



Karolina Anna Maria Zalewska

Ms. in Organic Chemistry Technology and Petrochemistry

Development of novel ionic liquids based on biological molecules

Dissertação para obtenção do Grau de Doutor em
Química Sustentável

Orientador: Doutor Luís Alexandre Almeida Fernandes Cobra Branco,
Investigador Auxiliar da Faculdade de Ciências e Tecnologia da
Universidade Nova de Lisboa.

Júri:

Presidente: Doutora Ana Maria Félix Trindade Lobo, Professora Catedrática
da Faculdade de Ciências e Tecnologia da Universidade Nova de Lisboa

Vogais: Doutor Carlos Alberto Mateus Afonso, Professor Catedrático da
Faculdade de Farmácia da Universidade de Lisboa;

Doutora Amélia Pilar Grases Santos Silva Rauter, Professora Associada com
Agregação da Faculdade de Ciências da Universidade de Lisboa;

Doutora Benilde de Jesus Vieira Saramago, Professora Associada do Instituto
Superior Técnico da Universidade de Lisboa;

Doutora Paula Cristina de Sérgio Branco, Professora Auxiliar da Faculdade de
Ciências e Tecnologia da Universidade Nova de Lisboa;

Doutora Isabel Maria Delgado Jana Marrucho Ferreira, Investigadora Auxiliar
do Instituto de Tecnologia Química e Biológica da Universidade Nova de
Lisboa



Dezembro de 2014

Development of Novel ionic liquids based on biological molecules

Copyright © Karolina Anna Maria Zalewska, Faculdade de Ciências e Tecnologia, Universidade Nova de Lisboa

A Faculdade de Ciências e Tecnologia e a Universidade Nova de Lisboa têm o direito, perpétuo e sem limites geográficos, de arquivar e publicar esta dissertação através de exemplares impressos reproduzidos em papel ou de forma digital, ou por qualquer outro meio conhecido ou que venha a ser inventado, e de a divulgar através de repositórios científicos e de admitir a sua cópia e distribuição com objectivos educacionais ou de investigação, não comerciais, desde que seja dado crédito ao autor e editor.

To my parents
Rodzicom

*‘Nothing in life is to be feared, it is only to be understood.
Now is the time to understand more, so that we may fear less.’*

Maria Skłodowska-Curie

Acknowledgments

In first place I would like to thank my supervisor, Dr. Luis C. Branco, for the opportunity to develop my knowledge while living in Portugal and for having the trust in me and my abilities. The continuous guidance, availability, advice when in my eyes nothing worked, support and encouragement, as well as the empathy that I felt from him throughout this four years trip was decisive to my personal growth. It has been a privilege to work with Dr. Luis C. Branco and the knowledge that I obtained from him will be unquestionably decisive in my future career. I would also like to thank Dr. Luis C. Branco's company Solchemar for providing some of the reagents used in this work.

I would like to extend special thanks to important personalities from the Photochemistry Group, namely to the Professor Fernando Pina, Dr. João Carlos Lima and Dr. Jorge Parola with whom I shared my love for caramels...

I would also like to leave a special thanks to Professor Carlos Afonso and all the other helpful members from the Faculty of Pharmacy's staff, for the guidance on using the HPLC, the scientific advices provided and also for performing some of the studies required for this project.

A sincere thank to all the people in the NMR service from FCT-UNL, for all the kindness and collaboration whenever it was needed to treat and analyse samples.

A gratefully thank to FCT for the funding sources that made my Ph.D. work possible.

I would like to leave a special thank to Dr. Luis Cabrita, a friend that was always present to advise me in professional and personal questions. His experience as a PhD student abroad, that he kindly shared with me, far away from his country and family, was extremely important in moments of doubt and the help provided in the understanding of the HPLC is deeply recognized.

A special thanks to João Avó that shared with me for almost 4 years the same office and many many candies... We have always been in tune because we are so similar and your friendship won't be forgotten.

I will never forget Andreinha, always a big help and support, Dra. Ana Marta for her good advices, Alexandra and Nuno for all the friendship and good times. You were with me since the beginning of this journey.

Special thanks to all colleagues in the Photochemistry and Supramolecular Group, Dra. Raquel, Dra. Márcia, Dra. Sandra, Dr. Artur, Dr. César Laia, Dr. Nuno, Joana, Noémi, Neuza.

I would also like to thanks my master thesis's orientator Dra. Agnieszka Siewniak, as well as the Professor of the Organic Chemistry Technology and Petrochemistry cathedral in Poland, Dra. Anna Chrobok, that during the last years became close friends. They are an excellent example of successful women and chemists. Thank you for not letting me give up!

And most of all for my loving, supportive, encouraging, and patient fiance João whose faithful support during this Ph.D. was so appreciated. Thank you.

Szczególne, z serca płynące podziękowania składam moim kochanym rodzicom, których miłość, wsparcie i nieustająca wiara we mnie zawsze pomagały mi przezwycięzać wszelkie trudności i dodawały sił, niezbędnych do realizacji życiowych planów.

Karolina

Resumo

Os Líquidos Iônicos (LIs) possuem algumas propriedades invulgares: pressão de vapor muito baixa; alta estabilidade química e térmica e a capacidade de se dissolver numa vasta gama de substâncias. Uma nova área de pesquisa está a avaliar a possibilidade de usar biomoléculas naturais quirais para a síntese de Líquidos Iônicos Quirais (LIQs). Este importante desafio pode abrir novos caminhos de pesquisa para evitar alguns problemas relacionados com a biodegradabilidade intrínseca e a toxicidade associada aos LIs convencionais.

O trabalho de pesquisa desenvolvido resultou na síntese de LIQs, com base em unidades biológicas utilizadas quer como catiões ou aniões quirais, dependendo da manipulação sintética dos derivados. No total, 28 sais orgânicos incluindo alguns LIQs foram sintetizados: 9 baseados em derivados de L-cisteína, 12 com base na L-prolina, 3 baseados em nucleosídeos e 4 em nucleotídeos. Estes novos LIQs foram completamente caracterizados a fim de avaliar as suas propriedades químicas e físicas e potenciais aplicações. Alguns destes LIQs, nomeadamente os baseados na L-cisteína e na L-prolina, foram aplicados em processos de discriminação, incluindo a síntese assimétrica, em particular como um meio de reação quiral para as reações assimétricas de Aldol e de Michael e a resolução de racematos.

Em paralelo, foram estudadas as interações de oligossacarídeos macrocíclicos denominados ciclodextrinas (CDs) com vários LIs. Foi possível melhorar a solubilidade das CDs em água e soro. A solubilidade dos ácidos gordos e esteróides em água também aumentou quando foram utilizados sistemas de LIs-CDs. O desenvolvimento de sistemas LIs-CDs eficientes e seletivos é indispensável para ampliar o leque das suas aplicações em interações *host-guest*, sistemas de administração de medicamentos ou reações catalíticas.

Novos sais derivados de nucleobases foram utilizados em estudos que visavam promover o aumento da fluorescência em meios aquosos.

Adicionalmente, foram realizados estudos preliminares para avaliar se o lactato de etilo poderia ser um solvente alternativo na organocatálise assimétrica.

PALAVRAS-CHAVE: Líquidos Iônicos, Moléculas Biológicas, Quiralidade, Catálise Assimétrica.

Abstract

Ionic Liquids (ILs) belong to a class of compounds with unusual properties: very low vapour pressure; high chemical and thermal stability and the ability to dissolve a wide range of substances. A new field in research is evaluating the possibility to use natural chiral biomolecules for the preparation of chiral ionic liquids (CILs). This important challenge in synthetic chemistry can open new avenues of research in order to avoid some problems related with the intrinsic biodegradability and toxicity associated to conventional ILs.

The research work developed aimed for the synthesis of CILs, their characterization and possible applications, based on biological moieties used either as chiral cations or anions, depending on the synthetic manipulation of the derivatives. Overall, a total of 28 organic salts, including CILs were synthesized: 9 based on L-cysteine derivatives, 12 based on L-proline, 3 based on nucleosides and 4 based on nucleotides. All these new CILs were completely characterized and their chemical and physical properties were evaluated. Some CILs based on L-cysteine have been applied for discrimination processes, including resolution of racemates and as a chiral catalyst for asymmetric Aldol condensation. L-proline derived CILs were also studied as chiral catalysts for Michael reaction.

In parallel, the interactions of macrocyclic oligosugars called cyclodextrins (CDs) with several ILs were studied. It was possible to improve the solubility of CDs in water and serum. Additionally, fatty acids and steroids showed an increase in water solubility when ILs-CDs systems were used. The development of efficient and selective ILs-CDs systems is indispensable to expand the range of their applications in host-guest interactions, drug delivery systems or catalytic reactions.

Novel salts derived from nucleobases were used in order to enhance the fluorescence in aqueous solution.

Additionally, preliminary studies regarding ethyl lactate as an alternative solvent for asymmetric organocatalysis were performed.

KEYWORDS: Ionic Liquids, Biological Molecules, Chirality, Asymmetric Catalysis.

Abbreviation List

[AcO]	acetate
[AOT]	docusate, (dioctyl sulfosuccinate)
[Bmim]	1-butyl-3-methylimidazolium
[Boc]	N-(<i>tert</i> -butoxycarbonyl)
[Bvim]	1-butyl-3-vinylimidazolium
[Bz]	benzyl
[C ₂ mim]	1-ethyl-3-methyl-imidazolium
[C ₂ OHDmim]	1-(2-hydroxyethyl)-2,3-dimethylimidazolium
[C ₂ OHmim]	1-(2-hydroxyethyl)-3-methylimidazolium
[C ₃ Omim]	1-(2-methoxyethyl)-3-methylimidazolium
[C ₄ mim]	1-butyl-3-methyl-imidazolium
[DCA]	dicyanamide
[Emim]	1-ethyl-3-methylimidazolium
[<i>i</i> -Pr]	<i>iso</i> -propyl
[<i>n</i> -Bu]	<i>n</i> -buthyl
[<i>n</i> -Pr]	<i>n</i> -propyl
[NTf ₂]	bis(trifluoromethylsulfonyl)imide
[Omim]	1-octyl-3-methylimidazolium
[P _{6,6,6,14}]	trihexyltetradecylphosphonium
[SAC]	saccharinate
[TfO]	trifluoromethanesulfonate
[TsO]	<i>p</i> -toluenosulfonate
AAs	Amino Acids
AD	Asymmetric Dihydroxylation
AMP	adenosine 5'-monophosphoric acid
AO	Acridine Orange
APIS	Active Pharmaceutical Ingredients
ATP	adenosine 5'-triphosphate
Bio-Ils	Bioinspired Ionic Liquids
BDM	dimethylated- β -cyclodextrin
BPM	permethylated- β -cyclodextrin
CD-CSPs	Cyclodextrin Chiral Stationary Phases

CDs	cyclodextrins
CE	Capillary Electrophoresis
CILs	Chiral Ionic Liquids
CMC	Critical Micellar Concentration
Cys	cysteine
DBU	1,8 – diazabicyclo[5.4.0]undec-7-ene
DCM	dichloromethane
DLS	Dynamic Light Scattering
DMF	dimethylformamide
DMSO	dimethylsulfoxide
DNA	deoxyribonucleic acid
DSC	Differential Scanning Calorimetry
E _a	Activation Energy
Ee	Enantiomeric Excess
EL	ethyl lactate
EPA	Enviromental Protection Agency
Et ₂ O	diethyl ether
EWG	Electron Withdrawing Group
FTIR	Fourier Transform Infrared Spectroscopy
GC	Gas Chromatography
HB	Hydrogen Bonds
HPLC	High Performance Liquid Chromatography
Ils	Ionic Liquids
K	Inclusion Complex Stability Constant
MB	Methylene Blue
MTBE	methyl <i>tert</i> -butyl ether
¹³ C NMR	Carbon Nuclear Magnetic Resonance Spectroscopy
¹⁹ F NMR	Fluor Nuclear Magnetic Resonance Spectroscopy
¹ H NMR	Proton Nuclear Magnetic Resonance Spectroscopy
2D NMR	Two-Dimensional Nuclear Magnetic Resonance Spectroscopy
ppm	parts per million
PRO	proline
RNA	ribonucleic acid
RT	Room Temperature
RTILs	Room Temperature Ionic Liquids

$scCO_2$	supercritical carbon dioxide
S-MeCys	S-methyl-L-cysteine
S-MeCysCO ₂	deprotonated S-methyl-L-cysteine
S-MeCysNH ₃	protonated S-methyl-L-cysteine
SNAP	Significant New Alternatives Policy
T _{dec}	Decomposition temperature
T _g	Glass Transition Temperature
TGA	Thermogravimetric Analysis
THF	tetrahydrofuran
T _m	melting temperature
TMG	tetramethylguanidine
TMS	tetramethylsilane
TS	Transition State
VOC	Volatile Organic Compounds
α_D	optical rotation
η	viscosity
Λ	conductance
ρ	density

Index

ACKNOWLEDGMENTS.....	V
RESUMO	VII
ABSTRACT	IX
ABBREVIATION LIST.....	XI
INDEX.....	XV
FIGURE INDEX.....	XXI
CHAPTER I. INTRODUCTION	1
I. INTRODUCTION	3
I.1. CHIRAL IONIC LIQUIDS	4
I.1.1. Chiral Ionic Liquids-historical background and applications.....	5
I.1.2. Chiral Ionic Liquids- design and synthesis.....	6
I.1.3. CILs of chiral cation	6
I.1.4. Imidazolium derivatives.....	7
I.1.5. Aminoacids derivatives.....	9
I.1.6. Pyridinium derivatives.....	12
I.1.7. Ammonium derivatives.....	12
I.1.8. Oxazolinium and Thiazolinium derivatives.....	13
I.1.9. Other derivatives	14
I.1.10. CILs based on chiral anion.....	15
I.2. CYCLODEXTRINS (CDs).....	17
I.2.1. Cyclodextrins (CDs)-Introduction, structure, applications	17
I.2.2. Interactions between ILs and CDs.....	19
I.3. NUCLEOBASES	22
I.3.1. Nucleobases-Introduction, structure, properties	22
I.3.2. Interactions between ILs and nucleobases.....	25
CHAPTER II. L-CYSTEINE BASED IONIC LIQUIDS	27
II. CHIRAL IONIC LIQUIS BASED ON CYSTEINE DERIVATIVES	29
II.1. BACKGROUND.....	29
II.2. SYNTHESIS OF NOVEL CILS BASED ON S-METHYL-L-CYSTEINE.....	30
II.3. THERMAL PROPERTIES OF NOVEL CILS BASED ON S-METHYL-L-CYSTEINE	33
II.4. PHYSICAL PROPERTIES OF NOVEL CILS BASED ON S-METHYL-L-CYSTEINE.....	34
II.5. NMR INTERACTION STUDY.....	34
II.6. APPLICATION OF S-ME-L-CYSTEINE BASED ILS FOR ENANTIOMERIC RESOLUTION.....	36
II.7. APPLICATION OF S-ME-L-CYSTEINE BASED ILS FOR ASYMMETRIC ALDOL REACTION	38
II.8. SYNTHESIS OF NOVEL CILS BASED ON OTHER L-CYSTEINE DERIVATIVES	42
II.9. CONCLUSIONS.....	44
II.10. EXPERIMENTAL PART	44

II.10.1. Synthesis of (S)-1-carboxy-2-(methylthio)ethanaminium bis((trifluoromethyl)sulfonyl)amide (2a)	45
II.10.2. Synthesis of (S)-1-carboxy-2-(methylthio)ethanaminium 1,4-bis((2-ethylhexyl)oxy)-1,4-dioxobutane-2-sulfonate (2b).....	45
II.10.3. Synthesis of trihexyl(tetradecyl)phosphonium (S)-2-amino-3-(methylthio) propanoate (3a)	46
II.10.4. Synthesis of 2-hydroxy-N,N,N-trimethylethanaminium (S)-2-amino-3-(methylthio)propanoate (3b).....	47
II.10.5. Synthesis of 1-ethyl-3-methyl-1H-imidazol-3-ium (S)-2-amino-3-(methylthio)propanoate (3c)	47
II.10.6. (S)-1-ethoxy-3-mercapto-1-oxopropan-2-aminium bis((trifluoromethyl)sulfonyl)amide (4a)	48
II.10.7. (S)-1-ethoxy-3-mercapto-1-oxopropan-2-aminium 1,4-bis((2-ethylhexyl)oxy)-1,4-dioxobutane-2-sulfonate (4b).....	48
II.10.8. (S)-1-carboxy-2-((carboxymethyl)thio)ethanaminium bis((trifluoromethyl)sulfonyl)amide (5a)	49
II.10.9. (S)-1-carboxy-2-((carboxymethyl)thio)ethanaminium 1,4-bis((2-ethylhexyl)oxy)-1,4-dioxobutane-2-sulfonate (5b).....	49
II.10.10. ¹⁹ F NMR Experiment- enantiomeric resolution	50
II.10.11. General procedure for asymmetric aldol reaction.....	50
CHAPTER III. L-PROLINE BASED IONIC LIQUIDS.....	53
III. L-PROLINE BASED IONIC LIQUIDS.....	55
III.1. BACKGROUND.....	55
III.2. SYNTHESIS AND CHARACTERIZATION	56
III.3. PHYSICAL PROPERTIES OF NOVEL L-PROLINE BASED SALTS	60
III.4. THERMAL PROPERTIES OF NOVEL L-PROLINE BASED SALTS	62
III.5. RHEOLOGY STUDIES OF NOVEL L-PROLINE BASED SALTS	65
III.6. PROLINE BASED CILS FOR ASYMMETRIC MICHAEL ADDITION	70
III.6.1. Extraction of Michael adduct with supercritical carbon dioxide (scCO ₂).....	75
III.7. OTHER EFFORTS RELATED WITH SYNTHESIS ATTEMPTS	77
III.8. CONCLUSIONS.....	79
III.9. EXPERIMENTAL PART	80
III.9.1. Synthesis of (S)-proline hydrochloride - cationic approach (7).....	81
III.9.2. Synthesis of (S)-2-carboxypyrrolidin-1-ium bis((trifluoromethyl)sulfonyl)amide (7a).....	81
III.9.3. Synthesis of (S)-2-carboxypyrrolidin-1-ium 1,4-bis((2-ethylhexyl)oxy)-1,4-dioxobutane-2-sulfonate (7b).....	82
III.9.4. Synthesis of (S)-2-carboxypyrrolidin-1-ium 4-methylbenzenesulfonate (7c).....	82
III.9.5. Synthesis of (S)-2-carboxypyrrolidin-1-ium 3-oxo-3H-benzo[d]isothiazol-2-ide 1,1-dioxide (7d).....	83
III.9.6. Synthesis of (S)-2-carboxypyrrolidin-1-ium ((1R, 4R)-7,7-dimethyl-2-oxobicyclo[2.2.1]heptan-1-yl)methanesulfonate (7e).....	83

III.9.7. Synthesis of (S)-2-carboxypyrrolidin-1-ium ((1S, 4R)-7,7-dimethyl-2-oxobicyclo[2.2.1]heptan-1-yl)methanesulfonate (7f)	84
III.9.8. Synthesis of trihexyl(tetradecyl)phosphonium (S)-pyrrolidine-2-carboxylate (8a).....	85
III.9.9. Synthesis of 1-ethyl-3-methyl-1H-imidazol-3-ium (S)-pyrrolidine-2-carboxylate (8b).....	85
III.9.10. Synthesis of 1-(2-methoxyethyl)-3-methyl-1H-imidazol-3-ium (S)- pyrrolidine-2-carboxylate (8c).....	86
III.9.11. Synthesis of 1-(2-hydroxyethyl)-3-methyl-1H-imidazol-3-ium (S)-pyrrolidine-2-carboxylate (8d).....	87
III.9.12. Synthesis of 1-(2-hydroxyethyl)-2,3-dimethyl-1H-imidazol-3-ium (S)-pyrrolidine-2-carboxylate (8e).....	87
III.9.13. Synthesis of 2-hydroxy-N,N,N-trimethylethanaminium (S)-pyrrolidine-2-carboxylate (8f)	88
III.9.14. General procedure for the Michael reaction of cyclohexanone and β -nitrostyrene	88
III.9.15. General procedure for extraction using scCO_2	89
CHAPTER IV. STUDIES OF CYCLODEXTRINS AND ILS.....	91
IV. STUDIES OF CYCLODEXTRINS AND IONIC LIQUIDS	93
IV.1. STUDIES ON DISSOLUTION OF BETA-CYCLODEXTRINS IN IONIC LIQUIDS.....	93
IV.2. RECOVERY OF BETA-CYCLODEXTRIN AND IONIC LIQUIDS.....	96
IV.3. APPLICATION OF BETA-CYCLODEXTRIN-IL GELS FOR THE STUDIES ON IMPROVEMENT OF WATER SOLUBILITY OF FATTY ACIDS AND STEROIDS.....	99
IV.4. DISSOLUTION OF ALFA- AND GAMMA-CYCLODEXTRINS IN IONIC LIQUIDS	100
IV.5. STUDIES ON SOLUBILITY BEHAVIOUR OF ALFA- AND GAMMA-CYCLODEXTRINS IN WATER AND SERUM	101
IV.6. INTERACTION OF ALFA- AND GAMMA-CYCLODEXTRINS WITH METHYLENE BLUE AND IONIC LIQUIDS	103
IV.7. CONCLUSIONS.....	106
IV.8. EXPERIMENTAL PART	106
IV.8.1. General procedure for the dissolution of β -CD in ILs.....	107
IV.8.2. General procedure for the recovery of β -CD and ILs.....	113
IV.8.3. General procedure for the studies on improvement of water solubility of fatty acids and steroids	113
IV.8.4. General procedure for the dissolution of α - and γ -CD in ILs.....	113
IV.8.5. General procedure for the studies on improvement of water solubility of α - and γ -CDs	114
CHAPTER V. NUCLEOBASES.....	115
V. IONIC LIQUIDS FROM NUCLEOBASES.....	117
V.1. SYNTHESIS OF ORGANIC SALTS DEVELOPED FROM NUCLEOSIDES AND AMP NUCLEOTIDE	117
V.2. CHARACTERIZATION OF SALTS DEVELOPED FROM NUCLEOSIDES AND AMP.....	122
V.3. NMR INTERACTION CATION-ANION STUDIES.....	123
V.4. CRITICAL MICELLAR CONCENTRATION STUDIES.....	125
V.5. FLUORESCENCE STUDIES.....	126
V.6. CONCLUSIONS.....	128

V.7.	EXPERIMENTAL PART.....	129
V.7.1.	General procedure for protonation of nucleosides (9a), (10a), (11a), (12a).....	130
V.7.2.	Synthesis of 9-(2 <i>R</i> ,3 <i>R</i> ,4 <i>S</i> ,5 <i>R</i>)-3,4-dihydroxy-5-(hydroxymethyl)tetrahydrofuran-2-yl)-6-oxo-6,9-dihydro-1 <i>H</i> -purin-2-aminium 1,4-bis((2-ethylhexyl)oxy)-1,4-dioxobutane-2-sulfonate (9b)	131
V.7.3.	Synthesis of 3-(2 <i>R</i> ,3 <i>R</i> ,4 <i>S</i> ,5 <i>R</i>)-3,4-dihydroxy-5-(hydroxymethyl)tetrahydrofuran-2-yl)-5-methyl-2,6-dioxo-1,2,3,6-tetrahydropyrimidin-1-ium 1,4-bis((2-ethylhexyl)oxy)-1,4-dioxobutane-2-sulfonate (11b).....	132
V.7.4.	Synthesis of 3-(2 <i>R</i> ,3 <i>R</i> ,4 <i>S</i> ,5 <i>R</i>)-3,4-dihydroxy-5-(hydroxymethyl)tetrahydrofuran-2-yl)-2,6-dioxo-1,2,3,6-tetrahydropyrimidin-1-ium 1,4-bis((2-ethylhexyl)oxy)-1,4-dioxobutane-2-sulfonate (12b)	133
V.7.5.	Synthesis of trihexyl(tetradecyl)phosphonium (2 <i>R</i> ,3 <i>S</i> ,4 <i>R</i> ,5 <i>R</i>)-5-(6-amino-9 <i>H</i> -purin-9-yl)-3,4-dihydroxytetrahydrofuran-2-yl)methyl hydrogenphosphate (13a)	134
V.7.6.	Synthesis of 1-ethyl-3-methyl-1 <i>H</i> -imidazol-3-ium (2 <i>R</i> ,3 <i>S</i> ,4 <i>R</i> ,5 <i>R</i>)-5-(6-amino-9 <i>H</i> -purin-9-yl)-3,4-dihydroxytetrahydrofuran-2-yl)methyl hydrogenphosphate (13b).....	134
V.7.7.	Synthesis of 1-(2-methoxyethyl)-3-methyl-1 <i>H</i> -imidazol-3-ium (2 <i>R</i> ,3 <i>S</i> ,4 <i>R</i> ,5 <i>R</i>)-5-(6-amino-9 <i>H</i> -purin-9-yl)-3,4-dihydroxytetrahydrofuran-2-yl)methyl hydrogenphosphate (13c).....	135
V.7.8.	Synthesis of 2-hydroxy- <i>N,N,N</i> -trimethylethanaminium (2 <i>R</i> ,3 <i>S</i> ,4 <i>R</i> ,5 <i>R</i>)-5-(6-amino-9 <i>H</i> -purin-9-yl)-3,4-dihydroxytetrahydrofuran-2-yl)methyl hydrogenphosphate (13d)	136
V.7.9.	General procedure for critical micelle concentration (CMC) of surfactant 9b and 11b.	137
V.7.10.	General procedure for fluorescence studies.....	137
CHAPTER VI. ETHYL LACTATE.....		139
VI.	ETHYL LACTATE.....	141
VI.1.	ETHYL LACTATE - AN ALTERNATIVE GREEN SOLVENT BESIDES ILS.....	141
VI.2.	ETHYL LACTATE- PROPERTIES AND APPLICATIONS	143
VI.3.	APPLICATION OF ETHYL LACTATE IN ORGANIC SYNTHESIS.....	144
VI.4.	APPLICATION OF ETHYL LACTATE IN ASYMMETRIC ORGANOCATALYSIS	147
VI.5.	CONCLUSIONS.....	150
VI.6.	EXPERIMENTAL PART	150
VI.6.1.	General procedure for asymmetric aldol reaction.....	150
VI.6.2.	General procedure for the Michael reaction of cyclohexanone and β -nitrostyrene	151
CHAPTER VII. ANNEX		153
VII.	ANNEX.....	155
VII.1.	NMR DATA FOR NMR ASSIGNMENT	155
VII.2.	FTIR DATA	169
VII.3.	DSC CURVES DATA.....	171
CHAPTER VIII. REFERENCES		175
VIII.	REFERENCES	177

Figure Index

Figure I.1 - Main families of Ionic Liquids cations.	4
Figure I.2 - Chiral Ionic Liquids general synthesis and application.	6
Figure I.3 - General design of CILs from naturally occurring amino acids.	9
Figure I.4 - Novel CILs based on L-proline developed by Luo (A) and Miao groups (B).	11
Figure I.5 - Novel CILs based on L-histidine developed by Erker (A) and Guillen groups (B).	11
Figure I.6 - Pyridinium CILs with urea functionality.	12
Figure I.7- CILs based on oxazolinium cation.	14
Figure I.8 - Structures of glucose (a), isosorbide (b) and isomannide (c) based CILs.	15
Figure I.9 - Structures of CILs based on chiral anion (a), (b), (c), (d) and (e).	17
Figure I.10 - Structural representations of α -cyclodextrin, β -cyclodextrin and γ -cyclodextrin.	18
Figure I.11 - The first RTILs derived from α - and β - CDs, the permethylated mono-6-deoxy-6-pyridin-1-ium and mono-6-deoxy-6(1-vinyl-1-H-imidazol-3-ium) α - and β - CDs trifluoromethanesulfonates.	21
Figure I.12 - Separation of the four enantiomers of whiskey lactone in a sample solution using novel RTILs derived from CDs.	22
Figure I.13 - Structural unit of common nucleotides.	23
Figure I.14 - Structure of adenosine 5'-phosphate (AMP) sodium salt in the state of ionization observed at neutral pH.	24
Figure I.15 - Protonation of adenosine 5'-phosphate (AMP) from strongly acidic solution (left) to strongly alkaline (right).	24
Figure I.16 - Studies on the dissolution mechanism of nucleobases in ILs.	26
Figure II.1 - Structures of synthesized S-methyl-L-cysteine based CILs.	30
Figure II.2- ^1H NMR spectrum of (S)-1-carboxy-2-(methylthio)ethanaminium 1,4-bis((2-ethylhexyl)oxy)-1,4-dioxobutane-2-sulfonate (2b) performed in CD_3OD	31
Figure II.3- ^1H NMR spectrum of -ethyl-3-methyl-1H-imidazol-3-ium (S)-2-amino-3-(methylthio)propanoate (3c) performed in CD_3OD	32
Figure II.4 - Photos of starting material S-methyl-L-cysteine and samples of synthesized ILs with the amino acid derivative either as cation (2a) or anion (3a).	32
Figure II.5 - ^1H NMR spectra of [S-Me-Cys][AOT] performed in different temperatures.	35
Figure II.6 - ^{19}F -NMR (CDCl_3) spectra of potassium Mosher's salt (A), potassium Mosher's salt with (1S,2R)-NorHEph[NTf ₂] as chiral selector (B), potassium Mosher's salt with (1S,2R)-HEphNTf ₂ as chiral selector (C), and potassium Mosher's salt with (1S,2R)-MeHEph [NTf ₂] as chiral selector (D).	37
Figure II.7 - ^{19}F NMR (DMSO) spectra of initial Mosher's sodium salt (A), Mosher's sodium salt with S-methyl-L-cysteine as chiral selector (B) and [Choline][S-MeCysCO ₂] as chiral selector (C).	38
Figure II.8 - Transition states (TS).	39
Figure II.9- Synthesis of CILs based on L-cysteine ethyl ester hydrochloride and S-carboxymethyl-L-cysteine.	43
Figure III.1 - Zwitterionic structure of both proline enantiomers: L-proline (left) and D-proline (right).	55
Figure III.2- Structures of chiral salts developed from L-proline.	56
Figure III.3 - ^1H NMR spectrum of trihexyl(tetradecyl)phosphonium (S)-pyrrolidine-2-carboxylate (8a) performed in CDCl_3 (Synthesis was carried out using ion exchange resin method).	59
Figure III.4 - ^1H NMR spectrum of (S)-2-carboxypyrrolidin-1-ium 1,4-bis((2-ethylhexyl)oxy)-1,4-dioxobutane-2-sulfonate (7b) performed in DMSO (Synthesis was carried out using anion metal exchange method).	59
Figure III.5 - Dubbling of peak from chiral carbon observed for [ProNH ₂][SAC] (7d) in ^1H NMR. The NMR description of the proton: 4.65-4.62 ppm (t, $^3J_{\text{H2-H3}}=4\text{Hz}$, 1H) and 4.47-4.44 ppm (t, $^3J_{\text{H2-H3}}=4\text{Hz}$, 1H).	60

Figure III.6- RTILs derived from L-proline [$P_{6,6,6,14}$][ProCO ₂] (left), [Emim][ProCO ₂] (middle) and [C ₃ Omim][ProCO ₂] (right).....	60
Figure III.7- DSC curve of [ProNH ₂][NTf ₂] (7a) in a heating cycle.....	64
Figure III.8- DSC curve of [Emim][ProCO ₂] 8b in a heating cycle.....	64
Figure III.9- Viscosity, the slope of each line, varies among materials.....	66
Figure III.10 - Studies on the Newtonian behaviour of CILs derived from L-proline.	66
Figure III.11 - Viscosity of proline based salts as a function of temperature at heating studies.	68
Figure III.12 -Viscosity of proline based salts as a function of temperature at cooling studies.	68
Figure III.13 - Scheme developed for [C ₂ OHmim][ProCO ₂] 8d in order to calculate the activation energy (E_a) and the R squared values during heating.....	69
Figure III.14 -Scheme developed for [C ₂ OHmim][ProCO ₂] 8d in order to calculate the activation energy (E_a) and the R squared values during cooling.....	69
Figure III.15 - Proposed ionic liquid strategy for acid replacement based on the example of the common organocatalyst (L)-1-[(pyrrolidin-2-yl)methyl]pyrrolidin.....	72
Figure III.16 - Carbon dioxide pressure-temperature phase diagram.	75
Figure III.17 - ¹ H NMR spectra of Michael adduct extrated with scCO ₂ (pure product up, mixture of product and catalyst down).....	77
Figure III.18 - Structures of counter-ions tried for synthesis of L-proline based salts.....	78
Figure IV.1 - Structure of β -CDs and ILs selected for dissolution studies.	94
Figure IV.2 - ¹ H NMR spectrum of the mixture β -CD dissolved in [Emim][EtSO ₄].....	95
Figure IV.3 - Novel chiral materials based on β -CD and ILs. (A)- gel, (B)- yellow liquid, (C)- transparent liquid.....	96
Figure IV.4 - Recovery strategy of β -CD and IL.....	96
Figure IV.5 - ¹ H NMR spectrum of the mixture β -CD dissolved in [Bmim][DCA] before recovery.....	97
Figure IV.6 - ¹ H NMR spectrum of the pure β -CD after recovery.....	98
Figure IV.7 - ¹ H NMR spectrum of the pure [Bmim][DCA] after recovery.	98
Figure IV.8 - Fatty acids and steroids chosen for the studies on improvment of their water solubility.....	99
Figure IV.9 - (A) squalene (left) and provit.D2 (right) in water with additive after 2 additions of steroids, (B) squalene (left) and provit. D2 (right) in water with additive after the last addition.	100
Figure IV.10- Structure of α - and γ -CDs and ILs selected for dissolution studies.	101
Figure IV.11 - CDs-ILs gels prepared for improvement of CDs water and serum solubility. ..	102
Figure IV.12 - Dissolution of α -CD with IL additive (KZ AC3) and γ -CD with IL additive (KZ AG4) in serum (first and last addition).	102
Figure IV.14 - Absorbtion spectra of MB (1.10^{-8} mol) with different proportions of α - and γ -CD solutions.	104
Figure IV.15 - Absorbtion spectra of MB (1.10^{-8} mol) with different proportions of α -CD [Bmim][DCA] solutions.....	104
Figure IV.13 - Methylene blue.	104
Figure IV.16 - Absorbtion spectra of MB (1.10^{-8} mol) with different proportions of γ -CD [Bmim][DCA] solutions.....	105
Figure IV.17 - Absorbtion spectra of MB (1.10^{-8} mol) with different proportions of α -CD [Aliquat][DCA] solutions.	105
Figure IV.18 - Absorbtion spectra of MB (1.10^{-8} mol) with different proportions of γ -CD [Aliquat][DCA] solutions.	105
Figure V.1 - Comparison of nucleic acids cations with imidazolium cation.	117
Figure V.2 - Structures of chiral salts synthesized from nucleosides as cations docusate [AOT] as anion.	120
Figure V.3- ¹ H NMR spectra of [T][AOT] 11b performed in dry DMSO.....	120
Figure V.4 - ¹ H NMR spectra of [U][AOT] 12b performed in dry DMSO.	121
Figure V.5 - Structures of the salts developed from AMP nucleotide.	121
Figure V.6- ¹ H NMR spectra of [Emim][AMP] 13b performed in dry DMSO.	122

Figure V.7 - Comparative ^1H -NMR study of $[\text{T}][\text{AOT}]$ for five temperatures (25, 40, 55, 70 and 85 °C) and two NMR regions (3.40 to 2.80 and at 2.10 ppm) in DMSO.....	124
Figure V.8 - Comparative ^1H -NMR study of $[\text{Emim}][\text{AMP}]$ for five temperatures (25, 40, 55, 70 and 85 °C) in DMSO.	125
Figure V.9 - An idealized model for a spherical micelle of sodium dodecyl sulfate	126
Figure V.10 -An example of fluorescence material- photo of $[\text{Emim}][\text{AMP}]$ (right) and the solid AMP nucleotide (left) under UV lamp.	127
Figure V.11- Emission spectra of AMP nucleotide (violet) and new AMP-based chiral salts $[\text{Emim}][\text{AMP}]$ in blue, and $[\text{C}_3\text{Omim}][\text{AMP}]$ in green at concentration 10^{-6} M.	127
Figure VI.1 - Twelve principles of green chemistry.....	141
Figure VI.2 – Green technologies in industry- Pfizer solvent selection guide for medicinal chemistry.	142
Figure VI.3 - Publications related to ethyl lactate since 1980 using all databases.....	143
Figure VI.4 - Synthesis of ethyl lactate (EL) from lactic acid.....	143
Figure VII.1 - ^1H NMR data for compound (S)-1-carboxy-2-(methylthio)ethanaminium 1,4-bis((2-ethylhexyl)oxy)-1,4-dioxobutane-2-sulfonate (2b).....	155
Figure VII.2 - ^{13}C NMR data for compound (S)-1-carboxy-2-(methylthio)ethanaminium 1,4-bis((2-ethylhexyl)oxy)-1,4-dioxobutane-2-sulfonate (2b).....	155
Figure VII.3 - ^1H NMR data of compound ethyl-3-methyl-1H-imidazol-3-ium (S)-2-amino-3-(methylthio)propanoate (3c).	156
Figure VII.4 - ^{13}C NMR data of compound ethyl-3-methyl-1H-imidazol-3-ium (S)-2-amino-3-(methylthio)propanoate (3c).	156
Figure VII.5 - ^1H NMR data of aldol product 4-hydroxy-4-(2-nitrophenyl)butan-2-one.....	157
Figure VII.6 - ^{13}C NMR data of aldol product 4-hydroxy-4-(2-nitrophenyl)butan-2-one.....	157
Figure VII.7 - ^1H NMR data of compound (S)-2-carboxypyrrolidin-1-ium 1,4-bis((2-ethylhexyl)oxy)-1,4-dioxobutane-2-sulfonate (7b).	158
Figure VII.8 - ^{13}C NMR data of compound (S)-2-carboxypyrrolidin-1-ium 1,4-bis((2-ethylhexyl)oxy)-1,4-dioxobutane-2-sulfonate (7b).	158
Figure VII.9 - ^1H NMR data of compound trihexyl(tetradecyl)phosphonium (S)-pyrrolidine-2-carboxylate (8a).	159
Figure VII.10 - ^{13}C NMR data of compound trihexyl(tetradecyl)phosphonium (S)-pyrrolidine-2-carboxylate (8a).	159
Figure VII.11 - ^1H NMR data of compound 1-ethyl-3-methyl-1H-imidazol-3-ium pyrrolidine-2-carboxylate (8b).	160
Figure VII.12 - ^{13}C NMR data of compound 1-ethyl-3-methyl-1H-imidazol-3-ium pyrrolidine-2-carboxylate (8b).	160
Figure VII.13- ^1H NMR data of compound (S)-2-[(R)-2-Nitro-1-phenylethyl]cyclohexanone (Michael product).....	161
Figure VII.14 - ^{13}C NMR data of compound (S)-2-[(R)-2-Nitro-1-phenylethyl]cyclohexanone (Michael product).....	161
Figure VII.15 - ^1H NMR data of compound α - CD.	162
Figure VII.16 - ^1H NMR data of compound γ - CD.....	162
Figure VII.17 - ^1H NMR data of compound 3-((2R,3R,4S,5R)-3,4-dihydroxy-5-(hydroxymethyl)tetrahydrofuran-2-yl)-5-methyl-2,6-dioxo-1,2,3,6-tetrahydropyrimidin-1-ium 1,4-bis((2-ethylhexyl)oxy)-1,4-dioxobutane-2-sulfonate (11b).	163
Figure VII.18 - ^{13}C NMR data of compound 3-((2R,3R,4S,5R)-3,4-dihydroxy-5-(hydroxymethyl)tetrahydrofuran-2-yl)-5-methyl-2,6-dioxo-1,2,3,6-tetrahydropyrimidin-1-ium 1,4-bis((2-ethylhexyl)oxy)-1,4-dioxobutane-2-sulfonate (11b).	163
Figure VII.19 - ^1H NMR data of compound 3-((2R,3R,4S,5R)-3,4-dihydroxy-5-(hydroxymethyl)tetrahydrofuran-2-yl)-2,6-dioxo-1,2,3,6-tetrahydropyrimidin-1-ium 1,4-bis((2-ethylhexyl)oxy)-1,4-dioxobutane-2-sulfonate (12b).	164
Figure VII.20 - ^{13}C NMR data of compound 3-((2R,3R,4S,5R)-3,4-dihydroxy-5-(hydroxymethyl)tetrahydrofuran-2-yl)-2,6-dioxo-1,2,3,6-tetrahydropyrimidin-1-ium 1,4-bis((2-ethylhexyl)oxy)-1,4-dioxobutane-2-sulfonate (12b).	164

Figure VII.21 - ^1H NMR data of compound trihexyl(tetradecyl)phosphonium ((2R,3S,4R,5R)-5-(6-amino-9H-purin-9-yl)-3,4-dihydroxytetrahydrofuran-2-yl)methyl hydrogenphosphate (13a).	165
Figure VII.22 - ^{13}C NMR data of compound trihexyl(tetradecyl)phosphonium ((2R,3S,4R,5R)-5-(6-amino-9H-purin-9-yl)-3,4-dihydroxytetrahydrofuran-2-yl)methyl hydrogenphosphate (13a).	165
Figure VII.23 - ^1H NMR data of compound 1-ethyl-3-methyl-1H-imidazol-3-ium ((2R,3S,4R,5R)-5-(6-amino-9H-purin-9-yl)-3,4-dihydroxytetrahydrofuran-2-yl)methyl hydrogenphosphate (13b).	166
Figure VII.24 - ^{13}C NMR data of compound 1-ethyl-3-methyl-1H-imidazol-3-ium ((2R,3S,4R,5R)-5-(6-amino-9H-purin-9-yl)-3,4-dihydroxytetrahydrofuran-2-yl)methyl hydrogenphosphate (13b).	166
Figure VII.25 - ^1H NMR data of compound 1-(2-methoxyethyl)-3-methyl-1H-imidazol-3-ium ((2R,3S,4R,5R)-5-(6-amino-9H-purin-9-yl)-3,4-dihydroxytetrahydrofuran-2-yl)methyl hydrogenphosphate (13c).	167
Figure VII.26 - ^{13}C NMR data of compound 1-(2-methoxyethyl)-3-methyl-1H-imidazol-3-ium ((2R,3S,4R,5R)-5-(6-amino-9H-purin-9-yl)-3,4-dihydroxytetrahydrofuran-2-yl)methyl hydrogenphosphate (13c).	167
Figure VII.27 - ^1H NMR data of compound 2-hydroxy-N,N,N-trimethylethanaminium ((2R,3S,4R,5R)-5-(6-amino-9H-purin-9-yl)-3,4-dihydroxytetrahydrofuran-2-yl)methyl hydrogenphosphate (13d).	168
Figure VII.28 - ^{13}C NMR data of compound 2-hydroxy-N,N,N-trimethylethanaminium ((2R,3S,4R,5R)-5-(6-amino-9H-purin-9-yl)-3,4-dihydroxytetrahydrofuran-2-yl)methyl hydrogenphosphate (13d).	168
Figure VII.29 - FTIR data for compound (L)-2-carboxypyrrolidin-1-ium bis((trifluoromethyl)sulfonyl)amide (7a).	169
Figure VII.30 - FTIR data for compound trihexyl(tetradecyl)phosphonium (L)-pyrrolidine-2-carboxylate (8a).	169
Figure VII.31 - FTIR data for compound 3-((2D,3D,4L,5D)-3,4-dihydroxy-5-(hydroxymethyl)tetrahydrofuran-2-yl)-5-methyl-2,6-dioxo-1,2,3,6-tetrahydropyrimidin-1-ium 1,4-bis((2-ethylhexyl)oxy)-1,4-dioxobutane-2-sulfonate (11b).	170
Figure VII.32 - FTIR data for compound trihexyl(tetradecyl)phosphonium ((2D,3L,4D,5D)-5-(6-amino-9H-purin-9-yl)-3,4-dihydroxytetrahydrofuran-2-yl)methyl hydrogenphosphate (13a).	170
Figure VII.33 - DSC curve for compound (L)-1-carboxy-2-(methylthio)ethanaminium bis((trifluoromethyl)sulfonyl)amide (2a) in a heating cycle.	171
Figure VII.34 - DSC curve for compound trihexyl(tetradecyl)phosphonium (S)-2-amino-3-(methylthio)propanoate (3a) in a heating cycle.	171
Figure VII.35 - DSC curve for compound 1-ethyl-3-methyl-1H-imidazol-3-ium pyrrolidine-2-carboxylate (8b) in a heating cycle.	172
Figure VII.36 - DSC curve for compound (L)-2-carboxypyrrolidin-1-ium bis((trifluoromethyl)sulfonyl)amide (7a) in a heating cycle.	172
Figure VII.37 - DSC curve for compound 1-(2-methoxyethyl)-3-methyl-1H-imidazol-3-ium ((2D,3L,4D,5D)-5-(6-amino-9H-purin-9-yl)-3,4-dihydroxytetrahydrofuran-2-yl)methyl hydrogenphosphate (13c) in heating cycle.	173
Figure VII.38 - DSC curve for compound 2-hydroxy-N,N,N-trimethylethanaminium ((2D,3L,4D,5D)-5-(6-amino-9H-purin-9-yl)-3,4-dihydroxytetrahydrofuran-2-yl)methyl hydrogenphosphate (13d) in heating cycle.	173

Scheme Index

<i>Scheme I.1 - Synthesis of the first CIL ([Bmim][lactate]) by Seddon and coworkers.</i>	<i>5</i>
<i>Scheme I.2 - Series of CILs synthesized from amino alcohols.</i>	<i>7</i>
<i>Scheme I.3 - Génisson's preparation of the imidazolium chiral RTILs.</i>	<i>8</i>
<i>Scheme I.4 - Synthesis of hydrophobic CILs using (L)-ethyl lactate.</i>	<i>8</i>
<i>Scheme I.5 - First synthesis of CILs from natural amino acids.</i>	<i>10</i>
<i>Scheme I.6 - Ammonium based CILs.</i>	<i>13</i>
<i>Scheme II.1 - General strategies for the synthesis of CILs starting from S-methyl-L-cysteine... </i>	<i>31</i>
<i>Scheme II.2 - General asymmetric aldol reaction between aldehydes and ketones.</i>	<i>39</i>
<i>Scheme II.3 - The original proposed mechanism of proline-catalyzed intermolecular aldol reaction. Proline acts through enamine catalysis. Enamine is formed from the pyrrolidine nitrogen and the carbonyl donor. Iminium ion, created by attack of the enamine on the re-face of the aldehyde, is then hydrolyzed to give chiral β-hydroxyketone.</i>	<i>40</i>
<i>Scheme III.1 - Hajos- Parrish- Eder- Sauer- Wiechert Reaction.</i>	<i>55</i>
<i>Scheme III.2 - General strategy for the synthesis of CILs based on L-proline as cationic unit.. </i>	<i>57</i>
<i>Scheme III.3 - Synthesis of L-proline based salts using ion exchange resins method.</i>	<i>58</i>
<i>Scheme III.4 –Enamine-, Enolate-, and Iminium- Catalytic Michael Reaction, where EWG=electron withdrawing group.</i>	<i>70</i>
<i>Scheme III.5 - Enamine-Catalyzed Michael Reaction.</i>	<i>71</i>
<i>Scheme III.6 - General scheme of the extraction of chiral Michael product using $scCO_2$.</i>	<i>76</i>
<i>Scheme V.1 - Protonation of nucleosides using hydrochloridic acid.</i>	<i>119</i>
<i>Scheme V.2 - Studies on the protonation of nucleosides using other organic acids.</i>	<i>119</i>

Table Index

Table I.1 – Some properties of α -, β - and γ - cyclodextrin	18
Table I.2 - Bases and their corresponding nucleosides.	23
Table II.1 Physical state, density, optical rotation, solubility and thermal properties of prepared S-methyl-L-cysteine based CILs.	33
Table II.2 Asymmetric aldol reaction using acetone or cyclohexanone with 2 or 4-nitrobenzaldehyde as model compounds and chiral RTILs based on S-protected-L-cysteine as organocatalysts.	41
Table II.3 Studies on asymmetric aldol reactions with different aromatic benzaldehydes.	42
Table III.1 Some properties of new synthesized salts based on L-proline scaffold.	61
Table III.2 Thermal Properties (T_m , T_{dec} and T_g) of ILs based on L-proline.	63
Table III.3- Parameters of Arrhenius plots calculated for CILs derived from L-proline.	68
Table III.4- Michael addition reaction of cyclohexanone to trans-nitrostyrene catalyzed by CILs based on L-proline.	74
Table IV.1 - Results of the dissolution studies of β -CD in ILs.	95
Table IV.2 - Amounts of β -CD and ILs used for recycling studies.	97
Table IV.3 - Results of water solubility of fatty acids and steroids using β -CD-[Emim][EtSO ₄] gel as additive.	100
Table IV.4 - Results of the dissolution studies of γ -CD in ILs.	101
Table IV.5 - Results of α – and γ -CDs water solubility.	102
Table V.1 - Characterization of new synthesized salts based on nucleosides and AMP scaffolds.	123
Table VI.1 Major advantages of using Ethyl Lactate.	144
Table VI.2 – Use of EL in Suzuki-Miyaura reaction	145
Table VI.3 - Synthesis of dihydropyridines with visible light using L-EL.	146
Table VI.4 - The use of EL in water used for 1, 3-dipolar cycloaddition reactions, optimization of solvent	147
Table VI.5 - Asymmetric aldol reaction using different solvents.	148
Table VI.6 - The effect of changing different conditions of Michael addition of cyclohexanone to trans-nitrostyrene.	149
Table VI.7 Michael addition reaction of cyclohexanone to trans-nitrostyrene catalyzed by L-proline in different solvents.	149

CHAPTER I. Introduction

I. Introduction

For economic and environmental reasons the chemistry society is confronted with the obligation to optimize their synthetic processes. Nowadays the organic solvents comprise 70% of all industrial emissions and 30% of overall volatile organic compounds (VOC) emissions nationwide^{1,2}.

One of the most important challenges of synthetic chemistry is related with the combination of efficiency, reduced costs and environmental impact in the production of relevant molecules, particularly in the preparation of chiral compounds. The creation of chiral centers can be achieved by several methodologies such as using chiral auxiliaries, readily obtained by chemical manipulation of chiral natural and non-natural compounds as well as by application of asymmetric catalysis including biocatalysis processes.

Recently, Ionic Liquids (ILs) have emerged as a possible environmentally benign alternative to common organic solvents, since they are typically liquids below 100 °C associated with their high thermal stability over a very wide temperature range¹. Since the first room temperature ionic liquid (RTIL), ethylammonium nitrate ever appeared, in 1914³, the field of ILs has undergone a rapid development mainly in last three decades. It is known that different RTILs can be synthesized from the combination of organic cations and relatively large, often poorly coordinating organic or inorganic anions⁴. Typically, a quaternary or protonated ammonium, phosphonium, pyridinium, pyrrolidinium, guanidinium, sulfonium or various N, N'-disubstituted imidazolium ions are distinguished as the cationic part of ILs (as shown in Figure I.1) and anions such as [AlX₄], [BF₄], [PF₆], docusate (dioctyl sulfosuccinate) [AOT], trifluoromethanesulfonate [TfO], bis(trifluoromethylsulfonyl)imide [NTf₂], dicyanamide [DCA] or halides represent some examples of the anionic part of ILs.

The interest of current research on ILs is mainly related with their almost negligible vapour pressure, high ionic conductivity, large electrochemical window, high chemical and thermal stability, peculiar interaction with supercritical CO₂ (ILs are insoluble in *sc*CO₂ but this supercritical gas is soluble in ILs) as well as their ability to dissolve a large range of organic molecules and transition metal complexes⁵. The physical and structural properties of the ILs are generally dependent on adequate selection of cation/anion combinations. The applications of ILs include their use as recyclable media for chemical processes, including non-catalytic and (bio)-catalytic reactions, CO₂ capture, biphasic extraction, gas chromatography, selective transport using supported liquid membranes, pervaporation, dissolution of cellulose, in fuel

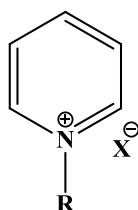
cells, and their potential use as a matrix for mass spectrometry or as solvent in nuclear electrical power plants, amongst others^{6,7,8,9}.

According to their properties and characteristics, ILs can be divided into three generations¹⁰. The first generation considers ILs as alternative solvents based on their peculiar physical properties (e.g. very low vapor pressure and high thermal stability) (*1st Generation*). The second-generation includes ILs with physical and chemical features that can act as advanced materials, such as lubricants, energetic materials and metal ion complexing agents (*2nd Generation*). Recently, the third generation of ILs (*3rd Generation*) has been described using active pharmaceutical ingredients (APIs) in order to design a wide range of new ILs with tunable biological activity, as well as the well known physical and chemical properties. This *3rd generation* of ILs can contribute for a considerable improve in solubility, stability, bioavailability or bioactivity of pharmaceutical drugs as well as the elimination of drug polymorphism.

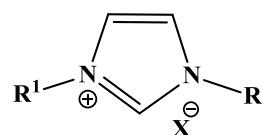
Alkyl ammonium salts



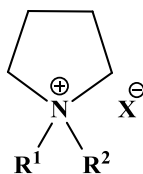
N-alkylpyridinium salts



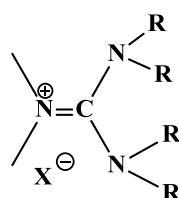
N,N'-dialkylimidazolium salts



Pyrrolidinium salts



Guanidinium salts



Sulfonium salts



where R= alkyl or other functional groups.

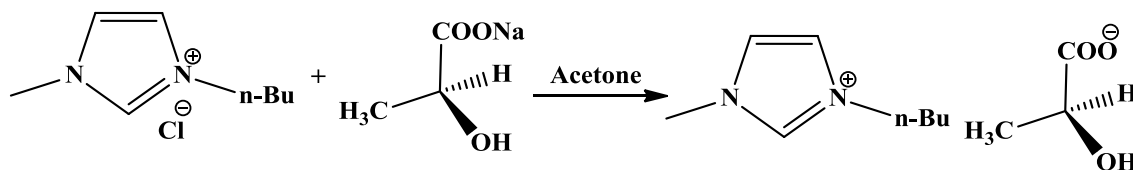
Figure I.1 - Main families of Ionic Liquids cations¹¹.

I.1. Chiral Ionic Liquids

The aim of this subsection is to introduce Chiral Ionic Liquids (CILs), starting with a historical background, reviewing the literature and proceeding with the discussion of most promising applications as well as future perspectives of their industrial use.

I.1.1. Chiral Ionic Liquids-historical background and applications

In 1975 Seebach described the first use of a chiral solvent in asymmetric synthesis¹². Using a chiral amino ether as solvent, modest enantioselectivities were obtained in the electrochemical reduction of ketones. In the case of ILs related with their high degree of organization, a transfer of chirality in these chiral media should be expected. It has been proved that many ILs possess a polymeric behavior and they are highly ordered H-bonded liquids, meaning 'three dimensional networks of anions and cations linked together by hydrogen bonds'¹³. These characteristics allow CILs to be tested as chiral reaction media for asymmetric processes. However, only few success reports appeared according the difficult syntheses of some CILs and their high cost. In 1999 Seddon and co-workers described the first example of CILs, 1-*n*-butyl-3-methylimidazolium 1-lactate ([Bmim][lactate]), simply synthesized by anion exchange between commercially available sodium (*S*)-2-hydroxypropionate and [Bmim]Cl in acetone (as shown in Scheme I.1)¹⁴. After the removal of NaCl by filtration and evaporation of acetone, it was possible to obtain the desired CIL.



Scheme I.1 - Synthesis of the first CIL ([Bmim][lactate]) by Seddon and coworkers.

Following the initial work on the preparation and application of CIL ([Bmim][lactate] by Seddon and coworkers), a number of new chiral ionic liquids have been synthesized and employed as chiral reaction media or additives, in order to induce moderate to high enantioselectivities in several reactions such as asymmetric Diels-Alder¹⁵, Aldol Reaction¹⁶, Michael Addition¹⁷, Sharpless Dihydroxylation (AD)^{18,19}.

One of the most significant examples is related with the Sharpless Osmium-catalyzed asymmetric dihydroxylation (AD) of olefins, one of the most reliable methods for the preparation of chiral vicinal diols, which act as intermediaries in the syntheses of many biologically active substances. The obstacles to its large-scale industrial application remain the osmium catalyst's high cost, toxicity, and potential product contamination. CILs based on guanidinium cations combined with quinic acid and mandelate as chiral anions were efficiently used as unique reaction and chirality-inducing media for asymmetric dihydroxylation of olefins¹⁸. For many cases the yields and enantiomeric excesses (*e.e.*'s) were comparable or higher than the conventional systems (using Sharpless alkaloid chiral ligands). The possibility

to recycle and recover the CILs and osmium catalyst by efficient extraction with *sc*CO₂ was presented as another advantage for the reaction processes.

CILs have been described as having potential application for chiral discrimination, which is one of the primary concerns in industry and academia. Despite the high number of applications of CILs in asymmetric reactions, other examples of applications have been reported (Figure I.2). Different CILs have been tested for chiral recognition as well as chiral separation processes. Also, the applications of CILs as chiral media for NMR²⁰, gas chromatography²¹, HPLC or mass spectra have been tested.

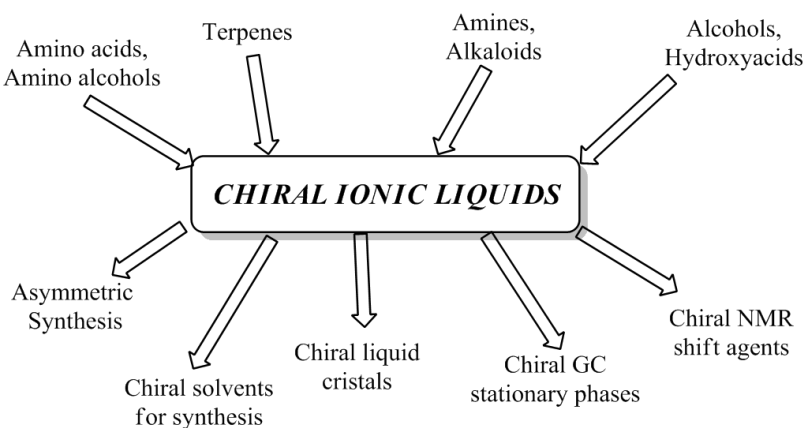


Figure I.2 - Chiral Ionic Liquids general synthesis and application.

I.1.2. Chiral Ionic Liquids- design and synthesis

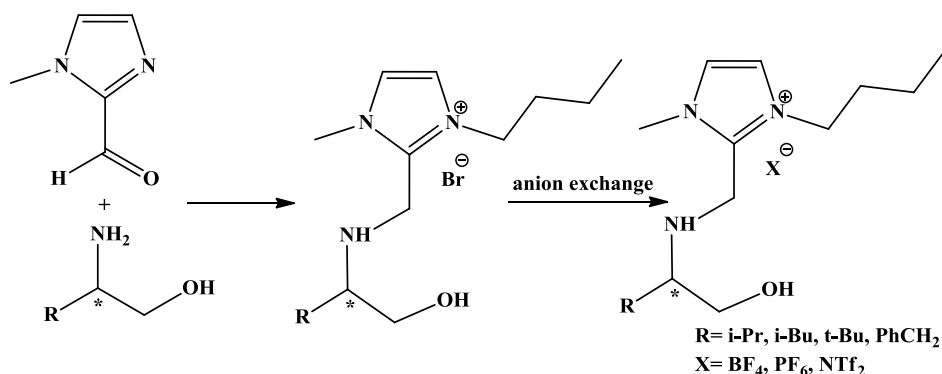
As mentioned previously, the research for synthesis, design and use of CILs is in its infancy. Nowadays, investigators try to develop more simple, economic and efficient methods in order to prepare alternative chiral RTILs. Therefore, natural materials are used as precursors derived from the 'chiral pool' for the generation of the CILs cation, anion or both. For this reason, CILs are described as mainly having a central chirality (nevertheless, some new CILs containing an axial or a planar chirality have been reported).

I.1.3. CILs of chiral cation

A larger number of known CILs obtain their chirality from the cationic moiety. The imidazolium cation is frequently used in ILs synthesis because it is known to produce salts with attractive properties, in particular lower melting points, tunable viscosities as well as high thermal and chemical stabilities.

I.1.4. Imidazolium derivatives

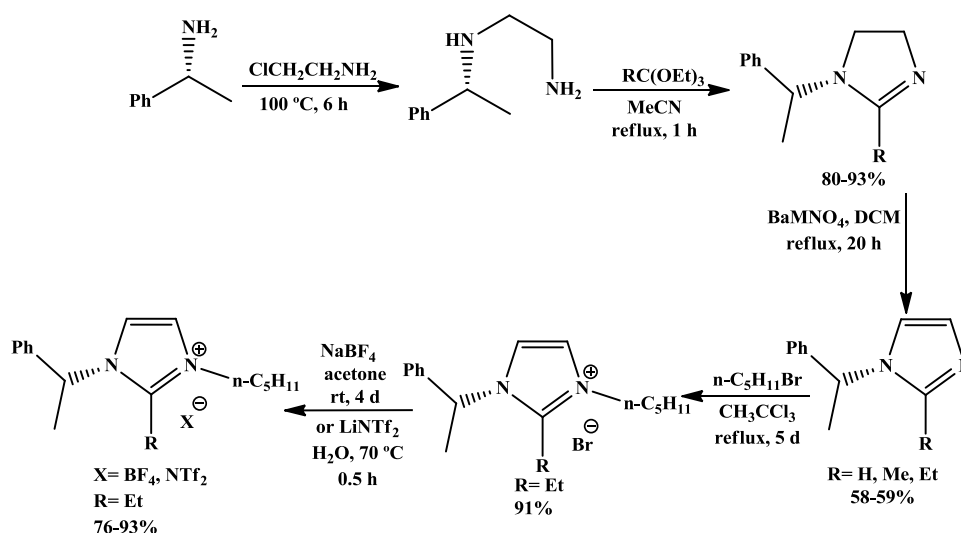
Herrmann et al. described the first CIL based on chiral imidazolium chloride obtained as an intermediate of the synthesis of N-heterocyclic imidazole carbenes²². In 2005, Headley and co-workers reported the attachment of a chiral group to C-2 position of the imidazolium ring. Commercially available chiral amino alcohols and 1-methyl-2-imidazol-carboxaldehyde have been tested by alkylation followed by anion exchange reactions (Scheme I.2)²³.



Scheme I.2 - Series of CILs synthesized from amino alcohols.

Other examples have included the incorporation of chiral amine (*R*)-(+)-methylbenzylamine in imidazolium unit by three synthetic steps: condensation of the chiral amine with ammonia, formaldehyde and glyoxal; alkylation with bromoethane in trichloromethane and then anion exchange using NaBF_4 in acetone²⁴. A similar strategy allowed the introduction of two chiral centers, each bonded to nitrogen atoms of the imidazolium ring using two equivalents of methylbenzylamine.

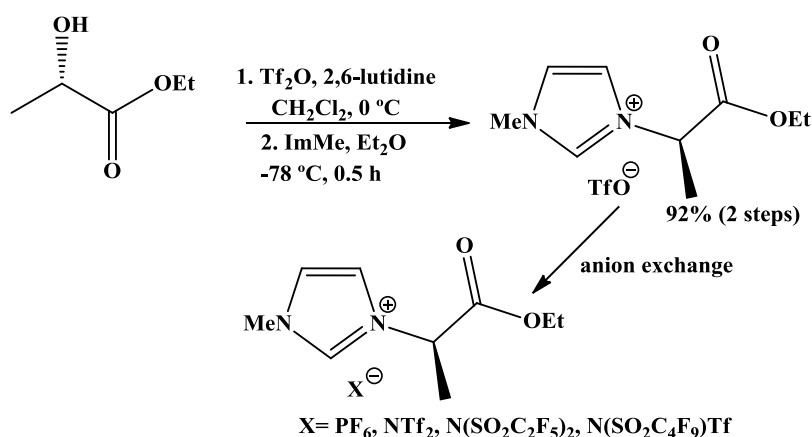
Génisson et al. described the development of several novel chiral imidazolium ILs using (*R*)-(+)-methylbenzylamine as starting material²⁵. Chiral 1,2-diamines were prepared from the alkylation of the starting material with chloroethylamine. These chiral 1,2-diamines were subjected to a ring-closing reaction with an appropriate ortho ester electrophile in order to obtain 4,5-dihydroimidazoles. Overall schematic of the synthesis is described in Scheme I.3. The final salts based on BF_4 and $[\text{NTf}_2]$ anions were obtained in relatively high yields, as water immiscible room temperature CILs.



Scheme I.3 - Génisson's preparation of the imidazolium chiral RTILs.

Different chiral alcohols have been used for the preparation of novel imidazolium CILs²⁶. Interesting results were obtained in the case of (*S*)-2-hexanol, (*1S*, *2S*, *5S*)-(-)-myrtanol²⁷ and (*3R*)-citronellol as chiral starting materials for the synthesis of chiral imidazolium ILs²⁸.

Jodry and Mikami reported the synthesis of hydrophobic chiral imidazolium ILs based on cheap and biodegradable L-ethyl lactate, which was firstly converted into a triflate derivative, followed by an alkylation and then an anion exchange reaction in order to give the desired imidazolium salt (Scheme I.4)²⁹.



Scheme I.4 - Synthesis of hydrophobic CILs using (L)-ethyl lactate.

Independent research groups of Bao³⁰ and Kubisa³¹ described the use of lactate as a starting material to incorporate into imidazolium units. Also, ethyl tartrate was employed as a chiral unit for dicationic CILs. Chiral tartrate bis(imidazolium) tetrafluoroborate and hexafluorophosphate were prepared as ILs with melting points lower than 90°C .

In 2006, Ni et al. explored another class of imidazolium CILs with urea functionality³². Urea derivatives, that contain effective hydrogen bonds formed by their amide hydrogens, are known as useful Lewis acid catalysts for organic reactions. Headley and coworkers published that the chirality comes from an amino acid ester derived isocyanate which reacts with 1-(3-aminopropyl)imidazole to yield the final urea derivatives. Many of them were obtained as viscous oils at room temperature.

I.1.5. Aminoacids derivatives

The natural chiral molecules such as Amino Acids (AAs) are considered the building blocks of life. It is possible to obtain pure AAs in big quantities at low cost, which is their great advantage, but there are further advantages, including biodegradability and biological activity. Currently, these biocompatible, small, natural molecules are receiving increasing attention due to their role as the most frequently employed chiral precursors for novel CILs³³. Since the AA contains both an amino and carboxylic acid group in a single molecule, with various side groups and a chiral carbon atom, they can be used as anions or cations for the design of various CILs (Figure I.3).

In the last years, the new synthesized CILs (from 'chiral pools') have enjoyed widespread attention and they are being used in the asymmetric synthesis, including direct aldol reaction, Michael Addition, Diels-Alder reaction, Baylis–Hillman, amongst others. It was been proved that they can be a great substitute for common asymmetric catalysts, presenting unprecedented opportunities to address some limitations in asymmetric catalysis.

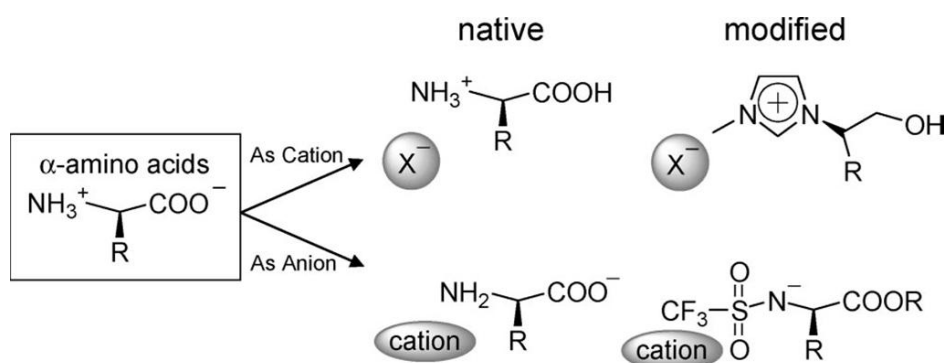
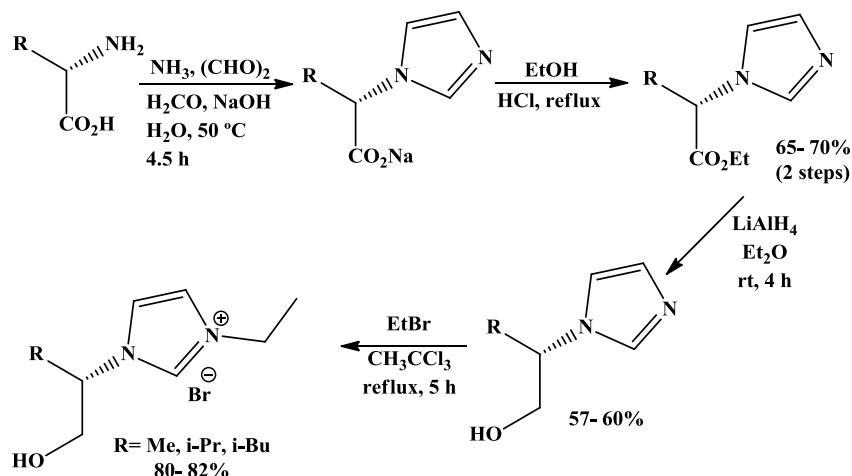


Figure I.3 - General design of CILs from naturally occurring amino acids³³.

In this context, the group of Bao reported the first synthesis of chiral imidazolium ILs from natural AAs, in particular using L-alanine, L-leucine and L-valine as chiral starting materials²⁴.

The imidazole ring was formed by condensation of the amino functionality of the amino acid with glyoxal, formaldehyde and aqueous ammonia under basic conditions. Different water miscible CILs with low melting points (5-16°C) were obtained using this synthetic methodology presented in Scheme I.5.



Scheme I.5 - First synthesis of CILs from natural amino acids.

In the same line, Xu and his coworkers developed novel chiral amine-functionalized ILs derived from L-alanine, L-valine, L-leucine, L-isoleucine and L-proline in four steps³⁴. All novel CILs possessed thermal stability up to 210 °C with higher solubility in polar solvents than less nonpolar solvents, when compared with the related unfunctionalized imidazolium-type ILs.

Amino acid derivatives in the form of amino alcohols are also good precursors for the development of CILs. Recently, chiral amino alcohols such as D or L-leucinol and L-3-phenyl-2-aminopropanol, amongst others, were used for the condensation with 1-methyl-2-imidazolecarboxaldehyde and after reduction *in situ* using NaBH₄, gave the desired chiral imidazole derivatives^{35,36}. The subsequent N-alkylation was performed by heating imidazoles with 1-bromobutane (1 equivalent) in toluene. The novel CILs based on chiral amino alcohols and BF₄ or [NTf₂] as anions, were obtained in moderate to high yields as colorless viscous oils at room temperature. Some variations of this synthetic method were also described by Ou et al.³⁷

Proline is a versatile and inexpensive chiral starting material which has been used for synthesis of CILs. Examples of CILs based on L-proline have been firstly described by Luo et al.³⁸ (series of pyrrolidine-containing chiral imidazolium ILs) and Miao and Chan³⁹ (using commercial available Boc-Pro-OH incorporated with imidazolium cation), as shown in Figure I.4.

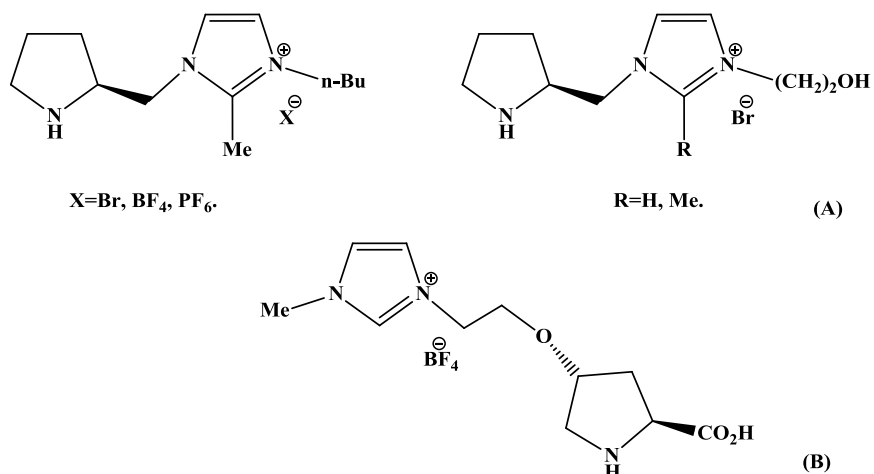


Figure I.4 - Novel CILs based on L-proline developed by Luo (A) and Miao groups (B).

Also, histidine as alternative amino acid was explored in order to attach imidazolium cations. Hannig et al. showed the two synthetic steps for the preparation of novel L-histidine CILs as water soluble salts with relatively lower melting points (39 to 55 °C), as shown in Figure I.5 (A)⁴⁰. One year later, Guillen et al. reported other O- and N-protected histidinium salts (Figure I.5 (B)⁴¹). In this case, the protection of histidine methyl ester via cyclic urea is followed by alkylation with iodomethane and the opening of the cyclic urea gave the desired histidine derivatives. Final alkylation with bromobutane allowed the formation of chiral imidazolium bromide salts.

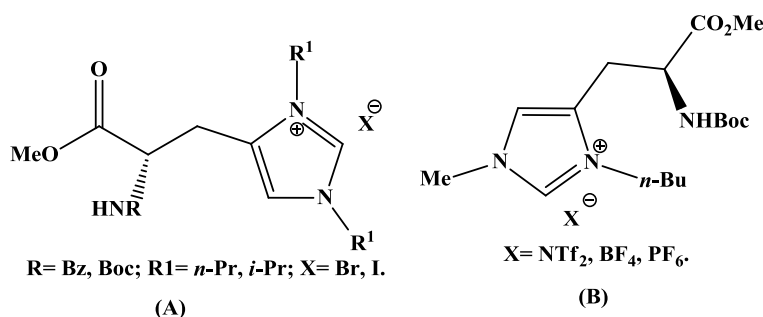


Figure I.5 - Novel CILs based on L-histidine developed by Erker (A) and Guillen groups (B).

Cyclophane-type imidazolium salts were developed by Saigo's group as first examples of planar-chiral ILs⁴². The introduction of a substituent in position 4 of the imidazolium ring can induce a planar chirality and dramatically reduce their melting points. The racemization of these planar chiral cyclophanes can be suppressed by the presence of a substituent at C-2 position. A similar approach was followed in the case of planar-chiral imidazolium chloride with tris(oxoethylene) bridge. At the same time, examples of CILs containing a fused and a spiro skeleton were reported in the literature by Headley⁴³ and Sasai⁴⁴ respectively.

I.1.6. Pyridinium derivatives

The use of pyridinium ion as the cationic moiety in order to create CILs is not as dominant as the use of imidazolium. However, due to its surface-active and antibacterial properties, pyridinium-based cations CILs remain an important class of compounds to be investigated.

In 2006, Headley and coworkers, already mentioned in the imidazolium subsection (I.1.4.), described pyridinium chiral ILs with urea functionality (Figure I.6)⁴⁵ as well. These class of CILs were synthesized starting from 2-(aminomethyl)pyridine and amino acid ester derived isocyanates. The use of pyridinium cation instead of imidazolium units can avoid the acidic hydrogen in the C-2 position of the imidazolium ring, which produces unwanted byproducts under basic conditions. In parallel, the same authors described pyridinium CILs with an appropriate pyrrolidine moiety⁴⁶. These CILs were prepared using commercially available (*S*)-2-aminomethyl-1-*N*-Boc-pyrrolidine and 1-(2,4-dinitrophenyl)pyridin-1-ium chloride (Zincke's salt). De Viguerie and coworkers also tested Zincke's salt as a precursor for pyridinium CILs by using Marazano's reaction based on the original work of Zincke⁴⁷. In this context, they synthesized an organometallic CIL (*R*) and (*S*)-bis-(1-phenylethylpyridinium) tetrachloropalladate, using enantiopure (*R*) and (*S*)-1-phenylethylamine as starting precursors. Pernak et al. reported a series of pyridinium CILs containing (*1R*, *2S*, *5R*)-(-)-menthyl unit using a similar synthetic approach already published for imidazolium CILs⁴⁸.

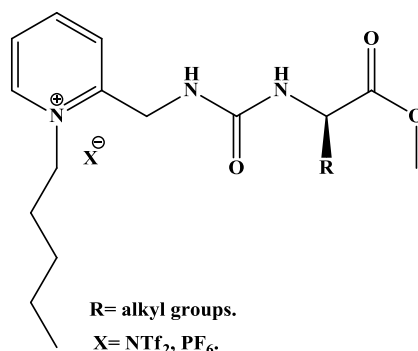
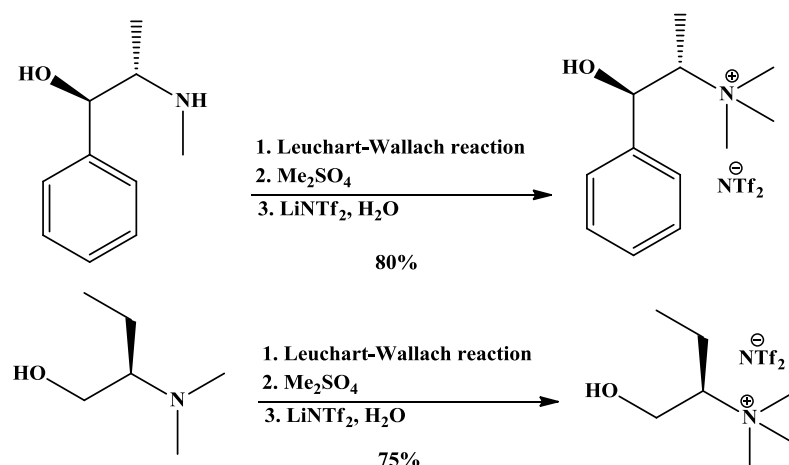


Figure I.6 - Pyridinium CILs with urea functionality^{45, 49}.

I.1.7. Ammonium derivatives

Two chiral hydroxyammonium salts were prepared in large scale from (-)-ephedrine and (*R*)-2-aminobutan-1-ol, as shown in Scheme I.6⁵⁰. The amino alcohols were converted in three steps into the desired CILs in moderate to high yields. Ephedrinium salt (based on NTf₂ anion) presented a low melting point (54 °C) and water immiscibility while (*R*)-2-aminobutanol salt (based on NTf₂ anion) is a room temperature CIL with low viscosity behavior.



Scheme I.6 - Ammonium based CILs.

Other ephedrinium salts have been described according to variable alkyl chain lengths on the nitrogen group⁵¹. In these cases, (1*R*, 2*S*)-*N*-methylephedrine was used as a starting material previously prepared by reductive amination of ephedrine. Then, alkylation reaction and anion metathesis gave the desired CILs in good yields and in most of the cases as viscous oils at room temperature. More recent examples of CILs were described by simply one-step acidification of natural α -amino acids and α -amino acid ester salts⁵². Due to the strong hydrogen bonds involving the carboxylic acid functionality, most of the salts derived from α -amino acid derivatives, showed higher melting points than correspondent esters salts (viscous oils at room temperature).

I.1.8. Oxazolinium and Thiazolinium derivatives

Wasserscheid and his group reported the first example of CILs based on oxazolinium cation, which were prepared in four steps starting from L-valine⁵⁰. The first step was the reduction of L-valine methyl ester, followed by the formation of aminoalcohols by Masamune's protocol ($\text{NaBH}_4\text{-H}_2\text{SO}_4$ in THF). Then, the cyclization step into oxazoline using propionic acid was performed and the final step related with alkylation of oxazoline using bromoalkanes gave the corresponding salts (Figure I.7). CILs based on oxazoline cation when combined with PF_6^- as anion, showed melting points in the range of 63 to 79 °C.

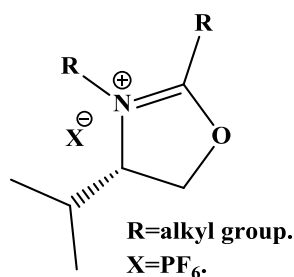


Figure I.7- CILs based on oxazolinium cation.

The group of Gaumont published a novel class of CILs based on thiazolinium salts, which are obtained in four steps using L-phenylalaninol or D-2-aminobutanol with relatively moderate yields (68% yield)⁵³. The first reaction was between dithioester and the aminoalcohol, followed by cyclisation of the intermediate thioamide in the presence of mesyl chloride and triethylamine. After the alkylation of the chiral thiazoline with an alkyl halides and further anion exchange using Li [NTf₂], HPF₆ or HBF₄, it was possible to obtain the corresponding CILs. Thiazolium ILs present good thermal and chemical stabilities (stable under basic and acidic conditions unlike their oxygen counterparts the oxazolinium salts).

I.1.9. Other derivatives

Several examples of CILs derived from chiral cations have been developed in the last years. The first sugar (fructose-based) IL was described in 2003 by Handy et al. and later the commercial available methyl-D-glucopyranoside served to develop a series of CILs^{54,55,56}. In this last case, novel CILs can act as chiral solvents in organic reactions showing appreciable stability. Therefore, the reactivity of hydroxyls was significantly lower by protection as methyl ethers, and the labile anomeric acetal was reduced to an inert methylene group.

Similar synthetic approaches were reported for the preparation of novel families of CILs based on isosorbide (derived from dehydration of inexpensive D-sorbitol) and isomannide (prepared by acid-catalyzed double dehydration of manitol)^{57, 58}. In 2008, Singh and coworkers described CILs based on D-arabinofuranose, D-ribofuranose and X-xylofuranose⁵⁹.

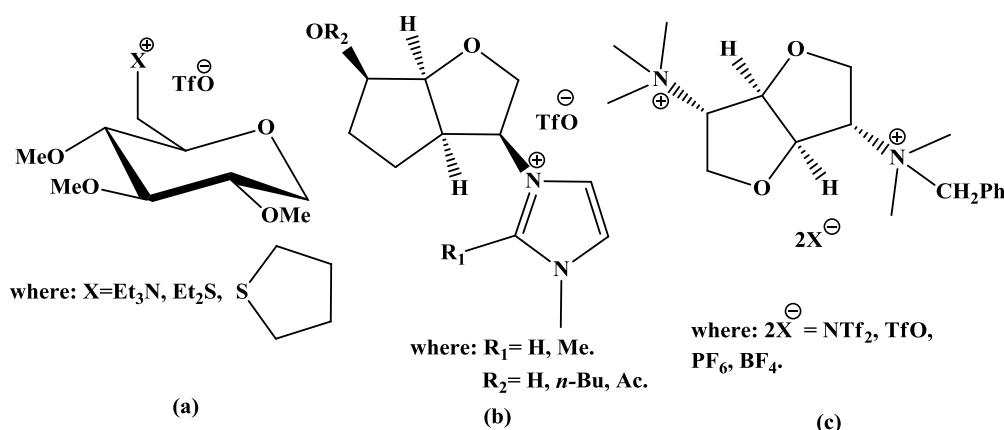


Figure I.8 - Structures of glucose (a), isosorbide (b) and isomannide (c) based CILs.

I.1.10. CILs based on chiral anion

The first example of chiral ILs based on chiral anions was at the same time the first example of CILs, described by Seddon in 1999, as it was mentioned in the historical background subchapter¹⁴ (I.1.1). Lactate anion was used as the source of chirality, combined with 1-butyl-3-methylimidazolium ([Bmim]) cation by simply anion exchange reaction. Then, Ohno and coworkers described the preparation of a series of 19 CILs based on natural amino acids as chiral anions⁶⁰. The synthesis involved two steps: first the conversion of 1-ethyl-3-methylimidazolium bromide ([Emim]Br) into hydroxide ([Emim]OH) using an anion-exchange resin method (Amberlite), followed by a neutralization reaction with the selected natural aminoacid. All CILs based on aminoacids were reported as almost colorless liquids at room temperature, as well as miscible in a variety of organic solvents such as alcohols, acetonitrile and chloroform. The authors observed that the increase of the alkyl chain of aminoacid leads to a small increase of the glass transition temperatures (T_g), while the presence of aromatic side chains induce a larger increase of T_g , probably due their π -stacking interactions. The same larger increase of T_g values were observed by introduction of very polar units such as carboxyl or amide groups.

Several examples of CILs incorporating aminocids have been described mainly because of their low cost, good enantiomeric purity, commercial availability and bio renewability. Fukumoto and Ohno reported the preparation of other class of CILs containing aminoacid derivatives as chiral anions³³. Previously the conversion of aminoacids into their methyl esters was carried out with thionyl chloride in methanol, followed by a treatment with trifluoromethanesulfonic anhydride and triethylamine in dichloromethane in order to give the desired methyl esters of N-trifluoromethanesulfonylamino acids. Final CILs were achieved by the anion exchange reaction between the correspondent esters and [Bmim]OH⁶⁰.

A similar synthetic approach was described in the case of the preparation of CILs containing tetrabutylphosphonium cation combined with deprotonated amino acid anions⁶¹. Also, Allen et al. reported a series of CILs based on tetrabutylammonium cation containing amino acid anions⁶².

Other available natural molecules have been tested as starting materials for the synthesis of CILs, containing chirality in the anionic moiety. Branco et al. reported the combination of tetrahexyldimethylguanidinium cations with a variety of chiral carboxylic acids and protected amino acids such as quinic, camphorsulfonate, mandelic, lactic, Boc-hydroxyproline, Boc-alanine and acetyl-hydroxyproline⁶³. All of them are examples of room temperature CILs with high thermal stability and tunable viscosity as well as solubility profile according to the selected anion.

Machado and Dorta prepared multigram chiral ILs based on the combination of [bmim] cation and (*S*)-10-camphorsulfonate (viscous oil) and (*R*)-1,1'-binaphthyl-2,2'-diylphosphate (mp. 80°C) as anions⁶⁴.

Recently, Weiss and coworkers reported reversible room temperature amidinium carbamate ILs, obtained by bubbling CO₂ gas through a equimolar mixture of an amidine (*N*'-alkyl-*N*, *N*-dimethylacetamide) and an amino acid ester or amino alcohol (40 examples)^{65, 66}. All CILs were stable under CO₂ atmosphere up to 50 °C and can be reconverted to the starting materials by purging with nitrogen gas. This reversibility concept has been explored as a CO₂ scavenging method or delivery system process.

In the last year, new reversible organic salts based on amino acids in the presence of organic superbases [1,8-diazabicyclo[5.4.0]undec-7-ene (DBU) and tetramethylguanidine (TMG)] have been reported⁶⁷. Novel protic amino acid salts with improved water-solubility profiles and unexpected phase behaviour were synthesized using an optimized acid–base reaction. It was proved that a phase separation between water and the amino acid salt occurs and that the process is reversible, depending on the temperature and the selected organic superbase. The work presented could show potencial for tuning miscibility and ionicity of organic salts and the design of reversible protic CILs or molten salts.

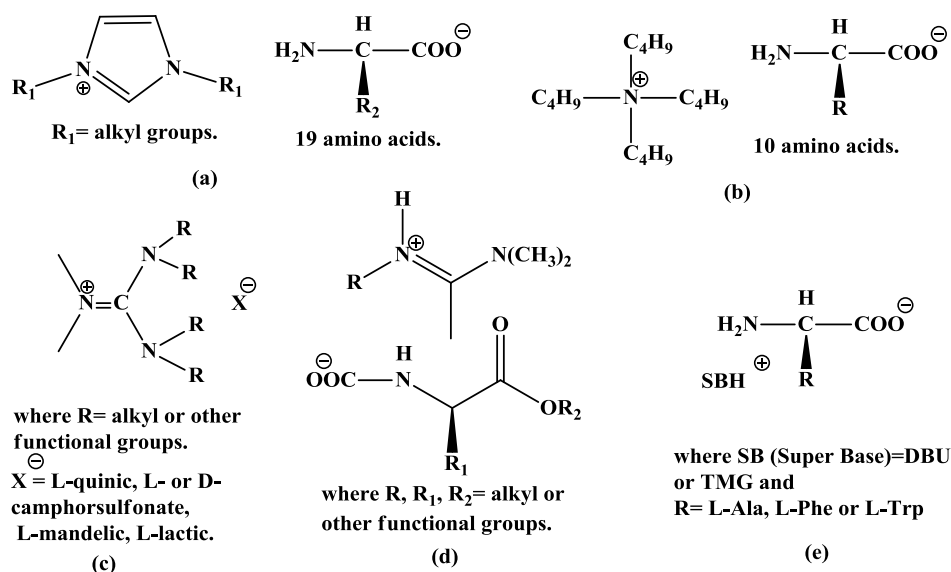


Figure I.9 - Structures of CILs based on chiral anion (a)⁶⁰, (b)⁶², (c)⁶³, (d)⁶⁵ and (e)⁶⁷.

I.2. Cyclodextrins (CDs)

The aim of this subchapter is to present a family of biological molecules called Cyclodextrins (CDs), which have enjoyed widespread attention and use in recent years. A relevant focus of current research is related with the chemistry of biomolecules and their crucial role in new fields. These useful functional excipients have gained most attention in the pharmaceutical area and drug delivery, by improving solubility and/or stability of several drug molecules. Within the field of supramolecular chemistry there is an increasing interest focused on the potential applications of cyclodextrin-based systems.

I.2.1. Cyclodextrins (CDs)-Introduction, structure, applications

Cyclodextrins (CDs) were first isolated by a French scientist, A. Villiers in 1891, who described them as a bacterial digest isolated from starch^{68, 69}. Experimental results proved that the substance was a dextrin and Villiers called it “cellulosine”. Later an Austrian microbiologist, Franz Schardinger, reported two crystalline compounds α -dextrin and β -dextrin which he had isolated from a bacterial digest of potato starch. Schardinger considered β -dextrin as Villiers' “cellulosine”^{70,71}. CDs, also known as cycloamyloses, cyclomaltoses and Schardinger dextrins, are cyclic oligosaccharides composed of six to eight α -D-glucose monomers linked by α -1,4 glycosidic bonds (α -, β -, γ - CD respectively, Figure I.10, Table I.1)⁷². They are produced as a result of enzymatic degradation of starch.

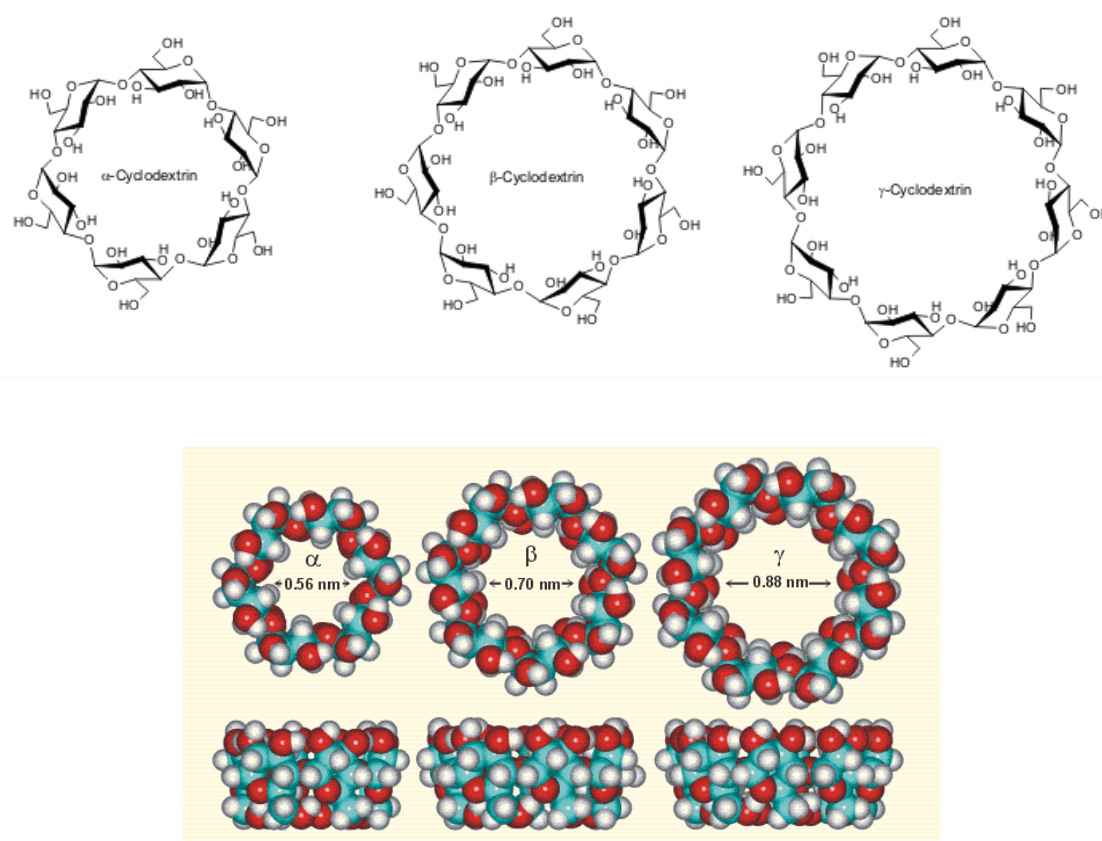


Figure I.10 - Structural representations of α -cyclodextrin, β -cyclodextrin and γ -cyclodextrin.

Table I.1 – Some properties of α -, β - and γ - cyclodextrin⁷².

Parameters	α -CD	β -CD	γ -CD
Number of glucose units	6	7	8
MW [g.mol ⁻¹]	972	1135	1297
Water solubility at room temperature [g.100ml ⁻¹]	14.5	1.85	23.2
Outer diameter [nm]	1.52	1.66	1.77
Cavity diameter [nm] inner rim/outer rim	0.45/ 0.53	0.60/ 0.65	0.75/ 0.85
Cavity volume [ml.g ⁻¹]	0.10	0.14	0.20
[α] _D at 25 °C	150±0.5	162.5±0.5	177.4±0.5
Melting temperature range [°C]	255-260	255-265	240-245

Among this class of host molecules, the β -CD is the most abundant natural oligomer because of its odd number of units and lower price. Owing to their unique structure, hydrophobic internal cavity and hydrophilic external surface, CDs have the property of forming inclusion complex with various guest molecules. The hydrophobic cavity provides relative good water solubility for the cyclodextrins and the hydrophilic surface causes a favourable environment for the hydrophobic parts of a guest molecule to be held in. This inclusion isolates the guest molecules from the aqueous media and can increase the guest's water solubility and/or stability. The

molecules from inclusion complex are only in contact by physical forces and without covalent binding⁷³. Furthermore, the dissociation-association equilibrium is one the most characteristic features of the host-guest processes.

The equilibrium between the guest and cyclodextrin is crucial in the measurement of the inclusion complex stability constant. The general equation can be defined as:



where n and m are the number of mole for the guest molecule and cyclodextrin, respectively. The equilibrium constant K or inclusion complex stability constant for the process can be defined as:

$$K = [\text{Guest}_n\text{CD}_m] / [\text{Guest}]_n [\text{CD}]_m \quad \text{Eq. I.2}$$

where n and m are the number of mole for the guest molecule and cyclodextrin, respectively. The simplest formation of a complex between the cyclodextrin and a guest molecule is a stoichiometric proportion of 1:1⁷³. Several techniques such as pH measurements, potentiometry, calorimetry, conductivity, absorption or fluorescence spectroscopy and capillary electrophoresis are used to determine their stoichiometry and stability.

The formation of host/guest complexes has been used in different areas, ranging from pharmaceutical and food industry to cosmetic, agrochemical and environmental applications^{74,75,76}. Generally these carbohydrates are used to enhance the solubility, stability, and bioavailability of drugs⁷⁷. They can also prevent drug-drug or drug additive interactions and reduce gastrointestinal or ocular irritation. At the same time, cyclodextrin complexations give rise to flavors, showed potential in asymmetric reactions, enantiomeric separations, self-assembled monolayers and enzyme mimics⁷⁷. The only limitation of those chiral biomolecules is related with their low solubility in water and many common organic solvents⁷⁸. Therefore, it is challenging to search for alternative solvents in order to enhance CDs applications⁷⁹.

I.2.2. Interactions between ILs and CDs

In the last years, wide attention has been focused on interactions between CDs and ILs. Formation of inclusion complexes of β -CD and ionic liquid surfactant was described by Gao et al⁸⁰. They concluded that β -CD and 1-butyl-3-methylimidazolium hexafluorophosphate

([Bmim] PF₆) could form 1:1 inclusion complexes in water with the whole imidazolium cation entering the cavity of β - CD. The group of Tran investigated the binding constants of CDs in 1-butylmethyimidazolium chloride ([Bmim]Cl) using the near-infrared spectrometry⁸¹.

According to the application of CDs in polymer chemistry, the group of Ritter studied the interactions between β - CD and 1-butyl-3-vinylimidazolium bis(trifluoromethylsulfonyl)imide ([Bvim][NTf₂]) in order to increase the solubility in water. The complexation between the CD and the bis(trifluoromethylsulfonyl)imide anion was proved using conductivity measurements, NMR and microcalorimetry⁸².

Besides β - CD, α - and γ - CD gain more attention and recently some work has been reported. Vranic and Uzunovic reported dissolution studies of indomethacin with α - and γ - CD resulting in an increase of solubility of non-steroidal anti-inflammatory drug (NSAID)⁸³.

In 2010, the group of Li reported the interaction between α -, β -, γ - CDs and two surfactant ILs 1-butyl-3-methyimidazolium tetrafluoroborate ([Bmim]BF₄) and 1-octyl-3-methyimidazolium tetrafluoroborate ([Omim]BF₄)⁸⁴. The measurements based on titration microcalorimetry, UV and NMR spectra, which were analyzed in terms of hydrophobic interactions between CD cavity with alkyl chain of IL cationic unit. The calorimetric studies confirmed that the stoichiometry of CDs and the two ILs was 1:1 and 1:2 except that α - CDs with [Omim]BF₄, which was only 1:1. ¹H NMR spectra showed the chemical shift data of all the CDs protons, proving the formation of inclusion complexes.

As it was mentioned before, CDs have been successfully applied for different chromatographic methods such as High Performance Liquid Chromatography (HPLC), Gas Chromatography (GC) and Capillary Electrophoresis (CE) for enantioseparation of racemic compounds^{85,86}. Modified CDs represent the leading type of chiral selectors for gas chromatography. They can be layered either as neat chiral stationary phases (CSPs), if they are viscous liquids at ambient temperatures, or as cyclodextrin-solvent mixtures if they have higher melting points and exist as solids at room temperatures.

On the other hand, ILs have been developed as a significant new class of GC stationary phase materials over the last few years^{87, 88}. In 2001 Armstrong and coworkers reported the use of achiral ionic liquids as stationary phase solvents for derivatized cyclodextrins⁸⁹. More recently, a study on ionic cyclodextrins in ionic liquid matrices as chiral stationary phases for gas chromatography (GC) resulted in a new ionic liquid-based stationary phase with broader enantioselectivities and higher thermal stabilities⁹⁰. This work was also presented by Armstrong

group that developed the first synthetic protocols for new class of ultra-high stability ILs⁹¹. In this paper, the authors used permethylated- β -cyclodextrins (BPM) and dimethylated- β -cyclodextrins (BDM) dissolved in 1-butyl-3-methylimidazolium chloride ([Bmim]Cl) and the column performances were evaluated against those of analogous polysiloxane-based commercial columns (Chiraldex BPM and Chiraldex BDM). It was proved that the IL-based column efficiencies were up to 10 times higher than the commercial columns.

Pereira and coworkers also developed the first room temperature ionic liquids (RTILs) derived from α - and β - CDs, the permethylated mono-6-deoxy-6-pyridin-1-ium and mono-6-deoxy-6(1-vinyl-1-H-imidazol-3-ium) α - and β - CDs trifluoromethanesulfonates at room temperature under solvent free conditions in low to moderate yields (34-71%)⁹². These new ILs were studied as stationary phases in capillary GC columns towards chiral discrimination in enantio-GC-analysis of racemic mixtures. This method resulted in good enantiomeric separation of some racemic lactones, esters and epoxides which were not achieved by using a common CD column (Figure I.12).

With the high number of ILs and variety of ionic cyclodextrin structures available nowadays, these types of Cyclodextrin Chiral Stationary Phases (CD-CSPs) offer a new avenue of potentially functional and interesting research and development.

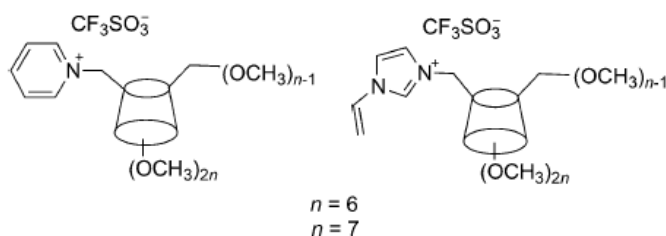


Figure I.11 - The first RTILs derived from α - and β - CDs, the permethylated mono-6-deoxy-6-pyridin-1-ium and mono-6-deoxy-6(1-vinyl-1-H-imidazol-3-ium) α - and β - CDs trifluoromethanesulfonates.

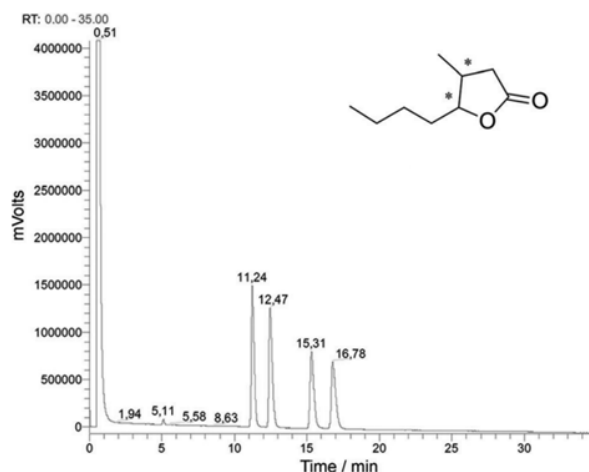


Figure I.12 - Separation of the four enantiomers of whiskey lactone in a sample solution using novel RTILs derived from CDs⁹².

I.3. Nucleobases

I.3.1. Nucleobases-Introduction, structure, properties

It was just 70 years ago discovered that DNA was the genetic material – the master draft of life⁹³. Since that time, nucleoside chemistry is a dynamic area of research both in industry and academia. Consequently, the nucleic acids DNA and RNA, which play an important role in storing genetic information and in protein biosynthesis, have been precisely studied and their properties are now a key factor in the education of both biologists and chemists⁹⁴. In fact, the double helical structure of DNA has grown to be a symbol of our time, appearing widely not only in the scientific literature, but also in the well-liked press and most recently as jewelry. Nucleoside derivatives have found wide-ranging application in agrochemistry (herbicides, fungicides, insecticides), biotechnology (e.g. DNA sequencing) and biology⁹³. Their chemistry defines a significant area of research for drug discovery related with cancer and viral chemotherapy, such as human immunodeficiency (HIV), herpes simplex virus (HSV) and hepatitis B virus (HBV)^{95,96,97}. According to this, the aim of this subchapter is to highlight the nucleosides chemistry that influences different pathways and ordered the structure and properties for living cells and organisms.

Nucleobases are the parts of Nucleic Acids (DNA, *deoxyribonucleic acid* and RNA, *ribonucleic acid*) that are involved in pairing, according to the Watson-Crick model⁹⁸.

Nucleoside is defined as the system of a base covalently bound to the 1' carbon of a ribose or deoxyribose and a nucleoside with one or more phosphate groups attached at the 5' carbon is

called a nucleotide⁹³. They involve the structural units of RNA and DNA. The structural elements of the most common nucleotides are presented in the Figure I.13.

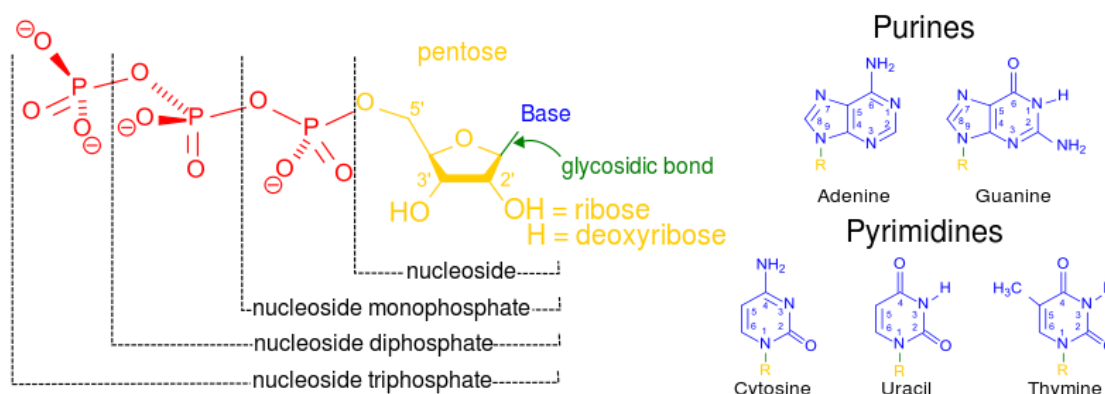


Figure I.13 - Structural unit of common nucleotides.

All nucleotides are made from three elements: a nitrogen heterocyclic base, a pentose sugar and a phosphate residue. The main bases are monocyclic pyrimidines or bicyclic purines. The major purines are adenine (A) and guanine (G) and are found in both DNA and RNA. Those bases and their corresponding nucleosides are described in Table I.2. The major pyrimidines are cytosine (C), thymine (T) and uracil (U). The simplest nucleotides, being the phosphate esters of nucleosides, have one of the hydroxyl groups of the pentose esterified by a single phosphate monoester function. Adenosine 5'-phosphate is a 5'-ribonucleotide, also called adenylic acid and abbreviated to AMP (Figure I.14). Nucleotides containing two phosphate monoesters on the same sugar are called nucleoside bisphosphates while nucleoside monoesters of pyrophosphoric acid are known as nucleoside diphosphates. Furthermore, nucleoside esters of tripolyphosphoric acid are nucleoside triphosphates with the classic example of adenosine 5'-triphosphate (ATP).

Table I.2 - Bases and their corresponding nucleosides.

Abbr.	Base	Nucleoside	Nucleic Acid
A	Adenine	deoxyadenosine	DNA
		adenosine	RNA
G	Guanine	deoxyguanosine	DNA
		guanosine	RNA
C	Cytosine	deoxycytidine	DNA
		cytidine	RNA
T	Thymine	deoxythymidine (thymidine)	DNA
U	Uracil	uridine	RNA

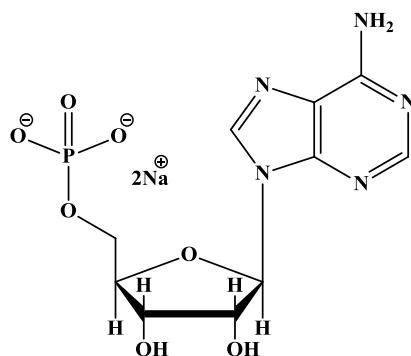


Figure I.14 - Structure of adenosine 5'-phosphate (AMP) sodium salt in the state of ionization observed at neutral pH.

Nucleic acids are soluble in water up to about 1% w/v according to size and they are precipitated by the addition of alcohol, due to their polyionic character. One of the most important physical characteristic of a nucleotide is its acid–base behavior. It keeps a tautomeric structure, its charge, and thus its ability to donate and accept hydrogen bonds. Apparently, all of the bases are uncharged in the physiological range $5 < \text{pH} < 9$. The same applies for the pentoses, where the ribose 2', 3'- diol loses a proton above pH 12. The nucleotide phosphates lose one proton at pH 1 and a second proton (in the case of monoesters) at pH 7. This model of proton equilibria is shown for AMP across the whole pH range (Figure I.15).

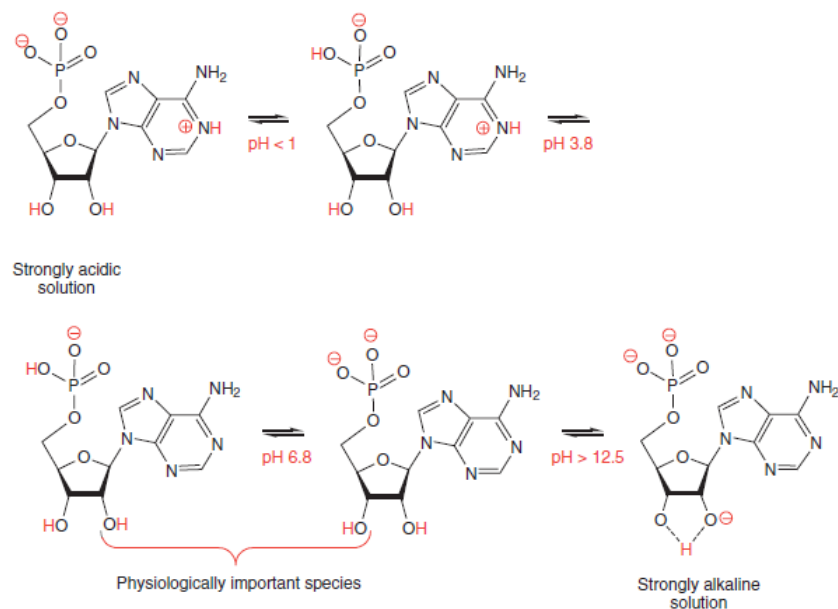


Figure I.15 - Protonation of adenosine 5'-phosphate (AMP) from strongly acidic solution (left) to strongly alkaline (right).

I.3.2. Interactions between ILs and nucleobases

Nucleosides are undeniably essential building blocks of biological systems with numerous applications. The widespread attention in nucleosides chemistry has motivated investigators to design efficient and practical synthetic routes for the development of nucleosides analogues. However, the development of new modified nucleosides presents a major drawback, which is related with their poor solubility in common organic solvents⁹⁹. Most of the common available methods use toxic high boiling solvents such as pyrimidine, *N,N*-dimethylformamide and *N*-methylpyrrolidone⁹⁹. Therefore, it is important to improve those methods using more environmentally benign media that could replace the harmful solvents and provide sufficient solubilization of nucleosides.

Previously discussed ILs, with the unique combination of their properties, are revolutionizing the world of solvents. Their tunable nature in the solubility of various compounds, including molecules of pharmaceutical and biological interest and its well known status of “green” alternatives for common solvent, confirmed that some not toxic ILs are excellent for dissolution of nucleobases (nucleic acids bases that from the structural units of DNA, RNA, nucleotides, and nucleosides).

Rebelo and coworkers investigated the dissolution mechanism of uracil, thymine, and adenine, in 1-ethyl-3-methylimidazolium ([C₂mim][AcO]) and 1-butyl-3-methylimidazolium acetate ([C₄mim][AcO]) ILs using NMR spectroscopy¹⁰⁰. The results proved that hydrogen bonds (HB) ruled the dissolution mechanism and that both cations and anions participate in the solvation process. The acetate anion influences the dissolution of nucleic acid bases into 1,3-dialkylimidazolium acetate ILs. Nevertheless, hydrogen bonding between nucleobases and the imidazolium cation also participated in the solubility process. The authors concluded that the ionic liquid must be a good hydrogen bond acceptor and a moderate hydrogen bond donor with a dissociation degree sufficiently high to dissolve the bases.

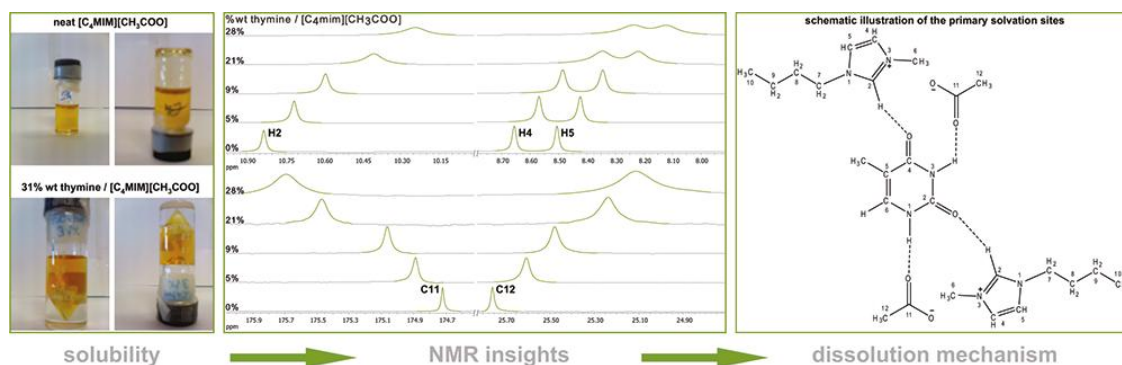


Figure I.16 - Studies on the dissolution mechanism of nucleobases in ILs¹⁰⁰.

It has been already reported in the literature that nucleobases, nucleosides, and nucleotides in biological fluids and herbal medicines can be separated and determined by numerous analytical methods, including immunoassays¹⁰¹, TLC¹⁰², HPLC¹⁰³, MEEKC¹⁰⁴ and many more. MEEKC is a powerful electrodriven separation technique with many applications in different disciplines, including environmental analysis, food analysis, pharmaceuticals analysis, partition coefficients study, bioanalysis and natural products analysis, due to its unique properties of microemulsion¹⁰⁵. According to this, in 2013, Li and coworkers simultaneously determined nucleobases, nucleosides and nucleotides using MEEKC method in the presence of IL 1-butyl-3-methylimidazolium hexafluorophosphate ([Bmim]PF₆) as oil phase¹⁰⁶. This particular IL has commonly been used as oil phase because of its strong hydrophobicity, which is related with the very chaotropic (able to interfere with the HB or van der Waals forces) counter-ion PF₆. The established method was successfully applied to obtain the contents of investigated compounds in three different widely used traditional Chinese medicines (cultured *Cordyceps sinensis*, *Radix Astragali*, and *Radix Isatidis*). Hence, the development of a MEEKC method with [Bmim]PF₆ as oil phase for simultaneous determination of nucleotides, nucleosides, and nucleobases should be the key for green analytical science, pharmaceutical analysis, and disease diagnosis.

CHAPTER II. L-cysteine based Ionic Liquids

II. Chiral Ionic Liquids based on cysteine derivatives

II.1. *Background*

The understanding of chiral biological molecules chemistry is a crucial role in new research fields⁵. Taking advantage of the relevance and natural chirality of these compounds, there is the possibility to use them for the preparation of bioinspired CILs¹⁰⁷. Applications of ILs include their use as chiral reaction media in many catalytic and non-catalytic synthetic methodologies and separation processes¹⁰⁸, including extractions with *sc*CO₂¹⁸ and their use as supporting liquid membranes¹⁰⁹. A transfer of chirality in these solvents should be expected, however only few CILs have been reported to date¹¹⁰. If in the past years the preparation of ILs was concentrated on obtaining unique physical-chemical properties (*1th Generation*), such as the absence of volatility or a high thermal stability, or a specific targeted behaviour (*2nd Generation*), now one of the main goal is the achieving of specific desirable biological features (*3th Generation*).

Many investigators have described the development of CILs mainly based on amino acids (AAs) and by the incorporation of chirality on cation, anion, or both units.

In this context, L-cysteine and its derivatives are interesting biological molecules with attractive properties for academia and industrial applications. In general, cysteine (Cys), mainly the L-enantiomer, is essential because of its prominent tasks in the food, pharmaceutical, and personal care industries¹¹¹. One of the biggest applications is related with the production of flavours. It is known that the reaction of cysteine with sugars in a Maillard reaction yields meat flavours¹¹². L-cysteine is also used as a processing aid for baking¹¹³. Cysteine derivatives are considered popular targets for site-directed labeling experiments to investigate biomolecular structure and dynamics.

In this context, we decided to develop novel CILs based on L-cysteine derivatives as cation or anion units, combined with appropriate counter-ions as described in Figure II.1. The development of efficient CILs is essential to expand the range of their applications.

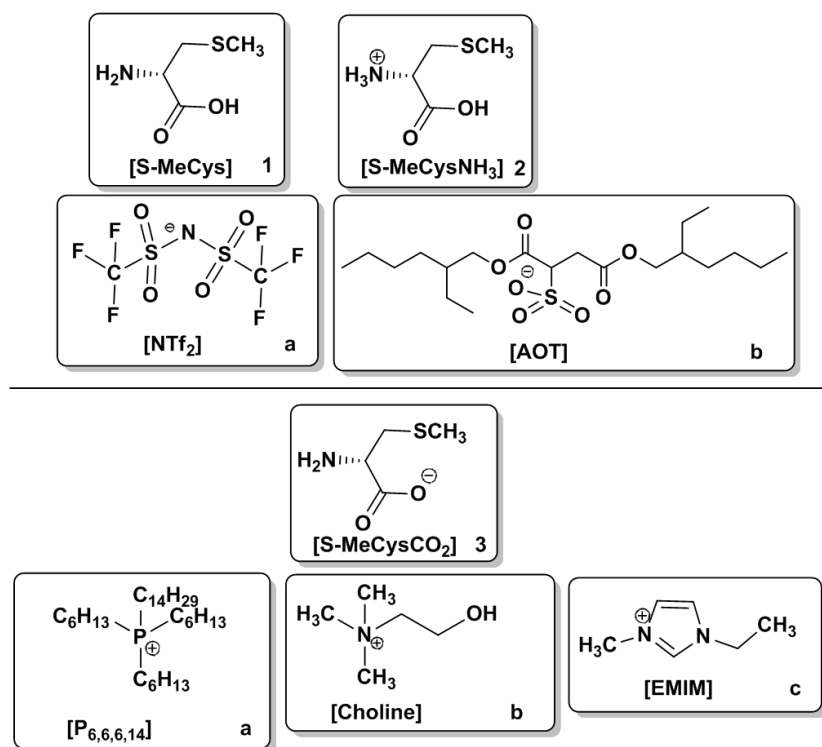
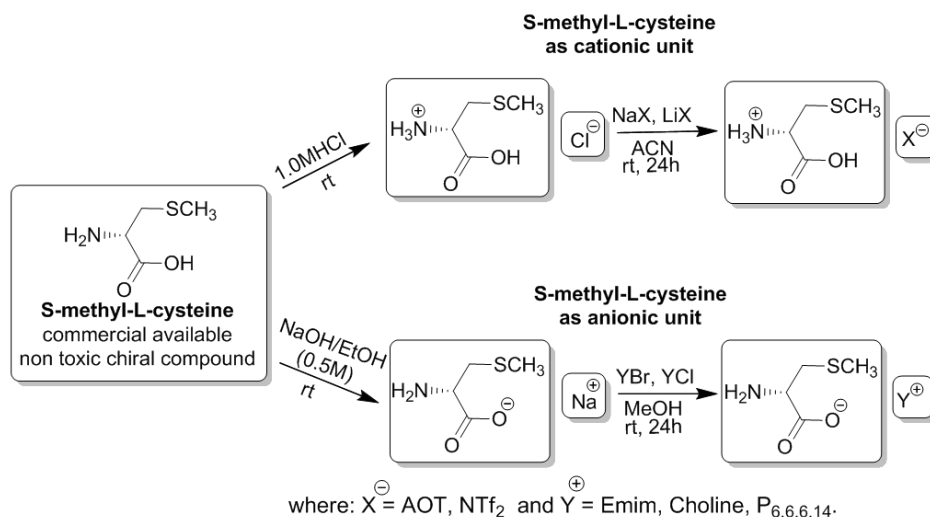


Figure II.1 - Structures of synthesized S-methyl-L-cysteine based CILs.

II.2. Synthesis of novel CILs based on S-methyl-L-cysteine

This work intended to develop an efficient and simple synthetic methodology for preparing CILs from natural amino acid derivatives. According to two different synthetic approaches, as described in Scheme II.1, novel S-methyl-L-cysteine based chiral ILs have been synthesized. The protonation of primary amine (NH_2) from S-methyl-L-cysteine scaffold was performed using hydrochloride acid in methanol solution. This correspondent chloride anion was then exchanged to more appropriate organic anions such as docusate ([AOT]) and bis(trifluoromethanesulfonyl)imide ([NTf₂]), in order to obtain room temperature CILs. Furthermore, the deprotonation of carboxylic acid from S-methyl-L-cysteine scaffold was carried out using sodium hydroxide in methanol solution. The resulting sodium salt was then exchanged to organic cations such as choline ([Choline]), 1-ethyl-3-methylimidazolium ([Emim]) and trihexyltetradecylphosphonium ([P_{6,6,6,14}]) structures, in order to obtain the desired CILs.

After optimizing the synthetic approach, CILs based on S-methyl-L-cysteine were obtained in moderate to high yields (69-92%) as well as high purities. For purity evaluation, the final water and halogen content was checked for each prepared CIL. For both parameters, it was considered a minimal quantity of 250 and 100 ppm, respectively.



Scheme II.1 - General strategies for the synthesis of CILs starting from S-methyl-L-cysteine.

All novel chiral ILs based on S-methyl-L-cysteine were completely characterized by 1H , ^{13}C and ^{19}F (in the case of NTf_2^- anion) NMR and elemental analysis (C, N, H), in order to check their structure, purity and chemical stability. The correct cation: anion (1:1) proportion could be also verified by 1H NMR except in the case of CIL with NTf_2^- anion. Figure II.2 and II.3 present the 1H NMR spectrum of 1-ethyl-3-methyl-1H-imidazol-3-ium (*S*)-2-amino-3-(methylthio)propanoate (**3c**) and (*S*)-1-carboxy-2-(methylthio)ethanaminium 1,4-bis((2-ethylhexyl)oxy)-1,4-dioxobutane-2-sulfonate (**2b**). The spectra clearly indicate the high purity (99%) and the correct proportion cation: anion (1:1.03) for both compounds respectively.

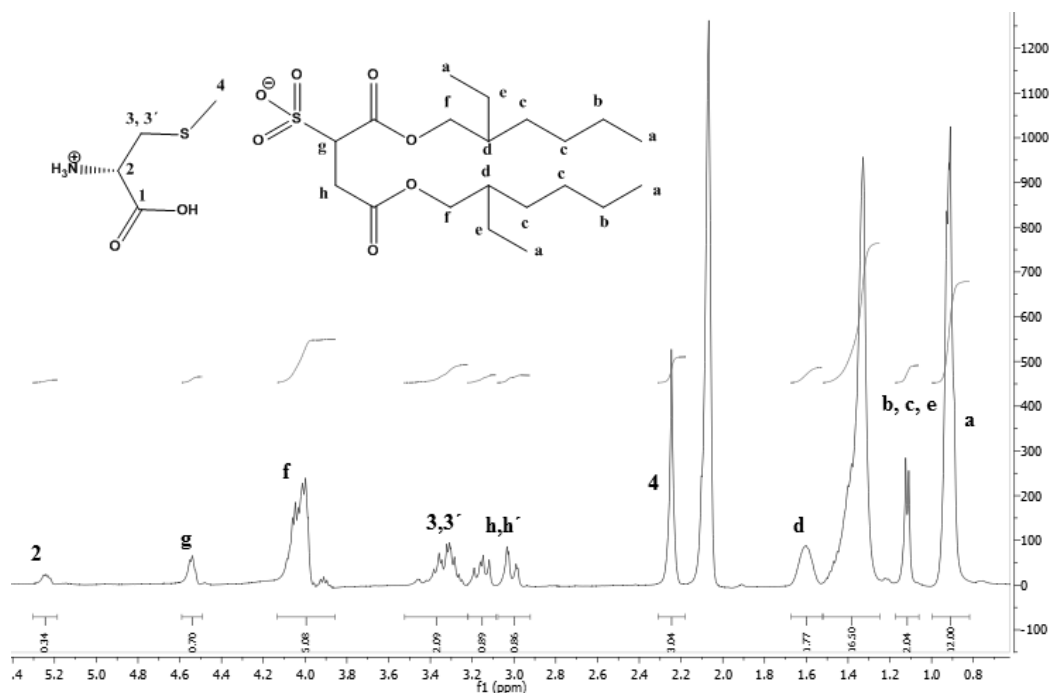


Figure II.2- 1H NMR spectrum of (*S*)-1-carboxy-2-(methylthio)ethanaminium 1,4-bis((2-ethylhexyl)oxy)-1,4-dioxobutane-2-sulfonate (2b**) performed in CD_3OD .**

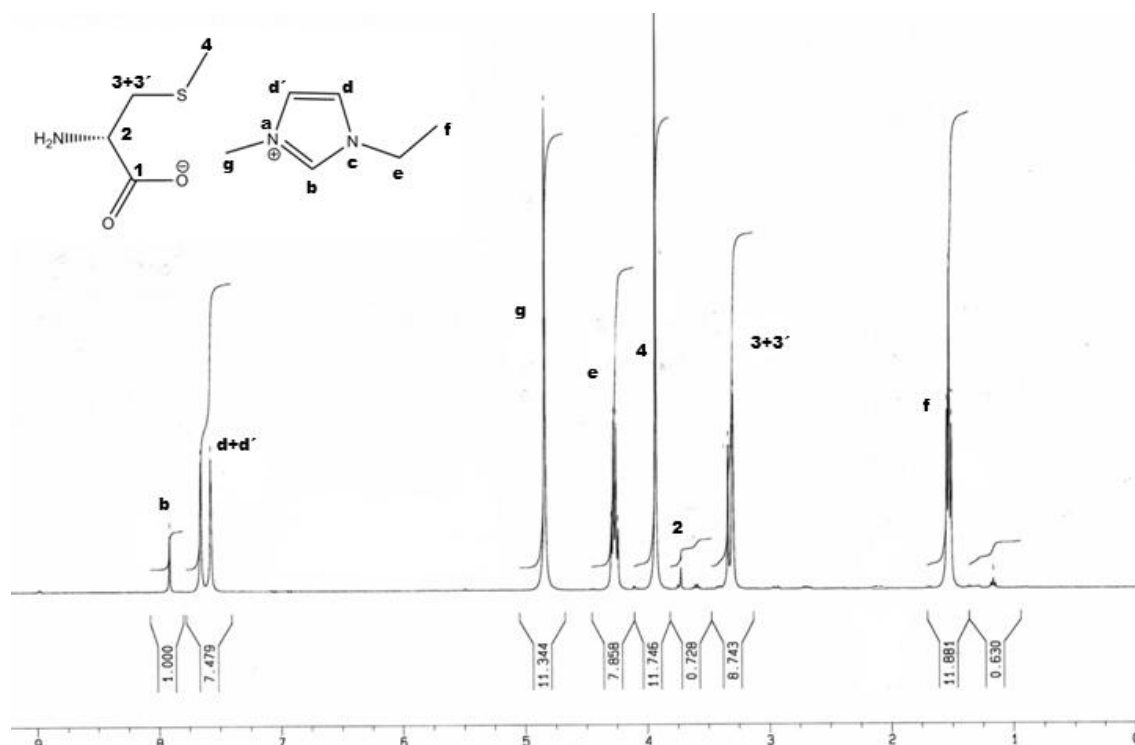


Figure II.3- ¹H NMR spectrum of -ethyl-3-methyl-1H-imidazol-3-ium (S)-2-amino-3-(methylthio)propanoate (3c) performed in CD₃OD.

Table II.1 summarizes the prepared CILs based on S-methyl-L-cysteine and some of their properties, such as optical rotation (α_D), solubility behaviour in water and common organic solvents, glass transition temperatures (T_g) and density (ρ) values. All CILs derived from S-methyl-L-cysteine were obtained as coloured viscous Room Temperature Ionic Liquids (RTILs). The colour of CILs changed according to the use of S-methyl-L-cysteine as a cation or anion and the type of counter-ions, between yellow, orange and brown viscous liquids (Figure II.4). The cation/anion interaction can justify the colour variation, when comparing with the initial white powder salts in the hydrochloride and sodium forms.

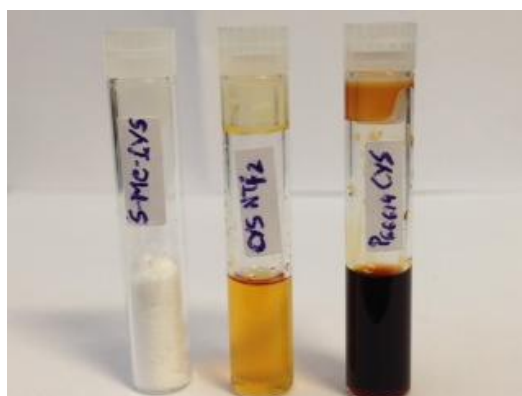


Figure II.4 - Photos of starting material S-methyl-L-cysteine and samples of synthesized ILs with the amino acid derivative either as cation (2a) or anion (3a).

Table II.1 Physical state, density, optical rotation, solubility and thermal properties of prepared S-methyl-L-cysteine based CILs.

CIL	Physical state	T_g [°C] ^[a]	Density ^[b] [g cm ⁻³]	α_D ^[c] [cm ² g ⁻¹]	Solubility ^[d]	
					Miscible	Immiscible
1	white powder	>240 (dec.)	---	+4.8±2°	H ₂ O, <i>i</i> -PrOH	ACN, Ac, DCM, hex, AcOEt, Et ₂ O
2a	orange liquid	-74.63	1.67	+3.0±2°	<i>i</i> -PrOH, ACN, Ac, DCM, AcOEt	H ₂ O, hex, Et ₂ O
2b	brown liquid	-- ^[e]	1.32	+6.0±2°	<i>i</i> -PrOH, ACN, Ac, DCM, AcOEt, Et ₂ O (pm)	H ₂ O, hex
3a	yellow liquid	-107.12	0.93	+6.0±2°	<i>i</i> -PrOH, ACN, Ac, DCM, AcOEt, Et ₂ O (pm)	H ₂ O, hex
3b	brown liquid	-56.11	0.98	+14.0±2°	H ₂ O, <i>i</i> -PrOH, ACN, Ac, DCM, AcOEt, Et ₂ O (pm)	hex
3c	brown liquid	-73.06	1.22	+12.0±2°	<i>i</i> -PrOH, ACN, Ac, DCM, AcOEt	H ₂ O, hex, Et ₂ O

^[a] Glass transition temperature (T_g) was determined by DSC measurements at a heating/cooling rate of 10 °C.min⁻¹ for all ILs. ^[b] Density was measured by pycnometer at room temperature. ^[c] Optical rotation values measured in ACN (1 mg/mL) by polarimetry at 20 °C. ^[d] Observed complete solubilization (miscible), partial solubilization (pm) or non-solubilization (immiscible) by adding solvent to a small amount of ionic liquid, *i*-PrOH (*i*-propanol), Ac (acetone), ACN (acetonitrile), hex (*n*-hexane), Et₂O (diethyl ether), DCM (dichloromethane) and AcOEt (ethyl acetate). ^[e] Not observed by DSC studies.

II.3. Thermal properties of novel CILs based on S-methyl-L-cysteine

All different CILs were studied by DSC measurements at heating/cooling rate of 10 °C.min⁻¹, in order to evaluate their thermal properties, in particular the characteristic glass transition temperature (T_g) values. Commercial S-methyl-L-cysteine, **1**, as a crystalline solid with higher melting point (T_m = 240 °C, decomposes), can be transformed in amorphous salts by a simple combination with appropriate counter-ions. Generally, the melting point of amino acids, including L-cysteine derivatives, is also their decomposition temperatures. In the case of novel CILs based on L-cysteine derivatives, it is possible to avoid the characteristic crystallization as well as take advantage of their room temperature liquid states. Glass transition temperatures were observed for all examples except in the case of [S-Me(Cys)NH₃][AOT], **2b**. The influence of the selected counter-ion in the T_g values is clearly observed for the examples where cysteine is combined as anion. [P_{6,6,6,14}], **3a**, cation decreases significantly the T_g value when compared with [choline], **3b**, or [Emim], **3c**, cations. [Emim][S-Me(Cys)CO₂], **3c**, and [S-Me(Cys)NH₃][NTf₂], **2a** showed similar T_g values, comparable with some values already reported in the literature. The detailed DSC spectra are attached in annex.

II.4. *Physical properties of novel CILs based on S-methyl-L-cysteine*

Optical rotation values in acetonitrile solution for all CILs and neutral S-methyl-L-cysteine were measured (1 mg.mL^{-1}) by polarimetry at 20°C . In the case of CILs **2a**, **2b** and **3a**, similar optical rotations to **1** were obtained. In contrast, a significant increase in the optical rotations for CILs **3b** and **3c** were observed. This difference can be explained by a stronger interaction between [Choline] and [Emim] cations with S-methyl-L-cysteine anion. In particular, the hydrogen bonding formation between OH group of choline cation, or H-2 acidic proton of imidazolium cation, with carboxylic group from cysteine derivative anion, is expected.

Density measurements were performed with the use of pycnometer at room temperature (25°C). The higher density values were obtained for CILs **2a**, **2b** and **3c** due to the presence of [NTf₂] or [AOT] anion and imidazolium cation respectively. As expected, the presence of ammonium or phosphonium cation contributed to density values lower than 1 g.cm^{-3} .

Solubility profiles of novel CILs were studied in water and different classes of common organic solvents, such as alcohols (methanol, ethanol and *i*-propanol); alkane (*n*-hexane); ether (diethyl ether); ketone (acetone); ester (ethyl acetate); dichloromethane and acetonitrile. Three novel CILs showed water immiscible behaviour, when compared with the initial water miscible S-methyl-L-cysteine, **1**. The combination of cysteine derivative with more hydrophobic counter-ions changes significantly the final water solubility profile. In general, all novel CILs are completely soluble in alcohols, acetone, acetonitrile and ethyl acetate but insoluble in *n*-hexane and diethyl ether. In the case of CILs **2b**, **3a** and **3b**, a partial miscibility in diethyl ether was observed.

According with the interest, it is possible to improve the initial cysteine derivative solubility (water and alcohols) by a simple combination with appropriate counter-ions. The possibility to tune the final solubility of cysteine derivative salts can be relevant for applications in asymmetric catalysis or chiral resolution.

II.5. *NMR interaction study*

Many studies have been performed to examine the structure and interactions of ILs, by using different approaches¹¹⁴. ILs are rather unique in the sense that in addition to the interactions existing in common organic solvents (hydrogen bonding, dipole–dipole and van der Waals interactions) ILs have other interactions, such as strong electrostatic interactions. ILs are

constituted only by ions and thus experience strong cation-anion interactions that yield long-lived association of ions¹¹⁵. Some authors suggested that cations and anions are held together through hydrogen bonding and others consider its relevance minor compared with the role of electrostatic interactions.

The nature of the forces in different ILs may differ from another and mainly control their physical and chemical properties. As it was mentioned before, all CILs based on crystalline S-methyl-L-cysteine were obtained as coloured viscous RTILs. This change of colour obviously indicates different interactions between the ions. NMR data allows extracting information on existence and strength of H-bondings present between cation and anion in ILs. Therefore, ¹H NMR spectroscopy has been used to determine the degree of cation-anion interactions of S-methyl-L-cysteine based ionic liquids. In particular, the [S-Me(Cys)NH₃][AOT] scaffold, **2b**, is presented in this subsection. Figure II.5 shows ¹H NMR spectra of **2b**, with variation of temperature (in DMSO as deuterated solvent due to its high boiling point). The CH₂ peaks close to the ion charge, both from the cationic cysteine moiety (3, 3') and the docusate anion (h, h') increase in higher temperature (facilitate the rotation of molecules). It seems that increase of temperature from 25 °C up to 70 °C (hence decrease of viscosity), facilitates the cation-anion interaction near the ion charge. These observations could be confirmed by using two-dimensional nuclear magnetic resonance spectroscopy (2D NMR). ¹H and ¹³C NMR of [S-Me(Cys)NH₃][AOT] spectra are included in the annex chapter (Figure VII.1).

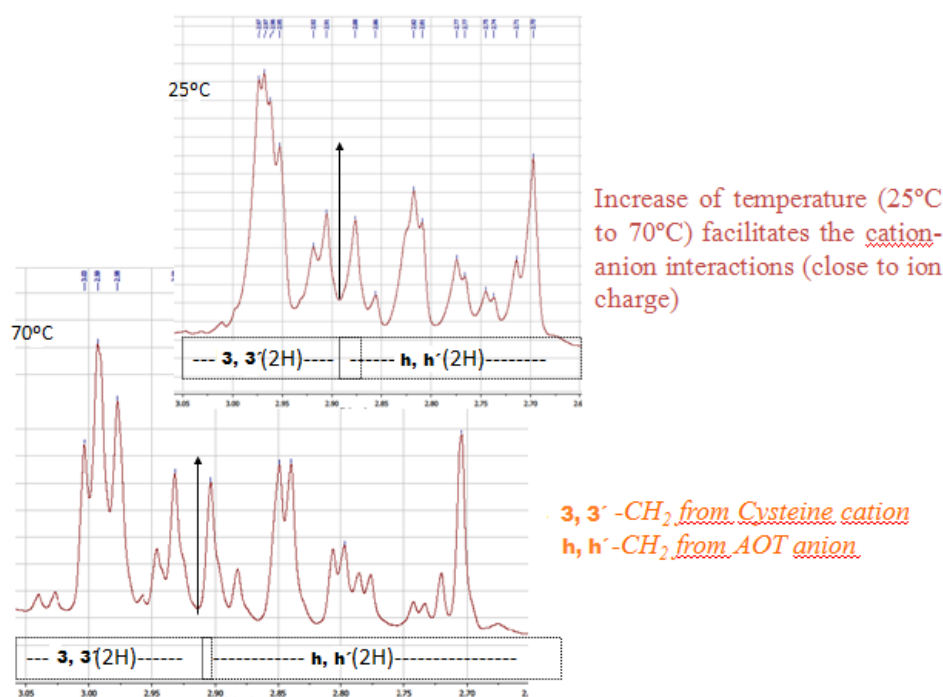


Figure II.5 - ¹H NMR spectra of [S-Me-Cys][AOT] performed in different temperatures.

In summary, cation- anion interactions have been studied to obtain a further understanding of the behavior of ILs that could expand their future applications such as chiral recognition. Many experimental and theoretical works from literature indicate strong cation- anion interactions through the interplay of hydrogen bond and Coulombic forces. Nevertheless, the relative importance of hydrogen bond and Coulombic forces in cation-anion interactions is still under discussion.

II.6. *Application of S-Me-L-cysteine based ILs for enantiomeric resolution*

Chiral analysis continues to play a crucial role in science and engineering. There are many compounds which have enantiomeric forms with different physiological and therapeutic effects⁵⁰. Generally, one enantiomer is pharmacologically active, while the other may be inactive or limit the effect of the desired form and/or be highly toxic. Single enantiomers of chiral drugs are continuously receiving more attention in the pharmaceutical industry. Therefore, the optimization of purification processes of enantiomeric pairs has become highly desirable. Many different chiral shift reagents (e.g. cyclodextrins, antibodies, antibiotics, crown ethers) have been proposed for enantiomeric recognition. More recently, the potential of CILs to be applied as NMR chiral shift reagents in spectroscopy has enjoyed considerable attention. In contrast to most of the chiral selectors, relatively simple to prepare, CILs show discrimination through the solvating power of ionic liquids¹¹⁶. Thus, the multiple solvation interactions may minimize solubility problems. In addition, CILs don't have the need to include the analyte into the selector's cavity to provide discrimination, thus adding to their universality.

The first example of the application of CILs in NMR spectroscopy was described in 2002 by Wasserscheid and his coworkers, who studied the interionic diastereomeric interactions between the enantiopure CIL and a racemic substrate monitoring the ¹⁹F NMR spectroscopy. In contrast to most of the chiral selectors, relatively simple to prepare, CILs show discrimination through the solvating power of ionic liquids¹¹⁶. Thus, the multiple solvation interactions may minimize solubility problems. In addition, CILs don't have the need to include the analyte into the selector's cavity to provide discrimination, thus adding to their universality.

In 2006, Jurcik et al. observed the diastereomeric interactions between a bis-imidazolinium salt containing an aromatic substituent at the C-2 position of the imidazolinic group and PF₆ counter anions with Mosher's carboxylate¹⁵. The splitting of both proton and fluorine signals of Mosher's carboxylate has been shown. In addition, while using a borate anion B[C₆H₃(CF₃)₂]₄ instead of PF₆, no ¹H NMR splitting and smaller chemical shift difference of fluorine signals in the ¹⁹F NMR were detected.

Malhotra and co-workers studied the use of a series of isomannide-based CILs for chiral discrimination in NMR¹¹⁷. Lindeman and coworkers showed the enantiomeric recognition using CILs based on chiral anions¹¹⁸. It was found that stronger chiral discrimination was given for anions with a relatively larger substituent group (e.g., phenylmethyl group, that led to better recognition compared to that with a phenyl group or the weakest isobutyl group). Their studies were performed by analyzing NMR spectra of CILs composed of chiral anions and a racemic 1-methyl-3-(2-methyl-butyl)imidazolium cation. In 2011, De Rooy et al. studied the interionic diastereomeric interactions between the enantiopure CIL and a racemic substrate monitoring the ¹⁹F NMR spectroscopy in the presence of crown ether¹¹⁹. A CIL based on ephedrine and racemic Mosher's acid sodium salt in deuterated CDCl₃, provide splitting of the CF₃-fluorine signal in ¹⁹F NMR as indicated in Figure II.6. All these efforts showed that these CILs may be attractive candidates for many applications in chemical synthesis and separation science.

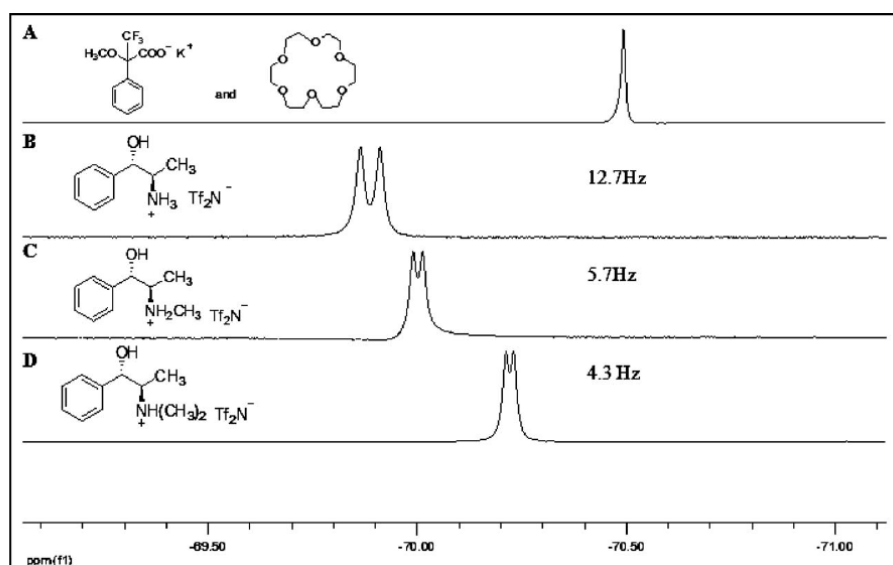


Figure II.6 - ¹⁹F-NMR (CDCl₃) spectra of potassium Mosher's salt (A), potassium Mosher's salt with (1S,2R)-NorHEph[NTf₂] as chiral selector (B), potassium Mosher's salt with (1S,2R)-HEphNTf₂ as chiral selector (C), and potassium Mosher's salt with (1S,2R)-MeHEph [NTf₂] as chiral selector (D)¹¹⁹.

In order to estimate the potential of our CILs based on S-methyl-L-cysteine, as chiral shift reagents for enantiomeric resolution, we studied the influence of the addition of CILs **3b** and **3c** (10 mol%) to racemic Mosher's acid sodium salt in deuterated DMSO. For both cases a splitting of the CF₃-fluorine signal in ¹⁹F NMR spectra was observed as indicated in Figure II.7 (for the case of CIL [Choline][S-Me(Cys)NH₃], **3b**). No influence in the case of original S-methyl-L-cysteine, **1**, addition was observed. In the case of other CILs no significant influence was also observed. It should be stated that no additional crown ether was needed in our studies.

In general, the chemical shift difference of fluorine signals in the ^{19}F NMR spectra, as well as an effective enantiomeric resolution of racemic Mosher salt, was achieved by the simple addition of a small quantity of selected CILs. The chiral separation was 4 Hz using 10 mol% of CILs. According to the quantity of CILs an improvement of this value is expected.

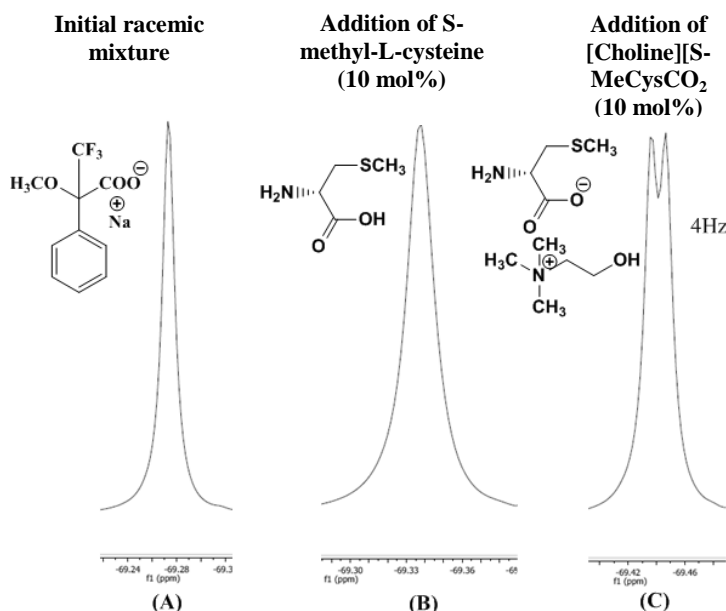
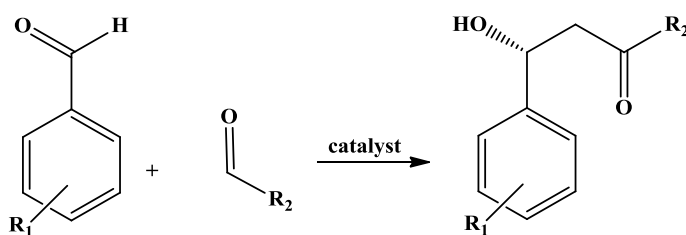


Figure II.7 - ^{19}F NMR (DMSO) spectra of initial Mosher's sodium salt (A), Mosher's sodium salt with S-methyl-L-cysteine as chiral selector (B) and [Choline][S-MeCysCO₂] as chiral selector (C).

II.7. Application of S-Me-L-cysteine based ILs for asymmetric aldol reaction

Asymmetric aldol reaction is largely studied in formation of C-C bonds as well as introducing chirality in organic synthesis¹²⁰. The discovery of novel catalysts which exhibit high activity and discriminating selectivity is a major focus of current research in the field of asymmetric synthesis. The use of CILs instead of common metallic organocatalysts led to overcome the complications related with the price, quantities and often toxicity of metals and the use of highly polar solvents like DMSO which make the reaction work-up and the recycling of catalyst impossible. In this context, the use of organocatalysis based on chiral small organic molecules has become a highly active area of research, with many opportunities to discover new reactions and their application in asymmetric synthesis. The aldol reaction is one of the most relevant carbon-carbon bond forming reactions for the preparation of small optically-active molecules (Scheme II.2).



Scheme II.2 - General asymmetric aldol reaction between aldehydes and ketones.

Hajos and Parrish first described the use of L-proline as the organocatalyst for aldol reaction¹²¹. Then, several examples involving proline and its derivatives confirmed their efficiency as catalysts for stereoselective organic reactions. Nevertheless, these approaches show some limitations such as the use of environmentally unfriendly solvents as DMF or DMSO as well as the difficulties of recycling large quantities of catalysts. In the last years, several groups studied the direct asymmetric aldol reaction catalyzed by hydrophobic proline derivatives in the presence of water.

The original proposed mechanism for the proline-catalyzed intermolecular aldol reaction was based on the launched class I aldolase-mechanism that includes carbinolamine, imine or iminium, and enamine intermediates¹²². The catalytically active functional groups in class-I aldolases, are an ϵ - amino group of a lysine residue and depending on the enzyme subtype, a set of Brønsted cocatalysts needed for the various proton-transfers of the multi-step reaction mechanism. In the proline-catalyzed case, the catalytic amine is proline's pyrrolidine. The carboxylate could function as multi-purpose Brønsted cocatalysts for the proton transfer (Scheme II.3)¹²³. The enantioselectivity was explained with a transition state (TS)- (**A**) that can be described as a metal free version of the common Zimmermann-Traxler model (**B**)¹²⁴, which justifies the stereoselectivity of metal enolate aldol reaction. Despite this, it is known that an N-H hydrogen bond does not lower the energy of a TS and model **A** has been advanced to model **C**¹²³, which is suitable with the calculated TS of the proline-catalyzed intermolecular aldol reaction.

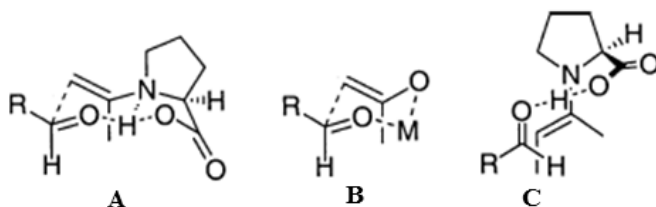
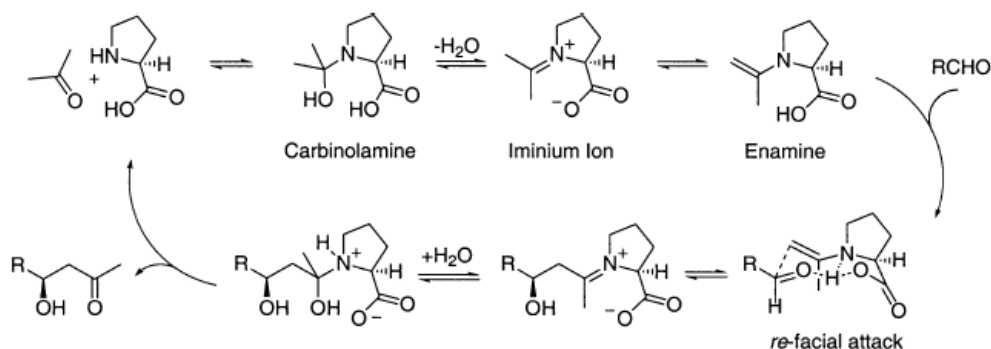


Figure II.8 - Transition states (TS)¹²³.



Scheme II.3 - The original proposed mechanism of proline-catalyzed intermolecular aldol reaction. Proline acts through enamine catalysis. Enamine is formed from the pyrrolidine nitrogen and the carbonyl donor. Iminium ion, created by attack of the enamine on the *re*-face of the aldehyde, is then hydrolyzed to give chiral β-hydroxyketone¹²³.

Miao and Chan reported the development of IL-anchored L-proline as an efficient and reusable catalyst for direct asymmetric aldol reaction³⁹. The prepared ILs combined with the chiral precursor in neat ketone reaction systems, showed higher catalytic activities than proline itself and made it possible to avoid the use of DMSO or DMF as a solvent for the reaction. In the same line, some L-proline and pyrrolidinium derivatives based CILs have been presented¹²⁵.

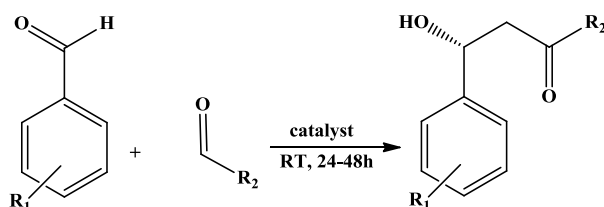
Yang et al. concluded that other amino acids such as threonine and serine derivatives are highly efficient organocatalysts for the asymmetric aldol reactions in aqueous media¹²⁶. The same authors described some novel cysteine, serine, and threonine based organocatalysts with the intention of creating a practical large scale process for asymmetric aldol reactions. The performed experiments showed that natural cysteine, serine and threonine are ineffective organocatalysts in water, but at the same time all new synthesized CILs derived from these amino acids, catalyzed the asymmetric direct aldol reaction of 4-nitrobenzaldehyde and cyclohexanone to give the desired product in good yields and enantiomeric excesses¹²⁷.

As it was presented in the previous paragraphs, the state of research concerning asymmetric aldol reactions with CILs based on small natural molecules as catalysts has been growing. Inspired by the work described in the literature, we studied the application of S-methyl-L-cysteine CILs previously synthesized and characterized, as chiral organocatalysts for asymmetric aldol reaction.

The model reaction was carried out in neat ketone reaction system using acetone or in water using cyclohexanone as ketones with 2- or 4-nitrobenzaldehyde in the presence of 10 to 20 mol% of catalyst, to find the optimum reaction conditions. Table II.2 summarizes the different yields and enantiomeric excesses of tested asymmetric aldol reactions. The initial investigation

confirmed that L-proline is an effective organocatalyst for asymmetric aldol reactions (Table II.2, Entries 1 and 2). However, novel chiral RTILs, essentially [S-MeCysNH₃][NTf₂], **2a**, catalyzed the asymmetric direct aldol reaction of 2- or 4-nitrobenzaldehyde and cyclohexanone to give the *anti* aldol product in moderate yields (70-79%), with the indicated range of *ee* values (53–90% *ee* for *anti*, Table II.2, Entries 5, 6, 16 and 17). Although longer reaction times were required in comparison with cyclic ketones, satisfactory results were obtained. As it was expected, in contrast with the *o*-NO₂ substituent group, the *p*-NO₂ substituent group gave higher yields as well as higher *ee* values. [Choline][S-MeCysCO₂], **3b**, and [Emim][S-MeCysCO₂], **3c**, showed a moderate performance in the case of acetone and 2 or 4-nitrobenzaldehyde (40% of yield and 66% of *ee* for **3b** and 77% yield with 68% *ee* in the case of **3c**) as model substrates.

Table II.2 Asymmetric aldol reaction using acetone or cyclohexanone with 2 or 4-nitrobenzaldehyde as model compounds and chiral RTILs based on S-protected-L-cysteine as organocatalysts.



where R₁ = *ortho*- or *para*-nitrobenzaldehyde
R₂ = acetone or cyclohexanone

Entry	Ketone/Benzaldehyde ^[a]	Catalyst ^[b]	Yield [%] ^[c]	<i>dr</i> (<i>anti</i> : <i>syn</i>) ^[d]	<i>ee</i> % ^[e]
1	Acetone/2-Nitro	L-PRO	85	--	89
2	Acetone/4-Nitro	L-PRO	90	--	91
3	Acetone/2-Nitro	L-CYS	no reaction	--	--
4	Acetone/4-Nitro	L-CYS	no reaction	--	--
5	Acetone/2-Nitro	2a	70	--	53
6	Acetone/4-Nitro	2a	79	--	70
7	Acetone/2-Nitro	2b	42	--	37
8	Acetone/2-Nitro	3a	no reaction	--	--
9	Acetone/2-Nitro	3b	40	--	66
10	Acetone/4-Nitro	3c	77	--	68
11	Acetone/2-Nitro	5a	no reaction	--	--
12	Cyclohexanone/2-Nitro	L-PRO	63	94:6	76
13	Cyclohexanone/4-Nitro	L-PRO	68	98:2	84
14	Cyclohexanone/2-Nitro	L-CYS	no reaction	--	--
15	Cyclohexanone/4-Nitro	L-CYS	no reaction	--	--
16	Cyclohexanone/2-Nitro	2a	63	89:11	88
17	Cyclohexanone/4-Nitro	2a	73	89:11	90
18	Cyclohexanone/2-Nitro	2b	no reaction	--	--
19	Cyclohexanone/2-Nitro	3c	no reaction	--	--
20	Cyclohexanone/2-Nitro	5a	21	91:9	n.d. ^[f]

^[a] Reaction conditions: acetone (2mmol) or cyclohexanone (1 mmol) in water (0.5ml) and 2 or 4-nitrobenzaldehyde (0.5 or 1 mmol) at room temperature, 24 h when acetone was used, 48 h when cyclohexanone. ^[b] Legend of Catalysts (20 mol% in the case of acetone examples and 10 mol% in the case of cyclohexanone examples) for : L-PRO- L-proline, 2a) [S-MeCysNH₃][NTf₂], 2b) [S-MeCysNH₃][AOT], 3a) [P_{6,6,6,14}][S-MeCysCO₂], 3b) [Choline][S-MeCysCO₂], 3c) [Emim][S-MeCysCO₂], 5a) [S-carboxyMeCysNH₃][NTf₂]. ^[c] Isolated yield. ^[d] *Anti*:*syn* diastereomers were determined from 400.13Hz ¹H NMR spectroscopy. ^[e] Enantiomeric excesses determined by ¹H NMR after use of chiral agent (Mosher's acid derivatives) and chiral HPLC analysis (AD-H column *i*-PrOH/hexane = 20:80; 0.5 mL.min⁻¹; 20 °C; λ = 254 nm). ^[f] n.d.: not determined.

With the optimal reaction condition at hand, we further studied the generality of the asymmetric direct aldol reaction of various substituted benzaldehydes in the presence of a catalyst: **L-proline** and **2a** as shown in Table II.3. It is important to note that changing the position of the substituent groups in benzaldehydes leads to different results. Thus, [S-MeCysNH₃][NTf₂], **2a**, in the case of 4-hydroxy-3-nitrobenzaldehyde, proved to be a better chiral catalyst than common L-proline (Table II.3, Entries 5, 6; 76% yield, 95% *ee*). This can be explained by the fact that electron-withdrawing groups enhance the electrophilicity of carbonyl carbons in aldehydes, which facilitates the reaction, while electron-donating groups reduce the electrophilicity. When 2-hydroxy-3-methoxy-5-nitrobenzaldehyde was used, similar results were obtained (Table II.3, Entries 10 and 11).

For all the cases using L-cysteine as organocatalyst no aldol product was observed. In the same line, other CILs based on S-methyl-L-cysteine have been tested without any efficiency to aldol reactions. Additionally, for this model reaction it was proved that the cysteine-based organocatalyst can be recovered and reused.

Table II.3 Studies on asymmetric aldol reactions with different aromatic benzaldehydes.

Entry ^[a]	Catalyst ^[b]	Ketone	Substituted benzaldehyde	Yield [%] ^[c]	dr (<i>anti</i> : <i>syn</i>) ^[d]	<i>ee</i> % ^[e]
1	1	Acetone	Benzaldehyde	68	--	84
2	2a	Acetone	Benzaldehyde	73	--	90
3	1	Cyclohexanone	Benzaldehyde	69	98:2	82
4	2a	Cyclohexanone	Benzaldehyde	70	90:10	85
5	L-PRO	Acetone	4-hydroxy-3-nitro	67	--	92
6	2a	Acetone	4-hydroxy-3-nitro	76	--	95
7	L-PRO	Acetone	2-hydroxy-5-nitro	70	--	95
8	2a	Acetone	2-hydroxy-5-nitro	58	--	96
9	L-PRO	Acetone	2-hydroxy-3-methoxy-5-nitro	41	--	94
10	2a	Acetone	2-hydroxy-3-methoxy-5-nitro	76	--	93

^[a] Reagents and conditions: ketone (1mmol), benzaldehyde or substituted benzaldehyde (0.5mmol), room temperature, 24h.

^[b] Legend of Catalysts (10 mol% loading) for: L-PRO- L-proline, 1) S-MeCys, 2a) [S-MeCysNH₃][NTf₂]. ^[c] Isolated yield.

^[d] *Anti*:*syn* diastereomers were determined from 400Hz ¹H NMR spectroscopy. ^[e] Enantiomeric excesses determined by ¹H NMR after use of chiral agent (Mosher's acid derivatives) and chiral HPLC analysis (AD-H column *i*-PrOH/hexane = 20:80; 0.5 mL.min⁻¹; 20 °C; λ = 254 nm).

II.8. Synthesis of novel CILs based on other L-cysteine derivatives

Due to the possibilities of applying amino acids (AA) as either cations or anions, because of their unique molecule structure and their close association with chirality and biomolecules, other L-cysteine derivatives were used for the development of novel CILs. In this context, additionally, four novel CILs were synthesized from L-cysteine ethyl ester hydrochloride and S-carboxymethyl-L-cysteine. Using a similar methodology as for the S-methyl-L-cysteine described before, it was possible to obtain the L-cysteine derivative scaffold as cation combined

with bis(trifluoromethanesulfonyl)imide ([NTf₂]) and docusate ([AOT]) as presented in Figure II.9. All four compounds were developed as RTILs with moderate to high yields (44-98%). Additionally, a complete characterization by ¹H, ¹³C and ¹⁹F (in the case of NTf₂ anion) NMR and elemental analysis (C, N, H), was performed in order to check their structure, purity and chemical stability. A chemical shift of the protons from protonated cysteine derivatives was observed (protons were more shielded). The proper cation: anion (1:1) proportion could be confirmed by ¹H NMR in the case of AOT anion. In relation with the water insoluble counter-ions chosen, all CILs were also water immiscible.

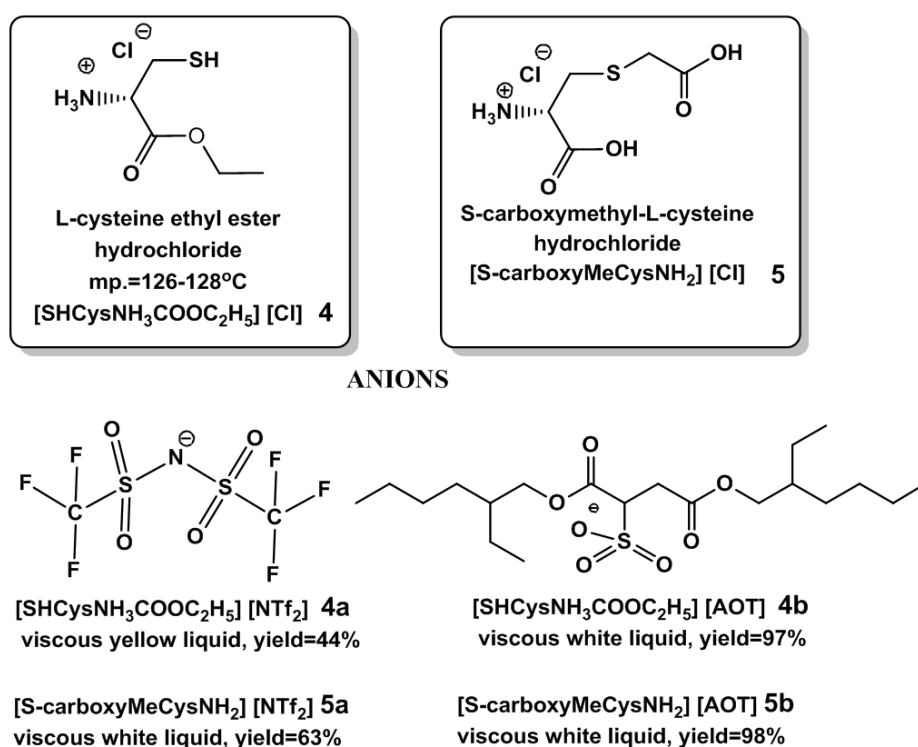


Figure II.9- Synthesis of CILs based on L-cysteine ethyl ester hydrochloride and S-carboxymethyl-L-cysteine.

After some main characterization of the prepared compounds, their further possible application as chiral organocatalysts for asymmetric aldol reaction was studied. In contrast to S-methyl-L-cysteine based CILs, these additionally synthesized CILs using other cysteine scaffolds didn't allowed to obtain good results. In all performed cases using the same conditions previously tested, no reaction occurred. This limitation in the case of L-cysteine ethyl ester is related with the tio-free group which throught dimmerization could form disulfides bound. L-cysteine with a not protected tio group causes problems with stability. Thus, this particular cysteine derivative may be used in acidic conditions but not in basic solutions.

II.9. *Conclusions*

Novel CILs based on S-methyl-L-cysteine as a cation or anion combined with appropriate counter-ions were developed. The optimized synthetic routes were appropriated in order to obtain the desired CILs in good yields and purities. No crystallization and glass transition temperatures were detected in the case of CILs, in contrast with initial S-methyl-L-cysteine.

With the use of cysteine derivative as a cation or anion and its combination with appropriate counter-ions, it was possible to adjust thermal (T_g) and physical (optical rotation, density and solubility profile in water and common organic solvents) properties of final CILs.

CILs [Choline][S-Me(Cys)CO₂] and [Emim][S-Me(Cys)CO₂] are the most promising examples as chiral shift reagents for enantiomeric resolution. The strong cation-anion interaction attributed to the H-bonding formation between OH group from choline or H-2 acidic proton from imidazolium ring, with the carboxylate group from cysteine anion, can justify the significant variation of their optical rotation as well as their effective use for chiral discrimination of racemic Mosher salt.

These novel CILs can open perspectives on their use for asymmetric catalytic reactions as chiral organocatalysts or chiral ligands and also for different chiral recognition processes in analytical chemistry or biological applications.

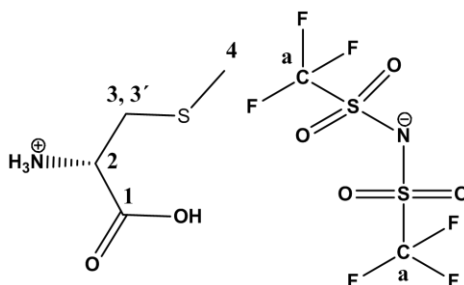
II.10. *Experimental Part*

General: Commercially available reagents S-methyl-L-cysteine (MW= 135.187 g.mol⁻¹, CAS No.187-84-4), L-cysteine ethyl ester hydrochloride (MW= 185.67 g.mol⁻¹, CAS No.868-59-7), S-carboxymethyl-L-cysteine (MW= 179.19 g.mol⁻¹, CAS No.638-23-3), 2-methoxy-2-(trifluoromethyl) phenylacetic acid-Mosher's acid (MW= 234.17 g.mol⁻¹, CAS No.17257-71-5), ionic liquids and solvents were purchased from Alfa Aesar, Aldrich, Solchemar and were used without further purification. ¹H and ¹³C NMR spectra were recorded at 25 °C on a Bruker AMX400 spectrometer with TMS as internal standard. Chemical shifts are reported downfield in parts per million (ppm). DSC analysis is carried out using a TA Instruments Q-series TM Q200 DSC with a refrigerated cooling system. The samples for elemental analysis were performed by Laboratório de Análises at REQUIMTE, Departamento de Química at Faculdade de Ciências e Tecnologia (Monte da Caparica), using Thermo Finnigan-CE Instruments

equipment, model Elementar Analyser 1112 series. Optical rotations were recorded on a Perkin Elmer 241MC. Density measurements were performed with the use of pycnometer at room temperature (25 °C).

II.10.1.Synthesis of (S)-1-carboxy-2-(methylthio)ethanaminium bis((trifluoromethyl)sulfonyl)amide (2a)

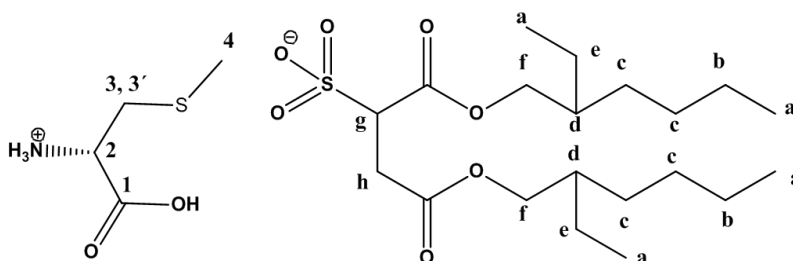
S-methyl-L-cysteine (0.5 g; 3.69 mmol) was dissolved in water and 1 M solution of HCl in H₂O (1:1 eq., 3.7 ml) was added slowly in order to protonate the amine group. The reaction mixture was stirred at room temperature for 1 hour. After the protonation was finished the solvent was evaporated



and the crude was redissolved in acetonitrile and isopropyl alcohol and Li[NTf₂] was added to perform the ion exchange (0.92 g; 3.21 mmol). The reaction was stirred for 24 hours at room temperature. Acetone was added in order to remove the inorganic salts by precipitation. The solution was evaporated and dried *in vacuo* for 24 hours. The desired product was obtained as a viscous orange liquid (1.1 g, 74%). T_g=-74.63 °C; [α]_D= 3.0±2° (c= 1 mg.mL⁻¹ in acetonitrile); ¹H NMR (400.13 MHz, CD₃CN) δ 4.30 (t, ³J_{H2-H3,H3'}=8Hz, 1H, H₂), 4.08 (s, 3H, -NH₃), 3.47 (m, 2H, H₃, H_{3'}), 2.40 (s, 3H, H₄). ¹³C NMR (100.61 MHz, CD₃CN) δ 172.94 (C₁), 122.55 (C_a), 56.13 (C₂), 34.41 (C₃), 14.68 (C₄). ¹⁹F NMR (376 MHz, (CD₃)₂SO) δ -79.23. Elemental analysis (%) calcd for C₆H₁₀F₆N₂O₆S₃ (MW=416.34 g.mol⁻¹): C 17.31, H 2.42, N 6.73, S 23.10; found: C 17.23, H 2.43, N 6.76, S 22.97.

II.10.2.Synthesis of (S)-1-carboxy-2-(methylthio)ethanaminium 1,4-bis((2-ethylhexyl)oxy)-1,4-dioxobutane-2-sulfonate (2b)

S-methyl-L-cysteine (0.5 g; 3.69 mmol) was dissolved in water and 1 M solution of HCl in H₂O (1:1 eq., 3.7 ml) was added slowly in

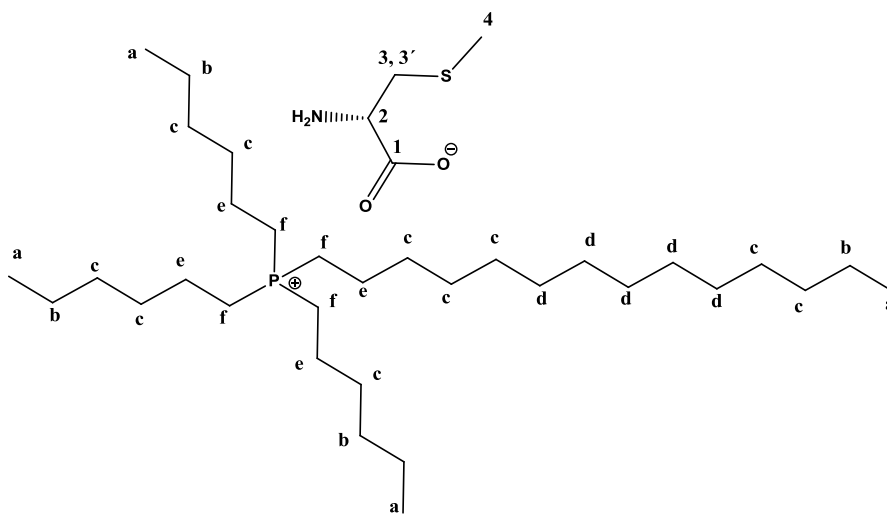


order to protonate the amine group. The reaction mixture was stirred at room temperature for 1 hour. After the protonation was finished the solvent was evaporated and the crude was redissolved in acetonitrile and isopropyl alcohol and Na[AOT] was added to perform the ion

exchange (1.54g; 3.46 mmol). The reaction was stirred for 24 hours at room temperature. Acetone was added in order to remove the inorganic salts by precipitation. The solution was evaporated and dried *in vacuo* for 24 hours. The desired product was obtained as a viscous brown liquid (1.8 g, 87%). $[\alpha]_D = 6.0 \pm 2^\circ$ ($c = 1 \text{ mg.mL}^{-1}$ in acetonitrile); ^1H NMR (400.13 MHz, $(\text{CD}_3)_2\text{CO}$) δ 5.25 (t, $^3J_{\text{H}_2-\text{H}_3, \text{H}_3-\text{H}_4} = 8\text{Hz}$, 1H, H_2), 4.54 (t, $^3J_{\text{H}_g-\text{H}_h} = 3.2\text{Hz}$, 1H, H_g), 4.01 (m, 4H, H_f), 3.32 (m, 2H, H_3 , H_3'), 3.15 (m, 2H, H_h), 2.25 (s, 3H, H_4), 1.60 (m, 2H, H_d), 1.41 – 1.15 (m, 16H, H_b , H_c , H_e), 0.92 (m, 12H, H_a). ^{13}C NMR (100.61 MHz, $(\text{CD}_3)_2\text{CO}$) δ 171.32 (C_1), 169.21 ($-\text{C}=\text{O}$), 168.75 ($-\text{C}=\text{O}$), 67.34 (C_f), 66.80 (C_f'), 62.25 (C_g), 52.47 (C_2), 39.14 (C_3 , C_d), 34.05 (C_c), 30.45 (C_c), 30.07 (C_h), 23.57 (C_e), 22.74 (C_b), 15.31 (C_4), 13.88 (C_a), 10.80 (C_a). Elemental analysis (%) calcd for $\text{C}_{24}\text{H}_{47}\text{NO}_9\text{S}_2$ (MW=557.76 g.mol $^{-1}$): C 51.68, H 8.49, N 2.51, S 11.50; found: C 51.42, H 8.44, N 2.50, S 11.46.

II.10.3. Synthesis of trihexyl(tetradecyl)phosphonium (S)-2-amino-3-(methylthio)propanoate (3a)

S-methyl-L-cysteine (0.5 g; 3.69 mmol) was dissolved in ethanol and 0.5M solution of NaOH in EtOH (1:1 eq., 7.4 ml) was added slowly in order to deprotonate the carboxylic acid

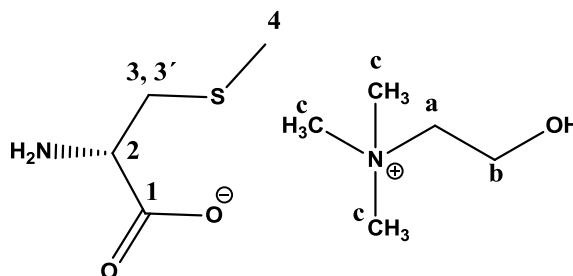


group. The reaction mixture was stirred at room temperature for 1 hour. After the deprotonation was finished the solvent was evaporated and the crude was redissolved in acetone and $[\text{P}_{6,6,6,14}]\text{Cl}$ was added to perform the ion exchange (2.25 g; 4.33 mmol). The reaction was stirred for 24 hours at room temperature. Dichloromethane was added in order to remove the inorganic salts by precipitation. The solution was evaporated and dried *in vacuo* for 24 hours. The desired product was obtained as a viscous brown liquid (2.4 g, 92%). $T_g = -73.06^\circ\text{C}$, $[\alpha]_D = 6.0 \pm 2^\circ$ ($c = 1 \text{ mg.mL}^{-1}$ in acetonitrile); ^1H NMR (400.13 MHz, CDCl_3) δ 6.09 (s, 1H, $-\text{OH}$), 5.30 (s, 3H, $-\text{NH}_3$), 4.32 (m, 1H, H_2), 3.64 (m, 2H, H_3), 2.40 (s, 3H, H_4), 2.32 (m, 8H, H_f), 1.27 (m, 16H, H_b , H_c), 1.26-1.20 (m, 32H, H_e), 0.83 (m, 12H, H_a). ^{13}C NMR (100.61 MHz, CDCl_3) δ 172.50 (C_1), 56.49 (C_2), 31.81 (C_3), 31.01 (C_c), 30.65 (C_c), 30.46 (C_c , C_d), 26.00 (C_4), 22.58 (C_f), 22.24 (C_b),

21.89 (C_e), 14.00 (C₄), 13.82 (C_a). Elemental analysis (%) calcd for C₃₆H₇₆NO₂PS (MW= 618.03 g.mol⁻¹): C 69.96, H 12.39, N 2.27, S 5.19; found: C 69.61, H 12.33, N 2.26, S 5.17.

II.10.4.Synthesis of 2-hydroxy-N,N,N-trimethylethanaminium (S)-2-amino-3-(methylthio)propanoate (3b)

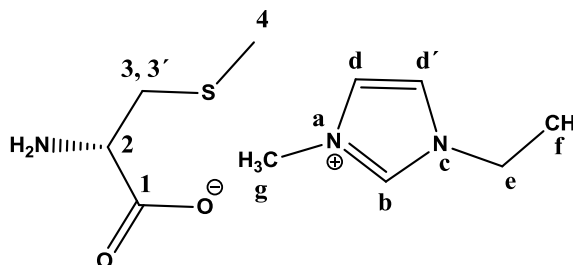
S-methyl-L-cysteine (0.5 g; 3.69 mmol) was dissolved in ethanol and 0.5M solution of NaOH in EtOH (1:1 eq., 7.4 ml) was added slowly in order to deprotonate the carboxylic acid group. The reaction mixture was stirred at room temperature for 1 hour.



After the deprotonation was finished the solvent was evaporated and the crude was redissolved in methanol and [Choline]Cl was added to perform the ion exchange (0.44 g; 3.18 mmol). The reaction was stirred for 24 hours at room temperature. Acetone was added in order to remove the inorganic salts by precipitation. The solution was evaporated and dried *in vacuo* for 24 hours. The desired product was obtained as a viscous brown liquid (1.1 g, 74%). $T_g = -56.11\text{ }^{\circ}\text{C}$; $[\alpha]_D = 12.0 \pm 2^{\circ}$ ($c = 1\text{ mg.mL}^{-1}$ in acetonitrile); $^1\text{H NMR}$ (400.13 MHz, CD₃OD) δ 4.88 (s, 1H, -OH), 4.02 (m, 2H, H_b), 3.53 (t, $^3J_{\text{H}_2\text{H}_3, \text{H}_3} = 8\text{ Hz}$, 1H, H₂), 3.44 (m, 2H, H_a), 3.24 (s, 9H, H_c), 2.96-2.92 (dd, $^3J_{\text{H}_3\text{H}_3} = 4\text{ Hz}$, 2H, H₃, H_{3'}), 2.12 (s, 3H, H₄). $^{13}\text{C NMR}$ (100.61 MHz, CD₃OD) δ 179.30 (C₁), 68.04 (C_a), 56.05 (C₂), 54.91 (C_b), 53.71 (C_c), 40.64 (C₃), 14.37 (C₄). Elemental analysis (%) calcd for C₉H₂₂N₂O₃S (MW= 238.35g.mol⁻¹): C 45.35, H 9.30, N 11.75, S 13.45; found: C 45.12, H 9.26, N 11.70, S 13.45.

II.10.5.Synthesis of 1-ethyl-3-methyl-1H-imidazol-3-ium (S)-2-amino-3-(methylthio)propanoate (3c)

S-methyl-L-cysteine (0.5 g; 3.69 mmol) was dissolved in ethanol and 0.5M solution of NaOH in EtOH (1:1 eq., 7.4 ml) was added slowly in order to deprotonate the carboxylic acid group. The reaction mixture was stirred at room temperature for 1 hour.

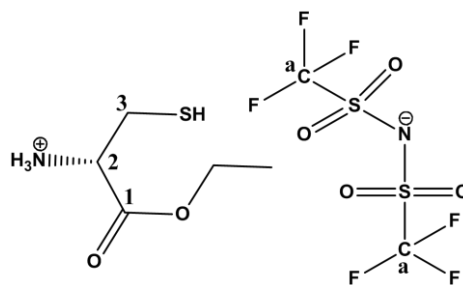


After the deprotonation was finished the solvent was evaporated and the crude was redissolved in methanol and [Emim]Br was added to perform the ion exchange (0.61 g; 3.18 mmol). The reaction was stirred for 24 hours at room temperature. Dichloromethane was added in order to remove the inorganic salts by precipitation. The solution was evaporated and dried *in vacuo* for 24 hours. The desired product was obtained as a viscous yellow liquid (0.62 g, 69%). $T_g =$

107.12 °C; $[\alpha]_D = 14.0 \pm 2^\circ$ ($c = 1 \text{ mg.mL}^{-1}$ in acetonitrile); ^1H NMR (400.13 MHz, CD_3OD) δ 7.69-7.61 (d, $^3J_{\text{Hd-Hd}} = 12 \text{ Hz}$, 2H, $\text{H}_{\text{d,d}}$), 4.96 (s, 3H, H_{g}), 4.29 (q, $^3J_{\text{He-Hf}} = 7.3 \text{ Hz}$, 2H, H_{e}), 3.76 (m, 2H, H_3), 3.33 (m, 1H, H_2), 2.16 (t, $^3J_{\text{Hf-He}} = 7.3 \text{ Hz}$, 3H, H_{f}). ^{13}C NMR (100.61 MHz, CD_3OD) δ 179.30 (C_1), 123.89 (C_{b}), 122.27 (C_{d}), 48.42 (C_2), 45.03 (C_{e}), 35.51 (C_3), 34.05 (C_{g}), 14.60 (C_4 , C_{f}). Elemental analysis (%) calcd for $\text{C}_{10}\text{H}_{19}\text{N}_3\text{O}_2\text{S}$ (MW = 245.34 g.mol^{-1}): C 48.95, H 7.81, N 17.13, S 13.07; found: C 48.95, H 7.79, N 17.05, S 13.05.

II.10.6. (S)-1-ethoxy-3-mercapto-1-oxopropan-2-aminium bis((trifluoromethyl)sulfonyl)amide (4a)

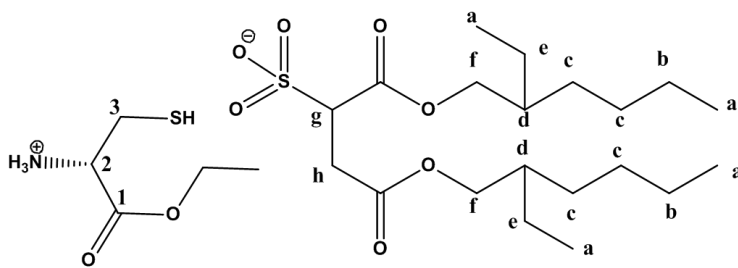
L-cysteine ethyl ester hydrochloride (0.5 g; 2.69 mmol) was dissolved in methanol and 1.2 eq. of $\text{Li}[\text{NTf}_2]$ was added to perform the ion exchange (0.93 g; 3.23 mmol). The reaction was stirred for 24 hours at room temperature. Acetone was added in order to remove the inorganic salts by precipitation.



The solution was evaporated and dried *in vacuo* for 24 hours. The desired product was obtained as a viscous yellow liquid (0.51 g, 44%). ^1H NMR (400.13 MHz, DMSO) δ 7.00 (s, 3H, $-\text{NH}_3$), 4.70 (t, $^3J_{\text{H}_2\text{-H}_3} = 6\text{Hz}$, 1H, H_2), 4.16 (m, 2H, $-\text{CH}_2$), 3.15 (m, 2H, H_3 , $\text{H}_{3'}$), 1.30 (t, $^3J_{\text{CH}_3\text{-CH}_2} = 6\text{Hz}$, 3H, $-\text{CH}_3$). ^{13}C NMR (100.61 MHz DMSO) δ 169.03 (C_1), 122.23 (C_{a}), 62.50 ($-\text{CH}_2$), 56.05 (C_2), 32.26 (C_3), 15.34 ($-\text{CH}_3$). ^{19}F NMR (376 MHz, DMSO) δ -79.23. Elemental analysis (%) calcd for $\text{C}_7\text{H}_{12}\text{F}_6\text{N}_2\text{O}_6\text{S}_3$ (MW = 430.37 g.mol^{-1}): C 19.54, H 2.81, N 6.51, S 22.35; found: C 19.44, H 2.80, N 6.48, S 22.25.

II.10.7. (S)-1-ethoxy-3-mercapto-1-oxopropan-2-aminium 1,4-bis((2-ethylhexyl)oxy)-1,4-dioxobutane-2-sulfonate (4b)

L-cysteine ethyl ester hydrochloride (0.5 g; 2.69 mmol) was dissolved in methanol and 1.2 eq. of $\text{Na}[\text{AOT}]$ was added to perform the ion exchange

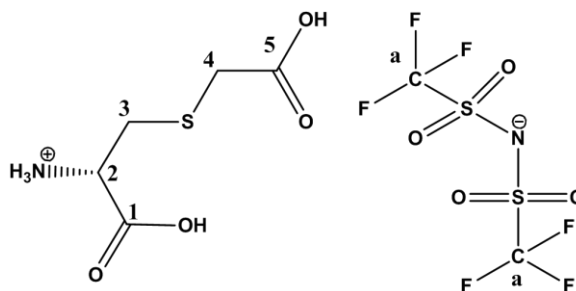


(1.32 g; 2.96 mmol). The reaction was stirred for 24 hours at room temperature. Acetone was added in order to remove the inorganic salts by precipitation. The solution was evaporated and dried *in vacuo* for 24 hours. The desired product was obtained as a viscous white liquid (1.49 g, 97%). ^1H NMR (400.13 MHz, $(\text{CD}_3)_2\text{CO}$) δ 5.25 (t, $^3J_{\text{H}_2\text{-H}_3, \text{H}_3'} = 6\text{Hz}$, 1H, H_2), 4.54 (t, $^3J_{\text{H}_{\text{g}}\text{-H}_{\text{h}}} = 3.2\text{Hz}$, 1H, H_{g}), 4.16 (m, 2H, $-\text{CH}_2$), 4.01 (m, 4H, H_{f}), 3.32 (m, 2H, H_3), 3.15 (m, 2H, H_{h}), 2.07

(m, 2H, H_d), 1.41 – 1.15 (m, 19H, H_b, H_c, H_e, -CH₃), 0.92 (m, 12H, H_a). ¹³C NMR (100.61 MHz, (CD₃)₂CO) δ 171.32 (C₁), 169.21 (-C=O), 168.75 (-C=O), 67.34 (C_f), 67.02 (C_f'), 63.70 (-CH₂), 62.25 (C_g), 52.47 (C₂), 39.14 (C₃, C_d), 35.51 (C_c), 30.45 (C_c), 30.07 (C_h), 23.57 (C_e), 22.74 (C_b), 14.60 (-CH₃), 13.88 (C_a), 10.80 (C_a). Elemental analysis (%) calcd for C₂₅H₄₉NO₉S₂ (MW= 571.79 g.mol⁻¹): C 52.51, H 8.64, N 2.45, S 11.22; found: C 52.24, H 8.58, N 2.45, S 11.17.

II.10.8.(S)-1-carboxy-2-((carboxymethyl)thio)ethanaminium bis((trifluoromethyl)sulfonyl)amide (5a)

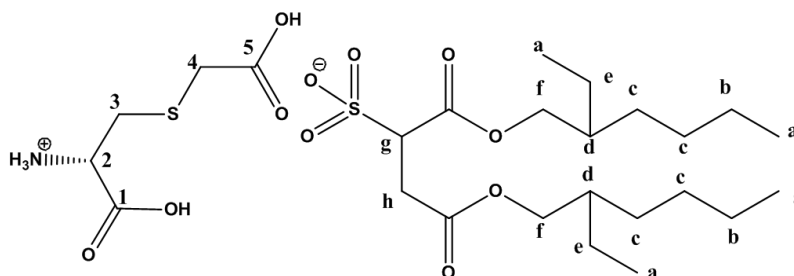
S-carboxymethyl-L-cysteine (0.5 g; 2.79 mmol) was dissolved in methanol and 1 M solution of HCl in MeOH (1:1 eq., 2.79 ml) was added slowly in order to protonate the primary amine group. The reaction mixture was stirred at room



temperature for 1 hour. After the protonation was finished Li[NTf₂] was added to perform the ion exchange (0.96 g; 3.35 mmol). The reaction was stirred for 24 hours at room temperature. Acetone was added in order to remove the inorganic salts by precipitation. The solution was evaporated and dried *in vacuo* for 24 hours. The desired product was obtained as a viscous yellow liquid (0.81 g, 63%). ¹H NMR (400.13 MHz, CD₃OD) δ 4.17 (m, 1H, H₂), 3.47 (s, 2H, H₄), 3.30 (m, 1H, H₃), 3.08 (m, 1H, H₃'). ¹³C NMR (100.61 MHz, CD₃OD) δ 172.89 (C₅), 122.79 (C₁), 119.61 (C_a), 53.56 (C₂), 34.44 (C₄), 33.96 (C₃). ¹⁹F NMR (376 MHz, (CD₃)₂SO) δ -79.23. Elemental analysis (%) calcd for C₇H₁₀F₆N₂O₈S₃ (MW= 460.35 g.mol⁻¹): C 18.26, H 2.19, N 6.09, S 20.90; found: C 18.16, H 2.18, N 6.06, S 21.00.

II.10.9.(S)-1-carboxy-2-((carboxymethyl)thio)ethanaminium 1,4-bis((2-ethylhexyl)oxy)-1,4-dioxobutane-2-sulfonate (5b)

S-carboxymethyl-L-cysteine (1 g; 5.58 mmol) was dissolved in methanol and 1.2 eq. of Na[AOT] was added to perform the ion exchange (2.97 g;

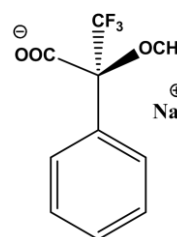


6.69 mmol). The reaction was stirred for 24 hours at room temperature. Acetone was added in order to remove the inorganic salts by precipitation. The solution was evaporated and dried *in vacuo* for 24 hours. The desired product was obtained as a viscous white liquid (2.74 g, 98%).

^1H NMR (400.13 MHz, $(\text{CD}_3)_2\text{CO}$) δ 4.30 (m, 1H, H_2), 4.10-4.01 (m, 5H, H_g , H_f), 3.77 (s, 2H, H_4), 3.53 (m, 1H, H_3), 3.36-3.13 (m, 3H, H_3' , H_h), 1.49 (m, 2H, H_d), 1.41 – 1.15 (m, 16H, H_b , H_c , H_e), 0.93 (m, 12H, H_a). ^{13}C NMR (100.61 MHz, $(\text{CD}_3)_2\text{CO}$) δ 171.39 (C_5), 171.22 ($-\text{C}=\text{O}$), 168.85 (C_1), 168.38 ($-\text{C}=\text{O}$), 67.34 (C_f), 67.02 (C_f'), 61.87(C_g), 51.82 (C_2), 40.04 (C_4), 39.14 (C_d), 35.51 (C_c), 30.45 (C_c), 30.07 (C_h), 29.18 (C_3), 23.57 (C_e), 22.74(C_b), 13.04 (C_a), 9.98 (C_a). . Elemental analysis (%) calcd for $\text{C}_{25}\text{H}_{47}\text{NO}_{11}\text{S}_2$ (MW= 601.77 $\text{g}\cdot\text{mol}^{-1}$): C 49.90, H 7.87, N 2.33, S 10.66; found: C 49.80, H 7.83, N 2.32, S 10.64.

II.10.10. ^{19}F NMR Experiment- enantiomeric resolution

Racemic Mosher's sodium salt was prepared from Mosher's acid by reacting with an equivalent of sodium hydroxide in water and the salt was dried under vacuum before ^{19}F NMR measurement. The racemic Mosher's sodium salt (8.38 mg, 0.03 mmol) and 77-159 mg (0.32 mmol) of chiral ionic compounds were dissolved in 0.5 ml of d-DMSO. The mixture was dissolved in ultrasonicator bath for 10 minutes at 35 °C before recording ^{19}F NMR spectra.



II.10.11. General procedure for asymmetric aldol reaction

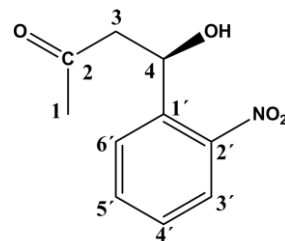
Asymmetric aldol reaction between aromatic aldehydes and acetone/cyclohexanone was carried out in neat ketone reaction system (acetone) and water or DMSO (cyclohexanone). The suspension of chiral catalyst based on cysteine scaffold (10-20 mol%) and ketone (100 μl , 2 mmol) was stirred for 30 minutes at RT. After that time aromatic aldehyde (0.0756 g, 1mmol) was added and the resulting mixture was allowed to stir at RT for 24-48 hours as indicated in Tables II.2 and II.3. In the next step, the solvent was evaporated in vacuo and the crude was redissolved in DCM, in order to be filtered through a silica gel pad (1 g) and washed with diethyl ether (Et_2O). The solvent was removed under vacuum to afford the desired aldol product as colourless solid. Relative and absolute configurations of the products and enantiomeric excess values were determined by comparison with the known ^1H NMR.

Procedure for Catalyst Recovery:

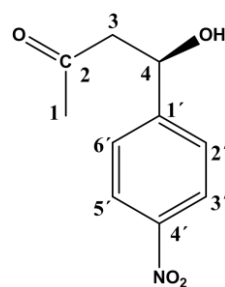
The reaction mixture was stirred at RT as specified in Tables II.2 and II.3. After the excess solvent was evaporated, Et_2O was added to the crude and vigorously stirred for 5 minutes. Later, an extraction using Et_2O (4x2ml) was performed. Then the organic layer was concentrated in vacuo to afford the aldol product. The catalyst phase remaining, according to the immiscibility

of the catalyst in Et₂O, was redissolved in acetone in order to be recovered and was dried under vacuum.

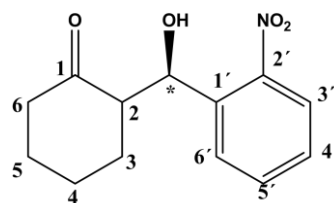
4-hydroxy-4-(2-nitrophenyl)butan-2-one: 93 mg, yield: 89%. ¹H NMR (400.13 MHz, CDCl₃) δ 7.95 (d, ³J_{H3'-H4'} = 8 Hz, 1H, H_{3'}), 7.90 (d, ³J_{H6'-H5'} = 8 Hz, 1H, H_{6'}), 7.65 (t, ³J_{H5'-H6'}, ⁴J_{H4'-H3'} = 8 Hz, 1H, H_{5'}), 7.43 (t, ³J_{H4'-H5'}, ³J_{H3'-H4'} = 8 Hz, 1H, H_{4'}), 5.68 (d, ³J_{H4-H3} = 8 Hz, 1H, H₄), 3.13 (dd, ³J_{H3-H3}, ⁴J_{H4-H3} = 8 Hz, 1H, H₃), 2.79 (dd, ³J_{H3-H3}, ⁴J_{H4-H3} = 8 Hz, 1H, H₃), 2.23 (s, 3H, H₁). ¹³C NMR (100.61 MHz, CDCl₃) δ 208.20 (C₂), 147.24 (C_{6'}), 138.28 (C_{5'}), 133.91 (C_{2'}), 128.27 (C_{3'}), 124.26 (C_{4'}), 65.53 (C₄), 51.18 (C₃), 30.00 (C₁).



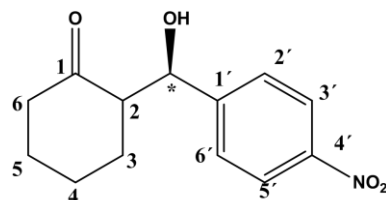
4-hydroxy-4-(4-nitrophenyl)butan-2-one: 95 mg, yield: 91%. ¹H NMR (400.13 MHz, CDCl₃) δ 8.38 (d, ³J_{H5'-H6'}, ³J_{H3'-H2'} = 8 Hz, 2H, H_{5'}, H_{3'}), 7.51 (d, ³J_{H6'-H5'}, ³J_{H2'-H3'} = 8 Hz, 2H, H_{6'}, H_{2'}), 5.29 (d, ³J_{H4-H3} = 8 Hz, 1H, H₄), 3.48 (t, ³J_{H3-H3}, ⁴J_{H4-H3} = 8 Hz, 1H, H₃), 2.13 (s, 3H, H₁). ¹³C NMR (100.61 MHz, CDCl₃) δ 190.47 (C₂), 150.93 (C_{1'}), 139.89 (C_{4'}), 128.72 (C_{6'}), 128.43 (C_{2'}), 125.27 (C_{3'}), 124.26 (C_{5'}), 65.71 (C₄), 50.18 (C₃), 30.81 (C₁).



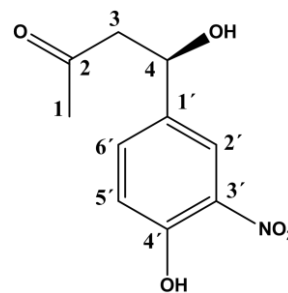
2-(hydroxy(2-nitrophenyl)methyl)cyclohexanone: 78 mg, yield: 63%. ¹H NMR (400.13 MHz, CDCl₃) δ 8.14 (dd, ³J_{H3'-H4'} = 8 Hz, ⁴J_{H3'-H5'} = 11 Hz, 1H, H_{3'}), 7.96 (dd, ³J_{H6'-H5'} = 8 Hz, ⁴J_{H6'-H4'} = 11 Hz, 1H, H_{6'}), 7.79 (m, 2H, H_{5'}, H_{4'}), 5.43 (d, ³J_{H*-H2} = 8 Hz, 1H, H*), 3.47 (t, ³J_{H2-H*}, ³J_{H3} = 8 Hz, 1H, H₂), 2.43 - 2.34 (m, 2H, H₆), 2.20 - 2.08 (m, 1H, H₃), 1.70 - 1.51 (m, 4H, H₄, H₅), 1.25 - 1.13 (m, 1H, H₃). ¹³C NMR (100.61 MHz, CDCl₃) δ 209.45 (C₁), 147.08 (C_{6'}), 140.46 (C_{5'}), 133.22 (C_{2'}), 131.53 (C_{3'}), 126.95 (C_{1'}), 121.46 (C_{4'}), 71.56 (C*), 57.48 (C₂), 39.34 (C₆), 29.20 (C₅), 23.12 (C₄), 20.53 (C₃).



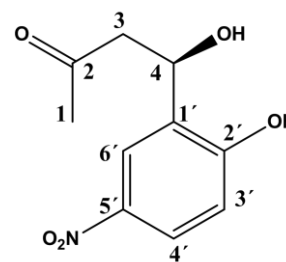
2-(hydroxy(4-nitrophenyl)methyl)cyclohexanone: 90 mg, yield: 73%. ¹H NMR (400.13 MHz, CDCl₃) δ 8.07 (d, ³J_{H5'-H6'}, ³J_{H3'-H2'} = 8 Hz, 2H, H_{5'}, H_{3'}), 7.48 (d, ³J_{H6'-H5'}, ³J_{H2'-H3'} = 8 Hz, 2H, H_{6'}, H_{2'}), 4.93 (d, ³J_{H*-H2} = 8 Hz, 1H, H*), 3.45 (t, ³J_{H2-H3}, ³J_{H2-H*} = 8 Hz, 1H, H₂), 2.82 - 2.44 (m, 2H, H₆), 2.34 - 2.15 (m, 1H, H₃), 1.90 - 1.71 (m, 4H, H₄, H₅), 1.55 - 1.38 (m, 1H, H₃). ¹³C NMR (100.61 MHz, CDCl₃) δ 207.02 (C₁), 151.08 (C_{1'}), 146.46 (C_{4'}), 127.39 (C_{6'}), 127.13 (C_{2'}), 123.95 (C_{3'}), 123.46 (C_{5'}), 76.56 (C*), 57.38 (C₂), 40.04 (C₆), 29.20 (C₅), 25.12 (C₄), 22.13 (C₃).



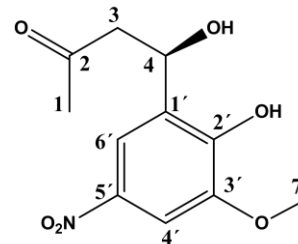
4-hydroxy-4-(4-hydroxy-3-nitrophenyl)butan-2-one: 77 mg, yield: 76%. ^1H NMR (400.13 MHz, CDCl_3) δ 8.63 (s, 1H, H_2), 8.13 (d, $^3J_{\text{H}_6'-\text{H}_5'} = 8$ Hz, 1H, H_6'), 7.30 (d, $^3J_{\text{H}_5'-\text{H}_6'} = 8$ Hz, 1H, H_5'), 3.47 (t, $^3J_{\text{H}_4-\text{H}_3} = 8$ Hz, 1H, H_4), 3.15 (dd, $^3J_{\text{H}_3-\text{H}_3, \text{H}_4} = 8$ Hz, 1H, H_3), 2.89 (dd, $^3J_{\text{H}_3-\text{H}_3, \text{H}_4} = 8$ Hz, 1H, H_3), 2.20 (s, 3H, H_1). ^{13}C NMR (100.61 MHz, CDCl_3) δ 188.52 (C_2), 159.22 (C_4'), 136.30 (C_3'), 133.55 (C_6'), 129.26 (C_1'), 128.53 (C_2'), 121.24 (C_5'), 68.88 (C_4), 53.27 (C_3), 29.66 (C_1).



4-hydroxy-4-(2-hydroxy-5-nitrophenyl)butan-2-one: 71 mg, yield: 70%. ^1H NMR (400.13 MHz, CDCl_3) δ 8.59 (s, 1H, H_6), 8.43 (d, $^3J_{\text{H}_4'-\text{H}_3'} = 8$ Hz, 1H, H_4'), 7.15 (d, $^3J_{\text{H}_3'-\text{H}_4'} = 8$ Hz, 1H, H_3'), 3.74 (t, $^3J_{\text{H}_4-\text{H}_3} = 8$ Hz, 1H, H_4), 3.12 (dd, $^3J_{\text{H}_3-\text{H}_3, \text{H}_4} = 8$ Hz, 1H, H_3), 2.78 (dd, $^3J_{\text{H}_3-\text{H}_3, \text{H}_4} = 8$ Hz, 1H, H_3), 2.25 (s, 3H, H_1). ^{13}C NMR (100.61 MHz, CDCl_3) δ 195.58 (C_2), 166.13 (C_2'), 140.63 (C_5'), 131.68 (C_1'), 129.78 (C_4'), 119.42 (C_6'), 119.00 (C_3'), 65.84 (C_4), 30.92 (C_3), 29.68 (C_1).



4-hydroxy-4-(2-hydroxy-3-methoxy-5-nitrophenyl)butan-2-one: 74 mg, yield: 76%. ^1H NMR (400.13 MHz, CDCl_3) δ 8.20 (s, 1H, H_6), 7.90 (s, 1H, H_4), 4.00 (s, 3H, H_7), 3.45 (t, $^3J_{\text{H}_4-\text{H}_3} = 8$ Hz, 1H, H_4), 3.07 (dd, $^3J_{\text{H}_3-\text{H}_3, \text{H}_4} = 8$ Hz, 1H, H_3), 2.88 (dd, $^3J_{\text{H}_3-\text{H}_3, \text{H}_4} = 8$ Hz, 1H, H_3), 1.39 (s, 3H, H_1). ^{13}C NMR (100.61 MHz, CDCl_3) δ 195.45 (C_2), 156.73 (C_3'), 148.90 (C_2'), 140.29 (C_5'), 120.34 (C_1'), 118.72 (C_6'), 111.24 (C_4'), 56.69 (C_4), 56.11 (C_7), 49.69 (C_3), 30.02 (C_1).



CHAPTER III. L-proline based Ionic Liquids

III. L-proline based ionic liquids

III.1. Background

Proline (Pro) is an abundant chiral scaffold as well as inexpensive secondary, cyclic pyrrolidine-based amino acid. This characteristic provides the increase in pK_a values of its amine compared to primary amino acids. Proline is a bifunctional amino acid available in both enantiomeric forms (Figure III.1). Concerning the amino and carboxylic acid group, they can both react as an acid or base and also facilitate the further chemical transformations. Those diverse reasons contribute to proline's role in catalysis as universal asymmetric catalyst.

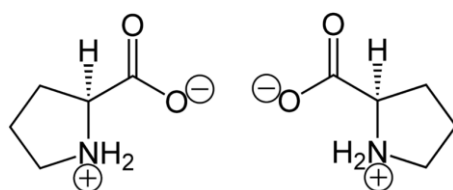
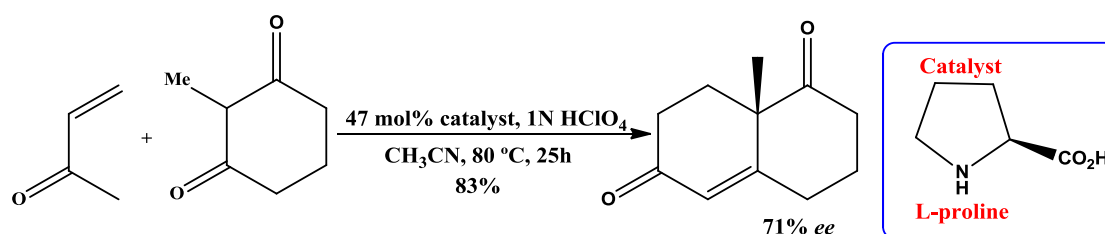


Figure III.1 - Zwitterionic structure of both proline enantiomers: L-proline (left) and D-proline (right).

Proline was firstly studied for catalysis in the Hajos-Parrish-Eder-Sauer-Wiechert reaction. In the 1970's, L-proline-catalyzed intramolecular aldol cyclizations in the synthesis of optically pure starting materials for the CD rings of steroids (C-one of three cyclohexane rings, D-cyclopentane ring)¹²⁸ were investigated. The skeleton of steroids consists in three fused cyclohexane rings and one cyclopentane ring. To each of the four rings was given an alphabet letter; the cyclohexane rings are A-C and the cyclopentane ring at the right edge is D.

Hajos and Parrish isolated the hydrindane dione from proline-catalyzed intramolecular aldol cyclization. The studies resulted in high yields and enantiomeric excesses as presented in Scheme III.1.



Scheme III.1 - Hajos- Parrish- Eder- Sauer- Wiechert Reaction.

Taking into account the versatile properties of this stable, non-toxic and powerful catalyst, it would seem daring to expect anything less than the discovery of novel proline-based ionic liquids. Therefore, in this chapter, the synthesis, characterization and application of a new class of chiral salts derived from commercially available L-proline are proposed.

III.2. Synthesis and characterization

Different structures of chiral salts developed from L-proline, including six using the amino acid unit as a cation and other six using it as an anion are shown in Figure III.2.

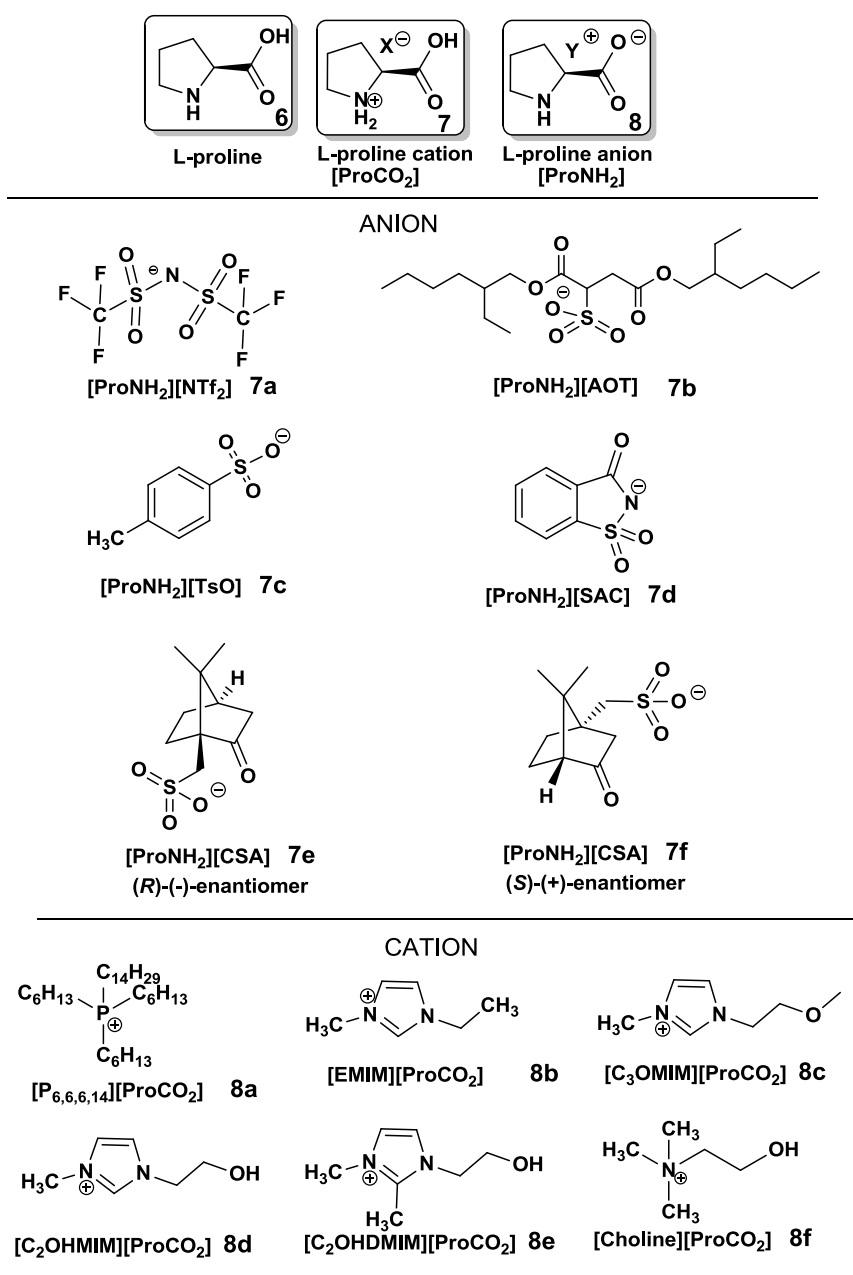
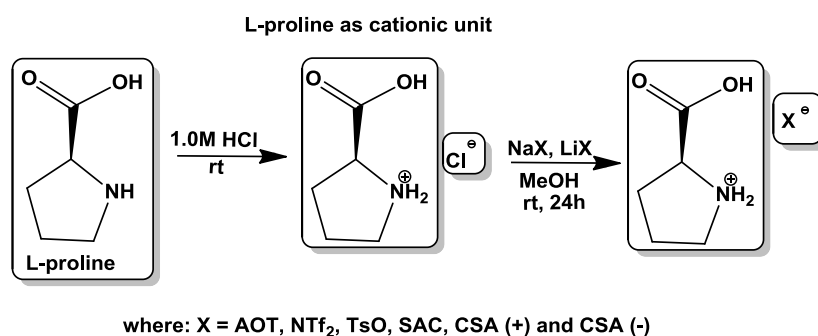


Figure III.2- Structures of chiral salts developed from L-proline.

According to synthesis of CILs derived from L-proline scaffold, similar approaches to those in the case of L-cysteine presented in chapter II have been used. The protonation of the secondary amine (NH) from L-proline was performed using hydrochloride acid in methanol solution. This correspondent chloride anion was then exchanged to more appropriate organic anions such as bis(trifluoromethanesulfonyl)imide ([NTf₂]), **7a**, docusate ([AOT]), **7b**, *p*-toluenesulfonate ([TsO]), **7c**, and saccharinate ([SAC]), **7d**, in order to obtain room temperature CILs (Scheme III.2). Additionally, two enantiomers from camphorsulfonic acid sodium salt, in the form of anions (*R*)-CSA, **7e**, and (*S*)-CSA, **7f**, were combined with the L-proline cation as examples of novel chiral salts containing chirality on both ionic units.

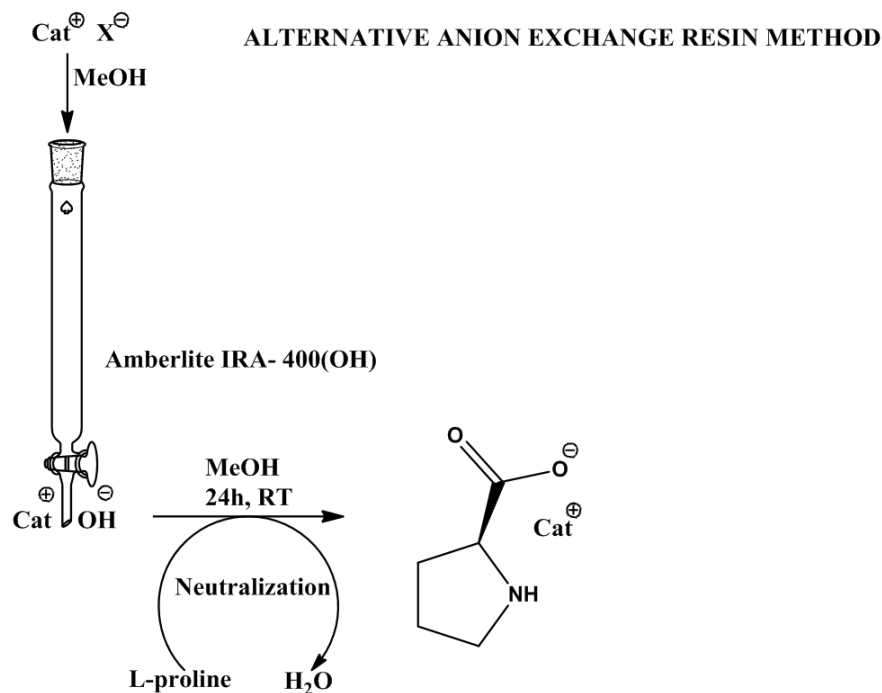


Scheme III.2 - General strategy for the synthesis of CILs based on L-proline as cationic unit.

The method selected to synthesize the proline- based salts with the amino acid as anion was the neutralization method. Ion exchange resin method developed by Ohno and coworkers is being effectively used as alternative anion exchange processes and it has been extended to other reactions¹²⁹. This strategy led to overcome many limitation related with the conventional method (anion metathesis), such as contamination of halides salts, limited variety of commercially available metal salt and adequate combination of amino acids to counter ions.

In this work, Amberlite resin (in the OH form) has been used in order to exchange halides (bromide or chloride) to the hydroxide form and then this basic solution was neutralized by the addition of an adequate acid solution, as described in Scheme III.3. The direct acid-base reaction allows the preparation of desired proline salt combined with organic cations such as trihexyltetradecylphosphonium ([P_{6,6,6,14}]), **8a**, 1-ethyl-3-methylimidazolium ([Emim]), **8b**, 1-(2-methoxyethyl)-3-methylimidazolium ([C₃Omim]), **8c**, 1-(2-hydroxyethyl)-3-methylimidazolium ([C₂OHmim]), **8d**, and 1-(2-hydroxyethyl)-2,3-dimethylimidazolium([C₂OHDmim]), **8e**. In the case of choline ([Choline]) cation, a direct acid- base reaction was performed due to the commercial available choline hydroxide in methanol solution (40% w/w), **8f**.

After optimizing the synthetic approach, CILs based on L-proline were obtained in moderate to high yields (66-99%) as well as high purities (confirmed by ^1H NMR spectroscopy and elemental analysis).



Scheme III.3 - Synthesis of L-proline based salts using ion exchange resins method.

All novel CILs based on L-proline were completely characterized by ^1H and ^{13}C NMR spectroscopy, Fourier transform infrared (FTIR) spectroscopy, elemental analysis (C, N, H) and differential scanning calorimetry (DSC) analysis, in order to check their structure, purity and chemical stability. In the ^1H - and ^{13}C -NMR spectra, no peaks attributable to impurities were found. NMR studies also elucidate about the expected cation/anion correlations by a quantitative integration of their characteristic ^1H resonance peaks. Figure II.3 shows the ^1H NMR spectrum of trihexyl(tetradecyl)phosphonium (*S*)-pyrrolidine-2-carboxylate, **8a**, with the correct cation /anion proportion 1:1.08 (value included in the 10% error) and 99% of purity. Figure II.4 presents (*S*)-2-carboxypyrrolidin-1-ium 1,4-bis((2-ethylhexyl)oxy)-1,4-dioxobutane-2-sulfonate, **7b**, where L-proline was used as a cation combined with the biocompatible docusate anion (cation /anion proportion 1:1.03 and 97% of purity).

It is important to emphasize that ^1H NMR spectra of the synthesized compounds based on L-proline as the cationic unit, show the dubbling of the peak belonging to the chiral proline carbon atom. This phenomenon is presented for (*S*)-2-carboxypyrrolidin-1-ium 3-oxo-3H-

benzo[d]isothiazol-2-ide 1,1-dioxide, **7d**, in Figure III.5. The corresponding triplet of H2 appeared at the same time at 4.65-4.62 ppm and 4.47-4.44 with the same coupling constant of 4Hz. It can be concluded that the chiral carbon is influenced by the protonation of the close amino group and for that reason this dubbling occurs.

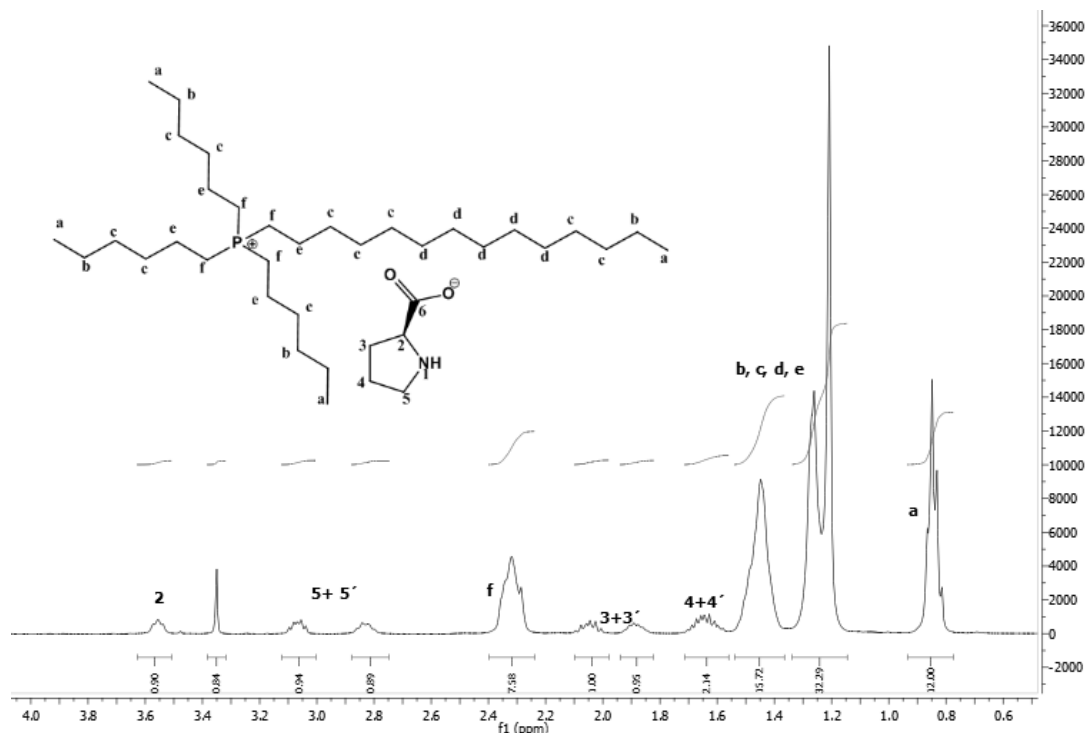


Figure III.3 - ^1H NMR spectrum of trihexyl(tetradecyl)phosphonium (*S*)-pyrrolidine-2-carboxylate (**8a**) performed in CDCl_3 (Synthesis was carried out using ion exchange resin method).

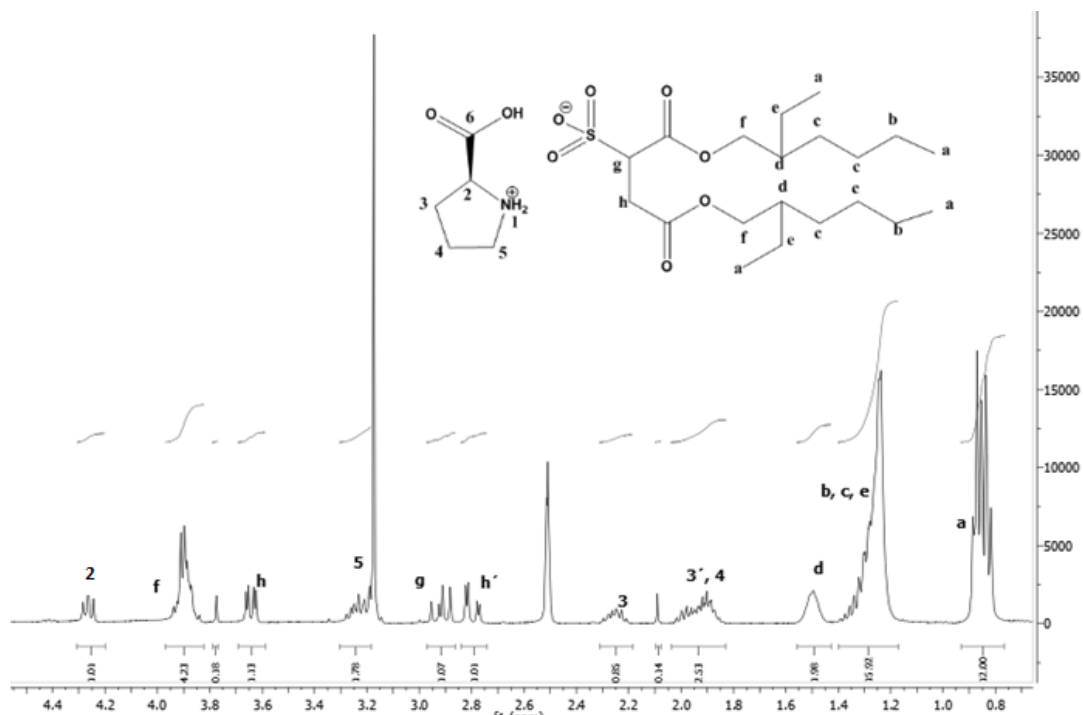


Figure III.4 - ^1H NMR spectrum of (*S*)-2-carboxypyrrolidin-1-ium 1,4-bis((2-ethylhexyl)oxy)-1,4-dioxobutane-2-sulfonate (**7b**) performed in DMSO (Synthesis was carried out using anion metal exchange method).

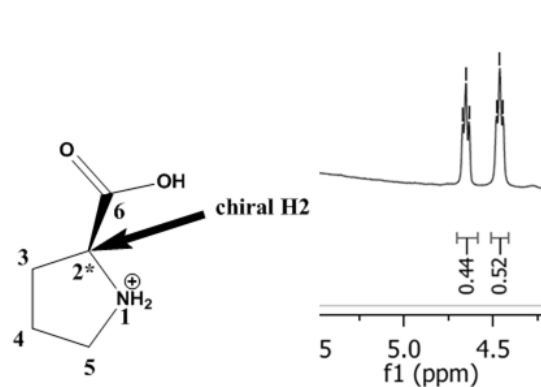


Figure III.5 - Dubbling of peak from chiral carbon observed for [ProNH₂][SAC] (**7d**) in ¹H NMR. The NMR description of the proton: 4.65-4.62 ppm (t, ³J_{H2-H3}=4Hz, 1H) and 4.47-4.44 ppm (t, ³J_{H2-H3}=4Hz, 1H).

Most of novel salts derived from L-proline were obtained as coloured viscous Room Temperature Ionic Liquids (RTILs), except in the case of [ProNH₂][(R)-CSA], **7e**, and [ProNH₂][(S)-CSA], **7f**, which were developed as white crystalline solids. The colour of CILs changed due to the use of L-proline as a cation or anion and the selected counter-ions between yellow, orange and brown viscous liquids as presented in Figure III.6. The cation/anion interaction can justify the colour variation when comparing with the initial white powder L-proline form.

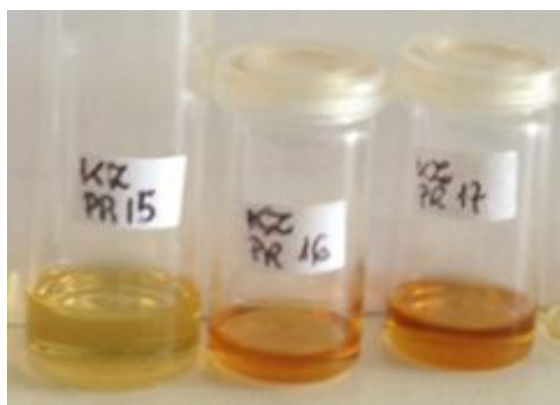


Figure III.6- RTILs derived from L-proline [P_{6,6,6,14}][ProCO₂] (left), [Emim][ProCO₂] (middle) and [C₃Omim][ProCO₂] (right).

III.3. *Physical properties of novel L-proline based salts*

Table III.1 summarizes all prepared CILs based on L-proline and some of their physical properties such as optical rotation (α_D) and density (ρ) values. Our optimized synthetic procedure allowed us to obtain pure compounds in high yields (75 to 99%).

Table III.1 Some properties of new synthesized salts based on L-proline scaffold.

CIL	Yield [%] ^[a]	Purity ^[b]	Density ^[c] [g cm ⁻³]	α_D ^[d] [cm ² g ⁻¹]
L-Pro 6	---	---	---	-41.3±2°
[ProNH ₂] [NTf ₂] 7a	90	>99	1.63	-12.7±2°
[ProNH ₂] [AOT] 7b	97	99	1.32	-12.0±2°
[ProNH ₂] [TsO] 7c	66	98	0.93	-4.0±2°
[ProNH ₂] [SAC] 7d	98	98	0.98	-4.5±2°
[ProNH ₂] [(-)CSA] 7e	99	99	---	-44.0±2°
[ProNH ₂] [(+)CSA] 7f	95	98	---	+66.0±2°
[P _{6,6,6,14}] [ProCO ₂] 8a	97	98	0.93	-17.3±2°
[Emim] [ProCO ₂] 8b	>99	98	1.19	-8.8±2°
[C ₃ Omim] [ProCO ₂] 8c	98	99	1.24	-5.3±2°
[C ₂ OHmim] [ProCO ₂] 8d	80	99	1.25	-6.7±2°
[C ₂ OHDmim] [ProCO ₂] 8e	75	99	1.28	-19.0±2°
[Choline] [ProCO ₂] 8f	99	>99	0.97	-12.7±2°

^[a] Isolated yields. ^[b] Purity obtained from ¹H NMR spectroscopy. ^[c] Density was measured by pycnometer at 25 °C. ^[d] Optical rotation values measured in MeOH (1 mg.mL⁻¹) by polarimetry at 20 °C recorded on a Perkin Elmer 241MC.

The optical rotation values were measured in methanol solution for all CILs and the initial L-proline protonated form (1 mg.mL⁻¹) by polarimetry at 20 °C. For most of the CILs, the optical rotations oscillated between -2.0 to -12.7° (with ±2° error). Higher optical rotation values were observed for CILs **8a** and **8e**. In general, salts derived from L-proline as chiral anion resulted in higher optical rotation values, but still significantly lower when compared with the initial L-proline (-41.3±2°). This difference can be explained by a stronger influence of organic cations combined with L-proline moiety as anion. Another relevant observation, all proline salts combined with methylimidazolium cations showed lower optical rotations (**8b**, **8c** and **8d** with values between -5.3 to -8.8°) except **8e** (-19.0°) comparing with phosphonium and ammonium cations. The presence of H-2 acidic proton from methylimidazolium cation can interact strongly with proline anion comparing with [C₂OHDmim] cation where the acidic proton is replaced by methyl group. Compounds **7e** and **7f** were developed with the idea of introducing chirality on both cation and anion units, showed the highest optical rotation values -44.0±2° for D and +66.0±2° for L enantiomers respectively (lit. -21.0° for D-camphorsulfonic acid and +19.9° for L-camphorsulfonic acid, c=2 in H₂O).

Density measurements were performed by the use of pycnometer at 25 °C. The higher density values were obtained for CILs **7a**, **7b** and **8e**, because of the presence of NTf₂ or AOT anion and the imidazolium cation, respectively. In the presence of ammonium or phosphonium cations, expected density values lower than 1 g.cm⁻³ were also observed. Obviously the ILs densities decrease with the increase of substituents chain lengths. This fact can be attributed to the increased number of interstices between ions caused by the more bulky cations, which

cannot pack closely with the anion. In fact, the density of many substances is compared to the density of water. These new CILs with significant difference in density value could be applied for biphasic systems using water (The denser ILs can be found on the bottom while the densest ILs are upper from water phase).

The same solubility behaviour studies and results, as previously described in chapter II, were performed for all L-proline based salts. The CILs were miscible with water, methanol, acetone, and other more polar organic solvents and immiscible with diethyl ether and other apolar organic solvents. The combination of proline derivative with more hydrophobic counter-ions can strongly influence the final water solubility profile, as already mentioned in the case of cysteine based ILs. Overall, it is possible to improve the neutral proline solubility by a simple combination with the appropriate counter-ions. This fact can be appropriate for the applications of L-proline as organocatalyst in asymmetric synthesis using alternative solvent mixtures.

III.4. *Thermal properties of novel L-proline based salts*

It is known that ILs are defined as organic salts with low melting points. Many of them have been broadly applied as liquid materials such as electrolytes, phase-transfer reagents, surfactants, fungicides and biocides⁵.

Commercial L-proline, **6**, as a crystalline solid with higher melting temperature ($T_m=228\text{ }^{\circ}\text{C}$, decomposes), can be transformed in amorphous salts by simple change in the counter-ions types. It is important to emphasize that melting points obtained as proline based salts were lower than the ones from the commercial available compound (from $198\text{ }^{\circ}\text{C}$ to $154\text{ }^{\circ}\text{C}$ in the case of (-) CSA and $196\text{--}200\text{ }^{\circ}\text{C}$ to $155\text{--}160\text{ }^{\circ}\text{C}$ for (+) CSA), according to the special cation-anion combination. The melting point of the salt decreases according with weaker coulombic interactions and efficient distribution of charge on the cation.

The thermal properties of twelve ILs were investigated, in particular their characteristic glass transition temperature (T_g) values, using a differential scanning calorimetry (DSC) analysis by heating/cooling rate of $10\text{ }^{\circ}\text{C}\cdot\text{min}^{-1}$.

Table III.2 summarizes the physical state, melting temperature (T_m) and glass transition temperature (T_g) for the series of selected salts. The DSC analysis showed that for most of the novel compounds, cooling from the liquid state caused glass formation at low temperatures except in the case of $[\text{ProNH}_2][\text{SAC}]$, **7d**, $[\text{ProNH}_2][\text{D-CSA}]$, **7e**, and $[\text{ProNH}_2][\text{L-CSA}]$, **7f**.

Similar values of glass transition temperatures were detected for most proline salts (-61.88 °C to -83.00 °C), except in the case of [C₂OHmim][ProCO₂], **8d**, [C₂OHDmim][ProCO₂], **8e**, and [ProNH₂][SAC], **7d**. As expected for [Emim] and [C₃Omim] cations, low glass transition temperatures were recorded in the typical region between -77.57 and -83.00. Figures III.7 and III.8 present the DSC curves of [ProNH₂][NTf₂], **7a**, where proline moiety was used as the cationic unit and [Emim][ProCO₂], **8b**, with the proline as anion in a cooling and heating cycle.

Decomposition temperatures (T_{dec}) were analysed by TGA analysis for some of the synthesized compounds. As expected, these studies indicated that the selection of the organic cation influences the thermal stability of CILs based on L-proline. [P_{6,6,6,14}][ProCO₂] presented higher thermal stability than those based on imidazolium cations. All proline based salts showed significantly higher decomposition temperatures (258 to 299°C) than original L-proline (238.60 °C).

Table III.2 Thermal Properties (T_m , T_{dec} and T_g) of ILs based on L-proline.

<i>CIL</i>	<i>Physical state</i>	T_g [°C] ^[a] (T_m)	T_{dec} [°C] ^[b]
L-Pro 6	white powder	(228 dec.)	238.60
[ProNH ₂] [NTf ₂] 7a	yellow liquid	-77.67	287.10
[ProNH ₂] [AOT] 7b	yellow liquid	-61.88	258.40
[ProNH ₂] [TsO] 7c	yellow liquid	-25.07	273.90
[ProNH ₂] [SAC] 7d	white liquid	-- ^[c]	299.50
[ProNH ₂] [(-)CSA] 7e	white solid	-- ^[c]	292.90
		(154) ^[d]	
[ProNH ₂] [(+)CSA] 7f	white solid	-- ^[c]	292.30
		(160) ^[d]	
[P _{6,6,6,14}] [ProCO ₂] 8a	orange liquid	-74.40	290.10
[Emim] [ProCO ₂] 8b	orange liquid	-77.57	247.80
[C ₃ Omim] [ProCO ₂] 8c	orange liquid	-83.00	256.30
[C ₂ OHmim] [ProCO ₂] 8d	yellow liquid	-52.60	270.40
[C ₂ OHDmim] [ProCO ₂] 8e	yellow liquid	-40.30	277.50
[Choline] [ProCO ₂] 8f	brown liquid	-79.85	^[e]

^[a] Glass transition temperature (T_g) was determined by DSC measurements at a heating/cooling rate of 10 °C.min⁻¹ for all salts. ^[b] Decomposition temperature (T_{dec}) was determined by TGA studies. ^[c] Not observed by DSC studies. ^[d] Melting temperature was determined on Electrothermal Melting Point Apparatus. ^[e] Not determined.

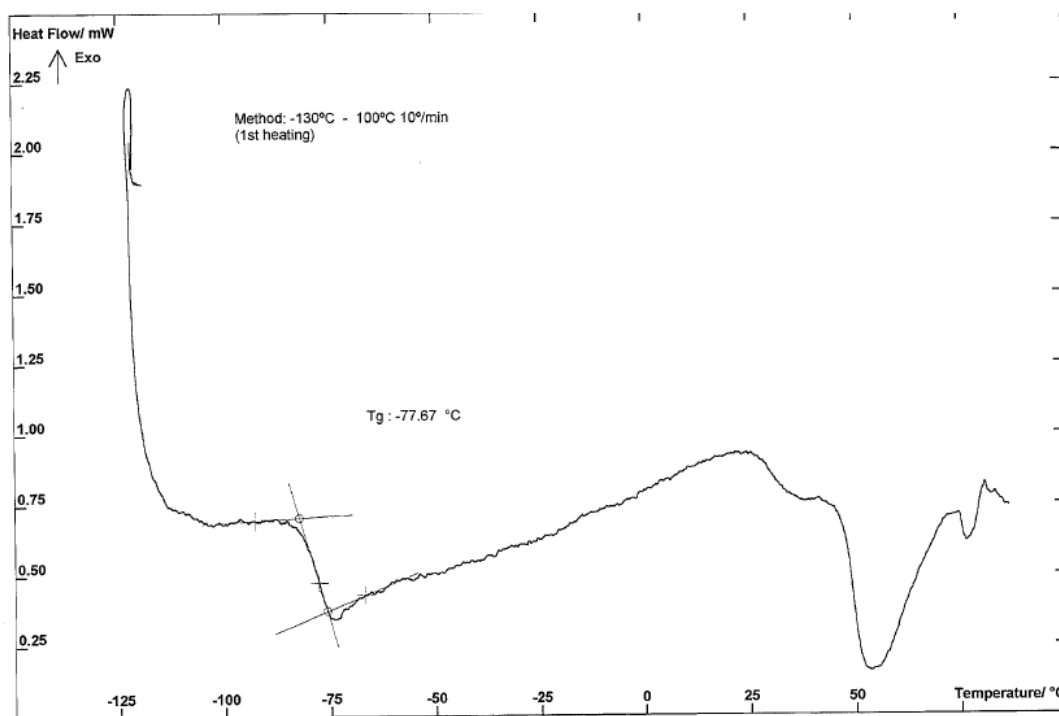


Figure III.7- DSC curve of $[\text{ProNH}_2][\text{NTf}_2]$ (7a) in a heating cycle.

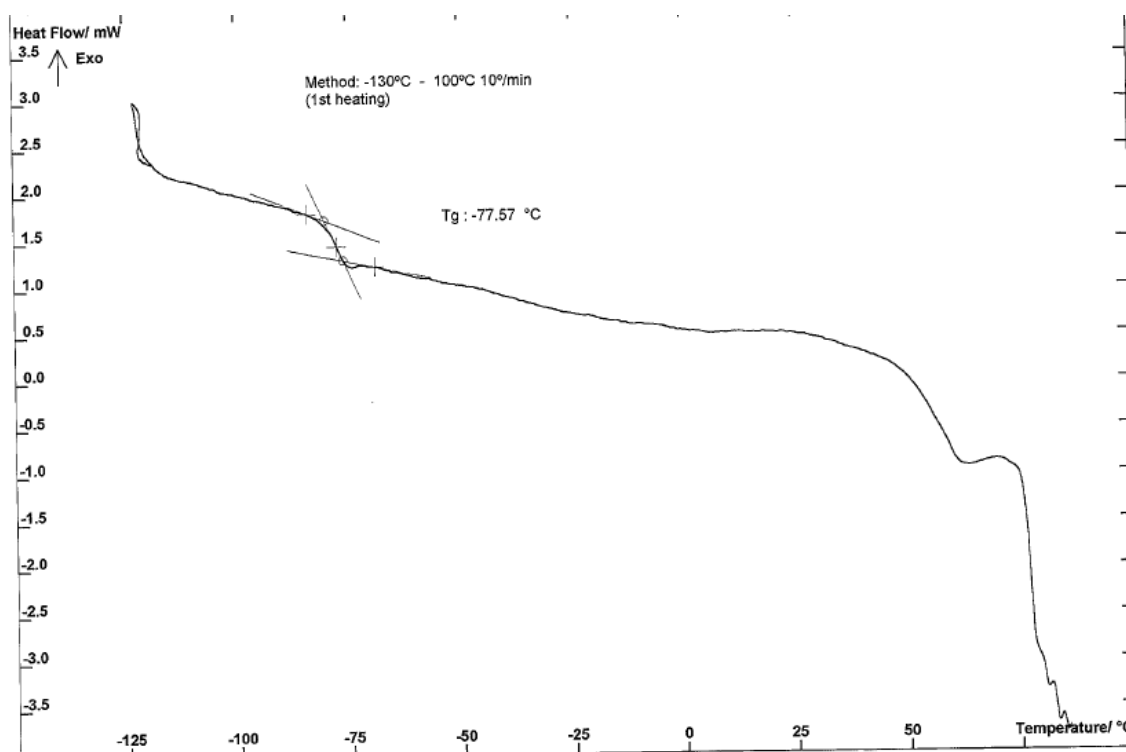


Figure III.8- DSC curve of $[\text{Emim}][\text{ProCO}_2]$ 8b in a heating cycle.

III.5. Rheology studies of novel *L*-proline based salts

The behavior of a fluid in a flow is very much correlated to two of its intrinsic characteristics: density and viscosity. The second is one of the most important physical properties of a liquid system. Measurements of viscosity have been performed on protein, polystyrene, pineapple juice, vegetable oil and dark beer among other (bio)materials¹³⁰. Viscosity changes upon shear rate, pressure, moisture, and concentration and all these changes can be described by equations. Viscosity decreases with increasing temperature and the relationship is normally fitted by Arrhenius-type relationship that is shown below:

$$\eta = Ae^{\frac{Ea}{RT}} \quad \text{Eq. III.1}$$

where η is dynamic viscosity (Pa.s); A is the pre-exponential factor (Pa.s); Ea is the exponential constant known as activation energy (J.mol⁻¹); R is the gas constant (J.(mol/K)⁻¹) and T is the absolute temperature (in Kelvin). The value of A can be described as the infinite-temperature viscosity η_{∞} , which is strict in the limit of infinite temperature. Therefore, equation III.1 can be composed in the following form:

$$\eta = \eta_{\infty} e^{\frac{Ea}{RT}} \quad \text{Eq. III.2}$$

Newtonian's law of viscosity defines the relationship between the shear stress and the shear rate of a fluid subjected to a mechanical stress. The ratio of share stress to share rate is a constant for a given temperature and pressure and it is defined as the viscosity or coefficient of viscosity.

In these terms, viscosity distinguishes two broad classes of fluids: Newtonian and non-Newtonian. Newtonian fluids have a constant viscosity despite of the strain rate (Figure III.9). Low-molecular-weight pure liquids are examples of Newtonian fluids. Non-Newtonian fluids do not have a constant viscosity and they will moreover thicken or thin when strain is applied. ILs are much more viscous than common solvents and commonly classified as Newtonian fluids.

In this part of work, we are interested in the study of Newtonian behaviour of some novel proline-based ILs, to model the changes in viscosity as a function of temperature, followed by the calculation of activation energy. In this context, several types of CILs derived from *L*-proline including [P_{6,6,14}][ProCO₂], **8a**, [C₃Omim][ProCO₂], **8c**, [C₂OHmim][ProCO₂], **8d**, and [C₂OHDmim][ProCO₂], **8e**, were chosen for the viscosity studies using a rotational

viscosimeter. This method could potentially give us information regarding the Newtonian behavior of the developed ILs. In the first step, all selected chiral RTILs were tested in order to evaluate if they follow the Newtonian's law. The profile of strain versus shear rate indicates that these CILs show a Newtonian fluid behavior. Although the viscosity changes with temperature, it does not change with the shear rate. So, at a given temperature, the viscosity of a Newtonian fluid remains constant regardless of which viscosimeter model, spindle or speed is used to measure it (Figure III.10).

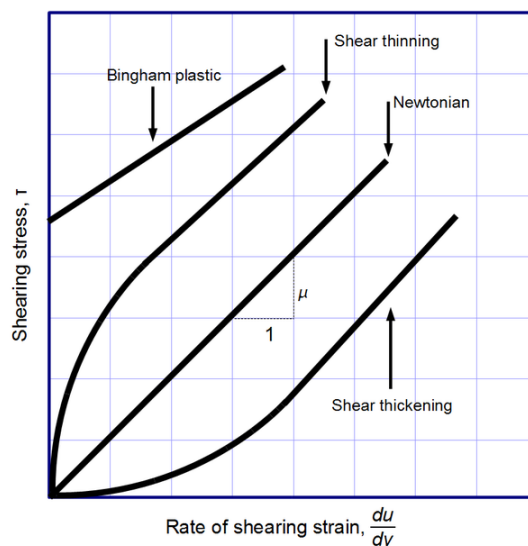


Figure III.9- Viscosity, the slope of each line, varies among materials.

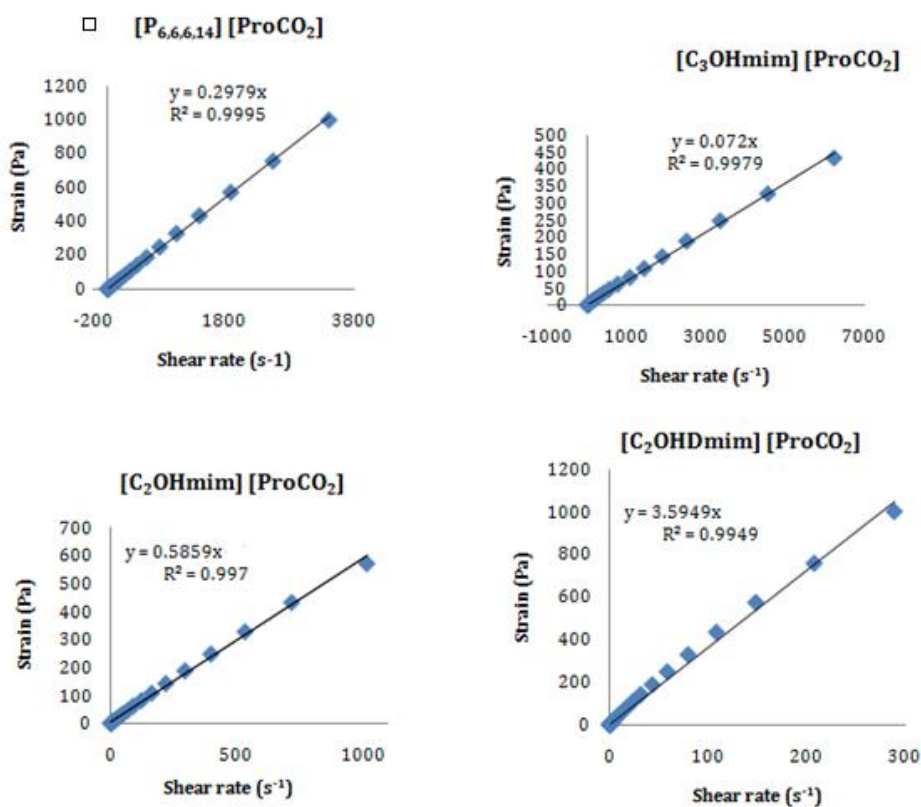


Figure III.10 - Studies on the Newtonian behaviour of CILs derived from L-proline.

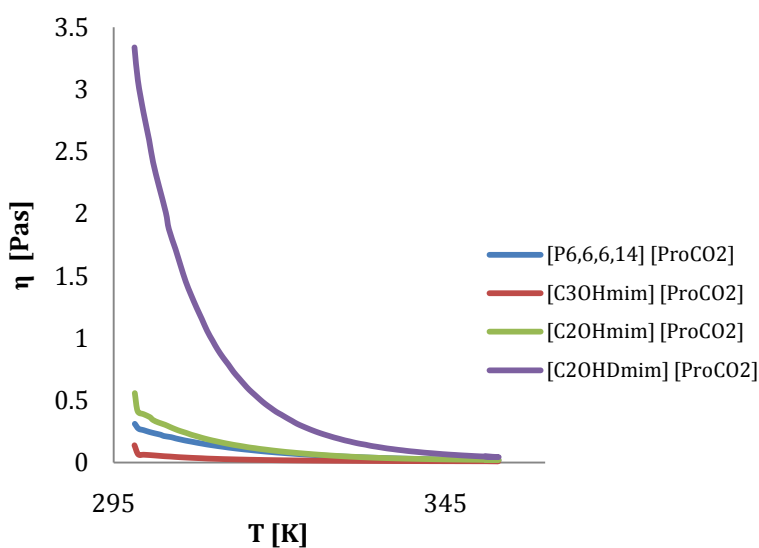
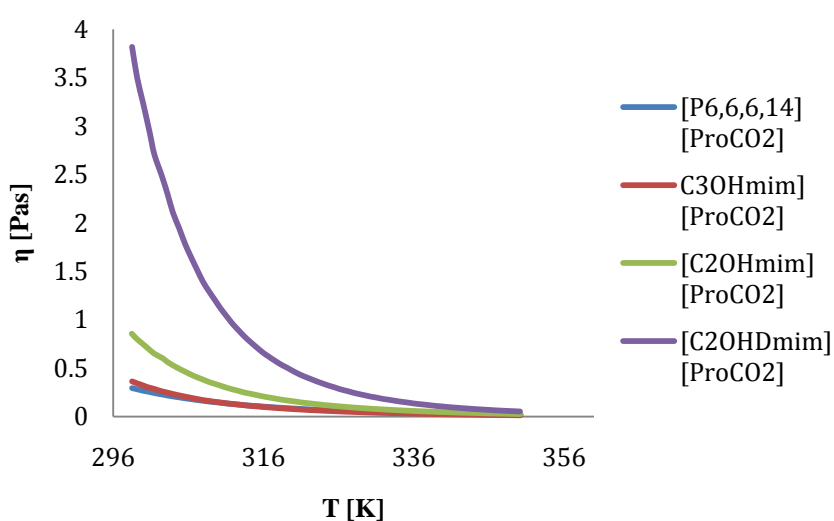
Table III.3 summarizes the viscosity values of L-proline based salts at room temperature. The viscosities of these CILs vary between 0.275 to 2.971 Pa.s depending on the cation species. $[C_3O\text{mim}][\text{ProCO}_2]$, **8c**, showed the lowest viscosity value (0.275 Pa.s) while $[C_2OHD\text{mim}][\text{ProCO}_2]$ indicated us a very viscous fluid at room temperature. Comparison of imidazolium based ILs followed a sequence $[C_3O\text{mim}] < [C_2OH\text{mim}] < [C_2OHD\text{mim}]$. As described in the literature, the overall contribution of the strong electrostatic terms to the interactions diminishes with an increase in the side-chain length⁵. Nevertheless, the contribution of weaker, non-associating, dispersion forces also improves the viscosity. Therefore, viscosity enhances with an increase on the size of the non-polar part of the cation. Also, the terminal hydroxy group of the cation might contribute to strong inter-molecular hydrogen bonding, explaining higher viscosity values. The water content according to the choice of counterions was also not without significance.

In the second part of the rheology studies, the relation between temperature and viscosity was monitored. In this context, studies related with viscosity variation as a function of temperature were performed. A temperature controller (temperature accuracy of ± 1 °C) was used to increase (heating studies) and decrease (cooling studies) the temperature of the CILs samples from 25 °C (298.15 K) to 80 °C (353.15 K) and from 80 °C back to 25 °C with an increment of 0.5 °C. The results are shown in Figures III.11 and III.12. As expected, the viscosity decreases with the increase of temperature. This kind of information could be important for our future work on optimization of the conditions for asymmetric catalysis using proline-based salts as catalysts. The activation energy of viscous fluids (E_a), was obtained by fitting the viscosity temperature dependence in the Arrhenius equation, for all ILs tested. Results collected in the case of $[C_2OHD\text{mim}][\text{ProCO}_2]$, **8d**, are presented in Figures III.13 and III.14. Activation energies vary from 46 to 77 kJ.mol⁻¹ at 25 until 80 °C (with accuracies of $R^2 > 0.990$ for all individual plots, except in case of **8c** in heating process). E_a values depend on the structure of the cation and anion (Table III.3).

In general, rheological relationships contributed for a better understanding of the fluids aimed in these studies, in terms of either knowing their behaviour or force them to behave according to the required.

Table III.3- Parameters of Arrhenius plots calculated for CILs derived from L-proline.

<i>CIL</i>	<i>Viscosity</i> (25°C) [Pa.s]	<i>Heating</i>		<i>Cooling</i>	
		<i>Ea</i> [kJ/mol]	<i>R</i> ² - <i>squared</i> <i>value</i>	<i>Ea</i> [kJ/mol]	<i>R</i> ² - <i>squared</i> <i>value</i>
[P _{6,6,6,14}][ProCO ₂] 8a	0.312	47	0.992	46	0.999
[C ₃ Omim][ProCO ₂] 8c	0.275	54	0.771	57	0.999
[C ₂ OHmim][ProCO ₂] 8d	0.558	56	0.990	63	0.999
[C ₂ OHDmim][ProCO ₂] 8e	2.971	75	0.999	77	0.999

**Figure III.11 - Viscosity of proline based salts as a function of temperature at heating studies.****Figure III.12 - Viscosity of proline based salts as a function of temperature at cooling studies.**

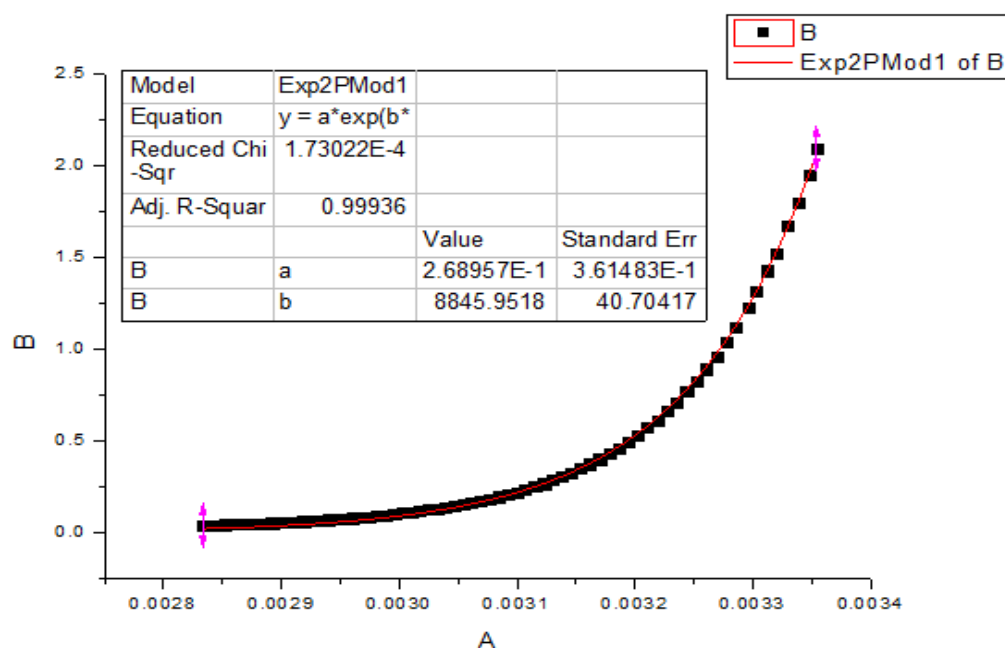


Figure III.13 - Scheme developed for $[\text{C}_2\text{OHmim}][\text{ProCO}_2]$ 8d in order to calculate the activation energy (E_a) and the R squared values during heating.

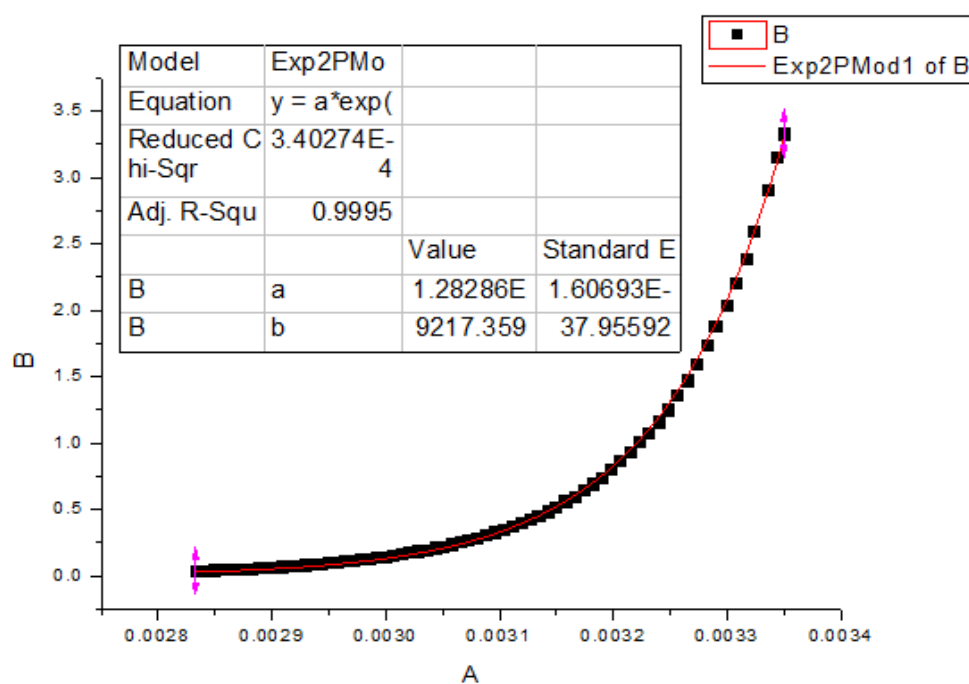


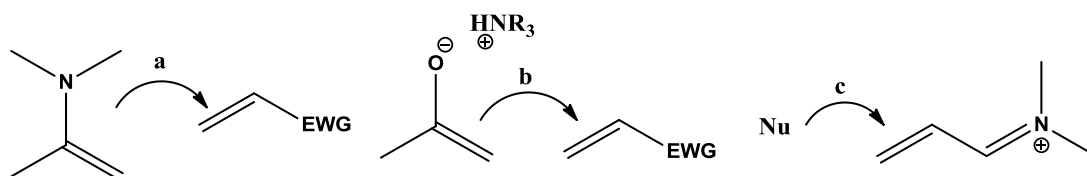
Figure III.14 -Scheme developed for $[\text{C}_2\text{OHmim}][\text{ProCO}_2]$ 8d in order to calculate the activation energy (E_a) and the R squared values during cooling.

III.6. *Proline based CILs for asymmetric Michael Addition*

The purpose of this new family of CILs, after its detailed characterization, is related with the evaluation of their potential as catalysts in asymmetric reactions. In contrast to cysteine-based CILs which were tested in asymmetric aldol reactions, as presented in chapter II, proline salts were examined in another important carbon-carbon bond forming reaction: asymmetric Michael reaction.

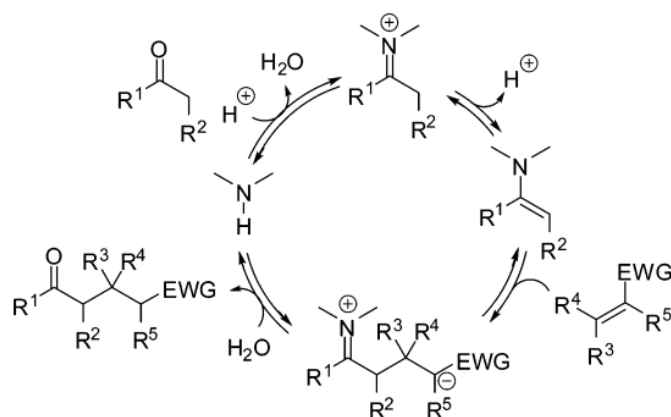
Since the Michael addition of ketone (Michael donor) to nitroalkenes (Michael acceptor) catalyzed by L-proline upraised, many research groups have been concentrated on development of more efficient and selective catalytic systems using CILs derived from natural acids for this functional transformation. The advantage of using proline as a nucleophile with carbonyl groups or Michael acceptors to form iminium ions or enamines is related with its enhanced nucleophilicity comparing with other amino acids due to its secondary amine functionality and higher pKa value¹³¹.

In general, the Michael donor can be catalytically activated either through enamine or enolate formation for the addition to a Michael acceptor (Scheme III.4, paths a and b). There is also the possibility for carbonyl-derived Michael acceptors to be activated via formation of an iminium species (Scheme III.4, path c)¹³².



Scheme III.4 –Enamine-, Enolate-, and Iminium- Catalytic Michael Reaction, where EWG=electron withdrawing group¹³².

The enamine-catalytic Michael addition of carbon nucleophiles to nitroalkenes is a useful synthetic method for the preparation of γ - nitrocarbonyl compounds due to its possible transformations, for example to pyrrolidines, aminocarbonyl compounds or aminoalkanes. Enamines can be formed reversibly from amines and carbonyl compounds and used as intermediates in a catalytic cycle (Scheme III.5). Similar to the well-studied reactions of preformed enamines, further reaction with an acceptor leads to the final Michael adduct. Interestingly, hydrolysis with in situ-generated water liberates the product and restores the catalyst.



Scheme III.5 - Enamine-Catalyzed Michael Reaction.

Common strategies often include the need of strongly acidic additives to obtain a protonated ammonium moiety as essential H-bonding unit, which is characteristic for enamine-based organocatalysis¹³³. Toxic and corrosive trifluoroacetic acid or other strong acids have to be added to observe high diastereo- and enantioselectivities, and therefore the development of novel effective catalysts is still desired. This new set of CILs based on L-proline was specifically designed to replace trifluoroacetic acid in enamine-based organocatalysis for asymmetric C-C bond formation. Based on their permanent charge, these CILs could be applied as organocatalysts in asymmetric Michael addition of cyclohexanone to *trans*-nitrostyrene and good conversions and selectivities up to 97 % *ee* were obtained without additional acid. The model reaction was promoted by using a chiral catalyst in a range of loading between 10-90 mol%. Ethanol or different ILs were tested as possible reaction media. Table III.4 summarizes the different conversions, *trans-cis* ratios and enantiomeric excesses of tested asymmetric Michael reactions. The stereoselectivities can be explained by a probable transition model proposed originally by Seebach and Golinski as shown in Figure III.15¹³⁴. In this hypothesis, the pyrrolidine scaffold of the catalyst reacts with cyclohexanone to form a nucleophilic enamine and the carbonyl oxygen directs the nitro group through hydrogen bonding to organize a favorable TS.

The partially positive nitrogen of the enamine and the partially negative nitro group should be situated close to each other, due to favorable electrostatic interactions. An intermolecular hydrogen bond between the carboxylic acid moiety and the nitro group was assumed to further fix the conformation.

The attack of this enamine on the *re*-face of the nitrostyrene leads to the formation of the observed major enantiomer of the *syn* diastereomer. The formation of a cyclic intermediate might also help to explain why the diastereoisomeric ratios are so high.

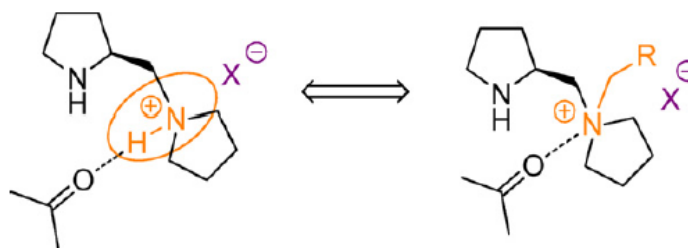


Figure III.15 - Proposed ionic liquid strategy for acid replacement based on the example of the common organocatalyst (L)-1-[(pyrrolidin-2-yl)methyl]pyrrolidin.

The initial investigation using ethanol as well as ILs as reaction media confirmed that well-known L-proline is an effective organocatalyst for asymmetric Michael addition yielding high enantioselectivities between 87 to higher than 99% (Table III.4, Entries 1-6).

The corresponding catalytic and enantioselective activities varied significantly with different ILs structures. In general, it was observed that better results could be obtained when L-proline moiety was used as the anionic unit. This fact confirms the importance of keeping the amine group not protonated (not modified). At the same time, ionic and highly polar nature of the imidazolium cation may also contribute in the TS. Interestingly, Wang and his group tested the asymmetric version of Michael addition of cyclohexanone with chalcone using [Emim][ProCO₂] in similar conditions and obtained *dr*: 15:85 and 69% of *ee*¹³⁵. In our studies different imidazolium based CILs such as [Emim] **8b**, [C₃Omim] **8c**, [C₂OHmim] **8d**, and [C₂OHDmim] **8e**, combined with the L-proline scaffold, allowed to obtain the desired product with moderate to high enantioselectivity, up to 94 % in the case of **8b** (Table III.4, Entries 20 and 21). Incorporation of a protic group in the side chain of the cation, as in **8d** and **8e**, led to a decrease in both the catalytic activity and selectivity (Table III.4, Entries 27 and 28). The use of biocompatible [Choline] cation **8f**, combined with the proline anion resulted in a significant increase of stereoselectivity to 97 %, comparing with other cations tested.

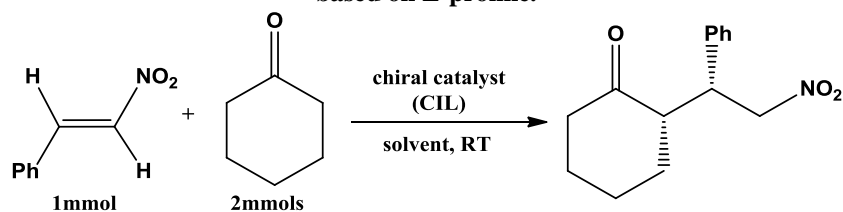
However, when the L-proline scaffold was used as cationic unit its catalytic ability drop drastically. Conversion values vary between 19 to 56% and 53-59% *ee*.

Taking in mind that ILs have been extensively tested as alternative and recyclable solvents for many catalytic and non-catalytic organic transformations, [Emim][EtSO₄] and [Bmim][DCA] as selected reaction media were also used. The replace of ethanol to these ILs provided with high enhanced on both the activities and selectivities in most of the cases. Particularly, it was possible to improve the conversion up to 100 %, *ee* and *dr* values, when docusate [AOT] and [NTf₂] were chosen as counter-ions (from 55 % to 65 % *ee* for **7b**, and from 58 % to 96 % *ee* for **7a**).

In general, the use of [Bmim][DCA] as alternative solvent showed better results when comparing with [Emim][EtSO₄].

The aim of this subsection is related with the the possibility to apply new developed L-proline based salts as asymmetric catalysts for Michael reaction. Functionalized CILs tested in this work showed comparable performance with previously reported chiral pyrrolidine catalysis in EtOH or ILs as reaction media. For example, only 30 mol% of L-proline based CILs without any additive was required to catalyze cyclohexanone addition to nitrostyrene in ILs with 100% conversion after 90 h (*d.r.*=91:9 and 97% *ee* for the *syn* diastereomer).

After the optimization of catalytic reaction conditions, further efforts to study several nitroalkenes in the presence of cyclohexanone should be performed, in order to emphasize the potential of these novel CILs based on L-proline for asymmetric Michael reaction.

Table III.4- Michael addition reaction of cyclohexanone to trans-nitrostyrene catalyzed by CILs based on L-proline.

Entry	Catalyst	Loading of catalyst [mol%]	Solvent	Conversion [%]	dr (syn: anti) ^[d]	ee [%] ^[e]
1 ^[a]	L-PRO 6	10	EtOH	98	95:5	94
2 ^[a]	L-PRO 6	30	EtOH	100	93:7	94
3 ^[b]	L-PRO 6	30	EtOH	100	90:10	>99
4 ^[b]	L-PRO 6	30	[Emim][EtSO ₄]	100	90:10	87
5 ^[b]	L-PRO 6	30	[Bmim][DCA]	100	93:7	96
6 ^[c]	L-PRO 6	60	EtOH	100	91:9	96
7 ^[c]	[ProNH ₂] [Cl] 7	30	EtOH	50	85:15	53
8 ^[c]	[ProNH ₂] [TsO] 7c	30	EtOH	50	75:25	n.d. ^[f]
9 ^[b]	[ProNH ₂] [AOT] 7b	30	EtOH	19	73:27	55
10 ^[c]	[ProNH ₂] [AOT] 7b	30	[Emim][EtSO ₄]	92	78:22	n.d. ^[f]
11 ^[c]	[ProNH ₂] [AOT] 7b	30	[Bmim][DCA]	100	90:10	65
12 ^[c]	[ProNH ₂] [AOT] 7b	60	EtOH	50	82:18	59
13 ^[c]	[ProNH ₂] [NTf ₂] 7a	30	EtOH	34	80:20	58
14 ^[c]	[ProNH ₂] [NTf ₂] 7a	30	[Emim][EtSO ₄]	92	64:36	n.d. ^[f]
15 ^[c]	[ProNH ₂] [NTf ₂] 7a	30	[Bmim][DCA]	100	91:9	96
16 ^[c]	[ProNH ₂] [(+)-CSA] 7f	30	EtOH	56	67:33	n.d. ^[f]
17 ^[c]	[Na] [ProCO ₂] 8	30	EtOH	100	78:22	73
18 ^[c]	[P _{6,6,6,14}] [ProCO ₂] 8a	30	EtOH	100	83:17	69
19 ^[c]	[Emim] [ProCO ₂] 8b	30	EtOH	100	86:14	78
20 ^[c]	[Emim] [ProCO ₂] 8b	30	[Emim][EtSO ₄]	100	94:6	94
21 ^[c]	[Emim] [ProCO ₂] 8b	30	[Bmim][DCA]	100	92:8	94
22 ^[c]	[Emim] [ProCO ₂] 8b	60	EtOH	100	69:31	81
23 ^[a]	[C ₃ Omim] [ProCO ₂] 8c	30	EtOH	100	72:28	74
24 ^[c]	[C ₃ Omim] [ProCO ₂] 8c	60	[Emim][EtSO ₄]	100	74:26	76
25 ^[c]	[C ₃ Omim] [ProCO ₂] 8c	90	[Emim][EtSO ₄]	100	75:25	83
26 ^[c]	[C ₃ Omim] [ProCO ₂] 8c	30	EtOH	100	75:25	93
27 ^[c]	[C ₂ OHmim] [ProCO ₂] 8d	30	EtOH	100	70:30	62
28 ^[c]	[C ₂ OHDmim][ProCO ₂] 8e	30	EtOH	100	65:35	55
29 ^[c]	[Choline] [ProCO ₂] 8f	30	[Emim][EtSO ₄]	100	91:9	95
30 ^[c]	[Choline] [ProCO ₂] 8f	30	[Bmim][DCA]	100	91:9	97

^[a] Reaction time: 48 h. ^[b] Reaction time: 66 h. ^[c] Reaction time: 90 h. ^[d] The trans-cis ratios were determined from 400.13 MHz ¹H NMR spectroscopy. ^[e] Determined by HPLC using Phenomenex Lux 5 um 250x10 cellulose column, flow 1ml.min⁻¹, 25 °C column oven, hexane: i-PrOH 90:10, λ=230nm. ^[f] Not determined.

III.6.1. Extraction of Michael adduct with supercritical carbon dioxide ($scCO_2$)

In the previous subchapter, studies on the optimization of asymmetric Michael addition using L-proline based CILs as organocatalysts were presented. Despite the high activities and selectivities, some limitations were observed during the isolation process of the chiral product. Following the purification methods reported in the literature, extractions with different organic solvents as n-hexane, diethyl ether (Et_2O) or methyl tert-butyl ether (MTBE) were tested. In non of those cases was possible to separate efficiently the desired Michael product from the CILs because of the good solubility of novel CILs in a large range of solvents. 1H NMR spectroscopy studies confirmed that some of the collected samples after simple extraction with organic solvents were still contaminated with CILs. Therefore, further purification of the resulting residue by flash column chromatography using ethyl acetate/hexane (1:2) allowed a pure isolation of the chiral products. Additionally, the reuse of chiral catalyst and IL reaction media was not possible using organic solvent extraction method. In this context the possibility to use supercritical carbon dioxide ($scCO_2$) as a more sustainable and efficient extraction and recycle methodology can be relevant.

Supercritical carbon dioxide ($scCO_2$) is a fluid state of carbon dioxide where it is held at or above its critical temperature and critical pressure as shown in Figure III.17¹³⁶. According to its role in chemical extraction, in addition to its low toxicity and environmental impact, $scCO_2$ is becoming a significant commercial and industrial green solvent^{137,138}. The quite low temperature of the process and the stability of CO_2 also allow most compounds to be extracted with little damage or denaturing. In addition, the solubility of many extracted compounds in CO_2 differs with pressure, permitting selective extractions¹³⁶.

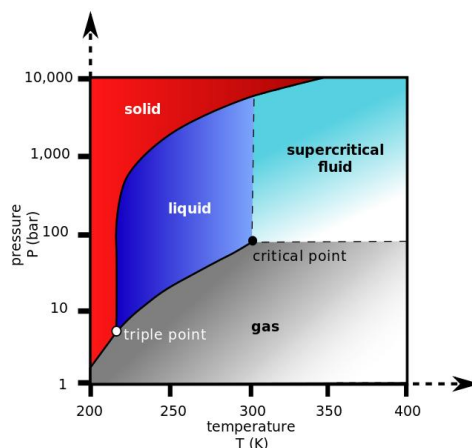
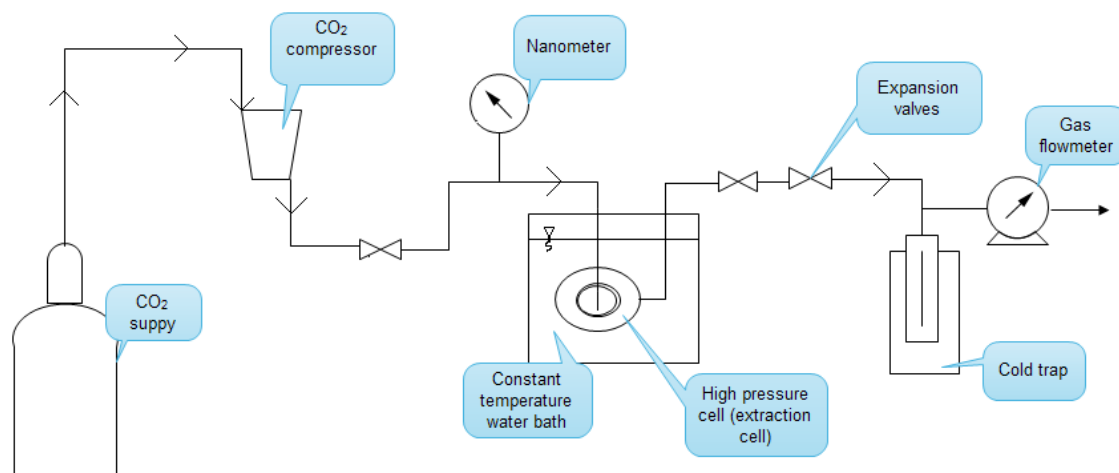


Figure III.16 - Carbon dioxide pressure-temperature phase diagram¹³².

As long as ILs are not soluble in $scCO_2$, there is a possibility to extract our Michael product from the reaction mixture. Therefore, advanced methods for separation and purification of

Michael adduct from ILs, by using *sc*CO₂ as a co-solvent have been performed in collaboration with Prof. M. N. Ponte and co-workers (PhD student Małgorzata Zakrzewska). The *sc*CO₂ extraction was carried out in the apparatus described in Scheme III.5. The model reaction was carried out using cyclohexanone and nitrostyrene, [Emim][ProCO₂] as asymmetric catalyst and [Emim][EtSO₄] as solvent.



Scheme III.6 - General scheme of the extraction of chiral Michael product using *sc*CO₂.

Some preliminary optimization of the conditions for extraction with *sc*CO₂ has been studied. Using ¹H NMR spectroscopy, it was concluded that the initial tests failed due to the presence of small amount of ILs impurities (8-16%). During the extraction experiments, different parameters such as extraction time, pressure, temperature, amount of *sc*CO₂ and speed of bubbling were changed in order not only to separate the 2-((*R*)-nitro-1-phenyl)cyclohexanone from the reaction mixture, but also to obtain the products with high yields. It was proved by ¹H NMR that the spectrum of the final product is pure and no peaks of ILs were detected as presented in Figure III.17. Nevertheless, further improvements of final Michael adduct yields and the reusability of the catalyst to perform more cycles are in progress in our laboratory in collaboration with Prof. M. N. Ponte group.

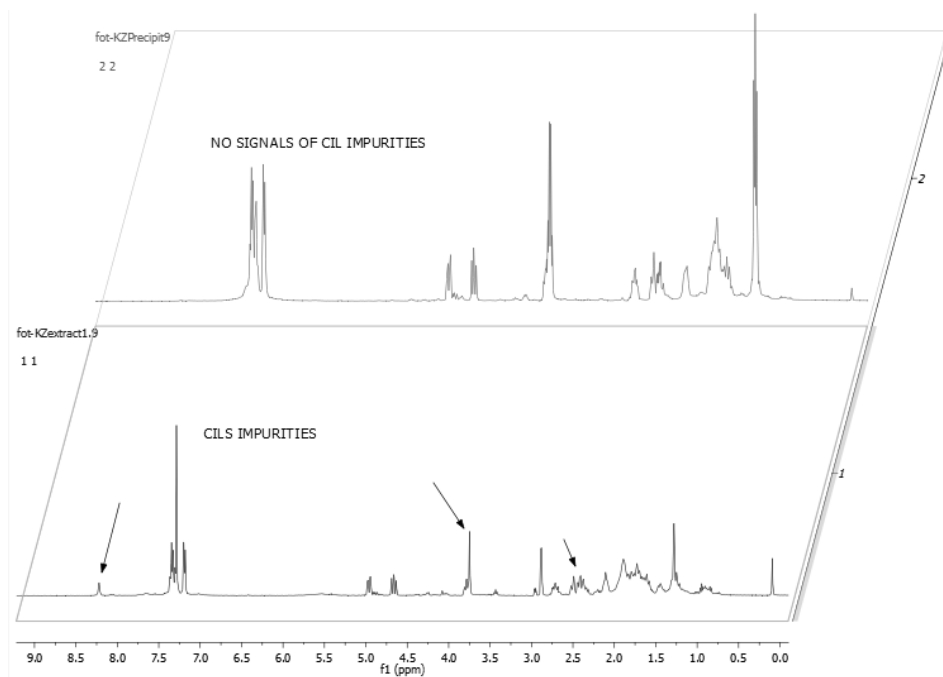


Figure III.17 - ^1H NMR spectra of Michael adduct extracted with scCO_2 (pure product up, mixture of product and catalyst down).

III.7. Other efforts related with synthesis attempts

Among those twelve CILs derived from L-proline successfully synthesized, characterized and applied for asymmetric organocatalysis, there were other attempts to develop new CILs based on L-proline scaffold as the cation combined with different anions, such as ascorbic [vitC] and dicyanamide [DCA] (Figure III.18). Studies on the protonation of L-proline amino group using acids stronger than hydrochloric acid, as mesylic and weaker, as glucolic acids, were also performed. All these efforts related with the synthesis resulted in failures. To understand and explain the reason of the methodology failure, more attention should be paid to the section of protic ILs. They are formed simply by proton transfer from pure Brønsted acid to pure Brønsted base. The presence of a variable proton activity is its special characteristic that makes them more conductive than in the aprotic cases. In fact, by taking advantage of these features, some of the most conductive liquids ever known have been obtained¹³⁹.

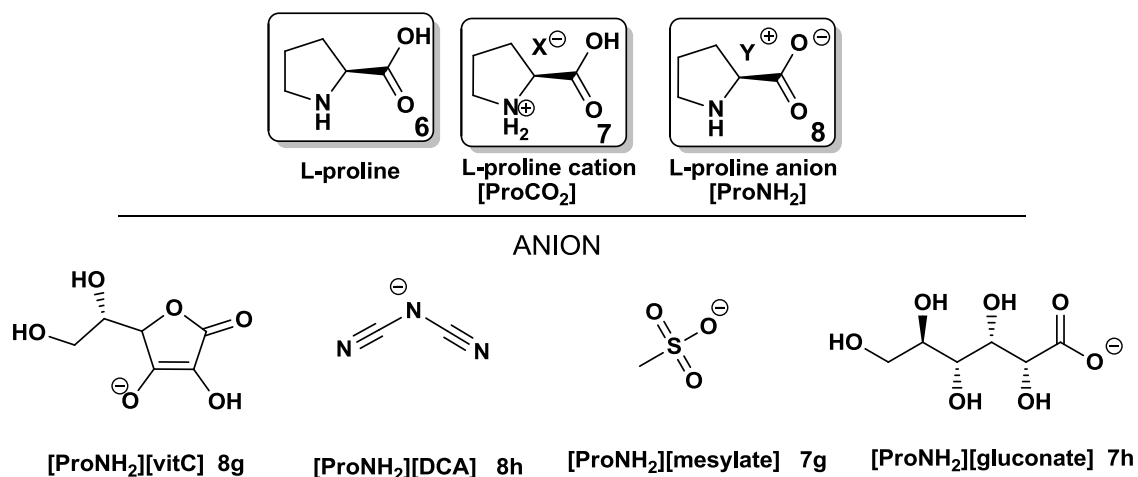


Figure III.18 - Structures of counter-ions tried for synthesis of L-proline based salts.

According to the information available in the literature, it is understandably possible to develop salts based on L-proline as the anion because there isn't a pK_a problem. The amino group stays unchanged while the carboxylic acid group gets deprotonated. Nevertheless, in the case of ILs derived from L-proline used as cation, the protonation of amino group must be achieved in order to check protic ionic liquids based on L-proline scaffold. In some cases the counter-ions were not strong enough to keep the positive charge on $-NH_2$ group of L-proline. Low pK_a values in comparison with those from L-proline ($pK_a=10.96$ for α -amino group) proved that a stronger acid is needed to obtain a stable salt and those anions used weren't enough acidic.

Due to the fact that sulfonates are good anionic scaffolds to maintain the positive charge on the cation, studies on the protonation of L-proline by mesylic acid were performed. All our attempts to use this protonation method failed. Tests on the optimization of conditions for the synthesis were carried out. Different parameters have been changed during the studies such as time (1-24 hours), substrates proportion and the molarity of the fresh prepared solution of mesylic acid (methanesulfonic acid) in methanol varying from 0.05-1M $CH_3SO_3H/MeOH$. 1H NMR spectra proved that the final compound was either a mixture of both forms, the neutral and the ionic (unfinished protonation), or a big excess of acid (the presence of a mixture of mesylate anion and the acid form). Unfortunately, none of our attempts allowed the desired proportion of L-proline mesylate, **7g**, to be obtained.

Another approach was focused in the protonation of amino acid moiety with gluconic acid, **7h**, which also failed. The 1H NMR studies showed that the protonation wasn't completed because of the weakness of the gluconic acid. Furthermore, it was also difficult to distinguish the peaks from both cation and anion because they overlapped on the NMR spectrum. Nevertheless, both of

these compounds **7g** and **7h** should be possible to obtain with a more precise control of the addition step.

According to the design of proline-camphorsulfonates (**7e** and **7f**), the proposal of proline ascorbate, **8g**, as another possible example of proline salt with chirality on both cation and anion was studied. In contrast to **7e** and **7f**, not good results were obtained. Our first attempt was to protonate the NH group of L-proline in order to create proline hydrochloride, followed by a simple ion exchange reaction using sodium ascorbate. Due to the poor solubility of sodium ascorbate in many common solvents, including methanol, water was selected as reaction media but no reaction occurred. In the case of [Pro][DCA], **8h**, after finishing the protonation of L-proline, the isolated proline hydrochloride reacted with sodium dicyanamide Na[DCA] in anion exchange reaction using methanol as solvent. Problems associated with purification of the final salt limited its characterization and future application.

III.8. Conclusions

A series of novel CILs have been prepared using L-proline, a naturally-derived and inexpensive material, as cation or anion. As expected according with counter ion type is possible to tune the physical, chemical and thermal properties of different CILs based on L-proline. The class of Amino Acids (AAs) again confirmed to be a good model to study the relation between ion structure and properties and significant in the designing of novel task-specific ILs. It was demonstrated that by using the simple ion exchange reaction and the alternative ion exchange resin method, it was possible to obtain the required CILs in good yields and purities. Properties like optical rotation, glass transition and decomposition temperatures (T_g , T_{dec}), density and viscosity of some bioinspired ionic liquids (Bio-ILs) were studied. In most of the cases glass transition temperatures were detected in contrast with initial crystalline L-proline. The objectives of the rheology studies were related with the Newtonian behaviour of the liquids, the relation between viscosity and activation energy (E_a) and reliable indicator of the viscosity – temperature stability of CILs from the comparison of the E_a and the experimental data. It was proved that E_a depends on the structure, the combination cation anion of the prepared salt and varies between 46 kJ.mol^{-1} and 77 kJ.mol^{-1} at $25 - 80^\circ\text{C}$ with accuracies of $R^2 > 0.990$ for individual plots.

L-proline based salts showed potential to be used as organocatalyst for asymmetric Michael reaction. Cyclohexanone could react with *trans*-nitrostyrene to afford Michael adducts with 100% of conversion and moderate to good enantioselectivities (53–94% *ee*), particular in the

presente of [Emim][ProCO₂], **8b**, [C₃Omim][ProCO₂], **8c**, [C₂OHmim][ProCO₂], **8d**, and [Choline][ProCO₂], **8f**. The precise design and selection of the cation (e.g., imidazole, choline) and anion scaffold of amino acid might lead to enhance levels of activity and selectivity. In addition, recovery of the product out of the CILs and ILs using *sc*CO₂ was studied experimentally. The extracted product was found to contain no detectable amount of ILs.

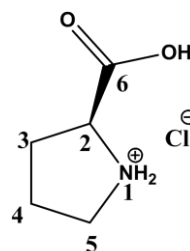
While the Bio-ILs developed are potential candidates as environmentally-benign and low-toxicity ILs, further research on their preparation method and toxicology should be addressed.

III.9. *Experimental Part*

General: Commercially available reagents L-proline (MW= 115.13 g.mol⁻¹, CAS No. 147-85-3), ionic liquids and solvents were purchased from Alfa Aesar, Aldrich, Solchemar and were used without further purification. The basic anion-exchange resin Amberlite IRA-400-OH (ion-exchange capacity 1.4 eq.mL⁻¹) was purchased from Supelco. ¹H and ¹³C NMR spectra were recorded at 25 [°C] on a Bruker AMX400 spectrometer with TMS as internal standard. Chemical shifts are reported downfield in ppm. IR spectra were performed by Perkin Elmer model Spectrum 1000 using NaCl plates for neat liquids. DSC analysis was carried out using a TA Instruments Q-series™ Q200 DSC with a refrigerated cooling system. The samples for elemental analysis were performed by Laboratório de Análises at REQUIMTE, Departamento de Química Faculdade de Ciências e Tecnologia (Monte da Caparica) using Thermo Finnigan-CE Instruments equipment, model Elemental Analyser 1112 series. Density measurements were performed with the use of pycnometer at room temperature (25 °C). Optical rotations were recorded on a Perkin Elmer 241MC. The melting point (mp) was determined by Electrothermal Melting Point Apparatus. The decomposition temperatures were measured with the Simultaneous Thermal Analyser STA 449 F3 Jupiter, using a nitrogen atmosphere (mass changed in % or mg). Rheology studies were performed at Instituto Jean Piaget in Almada, Portugal by using a Rheometer (RS-300, Haake, Germany). Measurements were carried out using a controlled-stress rheometer fitted with a coneplate sensor C20/2 °Ti. The torque amplitude was imposed by using a logarithmic ramp of shear stress, which was increased in 30 min intervals from 0.01 to 1000 Pa to decrease the initial acceleration and the effects due to instrument inertia. The temperatures of the samples were maintained at (20±0.5) °C by means of a circulating water bath (DC30, Haake, Germany), and they were measured with a thermocouple attached to the stationary element. The temperature dependence of the viscosity was also studied. The ILs were heated from 20 to 70 °C (0.5 °C.min⁻¹), using a constant shear stress of 5 Pa. All the measurements were performed at least twice.

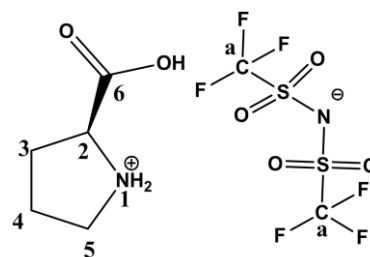
III.9.1. Synthesis of (S)-proline hydrochloride - cationic approach (7)

In the first step (S)-proline **1** (1 g; 8.69 mmol) was dissolved in 15 ml of methanol and 1M solution of HCl in MeOH (1:1 eq., 8.69 ml) was added slowly in order to protonate the amine group. The reaction mixture was stirred at room temperature for 24 hours. The solution was evaporated and dried *in vacuo* for ~5 hours. The (S)-proline hydrochloride **2** was obtained as a viscous yellow liquid (1.31 g, 100%). ^1H NMR (400.13 MHz, D_2O) δ 4.27 (t, $^3J_{\text{H}_2\text{-H}_3} = 8\text{Hz}$, 1H), 3.32 – 3.20 (m, 2H, H_5 , H_5'), 2.32-2.27 (m, 1H, H_3), 2.06-2.00 (m, 1H, H_3'), 1.95 – 1.86 (m, 2H, H_4 , H_4'). ^{13}C NMR (100.61 MHz, D_2O) δ 172.12 (C_6), 59.69 (C_2), 46.20 (C_5), 28.31 (C_4), 23.37 (C_3).



III.9.2. Synthesis of (S)-2-carboxypyrrolidin-1-ium bis((trifluoromethyl)sulfonyl)amide (7a)

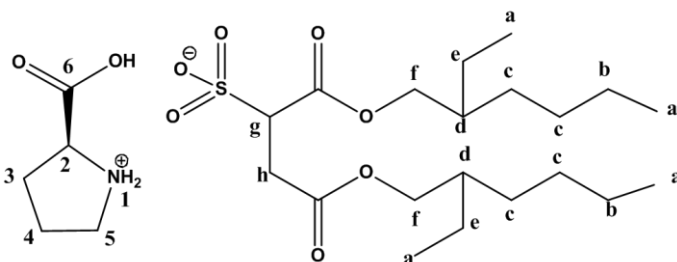
After the protonation was finished, the isolated L-proline hydrochloride (0.4 g; 2.64 mmol) was dissolved in 5ml of methanol and $\text{Li}[\text{NTf}_2]$ was added to perform the ion exchange (0.79 g; 2.77 mmol). The reaction was stirred for 24 hours at room temperature. Acetone was added in order to remove the inorganic salts by precipitation. The solution was



evaporated and dried *in vacuo* for 8 hours. The desired product was obtained as a viscous yellow liquid (0.94 g, 90%). $T_g = -77.67^\circ\text{C}$; $[\alpha]_D = -12.7 \pm 2^\circ$ ($c = 1 \text{ mg.mL}^{-1}$ in MeOH); ^1H NMR (400.13 MHz, D_2O) δ 4.27 (t, $^3J_{\text{H}_2\text{-H}_3} = 8\text{Hz}$, 1H), 3.38 – 3.25 (m, 2H, H_5 , H_5'), 2.38-2.278 (m, 1H, H_3), 2.13-2.02 (m, 1H, H_3'), 1.99 – 1.92 (m, 2H, H_4 , H_4'). ^{13}C NMR (100.61 MHz, D_2O) δ 172.12 (C_6), 120.79 (C_a), 59.69 (C_2), 46.20 (C_5), 28.31 (C_4), 23.37 (C_3). ^{19}F NMR (376 MHz, DMSO) δ -79.19. FTIR (NaCl) $\nu = 3414, 2362, 2345, 2067, 1638, 1350, 1199, 1133, 1056, 793, 766, 743, 666 \text{ cm}^{-1}$. Elemental analysis (%) calcd for $\text{C}_7\text{H}_{10}\text{F}_6\text{N}_2\text{O}_6\text{S}_2$ (MW= 396.28g.mol $^{-1}$): C 21.22, H 2.54, N 7.07, S 15.48; found: C 21.12, H 2.52, N 7.04, S 15.4.

III.9.3. Synthesis of (S)-2-carboxypyrrolidin-1-ium 1,4-bis((2-ethylhexyl)oxy)-1,4-dioxobutane-2-sulfonate (7b)

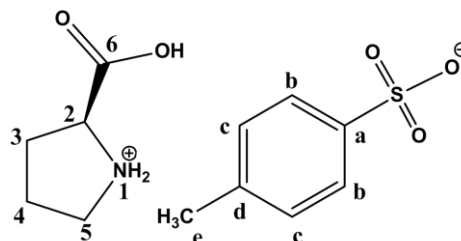
The protonated L-proline (0.5 g; 3.30 mmol) was dissolved in 5ml of methanol and sodium docusate Na[AOT] was added to perform the ion exchange (1.76 g; 1.96 mmol). The reaction was stirred for 24



hours at room temperature. Then the solvent was evaporated and the crude was redissolved in acetone in order to remove the inorganic salts by precipitation. The solution was evaporated and dried *in vacuo* for 8 hours. The desired product was obtained as a viscous yellow liquid (1.73 g, 97%). $T_g = -61.88^\circ\text{C}$; $[\alpha]_D = -12.0 \pm 2^\circ$ ($c = 1 \text{ mg.mL}^{-1}$ in MeOH); $^1\text{H NMR}$ (400.13 MHz, DMSO) δ 4.26 (t, $^3J_{\text{H}_2\text{H}_3} = 8\text{Hz}$, 1H, H_2), 3.92 – 3.87 (m, 4H, H_f), 3.62 (dd, $^2J_{\text{H}_h\text{H}_h} = 4 \text{ Hz}$, $^3J_{\text{H}_h\text{H}_g} = 8 \text{ Hz}$, 1H, H_h), 3.23 – 3.19 (m, 1H, H_5), 2.89 (m, 1H, H_g), 2.80 (dd, $^2J_{\text{H}_h\text{H}_h} = 4 \text{ Hz}$, $^3J_{\text{H}_h\text{H}_g} = 8 \text{ Hz}$, 1H, H_h), 2.25 (m, 1H, H_3), 2.03 – 1.82 (m, 3H, H_3' , H_4), 1.49 (m, 2H, H_d), 1.41 – 1.15 (m, 16H, H_b , H_c , H_e), 0.84 (m, 12H, H_a). $^{13}\text{C NMR}$ (100.61 MHz, DMSO) δ 171.49 (C_6), 170.99 ($-\text{C}=\text{O}$), 168.81 ($-\text{C}=\text{O}$), 66.65 (C_f), 66.58 (C_f'), 61.88 (C_g), 59.42 (C_2), 49.05 (C_5), 45.92 (C_d), 30.20 (C_3), 30.02 (C_c), 28.80 (C_c), 28.36 (C_h), 23.62 (C_e), 23.47 (C_b), 22.86 (C_4), 14.35 (C_a), 11.24 (C_a). FTIR (NaCl) $\nu = 3450, 2960, 2932, 2874, 2861, 2362, 2343, 1736, 1638, 1508, 1460, 1414, 1390, 1356, 1243, 1091, 1041, 855, 768, 730, 666 \text{ cm}^{-1}$. Elemental analysis (%) calcd for $\text{C}_{25}\text{H}_{47}\text{NO}_9\text{S}$ (MW= 537.71g.mol $^{-1}$): C 55.84, H 8.81, N 2.60; found: C 55.57, H 8.87, N 2.57.

III.9.4. Synthesis of (S)-2-carboxypyrrolidin-1-ium 4-methylbenzenesulfonate (7c)

The protonated L-proline (0.30 g; 1.98 mmol) was dissolved in 5ml of methanol and p-toluenesulfonic sodium salt Na[TsO] was added to perform the ion exchange (0.39 g; 2.0 mmol). The reaction was stirred for 24 hours at room temperature. Then the solvent was evaporated and the crude was redissolved in acetone in order to

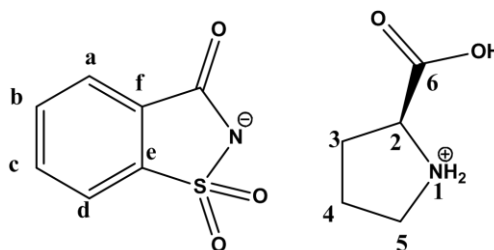


remove the inorganic salts by precipitation. The solution was evaporated and dried *in vacuo* for 8 hours. The desired product was obtained as a viscous yellow gel (0.38 g, 66%). $T_g = -25.07^\circ\text{C}$; $[\alpha]_D = -4.0 \pm 2^\circ$ ($c = 1 \text{ mg.mL}^{-1}$ in MeOH); $^1\text{H NMR}$ (400.13 MHz, CDCl_3) δ 7.70 (d, $^3J = 7.5 \text{ Hz}$, 2H, H_b), 7.16 (d, $^3J = 7.5 \text{ Hz}$, 2H, H_c), 4.48 (t, $^3J_{\text{H}_2\text{H}_3} = 8\text{Hz}$, 1H, H_2), 3.43 (m, 2H, H_5), 3.33 (m,

^1H , H_3), 2.34 (s, 3H, H_e), 2.08 (m, 1H, H_3), 1.90 (m, 2H, H_4). ^{13}C NMR (100.61 MHz, CDCl_3) δ 171.17 (C_6), 141.01 (C_a), 140.83 (C_d), 129.07 (C_c), 125.84 (C_b), 59.76 (C_2), 46.52 (C_5), 28.48 (C_3), 23.51 (C_4), 21.35 (C_e). FTIR (NaCl) ν = 3430, 2361, 2343, 2092, 1736, 1639, 1458, 1181, 1126, 1036, 1012, 819, 750, 689, 666 cm^{-1} . Elemental analysis (%) calcd for $\text{C}_{12}\text{H}_{17}\text{NO}_5\text{S}$ (MW= 287.33 $\text{g}\cdot\text{mol}^{-1}$): C 50.16, H 5.96, N 4.87, S 11.16; found: C 50.01, H 5.98, N 4.85, S: 11.12.

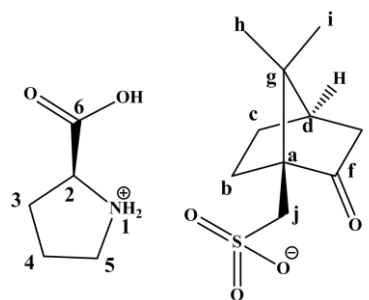
III.9.5. Synthesis of (S)-2-carboxypyrrolidin-1-ium 3-oxo-3H-benzo[d]isothiazol-2-ide 1,1-dioxide (7d)

The protonated L-proline (0.5 g; 3.30 mmol) was dissolved in 5ml of methanol and 5ml water and sodium saccharin Na[SAC] was added to perform the ion exchange (0.82 g; 3.96 mmol). The reaction was stirred for 24 hours at room temperature. Then the solvent was evaporated and the crude was redissolved in acetone in order to remove the inorganic salts by precipitation. The solution was evaporated and dried *in vacuo* for 8 hours. The desired product was obtained as a viscous yellow gel (0.96 g, 98%). $[\alpha]_D^{20} = -4.5 \pm 2^\circ$ ($c = 1 \text{ mg}\cdot\text{mL}^{-1}$ in MeOH); ^1H NMR (400.13 MHz, CDCl_3) δ 7.74 (m, 4H, H_a , H_b , H_c , H_d), 4.65-4.62 (t, $^3J_{\text{H}_2-\text{H}_3}=8\text{Hz}$, 1H), 4.47-4.44 (t, $^3J_{\text{H}_2-\text{H}_3}=8\text{Hz}$, 1H, H_2), 3.61- 3.46 (m, 2H, H_5 , H_5), 2.51 – 2.30 (m, 1H, H_3), 2.24 – 2.13 (m, 1H, H_3), 2.10 – 1.96 (m, 2H, H_4 , H_4). ^{13}C NMR (100.61 MHz, CDCl_3) δ 169.86 ($-\text{C}=\text{O}$), 167.82 (C_6), 142.36 (C_e), 133.09 (C_c), 131.54 (C_f , C_b), 124.13 (C_a), 120.43 (C_d), 59.30 (C_2), 46.30 (C_5), 29.00 (C_4), 24.24 (C_3). FTIR (NaCl) ν = 3430, 2960, 1720, 1630, 1335, 1258, 1148, 1120, 1053, 951, 758, 681 cm^{-1} . Elemental analysis (%) calcd for $\text{C}_{12}\text{H}_{14}\text{N}_2\text{O}_5\text{S}$ (MW= 298.31 $\text{g}\cdot\text{mol}^{-1}$): C 48.31; H 4.73; N 9.39; S 10.75; found: C 48.25, H 4.57, N 9.35, S: 10.80.



III.9.6. Synthesis of (S)-2-carboxypyrrolidin-1-ium ((1R, 4R)-7,7-dimethyl-2-oxobicyclo[2.2.1]heptan-1-yl)methanesulfonate (7e)

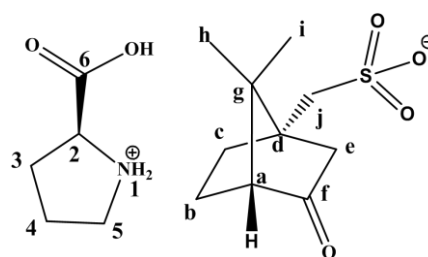
First, the (1R)-(-)-10-camphorsulfonic acid was transformed in a sodium salt. Then the acid (0.5 g, 2.12 mmol) was dissolved in 15 ml of ethanol and 0.5 M solution of NaOH in EtOH (1 eq., 4.31ml) was added dropwise. The mixture was stirred overnight at room temperature. The final salt was isolated and used for ion



exchange in the second step with [ProNH₂]Cl. The protonated L-proline (0.34 g; 2.24 mmol) was dissolved in 5 ml of methanol and camphorsulfonic acid sodium salt Na[CSA] was added to perform the ion exchange (0.57 g; 2.24 mmol). The reaction was stirred for 24 hours at room temperature. Then the solvent was evaporated and the crude was redissolved in acetone in order to remove the inorganic salts by precipitation. The solution was evaporated and dried *in vacuo* for 8 hours. The desired product was obtained as a white solid (0.78 g, 99%); *T_m* = 154 [°C]; [α]_D = -44.0 ± 2° (*c* = 1 mg.mL⁻¹ in MeOH); ¹H NMR (400.13 MHz, D₂O) δ 4.27 (t, ³*J*_{H₂-H₃} = 8 Hz, 1H, H₂), 3.34-3.29 (m, 2H, H₅), 3.17 (d, ²*J*_{H_j-H_j} = 16 Hz, 1H, H_j), 2.75 (d, ²*J*_{H_j-H_j} = 16 Hz, 1H, H_j), 2.30 (m, 3H, H₃, H₄), 2.03-1.84 (m, 6H, H₃, H_b, H_e, H_k), 1.52 (m, 1H, H_c), 1.33 (m, 1H, H_c), 0.91 (s, 3H, H_h), 0.71 (s, 3H, H_i). ¹³C NMR (100.61 MHz, D₂O) δ 210.0 (C_f), 172.19 (C₆), 59.73 (C₂), 58.43 (C_a), 48.15 (C_j), 47.09 (C₅), 46.18 (C_e), 42.54 (C_g), 28.35 (C_c), 26.15 (C₄), 24.51 (C₃), 3.22 (C_b), 18.67 (C_h, C_i). Elemental analysis (%) calcd for C₁₅H₂₅NO₆S (MW = 347.43 g.mol⁻¹): C 51.86, H 7.25, N 4.03, S 9.23; found: C 51.70, H 7.22, N 3.99, S 9.18.

III.9.7. Synthesis of (S)-2-carboxypyrrolidin-1-ium ((1S, 4R)-7,7-dimethyl-2-oxobicyclo[2.2.1]heptan-1-yl)methanesulfonate (7f)

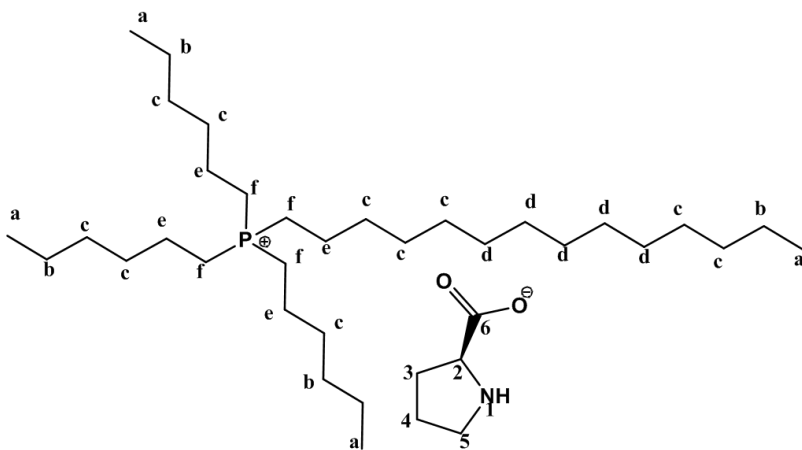
First, the (1S)-(+)-10-camphorsulfonic acid was transformed in a sodium salt. Then the acid (0.5 g, 2.12 mmol) was dissolved in 15 ml of ethanol and 0.5M solution of NaOH in EtOH (1 eq., 4.31 ml) was added dropwise. The mixture was stirred overnight at room temperature. The final salt was isolated and used for ion



exchange in the second step with [ProNH₂]Cl. The protonated L-proline (0.3 g; 2.24 mmol) was dissolved in 5 ml of methanol and camphorsulfonic acid sodium salt Na[CSA] was added to perform the ion exchange (0.57 g; 2.24 mmol). The reaction was stirred for 24 hours at room temperature. Then the solvent was evaporated and the crude was redissolved in acetone in order to remove the inorganic salts by precipitation. The solution was evaporated and dried *in vacuo* for 8 hours. The desired product was obtained as a white solid (0.74 g, 95%); *T_m* = 155-160 [°C]; [α]_D = +66.0 ± 2° (*c* = 1 mg.mL⁻¹ in MeOH); ¹H NMR (400.13 MHz, D₂O) δ 4.27 (t, ³*J*_{H₂-H₃} = 8 Hz, 1H, H₂), 3.34-3.29 (m, 2H, H₅), 3.17 (d, ²*J*_{H_j-H_j} = 16 Hz, 1H, H_j), 2.75 (d, ²*J*_{H_j-H_j} = 16 Hz, 1H, H_j), 2.30 (m, 3H, H₃, H₄), 2.03-1.84 (m, 6H, H₃, H_b, H_e, H_k), 1.52 (m, 1H, H_c), 1.33 (m, 1H, H_c), 0.91 (s, 3H, H_h), 0.71 (s, 3H, H_i). ¹³C NMR (100.61 MHz, D₂O) δ 210.0 (C_f), 172.19 (C₆), 59.73 (C₂), 58.43 (C_a), 48.15 (C_j), 47.09 (C₅), 46.18 (C_e), 42.54 (C_g), 28.35 (C_c), 26.15 (C₄), 24.51 (C₃), 3.22 (C_b), 18.67 (C_h, C_i). Elemental analysis (%) calcd for C₁₅H₂₅NO₆S (MW = 347.43 g.mol⁻¹): C 51.86, H 7.25, N 4.03, S 9.23; found: C 51.80, H 7.25, N 4.00, S 9.19.

III.9.8. Synthesis of trihexyl(tetradecyl)phosphonium (*S*)-pyrrolidine-2-carboxylate (8a)

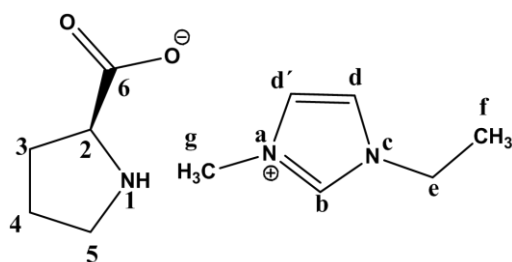
For the preparation of trihexyl(tetradecyl)phosphonium (*S*)-pyrrolidine-2-carboxylate a column ion exchange method was used. The phosphonium chloride [P_{6,6,6,14}]Cl (2.26 g; 4.34 mmol) which was first transformed into hydroxide by the use of an ionic exchange column (Amberlite IRA-400 OH) in methanol and



then this basic solution was neutralized by reacting with the (*S*)-proline (0.5 g; 4.34 mmol) in methanol solution. The mixture was stirred at room temperature for 24 hours. After the indicated time the established water was evaporated and dried *in vacuo* for 8 hours. The final product was obtained as a viscous yellow liquid (2.52 g, 97%). $T_g = -74.40\text{ }^\circ\text{C}$; $[\alpha]_D = -17.3 \pm 2^\circ$ ($c = 1\text{ mg.mL}^{-1}$ in MeOH). ^1H NMR (400.13 MHz, CDCl_3) δ 3.56 (t, $^3J_{\text{H}_2\text{-H}_3} = 8\text{ Hz}$, 1H, H_2), 3.07 (m, 1H, H_5), 2.82 (m, 1H, H_5'), 2.32 (m, 8H, H_f), 2.03 (m, 1H, H_3), 1.66 (m, 1H, H_3'), 1.45 (m, 2H, H_4), 1.27 (m, 16H, H_b, e), 1.26-1.20 (m, 32H, H_c), 0.83 (m, 12H, H_a). ^{13}C NMR (100.61 MHz, CDCl_3) δ 178.50 (C_6), 62.49 (C_2), 47.06 (C_5), 31.79 (C_c), 30.99 (C_3), 30.45 (C_e, C_d), 26.00 (C_4), 22.52 (C_f), 22.22 (C_b), 21.77 (C_e), 13.82 (C_a). FTIR (NaCl) $\nu = 3400, 2956, 2927, 2856, 2361, 1586, 1458, 1414, 1310, 1268, 1214, 1173, 1112, 1044, 986, 917, 862, 820, 721, 667\text{ cm}^{-1}$. ¹. Elemental analysis (%) calcd for $\text{C}_{37}\text{H}_{76}\text{NO}_2\text{P}$ (MW = 597.98 g.mol^{-1}): C 74.32; H 12.81; N 2.34; found: C 73.97, H 12.87, N 2.30.

III.9.9. Synthesis of 1-ethyl-3-methyl-1H-imidazol-3-ium (*S*)-pyrrolidine-2-carboxylate (8b)

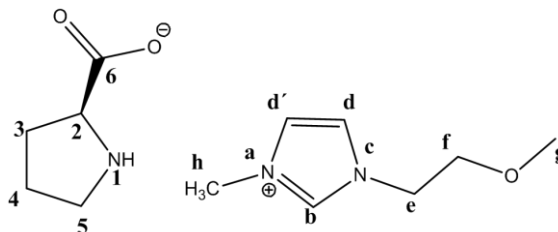
For the preparation of 1-ethyl-3-methyl-1H-imidazol-3-ium (*S*)-pyrrolidine-2-carboxylate a column ion exchange method was used. The 1-ethyl-3-methyl-1H-imidazol-3-ium bromide chloride [Emim]Br (0.83 g; 4.34 mmol) which was first transformed into hydroxide by the use of



an ionic exchange column (Amberlite IRA-400 OH) in methanol and then this basic solution was neutralized by reacting with the (*S*)-proline (0.5 g; 4.34 mmol) in methanol solution. The mixture was stirred at room temperature for 24 hours. After the indicated time the established water was evaporated and dried *in vacuo* for 8 hours. The final product was obtained as a viscous yellow liquid (1.08 g, 100%). $T_g = -77.57^\circ\text{C}$; $[\alpha]_D = -8.8 \pm 2^\circ$ ($c = 1 \text{ mg.mL}^{-1}$ in MeOH). ^1H NMR (400.13 MHz, CDCl_3) δ 7.28 (m, 3H, $\text{H}_{b, d, d'}$), 4.36 (q, $^3J_{\text{He-Hf}} = 10\text{Hz}$, 2H, H_e), 4.05 (s, 3H, H_g), 3.60 (t, $^3J_{\text{H}_2-\text{H}_3} = 8\text{Hz}$, 1H, H_2), 3.12 (m, 1H, H_5), 2.83 (m, 1H, $\text{H}_{5'}$), 2.13 (m, 1H, H_3), 1.88 (m, 1H, $\text{H}_{3'}$), 1.66 (m, 2H, H_4), 1.66 (m, 2H, $\text{H}_{4'}$), 1.56 (t, $^3J_{\text{Hf-He}} = 4 \text{ ppm Hz}$, 3H, H_f). ^{13}C NMR (100.61 MHz, CDCl_3) δ 179.63 (C_6), 122.69 (C_b), 120.73 (C_d), 62.62 (C_2), 47.04 (C_5), 44.99 (C_e), 36.26 (C_g), 31.45 (C_3), 26.17 (C_4), 15.44 (C_f). FTIR (NaCl) $\nu = 3400, 3154, 3108, 2973, 2876, 2361, 2343, 1578, 1390, 1171, 1092, 1032, 959, 917, 856, 766, 702, 667, 649, 623 \text{ cm}^{-1}$. Elemental analysis (%) calcd for $\text{C}_{11}\text{H}_{19}\text{N}_3\text{O}_2$ (MW = 225.29 g.mol^{-1}): C 58.64; H 8.50; N 18.65; found: C 58.40, H 8.53, N 18.57.

III.9.10. Synthesis of 1-(2-methoxyethyl)-3-methyl-1H-imidazol-3-ium (*S*)-pyrrolidine-2-carboxylate (8c)

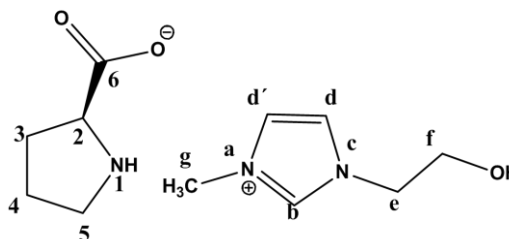
For the preparation of 1-(2-methoxyethyl)-3-methyl-1H-imidazol-3-ium (*S*)-pyrrolidine-2-carboxylate a column ion exchange method was used. The 1-(2-methoxyethyl)-3-methyl-1H-imidazol-3-



ium chloride [C_3Oimim] Cl (0.77 g; 4.34 mmol) which was first transformed into hydroxide by the use of an ionic exchange column (Amberlite IRA-400 OH) in methanol and then this basic solution was neutralized by reacting with the (*L*)-proline (0.5 g; 4.34 mmol) in methanol solution. The mixture was stirred at room temperature for 24 hours. After the indicated time the established water was evaporated and dried *in vacuo* for 8 hours. The final product was obtained as a viscous yellow liquid (0.83 g, 99%). $T_g = -83^\circ\text{C}$; $[\alpha]_D = -5.3 \pm 2^\circ$ ($c = 1 \text{ mg.mL}^{-1}$ in MeOH). ^1H NMR (400.13 MHz, CDCl_3) δ 7.34 (m, 1H, H_b), 7.12 (m, 2H, $\text{H}_{d, d'}$), 4.56 (t, $^3J_{\text{He-Hf}} = 4 \text{ Hz}$, 2H, H_e), 4.01 (s, 3H, H_h), 3.75 (t, $^3J_{\text{Hf-He}} = 4 \text{ Hz}$, 2H, H_f), 3.56 (t, $^3J_{\text{H}_2-\text{H}_3} = 4 \text{ Hz}$, 1H, H_2), 3.33 (s, 3H, H_g), 3.15 (m, 1H, H_5), 2.80 (m, 1H, $\text{H}_{5'}$), 2.11 (m, 1H, H_3), 1.84-1.65 (m, 3H, $\text{H}_{3', \text{H}_4}$). ^{13}C NMR (100.61 MHz, CDCl_3) δ 179.91 (C_6), 122.84 (C_b), 121.90 (C_d), 70.62 (C_f), 62.68 (C_2), 58.91 (C_g), 49.65 (C_5), 47.08 (C_e), 36.24 (C_h), 31.49 (C_3), 26.21 (C_4). FTIR (NaCl) $\nu = 3402, 2359, 2341, 2136, 1622, 1574, 1428, 1353, 1311, 1171, 1118, 1081, 1035, 1013, 833, 750, 666, 623 \text{ cm}^{-1}$. Elemental analysis (%) calcd for $\text{C}_{12}\text{H}_{21}\text{N}_3\text{O}_3$ (MW = 255.31 g.mol^{-1}): C 56.45; H 8.29; N 16.46; found: C 56.18, H 8.32, N 16.38.

III.9.11. Synthesis of 1-(2-hydroxyethyl)-3-methyl-1H-imidazol-3-ium (S)-pyrrolidine-2-carboxylate (8d)

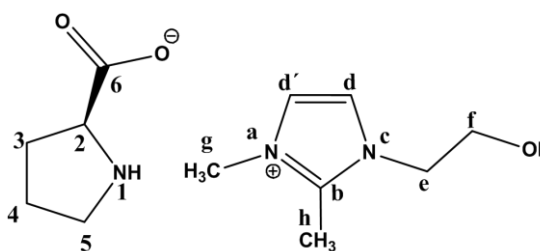
For the preparation of 1-(2-hydroxyethyl)-3-methyl-1H-imidazol-3-ium (S)-pyrrolidine-2-carboxylate a column ion exchange method was used. The 1-(2-hydroxyethyl)-3-methyl-1H-imidazol-3-ium chloride [C₂OHmim]Cl (0.71 g; 4.34 mmol) which was first transformed into



hydroxide by the use of an ionic exchange column (Amberlite IRA-400 OH) in methanol and then this basic solution was neutralized by reacting with the (L)-proline (0.5 g; 4.34 mmol) in methanol solution. The mixture was stirred at room temperature for 24 hours. After the indicated time the established water was evaporated and dried *in vacuo* for 8 hours. The final product was obtained as a viscous yellow liquid (0.94 g, 80%). $T_g = -52.06^\circ\text{C}$; $[\alpha]_D = -6.7 \pm 2^\circ$ ($c = 1 \text{ mg.mL}^{-1}$ in MeOH). ^1H NMR (400.13 MHz, D₂O) δ 7.37 (m, 3H, H_{b, d, d'}), 4.20 (t, $^3J_{\text{He-Hf}} = 4 \text{ Hz}$, 2H, H_e), 4.01 (s, 3H, H_g), 3.79 (t, $^3J_{\text{Hf-He}} = 4 \text{ Hz}$, 2H, H_f), 3.45 (t, $^3J_{\text{H2-H3}} = 4 \text{ Hz}$, 1H, H₂), 3.33 (s, 3H, H_g), 3.15 (m, 1H, H₅), 2.73 (m, 1H, H_{5'}), 2.11 (m, 1H, H₃), 1.84-1.65 (m, 3H, H_{3', H4}). ^{13}C NMR (100.61 MHz, D₂O) δ 180.85 (C₆), 136.28 (C_b), 123.52 (C_d), 61.42 (C₂), 59.70 (C_f), 51.46 (C₃), 45.94 (C_e), 35.61 (C_g), 30.37 (C₃), 24.81 (C₄). FTIR (NaCl) $\nu = 3410$, 2361, 2342, 2142, 1630, 1578, 1420, 1168, 1073, 947, 872, 751, 667, 622 cm^{-1} . Elemental analysis (%) calcd for C₁₁H₁₉N₃O₃ (MW = 241.29 g.mol^{-1}): C 54.76; H 7.94; N 17.41; found: C 54.50, H 7.91, N 17.31.

III.9.12. Synthesis of 1-(2-hydroxyethyl)-2,3-dimethyl-1H-imidazol-3-ium (S)-pyrrolidine-2-carboxylate (8e)

For the preparation of 1-(2-hydroxyethyl)-2,3-dimethyl-1H-imidazol-3-ium (S)-pyrrolidine-2-carboxylate a column ion exchange method was used. The 1-(2-hydroxyethyl)-2,3-dimethyl-1H-imidazol-3-ium chloride [C₂OHDMim]Cl (0.76 g; 4.34 mmol) which was first transformed into

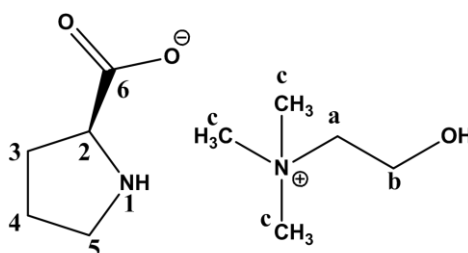


hydroxide by the use of an ionic exchange column (Amberlite IRA-400 OH) in methanol and then this basic solution was neutralized by reacting with the (L)-proline (0.5 g; 4.34 mmol) in methanol solution. The mixture was stirred at room temperature for 24 hours. After the indicated time the established water was evaporated and dried *in vacuo* for 8 hours. The final product was obtained as a viscous yellow liquid (0.82 g, 75%). $T_g = -40.30^\circ\text{C}$; $[\alpha]_D = -19.0 \pm 2^\circ$ ($c = 1 \text{ mg.mL}^{-1}$ in MeOH). ^1H NMR (400.13 MHz, D₂O) δ 7.24 (m, 3H, H_{b, d, d'}), 4.20 (t, $^3J_{\text{He-Hf}} =$

4 Hz, 2H, H_e), 4.01 (s, 3H, H_g), 3.79 (t, $^3J_{\text{Hf-He}} = 4$ Hz, 2H, H_f), 3.45 (t, $^3J_{\text{H2-H3}} = 4$ Hz, 1H, H₂), 3.33 (s, 3H, H_g), 3.15 (m, 1H, H₅), 2.73 (m, 1H, H₅), 2.45 (s, 3H, H_h), 2.11 (m, 1H, H₃), 1.84-1.65 (m, 3H, H₃, H₄). ^{13}C NMR (100.61 MHz, D₂O) δ 180.85 (C₆), 136.28 (C_b), 123.52 (C_d), 61.42 (C₂), 59.70 (C_f), 51.46 (C₅), 45.94 (C_e), 35.61 (C_g), 30.37 (C₃), 24.81 (C₄), 8.97 (C_h). FTIR (NaCl) $\nu = 3390, 2360, 2339, 2142, 1630, 1588, 1416, 1169, 1076, 872, 771, 666$ cm⁻¹. Elemental analysis (%) calcd for C₁₃H₂₅N₃O₃ (MW= 271.36 g.mol⁻¹): C 57.54; H 9.29; N 15.49; found: C 57.27, H 9.26, N 15.48.

III.9.13. Synthesis of 2-hydroxy-N,N,N-trimethylethanaminium (S)-pyrrolidine-2-carboxylate (8f)

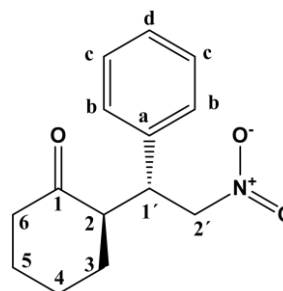
For the synthesis of 2-hydroxy-N,N,N-trimethylethanaminium (S)-pyrrolidine-2-carboxylate a simple acid base reaction was performed. Primary the choline hydroxide in MeOH 45% (0.25 g; 2.06mmol) was diluted with additional 10ml of methanol and next added drop wise to the



solution of (L)-proline in 20 ml methanol. The mixture was stirred at room temperature for 24 hours. After the indicated time the established water was evaporated and dried *in vacuo* for 8 hours. The final product was obtained as a viscous brown liquid (0.65 g, 100%). Tg=-79.85 °C; $[\alpha]_D = -12.7 \pm 2^\circ$ (c= 1 mg.mL⁻¹ in MeOH). ^1H NMR (400.13 MHz, DMSO) δ 5.26 (m, -OH), 3.84 (m, 2H, H_b), 3.43 (m, 2H, H_a), 3.47 (m, 1H, H₂), 3.12 (s, 9H, H_c), 2.88 (m, 2H, H₅), 2.11 (m, 1H, H₃), 1.84-1.65 (m, 3H, H₃, H₄). ^{13}C NMR (100.61 MHz, DMSO) δ 182.41(C₆), 67.49 (C_a), 61.48 (C₂), 55.56 (C_b), 53.85 (C_c), 45.94(C₅), 30.64 (C₃), 24.99 (C₄). FTIR (NaCl) $\nu = 3401, 2360, 2341, 2134, 1633, 1574, 1488, 1417, 1352, 1204, 1134, 1086, 1052, 957, 865, 750, 667$ cm⁻¹. Elemental analysis (%) calcd for C₁₁H₂₆N₂O₃ (MW=234.34 g.mol⁻¹): C 56.38; H 11.18; N 11.95; found: C 56.12, H 11.12, N 11.92.

III.9.14. General procedure for the Michael reaction of cyclohexanone and β -nitrostyrene

To a suspension of catalyst (10-30 mol%) and cyclohexanone (210 μl , 2 mmol) in 1ml of solvent (EtOH, Emim EtSO₄ or Bmim DCA) *trans*- β -nitrostyrene (0.149 g, 1.0 mmol) was added. The resulting mixture was allowed to stir at room temperature, for 48-90 hours, then evaporated in vacuo and the resulting residue was purified by extraction with Et₂O and



flash column chromatography using ethyl acetate/hexane (1:2) giving the desired product. If necessary the product was additionally purified by filtration using neutral aluminium and Et₂O as washing solvent. Relative and absolute configurations of the products were determined by comparison with the known ¹H NMR and chiral HPLC analysis. The enantiomeric excess was determined by chiral HPLC analysis on a Phenomenex Lux 5 um 250x10 cellulose column, flow 1ml.min⁻¹, 25 °C column oven, hexane: i-PrOH 90:10, λ=230 nm. *t* major = 13.7 min and *t* minor = 15.0 min.

(S)-2-(R)-2-nitro-1-phenylethyl)cyclohexanone: colourless solid; mp 128-130 °C; conversion 100%; *dr* (*syn/anti*): 93:7, % *ee*. ¹H NMR (400 MHz, CDCl₃) δ 7.36 – 7.26 (m, 3H, H_c, H_d), 7.17 (d, ⁴J_{Hb-Hb} = 8 Hz, 2H, H_b), 4.94 (dd, ²J_{H2'-H2'} = 4 Hz, ³J_{H2'-H1'} = 8 Hz, 1H, H_{2'}), 4.64 (dd, ²J_{H2'-H2'} = 4 Hz, ³J_{H2'-H1'} = 8 Hz, 1H, H_{2'}), 4.19 (dt, ³J_{H1'-H2'} = 8 Hz, ³J_{H1'-H2} = 10 Hz, 1H, H_{1'}), 3.76 (ddd, ³J_{H2-H1'} = 8 Hz, ³J_{H1'-H3} = 8 Hz, ³J_{H1'-H4} = 10 Hz, 1H, H₂), 2.74 - 2.67 (m, 2H, H₆), 2.51 - 2.36 (m, 1H, H₃), 1.81–1.59 (m, 4H, H₄, H₅), 1.30–1.20 (m, 1H, H₃). ¹³C NMR (101 MHz, CDCl₃) δ 211.88 (C₁), 137.73 (C_a), 128.90 (C_c), 128.14 (C_c), 127.74 (C_d), 78.86 (C_{2'}), 52.51 (C₂), 43.91 (C₆), 42.71 (C_{1'}), 33.18 (C₅), 28.49 (C₃), 25.00 (C₄).

III.9.15. General procedure for extraction using *sc*CO₂

The *sc*CO₂ extraction was carried out in the apparatus schematically presented in Scheme III.5. The core of the apparatus is a 3.5 mL high-pressure cell, with two sapphire windows allowing visualization of the internal volume. In order to perform the extraction, the cell is charged with a desired amount of the reaction mixture (0.9 mL), placed inside a constant temperature (40 °C) water bath and pressurized with CO₂ until the desired pressure (250 bar) is brought into the cell. Supercritical extraction starts by careful opening the venting valves and allowing the extract to be collected in a cold trap filled with ethanol and cooled with ice. The drop of pressure is continuously compensated with the introduction of fresh CO₂. The total quantity of CO₂ passed through the system is measured by a gas flow meter placed at the exit of an ethanol trap. The extraction is considered finished when 0.55 mol of CO₂ passes through the system. After a careful depressurisation of the system, some additional solvent (ethanol) is injected through the expansion lines to ensure that all the solute is recovered in the trap.

CHAPTER IV. Studies of Cyclodextrins and ILs

IV. Studies of Cyclodextrins and Ionic Liquids

Cyclodextrins (CDs), mainly β -CD is difficult to dissolve in water and in many common solvents and the search of more appropriate solvents is a key step to expand its application. Nowadays, up to 40% of new chemical entities developed by the pharmaceutical industry are poorly soluble or lipophilic compounds¹⁴⁰. The solubility issues difficult the delivery of these new drugs as well as affects the delivery of many existing drugs. Thus, the dissolution characteristics of poorly soluble drugs could be enhanced by several methods.

In last decades, ILs have emerged as a possible environmentally benign alternative to common organic solvents, mainly related with their peculiar properties. Understanding the interaction between IL and CD is important to analytical chemistry and material synthesis. The main goal of this chapter is related with the development of novel chiral biological compounds based on the interaction of biocompatible ILs and CDs. In this context, dissolution and interaction studies of α -, β - and γ -CDs with several ILs were investigated. Novel biomaterials based on simple combination of ILs and CDs can be applied for host-guest and drug delivery processes. Novel biocompatible materials based on the combination of ILs and CDs can be explored for relevant chiral discrimination or separation processes.

IV.1. *Studies on dissolution of beta-cyclodextrins in Ionic Liquids*

In order to develop novel chiral biological molecules the effect of several ILs as solvents on β -CD has been first studied. The dissolution of β -CD in different classes of RTILs based on methylimidazolium, ammonium, pyridinium, sulfonium, guanidinium and phosphonium cations combined with halogenate (chloride or bromide), dicyanamide, acetate, tetrafluoroborate, saccharine and ethylsulfate anions were tested (Figure IV.1). Table IV.1 summarizes the dissolution performance of different examples of RTILs. The maximum percentage of β -CD dissolved in ILs was verified by ^1H NMR spectra of the mixture comparing the well known peaks of β -CD with some characteristic ILs peaks. ^1H NMR spectrum of dissolution of β -CD in [Emim][EtSO₄] is presented in Figure IV.2. The same experimental protocol was repeated for all of the β -CD and ILs mixtures.

All dissolution experiments are presented in Table IV.1. It was possible to change the solubility behavior of β -CD scaffold due to the choice of the counter-ion. In general, the family of cations that showed the best dissolution with [DCA] as the anion was the sulfonium and the

phosphonium, followed by the imidazolium and at last the ammonium family. Regarding the selection of the cation, different results were observed while using BF_4 as the anion. The highest percentage of β -CD dissolved into IL was obtained for the family of imidazolium combined with BF_4 in sequence $[\text{Bmim}] > [\text{C}_2\text{OHmim}] > [\text{C}_3\text{Omim}] > [\text{Omim}] > [\text{C}_{10}\text{mim}]$, respectively. The increase of alkyl chain connected to the imidazolium ring resulted in the decrease of β -CD solubility profile. The influence of anion was also not irrelevant. Changing the anion from BF_4 to $[\text{DCA}]$, when $[\text{Bmim}]$ was used as the cation, resulted in lower percentage of β -CD dissolved (from 99.3% to 76.8%). According to the biocompatibility and dissolution performance of the different ILs tested, it was possible to classify the chiral biological materials based on β -CDs and ILs as good candidates or not so good for future applications. The best candidates for applications are in particular based on sulfonium and imidazolium cations combined with dicyanamide and ethylsulfate anions ($[\text{Emim}][\text{EtSO}_4]$ or $[\text{C}_5\text{O}_2\text{mim}][\text{Cl}]$). It is important to emphasize that all the β -CD- ILs mixtures were obtained either as gels or viscous liquids as shown in Figure IV.3.

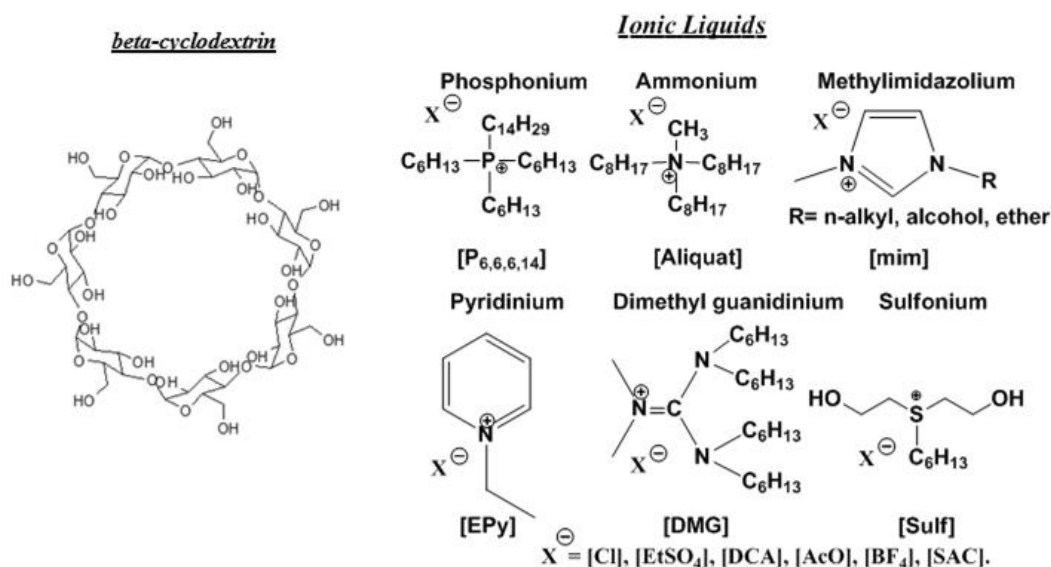
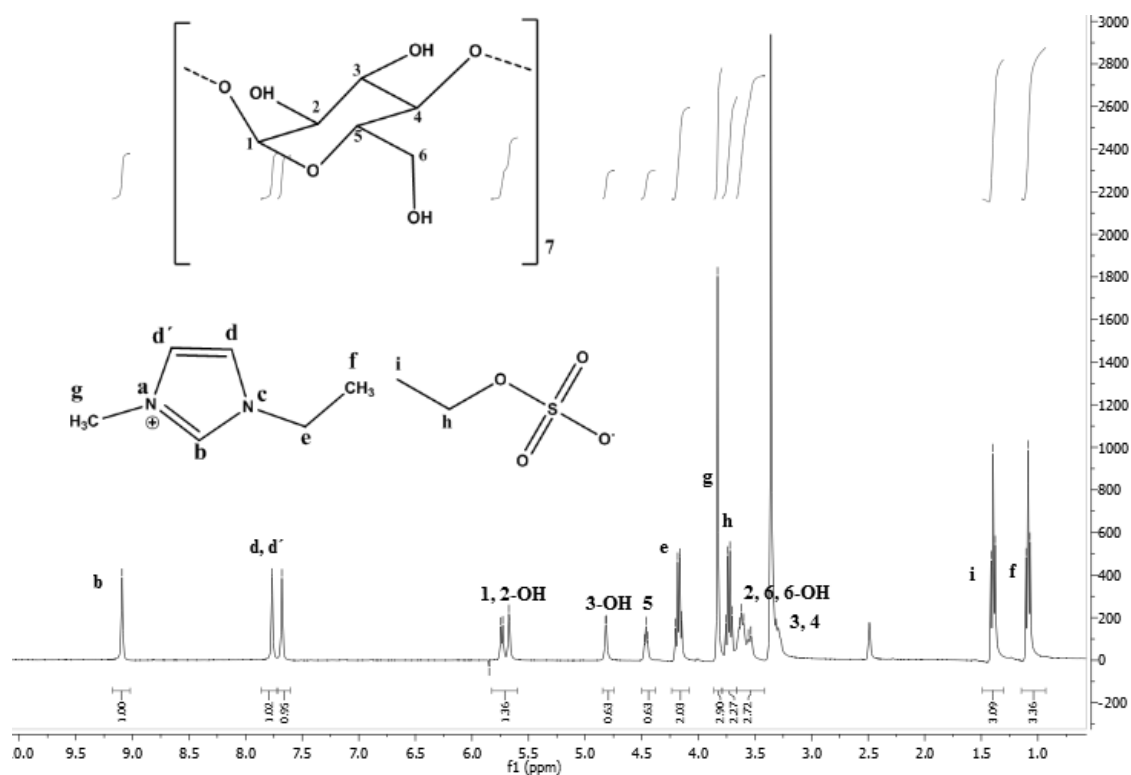


Figure IV.1 - Structure of β -CDs and ILs selected for dissolution studies.

Table IV.1 - Results of the dissolution studies of β -CD in ILs.

Family of ILs	ILs	Mass of β -CD per mass of IL [mg CD/mg IL]	[%] of β -CD dissolved in ILs
IMIDAZOLIUM	[Emim][EtSO ₄]	100.6/206	99.3
	[Bmim][BF ₄]	50.6/204	99.3
	[Bmim][DCA]	151.5/202	76.8
	[Omim][Cl]	100.3/205	100
	[Omim][DCA]	50.1/209	92.4
	[Omim][BF ₄]	50.2/208	5.8
	[C ₁₀ mim][SAC]	100.4/217	97
	[C ₁₀ mim][DCA]	50.1/202	89.2
	[C ₁₀ mim][BF ₄]	50.0/216	3
	[C ₂ OHmim][BF ₄]	50.2/200	95.5
	[C ₂ OHmim][DCA]	100.4/202	68.5
	[C ₃ Omim][BF ₄]	50.2/216	80.1
	[C ₅ O ₂ mim][Cl]	150.3/205	100
AMMONIUM	[Aliquat][DCA]	100.9/302	62.2
	[Aliquat][SAC]	100.5/212	33.4
	[Aliquat][Cl]	50.2/304	22
PHOSPHONIUM	[P _{6,6,6,14}][DCA]	100.7/301	100
	[P _{6,6,6,14}][Cl]	50.0/302	12.4
SULFONIUM	[(C ₂ OH) ₂ C ₆ S][DCA]	50.6/219	100
	[(C ₂ OH) ₂ C ₆ S][Br]	101.1/205	64.1
GUANIDINIUM	[DMG][Cl]	101.7/200	83.5
	[DMG][SAC]	100.2/215	79
PYRIDINIUM	[Epy][EtSO ₄]	150.5/202	88

Solubility was checked by visual observation and then proofed by ¹H NMR analysis.

Figure IV.2 - ¹H NMR spectrum of the mixture β -CD dissolved in [Emim][EtSO₄].

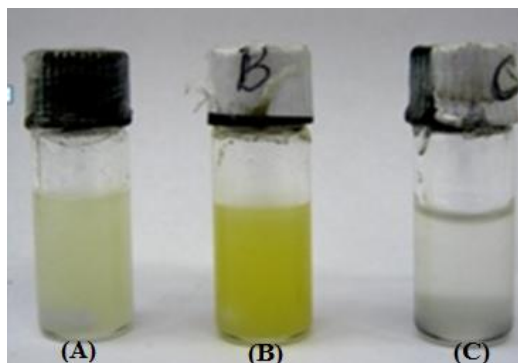


Figure IV.3 - Novel chiral materials based on β -CD and ILs. (A)- gel, (B)- yellow liquid, (C)- transparent liquid.

IV.2. Recovery of beta-cyclodextrin and Ionic Liquids

It was also proved that recovering of pure β -CD as well as the original ILs is possible by simple addition of acetone to the mixture (Figure IV.4). The recycled β -CD and ILs were recovered without any decomposition and not a significant lost as indicated in Table IV.2. Their stability and purity was checked by ^1H NMR spectra presented in Figures IV.5, IV.6 and IV.7.

Using this approach is possible to create chiral materials as gels or viscous liquids based on the simple combination of biocompatible task specific ILs and CDs and then recover the original components if required. These chiral liquid materials based CDs can be useful for asymmetric catalysis or chiral separation processes.

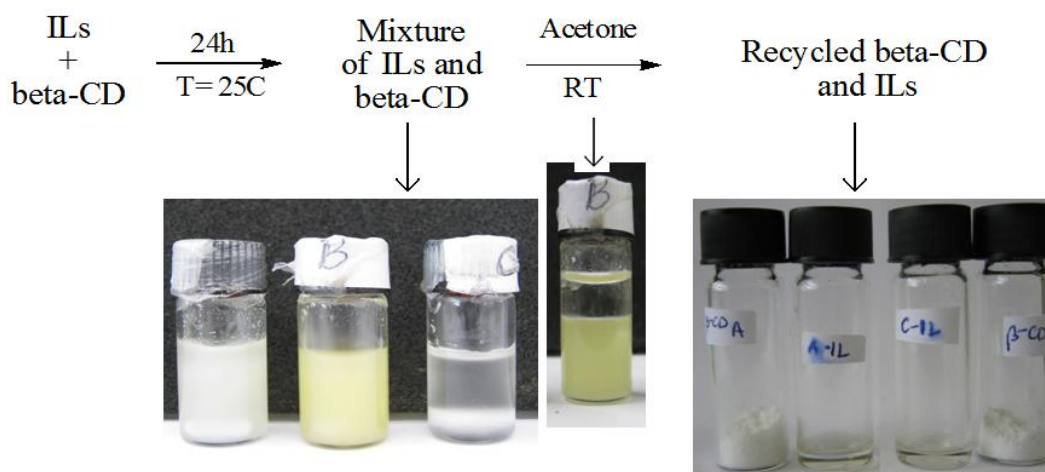
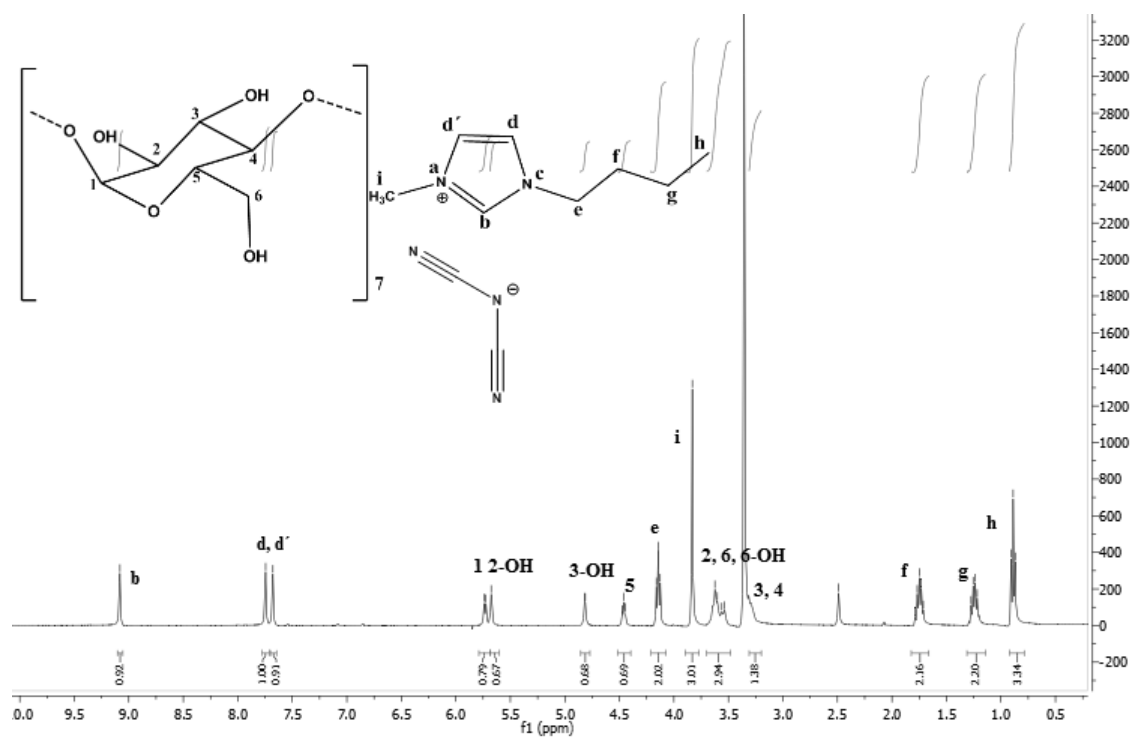
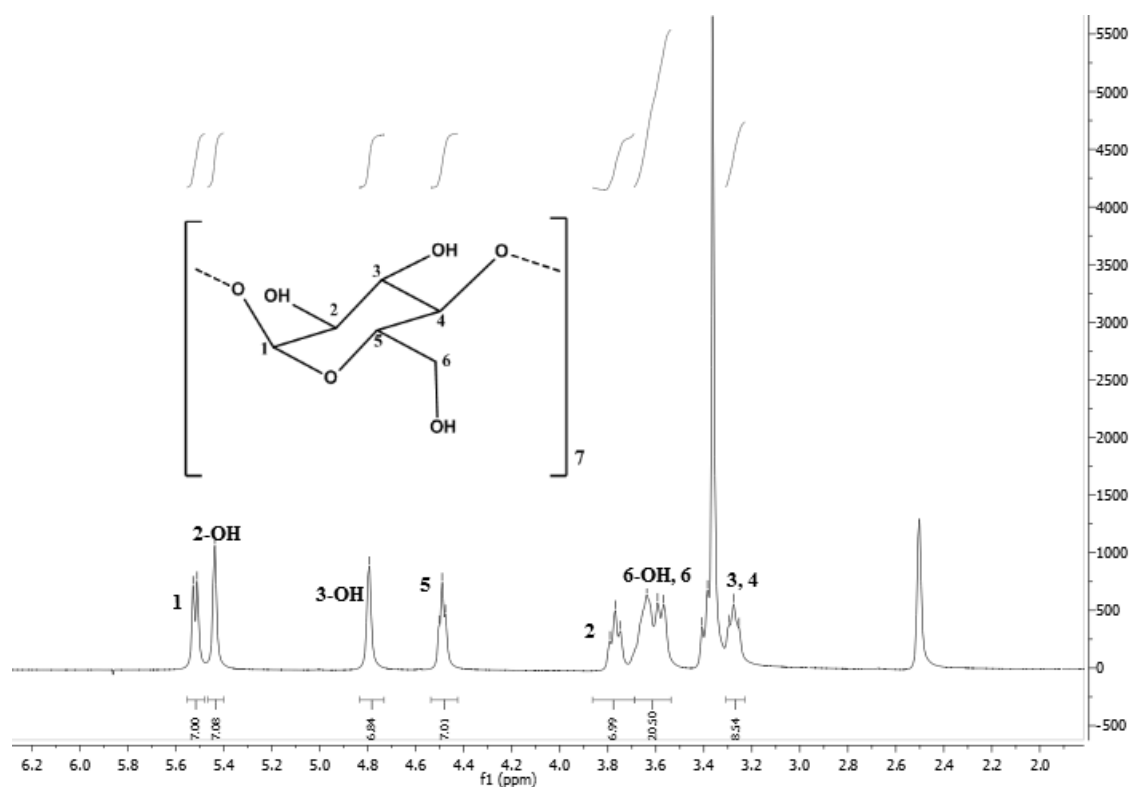
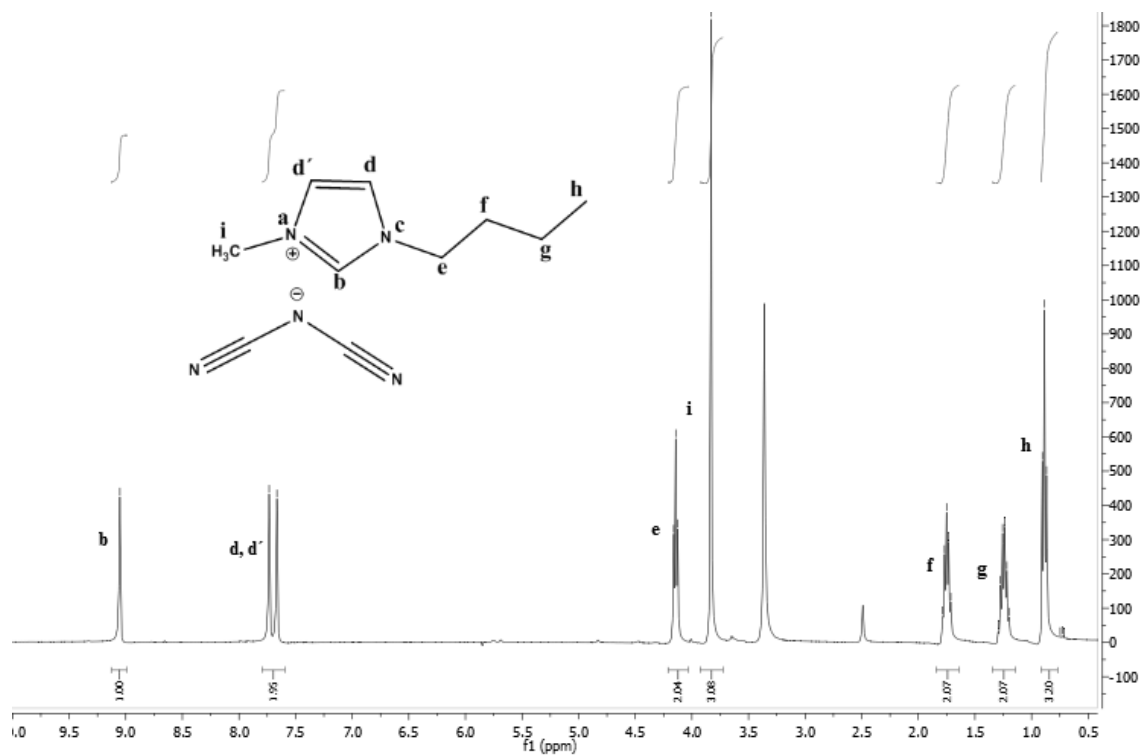


Figure IV.4 - Recovery strategy of β -CD and IL.

Table IV.2 - Amounts of β -CD and ILs used for recycling studies.

IL	Mass of IL before recovery[mg]	Mass of β -CD before recovery [mg]	Mass of IL after recovery[mg]	Mass of β -CD after recovery [mg]
[Bmim][DCA] A	805.7	601.2	624.7 (78%)	395.5 (66%)
[C ₅ O ₂ mim][Cl] B	800.5	600.0	600.3 (75%)	394.6 (66%)
[Emim][EtSO ₄] C	801.9	603.9	509.3 (64%)	353.1 (59%)

Figure IV.5 - ^1H NMR spectrum of the mixture β -CD dissolved in [Bmim][DCA] before recovery.


 Figure IV.6 - ^1H NMR spectrum of the pure β -CD after recovery.

 Figure IV.7 - ^1H NMR spectrum of the pure [Bmim][DCA] after recovery.

IV.3. *Application of beta-cyclodextrin-IL gels for the studies on improvement of water solubility of fatty acids and steroids*

Saturated fatty acids such as: capric acid (decanoic acid), lauric acid (dodecanoic acid), ester lauryl gallate (dodecyl gallate) and steroids: squalene and Provitamin D2 (Ergosterol) are examples of compounds poorly soluble in water (Figure IV.8). These fatty acids and steroids have certain significant applications in different areas (eg. pharmaceutical, food, cosmetics, lubricant and chemical). Because ergosterol is present in cell membranes of fungi, yet absent in those of animals, it is a useful target for antifungal drugs¹⁴¹. In animals, squalene is the biochemical precursor to the whole family of steroids. Squalene anti-tumor activity in animal experiments and epidemiological proof based on olive oil consumption also suggest reduction of cancer risk by squalene¹⁴². Lauryl gallate is a food additive and used under the E number E312 as an antioxidant and preservative compound. To overcome solubility problems of unpolar or weakly polar substances, the addition of a solubiliser to the solvent is necessary. In this context, β -CD- [Emim][EtSO₄] gel was added to the water as additive. The results presented in Table IV.3 clearly show that the use of β -CD- [Emim][EtSO₄] mixture facilitates the water solubility of fatty acids and steroids. It was possible to improve the values for capric and lauric acid up to 5 and 22%. At the same time, practically water-insoluble squalene and provitamin D2 proved to be totally soluble in water with additive after two additions of the steroids (80.10^{-5} g) and only after the last addition was visible a precipitate in both cases as presented in Figure IV.9.

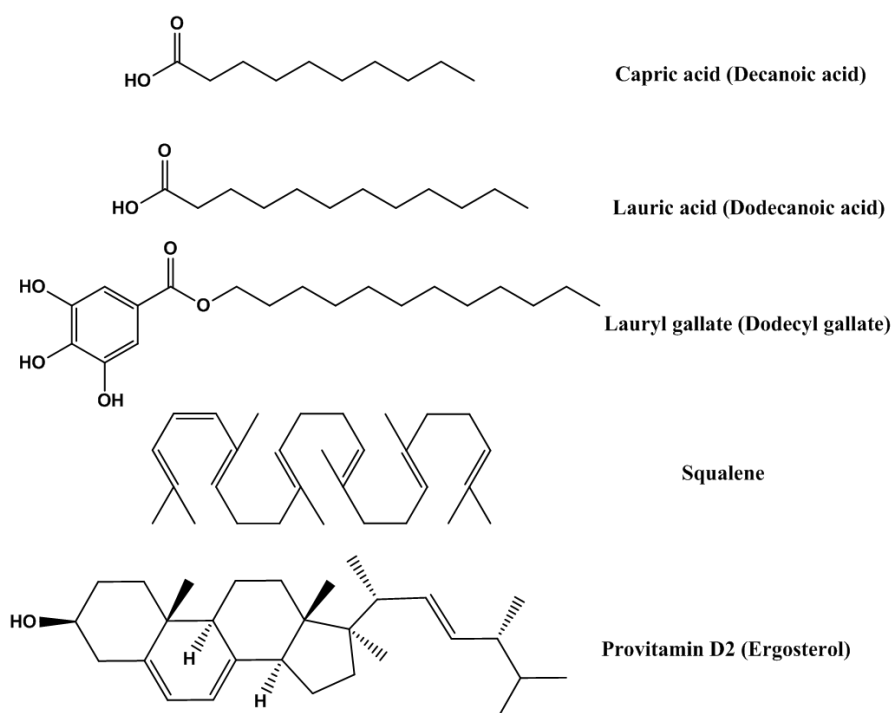


Figure IV.8 - Fatty acids and steroids chosen for the studies on improvement of their water solubility.

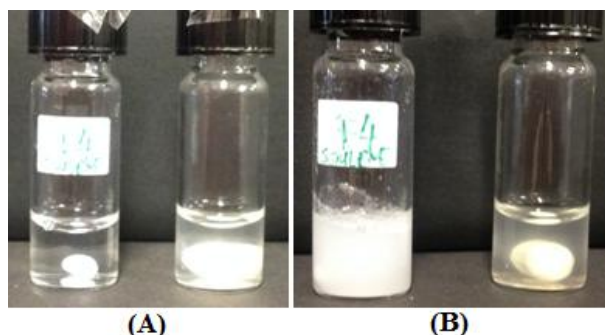


Figure IV.9 - (A) squalene (left) and provit.D2 (right) in water with additive after 2 additions of steroids, (B) squalene (left) and provit. D2 (right) in water with additive after the last addition.

Table IV.3 - Results of water solubility of fatty acids and steroids using β -CD-[Emim][EtSO₄] gel as additive.

<i>Fatty acid, steroid</i>	<i>Water solubility [g.mL⁻¹.10⁻⁵], (lit.)</i>	<i>Amount solubilized in water with additive [g.mL⁻¹.10⁻⁵]^[a]</i>
Capric acid	15	80
Lauric acid	6	130
Lauryl gallate	0	40
Squalene	0	600
Provitamin D2	0	155

^[a] Amount of fatty acid or steroid dissolved in water after the β -CD- [Emim][EtSO₄] gel (50 μ l) was used as additive. The results were concluded by visual observation.

IV.4. Dissolution of α - and γ -cyclodextrins in Ionic Liquids

In this part of the work, we are interested in the complexation and dissolution of α - and γ -CD with different ILs. In this context, the possibility to combine task specific ILs with CDs by simple dissolution process can be relevant in order to expand the range of their applications as a chiral media for asymmetric catalysis and chiral recognition. For these experiments, different RTILs were selected as indicated in Figure IV.10. The mixtures of α - and γ -CDs (100-150 mg) and ILs (200-300 mg) were stirred for 24 hours at room temperature. The percentage of α - and γ -CDs dissolved in ILs was confirmed by ¹H NMR spectra of the mixture by comparing the well known peaks of α - and γ -CDs with the ILs peaks. All dissolution studies are presented in Table IV.4.

According the selection of the counter-ion, it was possible to change the solubility behavior of α - and γ -CDs scaffolds. The highest percentage of α -CD dissolved into IL was obtained for the family of imidazolium cations, in particular [C₅O₂mim][Cl], [Emim][EtSO₄] (Table IV.4, Entries 4 and 5). These results indicated us that the alkyl chain of imidazolium ring can interact inside of α -CD cavity as inclusion complex (This possible inclusion structure was confirmed by ¹H NMR). In the case of ammonium IL combined with dicyanamide (Table IV.4, Entry 2) moderate dissolution results were obtain. It is important to note, that when the aliquat cation was substituted by the hydrophobic phosphonium cation, the solubility of α -CD dropped

dramatically (Table IV.4, Entry1). The cavity size can explain the solubility profile differences between ammonium and phosphonium salts. In general, γ -CD showed less miscibility with the chosen ILs. Furthermore, a diverse behaviour was observed when [Aliquat][DCA] was examined, while the small α -CD scaffold showed moderate solubility of 77.8 %, in the case of bigger γ -CD only 3.6 % dissolution was obtained. This fact indicates that depending of the size of the CD moiety different interactions with ILs can occur. The ^1H NMR spectra revealed that chemical shift data of all protons in α - and γ -CD molecules move to higher field in the presence of ILs.

Table IV.4 - Results of the dissolution studies of γ -CD in ILs.

Entry	ILs	Mass of α -CD per mass of IL [mg CD/mg IL]	[%] of α -CD dissolved in ILs	Mass of γ -CD per mass of IL [mg CD/mg IL]	[%] of γ -CD dissolved in ILs
1	[P _{6,6,6,14}] [DCA]	101.5/212	2.1	104.9/200	2.5
2	[Aliquat] [DCA]	101.4/209	77.8	100.0/205	3.6
3	[Bmim] [DCA]	150.3/211	48.1	151.2/206	31.2
4	[C ₅ O ₂ MIM] [Cl]	151.0/206	100	151.4/204	66.5
5	[Emim] [EtSO ₄]	150.2/207	93.5	151.2/210	81.0

Solubility was checked by visual observation and then proofed by ^1H NMR analysis.

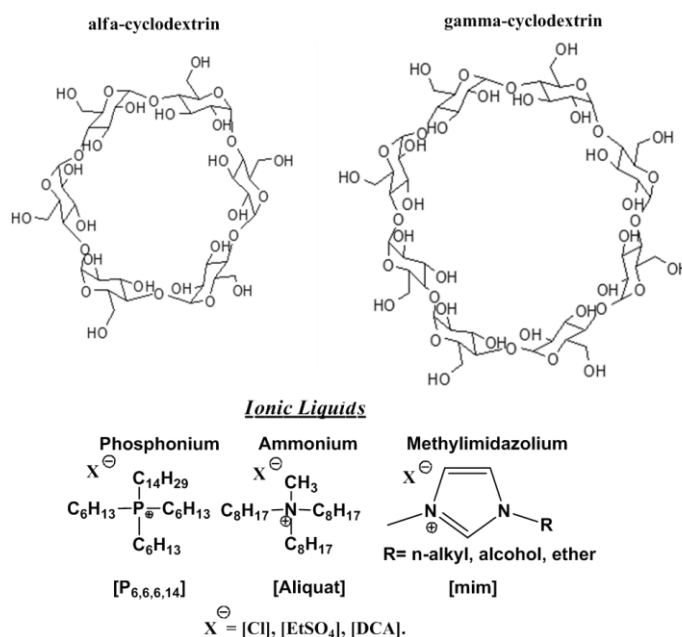


Figure IV.10- Structure of α - and γ -CDs and ILs selected for dissolution studies.

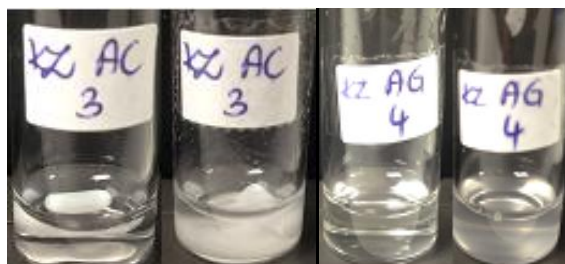
IV.5. *Studies on solubility behaviour of α - and γ -cyclodextrins in water and serum*

The natural CDs have limited water solubility, meaning that complexes resulting from interaction of lipophiles with these CDs can be of limited solubility resulting in precipitation of solid cyclodextrin complexes from water and other aqueous systems. In fact, the aqueous

solubility of the CDs is much lower comparing with other acyclic saccharides⁶⁹. This is thought to be due to relatively strong intermolecular hydrogen bonding in the crystal state. In order to increase its apparent water solubility α - and γ -CDs were combined with [Emim][EtSO₄] and portions of these gels were added to water as presented in Figure IV.11 and 12. The addition of IL resulted in dramatic improvement of their aqueous solubility. In the second part of our studies, the dissolution of α - and γ -CDs in serum (water with sodium chloride buffer, pH=7) was examined. Table IV.5 summarizes all the water and serum solubility experiments. It was found that the presence of [Emim][EtSO₄] involves an increase in the solubility of α - and γ -CD in serum.



Figure IV.11 - CDs-ILs gels prepared for improvement of CDs water and serum solubility.



1th addition / last addition 1th addition / last addition

Figure IV.12 - Dissolution of α -CD with IL additive (KZ AC3) and γ -CD with IL additive (KZ AG4) in serum (first and last addition).

Table IV.5 - Results of α – and γ -CDs water solubility.

CDs or gels	Dissolution in water [g/0.5ml] ^[a]	Dissolution in serum [g/0.5ml] ^[a]
α -CD	0.041	0.050
α -CD+[Emim] [EtSO ₄]	0.250 (x6 times)	0.156 (x3 times)
γ -CD	0.025	0.046
γ -CD+[Emim] [EtSO ₄]	0.050 (x2 times)	0.100 (x2 times)

^[a]Dissolution studies were performed at 20 °C.

IV.6. *Interaction of alfa- and gamma-cyclodextrins with methylene blue and Ionic Liquids*

Methylene blue (MB) is a heterocyclic aromatic compound and as example of phenothiazine dyes with a planar structure (Figure IV.13). Phenothiazine dyes have found a wide range of applications such as sensitizers in solar energy conversion, active species in electrochromism and dye lasers, ingredients in pharmaceutical preparation, redox mediators in catalytic oxidation reactions and candidates for cancer therapy by intercalating in between DNA base layers¹⁴³. Nevertheless, according to the dimerization of dye molecules in aqueous media such as the great decrease of light sensitivity, there are some limitations for these applications. Therefore, it is important to improve the sensitivity of dyes towards obtaining a high number of monomers.

The property of CDs to form host-guest complexes can be used to control the position of monomer/dimer equilibrium and aggregation ability of dye, affecting electronic absorption and fluorescence spectra as the photochemical and electrochemical properties of dyes. Many analytical methods for the study on the complex of CD with MB including electrochemical method and UV/ Vis spectrometry have been reported¹⁴³. The recent methods are limited to parent β -CD.

The purpose of this subchapter is related with the study of complexing behavior of MB with initial α - and γ -CDs as well as α - and γ -CD/IL systems by absorption spectroscopy analysis. In this context, solutions with initial MB, α - and γ -CDs and α - and γ -CDs with either [Bmim][DCA] or [Aliquat][DCA] were prepared (proportions: 1.0: 0.5; 1.0: 1.0; 1.0: 1.5 and 1.0: 2:0). Figure IV.14 shows the absorption spectra of MB monomer (666 nm) and dimer (612 nm). In the presence of α - or γ -CD, the initial maximum absorption of MB at 612 and 666 nm decreases (see Figure IV.14). In the case in which CDs were used in a form of gel with ILs, similar profile was observed. These results were in contrast to those obtained in the literature. Some reports show a large increase of absorption in MB monomer peak and a slight decrease in MB dimer peak that proved the breaking of the aggregate of the MB. The initial idea of these studies was to rationalize the different dissolution results obtained with these ILs for both CDs. Unfortunately, no clear conclusions could be taken out of the studies. The absorption method was not sensitive enough to elucidate us. In this context, further studies using other methods such as NMR and fluorescence should be performed.

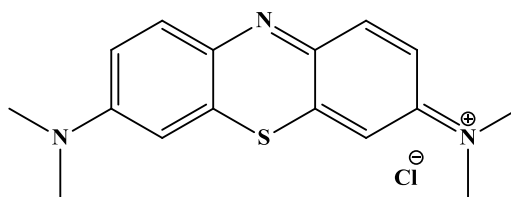


Figure IV.13 - Methylene blue.

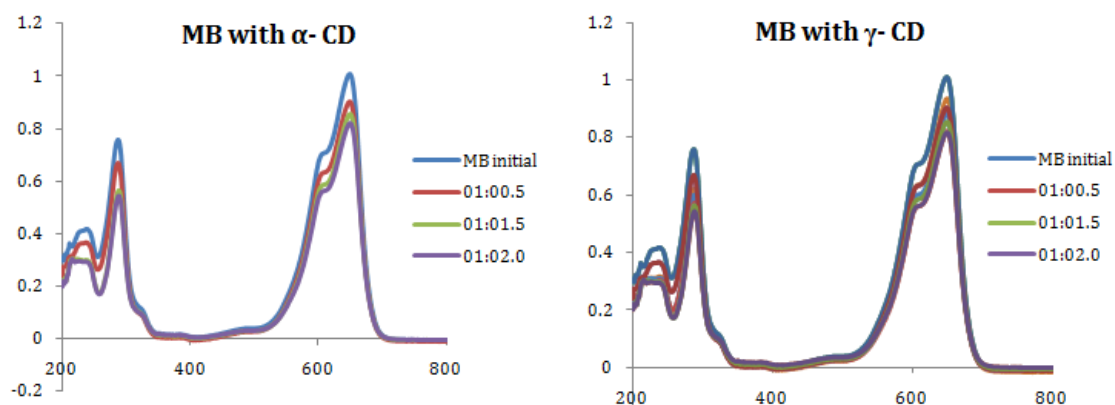


Figure IV.14 - Absorbance spectra of MB (1.10^{-8} mol) with different proportions of α - and γ -CD solutions.

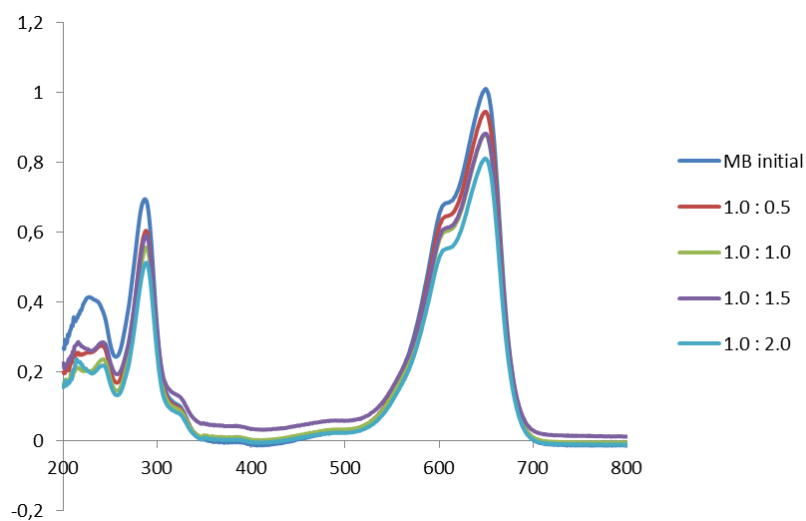


Figure IV.15 - Absorbance spectra of MB (1.10^{-8} mol) with different proportions of α -CD [Bmim][DCA] solutions.

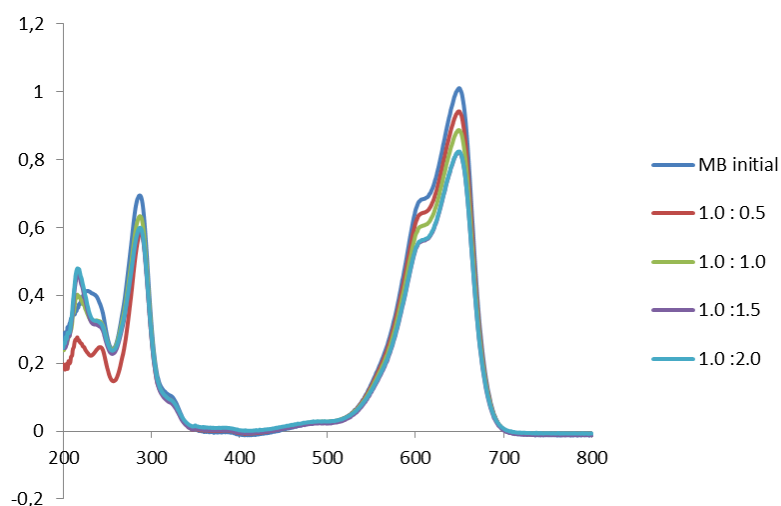


Figure IV.16 - Absorbance spectra of MB (1.10^{-8} mol) with different proportions of γ -CD [Bmim][DCA] solutions.

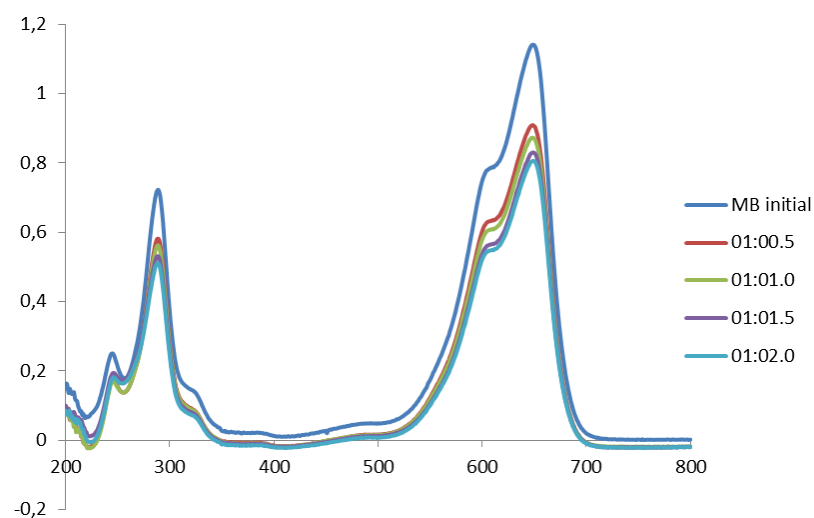


Figure IV.17 - Absorbance spectra of MB (1.10^{-8} mol) with different proportions of α -CD [Aliquat][DCA] solutions.

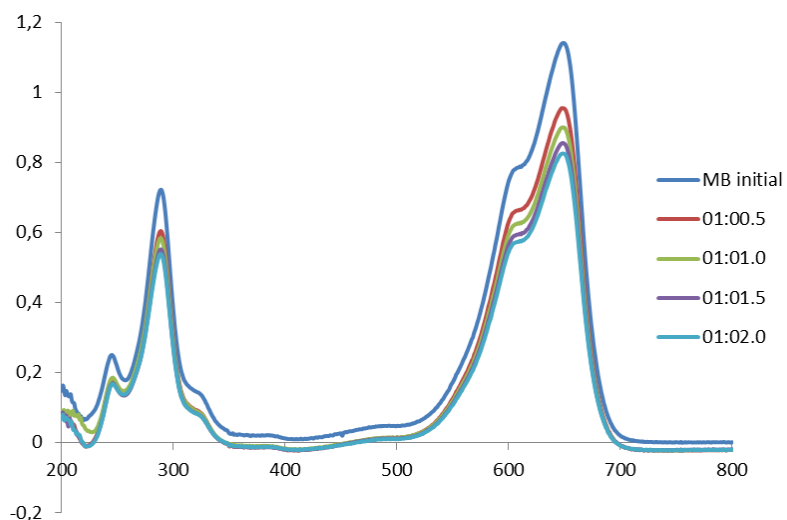


Figure IV.18 - Absorbance spectra of MB (1.10^{-8} mol) with different proportions of γ -CD [Aliquat][DCA] solutions.

IV.7. *Conclusions*

This chapter was focused on the possible interactions of oligosaccharides with ILs. The studies showed a high potencial of some ILs for the dissolution of CDs. In particular, in the case of β -CD, it was possible to find ILs that can be used as an alternative to organic solvents (DMSO) with very high solubility profiles. The difference observed for α -, β -, γ -CDs dissolution in the same ILs makes them task specific ILs and it is a relevant point to study in more detail in the future. One of the explanations for this variable behavior could be the size of each CD and possible hydrophobic interactions present inside CDs and more hydrophobic ILs as well as external hydrophilic interactions of CDs with specific ILs (acidic protons or OH groups from imidazolium cations).

Additionally, some CDs and ILs mixtures seems to be novel (bio)materials as additives to improve the solubility of drugs, fatty acids and steroids as well as to improve the original CDs solubility in aqueous and serum solutions.

Observing the chirality applications of CDs, we are interested in the use of ILs- CDs systems for asymmetric catalysis, chiral separation as well as in pharmaceutical industry. Some preliminary studies using β -CD as a chiral media for asymmetric epoxidation reactions were performed. Moreover, preliminary synthetic approaches in order to incorporate ionic scaffolds in the CD structure were also tested. In particular the functionalization of β -cyclodextrin was developed using three synthetic steps: the synthesis of 6-O-Monotosyl-6-deoxy- β -cyclodextrin, followed by the synthesis of 6-Monodeoxy-6-azido- β -cyclodextrin in order to obtain the final 6-Monodeoxy-6-amino- β -cyclodextrin. The preparation of these CDs based ILs is in progress.

IV.8. *Experimental Part*

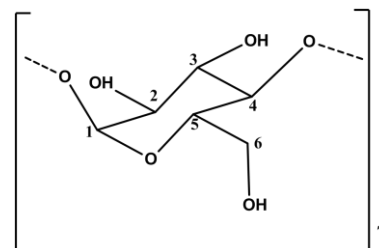
General: Commercially available reagents α -CD ($M = 972.84 \text{ g.mol}^{-1}$, CAS No. 10016-20-3), β -CD ($M = 1134.98 \text{ g.mol}^{-1}$, CAS No. 7585-39-9), γ -CD ($M = 1296.42 \text{ g.mol}^{-1}$, CAS No. 17465-86-0) ionic liquids and solvents were purchased from TCI Europe nv (Zwijndrecht, Belgium), Fluka (Buchs, Switzerland), Alfa Aesar, Aldrich, Solchemar and were used without further purification. ^1H NMR spectra were recorded on a Bruker AMX 400 Spectrometer. Chemical shifts are reported downfield in ppm from a TMS reference.

Absorption measurements: UV/Vis absorption spectra were recorded with a Varian-Cary 100 Bio UV/Vis spectrophotometer.

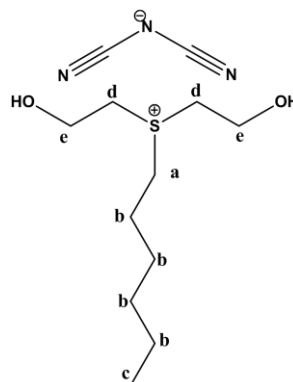
IV.8.1. General procedure for the dissolution of β -CD in ILs

Following the general procedure for the β -CD dissolution studies for these experiments, RTILs were selected based on phosphonium, ammonium, methylimidazolium, pyridinium, dimethyl guanidinium and sulfonium cations connected with chloride, bromide, dicyanamide, acetate, tetrafluoroborate, saccharine and ethylsulfate as anions. To a 1 ml vial, 200-300 mg of ILs were added and also 50-150 mg of β -CD until saturation was observed. The samples were stirred for 24 hours at room temperature and filtrated. The percentage of β -CD dissolved in ILs was confirmed using ^1H NMR spectra of the mixture after 24 hours by comparing the well known peaks of β -CD with the ILs peaks.

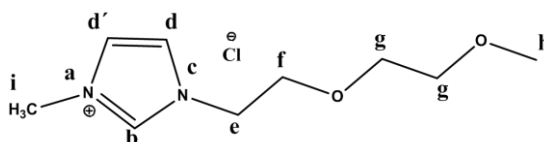
β -CD ^1H NMR (400.13 MHz, DMSO) δ 5.53 (m, 7H, H_1), 5.44 (s, 7H, 2-OH), 4.79 (s, 7H, 3-OH), 4.45 (t, $^3J_{\text{H}_5-\text{H}_6}=4$ Hz, $^3J_{\text{H}_5-\text{H}_6}=8$ Hz, 7H, H_5), 3.61 (m, 7H, H_2), 3.55-3.53 (m, 14H, 6-OH, H_6), 3.28 (m, 14H, H_3 , H_4). ^{13}C NMR (100.61 MHz, DMSO) δ 101.99 (C_1), 81.58 (C_4), 73.09 (C_5), 72.45 (C_2), 72.08 (C_3), 59.97 (C_6).



β -CD + $[(\text{C}_2\text{OH})_2\text{C}_6\text{S}][\text{DCA}]$ ^1H NMR (400.13 MHz, DMSO) δ 5.72 (m, 7H, H_1), 5.51 (s, 7H, 2-OH), 4.80 (s, 7H, 3-OH), 4.46 (t, $^3J_{\text{H}_5-\text{H}_6}=4$ Hz, $^3J_{\text{H}_5-\text{H}_6}=8$ Hz, 7H, H_5), 3.84 (m, 7H, H_2), 3.62-3.46 (m, 20H, 6-OH, H_6 , H_e , e-OH), 3.28 (m, 14H, H_3 , H_4), 2.54 (t, $^3J_{\text{H}_d-\text{H}_e}=4$ Hz, 4H, H_d), 1.74 (m, 2H, H_a), 1.37-1.27 (m, 8H, H_b), 0.85 (t, $^3J_{\text{H}_c-\text{H}_b}=8$ Hz, 3H, H_c).



β -CD + $[\text{C}_5\text{O}_2\text{MIM}][\text{Cl}]$ ^1H NMR (400.13 MHz, DMSO) δ 9.25 (s, 1H, H_b), 7.76 (s, 1H, H_d), 7.71 (s, 1H, $\text{H}_{d'}$), 5.85 (m, 7H, H_1), 5.67 (s, 7H, 2-OH), 4.81 (s, 7H, 3-OH), 4.35 (t, $^3J_{\text{H}_5-\text{H}_6}=4$ Hz, $^3J_{\text{H}_5-\text{H}_6}=8$ Hz, 7H, H_5), 3.89 (m, 3H, H_i), 3.75 (t, $^2J_{\text{H}_e-\text{H}_f}=4$ Hz, $^3J_{\text{H}_e-\text{H}_f}=8$ Hz, 2H, H_e), 3.63 (m, 7H, H_2), 3.60-3.51 (m, 16H, 6-OH, H_6 , H_f), 3.40 (s, 4H, H_g), 3.36 (m, 14H, H_3 , H_4), 3.19 (s, 3H, H_h).

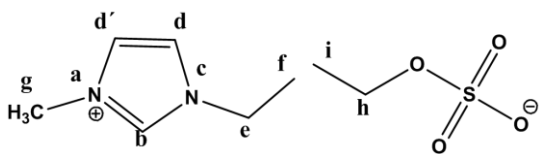


β -CD + [Emim][EtSO₄] ¹H NMR (400.13

MHz, DMSO) δ 9.09 (s, 1H, H_b), 7.76 (s, 1H,

H_d), 7.68 (s, 1H, H_{d'}), 5.85 (m, 7H, H₁), 5.67

(s, 7H, 2-OH), 4.82 (s, 7H, 3-OH), 4.46 (t, ³J_{H5-H6}=4 Hz, ³J_{H5-H6}=8 Hz, 7H, H₅), 4.16 (t, ²J_{He-He}=4 Hz, ³J_{He-Hf}=8 Hz, 2H, H_e), 3.83 (m, 3H, H_g), 3.72 (m, 2H, H_h), 3.62 (m, 7H, H₂), 3.60-3.53 (m, 14H, 6-OH, H₆), 3.28 (m, 14H, H₃, H₄), 1.40 (t, ³J_{Hi-Hh}=8 Hz, 3H, H_i), 1.09 (t, ³J_{Hf-He}=8 Hz, 3H, H_f).



β -CD + [Epy][EtSO₄] ¹H NMR (400.13 MHz, DMSO) δ

8.92 (d, ³J_{Ha-Hb}=8 Hz, 2H, H_a), 8.44 (d, ³J_{Hb-Ha}=8 Hz, 2H,

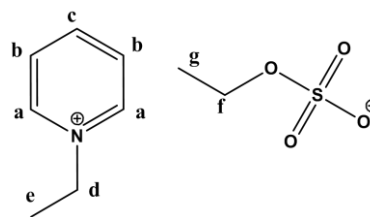
H_b), 8.92 (d, ³J_{Ha-Hb}=8 Hz, 2H, H_a), 8.04 (t, ³J_{He-Hb}=8 Hz,

1H, H_c), 5.82 (m, 7H, H₁), 5.68 (s, 7H, 2-OH), 4.82 (s,

7H, 3-OH), 4.58 (q, ³J_{Hd-He}=8 Hz, 2H, H_d), 3.76 (q, ³J_{Hf-}

H_g=8 Hz, 2H, H_f), 3.67-3.54 (m, 7H, H₂), 3.44 (m, 14H, 6-OH, H₆), 3.28 (m, 14H, H₃, H₄), 1.53

(t, ³J_{He-Hd}=8 Hz, 3H, H_e), 1.06 (t, ³J_{Hg-Hf}=8 Hz, 3H, H_g).



β -CD + [Bmim][DCA] ¹H NMR (400.13 MHz, DMSO) δ

9.08 (s, 1H, H_b), 7.74 (s, 1H, H_d), 7.68 (s, 1H, H_{d'}), 5.74

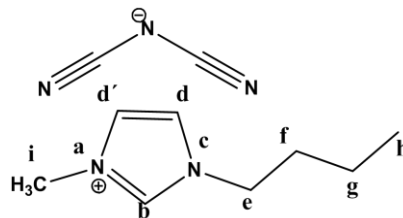
(m, 7H, H₁), 5.68 (s, 7H, 2-OH), 4.82 (s, 7H, 3-OH), 4.46

(t, ³J_{H5-H6}=4 Hz, ³J_{H5-H6}=8 Hz, 7H, H₅), 4.14 (t, ²J_{He-He}=4

Hz, ³J_{He-Hf}=8 Hz, 2H, H_e), 3.83 (, 3H, H_i), 3.62 (m, 7H,

H₂), 3.61-3.54 (m, 14H, 6-OH, H₆), 3.28 (m, 14H, H₃, H₄), 1.75 (m, 2H, H_f), 1.25 (m, 2H, H_g),

0.89 (t, ³J_{Hh-Hf}=8 Hz, 3H, H_h).



β -CD + [Omim][Cl] ¹H NMR (400.13 MHz,

DMSO) δ 9.07 (s, 1H, H_b), 7.74 (s, 1H, H_d),

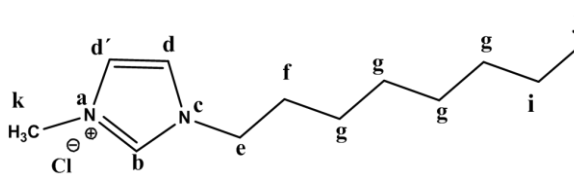
7.67 (s, 1H, H_{d'}), 5.76 (m, 7H, H₁), 5.68 (s,

7H, 2-OH), 4.82 (s, 7H, 3-OH), 4.46 (t, ³J_{H5-}

H₆=4 Hz, ³J_{H5-H6}=8 Hz, 7H, H₅), 4.13 (t, ²J_{He-He}=4 Hz, ³J_{He-Hf}=8 Hz, 2H, H_e), 3.83 (, 3H, H_k),

3.62 (m, 7H, H₂), 3.61-3.54 (m, 14H, 6-OH, H₆), 3.38 (m, 14H, H₃, H₄), 1.77 (m, 2H, H_f), 1.25

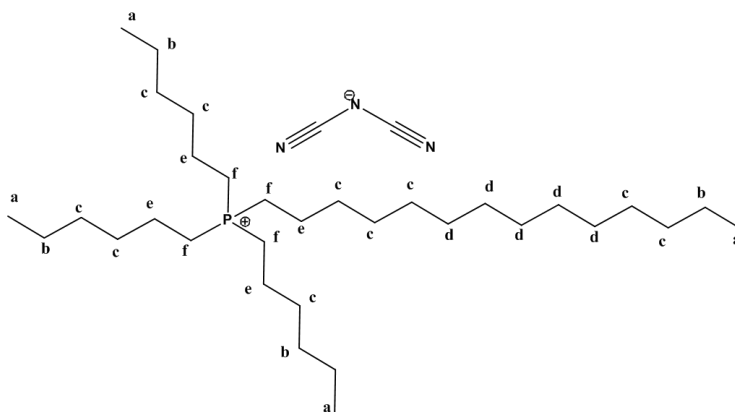
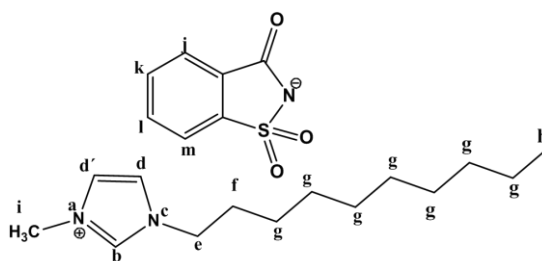
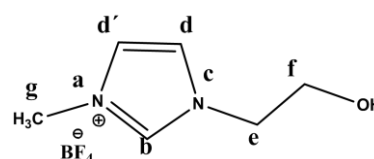
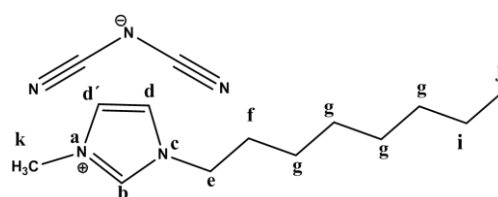
(m, 10H, H_g, H_i), 0.84 (t, ³J_{Hj-Hi}=8 Hz, 3H, H_j).



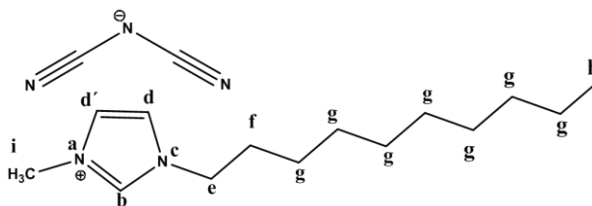
β -CD + [P_{6,6,6,14}][DCA] ¹H

NMR (400.13 MHz, DMSO)

δ 5.74 (m, 7H, H₁), 5.70 (s, 7H, 2-OH), 5.17 (s, 7H, 3-OH), 4.82 (t, ³J_{H5-H6}=4 Hz, ³J_{H5-H6'}=8 Hz, 7H, H₅), 3.62 (m, 7H, H₂), 3.60-3.53 (m, 14H, 6-OH, H₆), 3.28 (m, 14H, H₃, H₄), 2.49 (m, 8H,

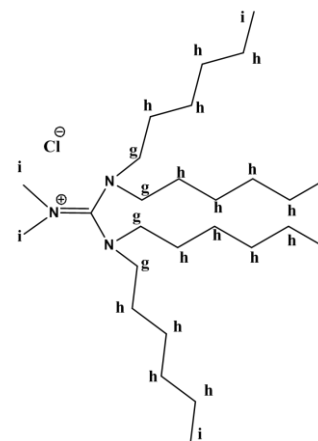
H_f), 1.46-1.27 (m, 16H, H_{b,e}), 1.26-1.20 (m, 32H, H_c), 0.84 (m, 12H, H_a). **β -CD + [C₁₀mim][SAC] ¹H NMR (400.13**MHz, DMSO) δ 9.08 (s, 1H, H_b), 7.74 (s, 1H,H_d), 7.68 (s, 1H, H_{d'}), 7.57 (m, 4H, H_j, H_k, H_l,H_m), 5.74 (m, 7H, H₁), 5.68 (s, 7H, 2-OH), 4.82(s, 7H, 3-OH), 4.46 (t, ³J_{H5-H6}=4 Hz, ³J_{H5-H6'}=8Hz, 7H, H₅), 4.13 (t, ²J_{He-He'}=4 Hz, ³J_{He-Hf}=8 Hz,2H, H_e), 3.82 (s, 3H, H_i), 3.62 (m, 7H, H₂), 3.61-3.54 (m, 14H, 6-OH, H₆), 3.38 (m, 14H, H₃, H₄),1.77 (m, 2H, H_f), 1.25 (m, 14H, H_g), 0.84 (t, ³J_{Hh-Hg}=8 Hz, 3H, H_h). **β -CD + [C₂OHMIM][BF₄] ¹H NMR (400.13 MHz, DMSO)** δ 9.04 (s, 1H, H_b), 7.69 (s, 1H, H_d), 7.66 (s, 1H, H_{d'}), 5.74 (m,7H, H₁), 5.70 (s, 7H, 2-OH), 5.17 (s, 7H, 3-OH), 4.82 (t, ³J_{H5-}H₆=4 Hz, ³J_{H5-H6'}=8 Hz, 7H, H₅), 4.19 (t, ²J_{He-He'}=4 Hz, ³J_{He-}H_f=8 Hz, 2H, H_e), 3.84 (m, 3H, H_g), 3.62 (m, 7H, H₂), 3.60-3.53 (m, 14H, 6-OH, H₆), 3.28 (m,14H, H₃, H₄), 1.40 (t, ³J_{Hf-He}= 8 Hz, 3H, H_f). **β -CD + [Omim][DCA] ¹H NMR (400.13 MHz,**DMSO) δ 9.07 (s, 1H, H_b), 7.74 (s, 1H, H_d), 7.67(s, 1H, H_{d'}), 5.76 (m, 7H, H₁), 5.68 (s, 7H, 2-OH),4.82 (s, 7H, 3-OH), 4.46 (t, ³J_{H5-H6}=4 Hz, ³J_{H5-}

(400.13 MHz, DMSO) δ 9.08 (s, 1H, H_b), 7.74 (s, 1H, H_d), 7.68 (s, 1H, H_{d'}), 5.74 (m, 7H, H_l), 5.68 (s, 7H, 2-OH), 4.82 (s, 7H, 3-OH), 4.46 (t, $^3J_{\text{H5-H6}}=4$ Hz, $^3J_{\text{H5-}}$



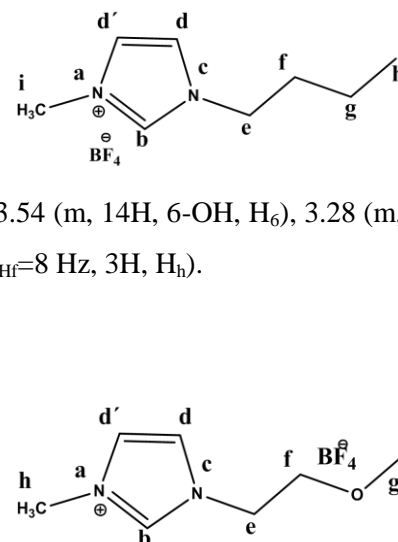
H₆=8 Hz, 7H, H₅), 4.13 (t, ²J_{He-He}=4 Hz, ³J_{He-Hf}=8 Hz, 2H, H_e), 3.83 (, 3H, H_i), 3.62 (m, 7H, H₂), 3.61-3.54 (m, 14H, 6-OH, H₆), 3.38 (m, 14H, H₃, H₄), 1.77 (m, 2H, H_f), 1.25 (m, 14H, H_g), 0.84 (t, ³J_{Hh-Hg}=8 Hz, 3H, H_h).

β -CD + [(C₆)₄DMG][Cl] ¹H NMR (400.13 MHz, DMSO) δ 5.74 (m, 7H, H₁), 5.68 (s, 7H, 2-OH), 4.82 (s, 7H, 3-OH), 4.45 (t, ³J_{H5-H6}=4 Hz, ³J_{H5-H6}=8 Hz, 7H, H₅), 3.63 (m, 7H, H₂), 3.61-3.54 (m, 22H, 6-OH, H₆, H_g), 3.38 (m, 14H, H₃, H₄), 1.52-1.23 (m, 16H, H_h), 0.84 (m, 12H, H_i).



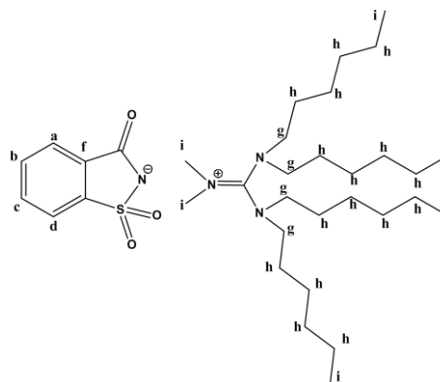
β -CD + [Bmim][BF₄] ¹H NMR (400.13 MHz, DMSO) δ
 9.08 (s, 1H, H_b), 7.74 (s, 1H, H_d), 7.68 (s, 1H, H_{d'}), 5.74 (m, 7H, H₁), 5.68 (s, 7H, 2-OH), 4.82 (s, 7H, 3-OH), 4.46 (t, ³J_{H5-H6}=4 Hz, ³J_{H5-H6'}=8 Hz, 7H, H₅), 4.14 (t, ²J_{He-Hc}=4 Hz, ³J_{He-Hf}=8 Hz, 2H, H_e), 3.83 (, 3H, H_i), 3.62 (m, 7H, H₂), 3.61-3.54 (m, 14H, 6-OH, H₆), 3.28 (m, 14H, H₃, H₄), 1.75 (m, 2H, H_f), 1.25 (m, 2H, H_g), 0.89 (t, ³J_{Hh-Hf}=8 Hz, 3H, H_h).

The chemical structure shows the [Bmim]⁺ cation and the BF₄⁻ anion. The imidazolium ring protons are labeled: a (H2), b (H3), c (H4), d (H5), and d' (H6). The methyl group is labeled i. The butyl chain protons are labeled: e (CH2), f (CH2), g (CH2), and h (CH3).

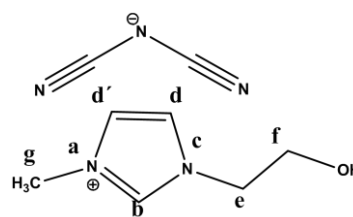


β -CD + [C₃O⁺mim][BF₄⁻] ¹H NMR (400.13 MHz, DMSO) δ
 9.09 (s, 1H, H_b), 7.71(s, 1H, H_d), 7.68 (s, 1H, H_{d'}), 5.74 (m, 7H, H₁), 5.67 (s, 7H, 2-OH), 5.22 (s, 7H, 3-OH), 4.46 (t, ³J_{H5-H6}=4 Hz, ³J_{H5-H6}=8 Hz, 7H, H₅), 4.16 (t, ²J_{He-He}=4 Hz, ³J_{He-Hf}=8 Hz, 2H, H_e), 3.83 (m, 3H, H_h), 3.72 (m, 2H, H_f), 3.63 (m, 7H, H₂), 3.60-3.53 (m, 14H, 6-OH, H₆), 3.34 (m, 14H, H₃, H₄), 3.15 (s, 3H, H_g).

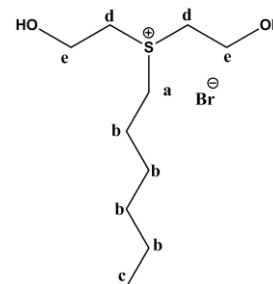
β -CD + [(C₆)₄DMG][SAC] ¹H NMR (400.13 MHz, DMSO) δ 7.57 (m, 4H, H_a, H_b, H_c, H_d), 5.74 (m, 7H, H₁), 5.68 (s, 7H, 2-OH), 4.82 (s, 7H, 3-OH), 4.45 (t, ³J_{H5-H6}=4 Hz, ³J_{H5-H6'}=8 Hz, 7H, H₅), 3.63 (m, 7H, H₂), 3.61-3.54 (m, 22H, 6-OH, H₆, H_g), 3.38 (m, 14H, H₃, H₄), 1.52-1.23 (m, 16H, H_h), 0.84 (m, 12H, H_i).



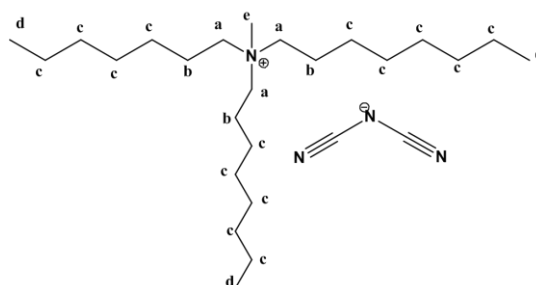
β -CD + [C₂OHMIM][DCA] ¹H NMR (400.13 MHz, DMSO) δ 9.09 (s, 1H, H_b), 7.68 (s, 1H, H_d), 7.65 (s, 1H, H_{d'}), 5.75 (m, 7H, H₁), 5.70 (s, 7H, 2-OH), 5.21 (s, 7H, 3-OH), 4.80 (t, ³J_{H5-H6}=4 Hz, ³J_{H5-H6'}=8 Hz, 7H, H₅), 4.19 (t, ²J_{He-Hc}=4 Hz, ³J_{He-Hf}=8 Hz, 2H, H_e), 3.84 (m, 3H, H_g), 3.62 (m, 7H, H₂), 3.60-3.53 (m, 14H, 6-OH, H₆), 3.28 (m, 14H, H₃, H₄), 1.40 (t, ³J_{Hf-Hc}=8 Hz, 3H, H_f).



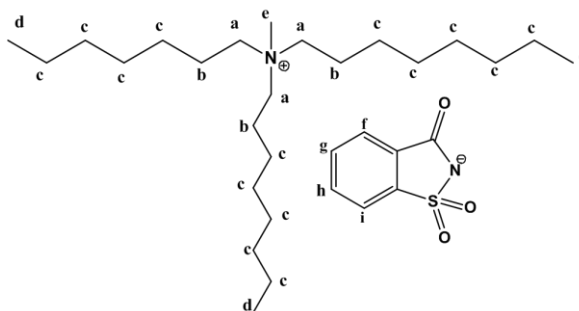
β -CD + [(C₂OH)₂C₆S][Br] ¹H NMR (400.13 MHz, DMSO) δ 5.72 (m, 7H, H₁), 5.52 (s, 7H, 2-OH), 4.80 (s, 7H, 3-OH), 4.45 (t, ³J_{H5-H6}=4 Hz, ³J_{H5-H6'}=8 Hz, 7H, H₅), 3.84 (m, 7H, H₂), 3.62-3.37 (m, 20H, 6-OH, H₆, H_e, e-OH), 3.28 (m, 14H, H₃, H₄), 2.55 (t, ³J_{Hd-Hc}=4 Hz, 4H, H_d), 1.74 (m, 2H, H_a), 1.37-1.27 (m, 8H, H_b), 0.85 (t, ³J_{Hc-Hb}=8 Hz, 3H, H_c).



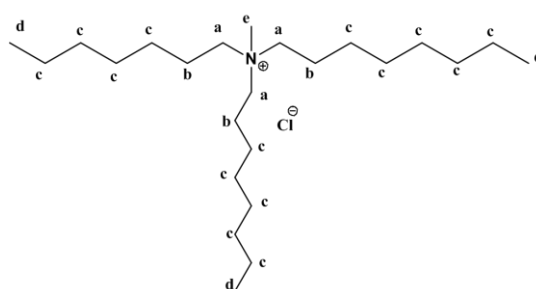
β -CD + [Aliquat][DCA] ¹H NMR (400.13 MHz, DMSO) δ 5.74 (m, 7H, H₁), 5.70 (s, 7H, 2-OH), 5.17 (s, 7H, 3-OH), 4.82 (t, ³J_{H5-H6}=4 Hz, ³J_{H5-H6'}=8 Hz, 7H, H₅), 3.62 (m, 7H, H₂), 3.60-3.53 (m, 14H, 6-OH, H₆), 3.35 (s, 3H, H_e), 3.28 (m, 14H, H₃, H₄), 3.20 (m, 6H, H_a), 1.58 (m, 6H, H_b), 1.23 (m, 28H, H_c), 0.85 (m, 9H, H_d).



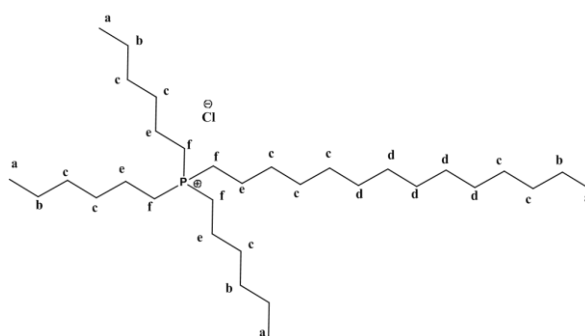
β -CD + [Aliquat][SAC] ^1H NMR (400.13 MHz, DMSO) δ 7.57 (m, 4H, H_f, H_g, H_h, H_i), 5.74 (m, 7H, H₁), 5.70 (s, 7H, 2-OH), 5.17 (s, 7H, 3-OH), 4.82 (t, $^3J_{\text{H5-H6}}=4$ Hz, $^3J_{\text{H5-H6}}=8$ Hz, 7H, H₅), 3.62 (m, 7H, H₂), 3.60-3.53 (m, 14H, 6-OH, H₆), 3.35 (s, 3H, H_c), 3.28 (m, 14H, H₃, H₄), 3.20 (m, 6H, H_a), 1.58 (m, 6H, H_b), 1.23 (m, 28H, H_c), 0.85 (m, 9H, H_d).



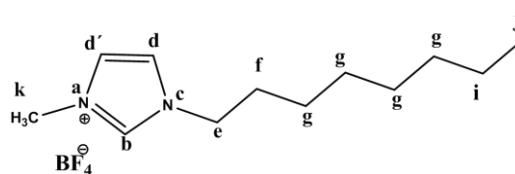
β -CD + [Aliquat][Cl] ^1H NMR (400.13 MHz, DMSO) δ 5.74 (m, 7H, H₁), 5.70 (s, 7H, 2-OH), 5.17 (s, 7H, 3-OH), 4.82 (t, $^3J_{\text{H5-H6}}=4$ Hz, $^3J_{\text{H5-H6}}=8$ Hz, 7H, H₅), 3.62 (m, 7H, H₂), 3.60-3.53 (m, 14H, 6-OH, H₆), 3.35 (s, 3H, H_c), 3.28 (m, 14H, H₃, H₄), 3.20 (m, 6H, H_a), 1.58 (m, 6H, H_b), 1.23 (m, 28H, H_c), 0.85 (m, 9H, H_d).



β -CD + [P_{6,6,6,14}][Cl] ^1H NMR (400.13 MHz, DMSO) δ 5.74 (m, 7H, H₁), 5.70 (s, 7H, 2-OH), 5.17 (s, 7H, 3-OH), 4.82 (t, $^3J_{\text{H5-H6}}=4$ Hz, $^3J_{\text{H5-H6}}=8$ Hz, 7H, H₅), 3.62 (m, 7H, H₂), 3.60-3.53 (m, 14H, 6-OH, H₆), 3.28 (m, 14H, H₃, H₄), 2.49 (m, 8H, H_f), 1.46-1.27 (m, 16H, H_b, e), 1.26-1.20 (m, 32H, H_c), 0.84 (m, 12H, H_a).



β -CD + [Omim][BF₄] ^1H NMR (400.13 MHz, DMSO) δ 9.09 (s, 1H, H_b), 7.74 (s, 1H, H_d), 7.67 (s, 1H, H_{d'}), 5.74 (m, 7H, H₁), 5.68 (s, 7H, 2-OH), 4.82 (s, 7H, 3-OH), 4.46 (t, $^3J_{\text{H5-H6}}=4$ Hz, $^3J_{\text{H5-H6}}=8$ Hz, 7H, H₅), 4.13 (t, $^2J_{\text{He-He}}=4$ Hz, $^3J_{\text{He-Hf}}=8$ Hz, 2H, H_e), 3.83 (s, 3H, H_k), 3.62 (m, 7H, H₂), 3.61-3.54 (m, 14H, 6-OH, H₆), 3.38 (m, 14H, H₃, H₄), 1.77 (m, 2H, H_f), 1.25 (m, 10H, H_g, H_i), 0.84 (t, $^3J_{\text{Hj-Hi}}=8$ Hz, 3H, H_j).



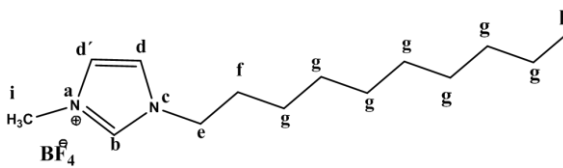
β -CD + [C₁₀mim][BF₄] ¹H NMR (400.13

MHz, DMSO) δ 9.07 (s, 1H, H_b), 7.74 (s, 1H,

H_d), 7.67 (s, 1H, H_{d'}), 5.74 (m, 7H, H_i), 5.68

(s, 7H, 2-OH), 4.82 (s, 7H, 3-OH), 4.46 (t,

³J_{H5-H6}=4 Hz, ³J_{H5-H6}=8 Hz, 7H, H₅), 4.13 (t, ²J_{He-Hc}=4 Hz, ³J_{He-Hf}=8 Hz, 2H, H_e), 3.83 (, 3H, H_i), 3.62 (m, 7H, H₂), 3.61-3.54 (m, 14H, 6-OH, H₆), 3.38 (m, 14H, H₃, H₄), 1.77 (m, 2H, H_f), 1.25 (m, 14H, H_g), 0.84 (t, ³J_{Hh-Hg}=8 Hz, 3H, H_h).



IV.8.2. General procedure for the recovery of β -CD and ILs

After 24 hours stirring the mixture of β -CD and ILs at RT, acetone was added to extract the cyclic oligosaccharide from the organic layer. This experiment confirmed the possibility to recover β -CD as well as the ILs. This addition caused a complete β -CD precipitation while the IL maintain soluble in the organic phase. The β -CD precipitate could be easily recovered from the solution. The chemical stability of the recycled β -CD and ILs were analyzed by ¹H NMR and ¹³C NMR spectroscopy.

IV.8.3. General procedure for the studies on improvement of water solubility of fatty acids and steroids

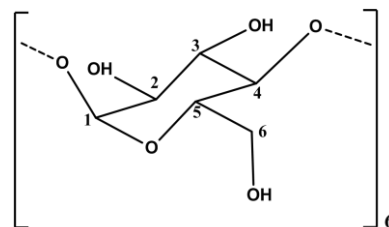
For the preparation of the β -CD- [Emim][EtSO₄] gel, β -CD (0.05 g, 0.04 mmol) was mixed with [Emim][EtSO₄] (0.2 g, 0.85 mmol) and stirred for 24h at RT. To a flask with 1 ml of water, 50 μ l of β -CD with [Emim][EtSO₄] additive was added and stirred to solubilize all the gel. Then a portion of fatty acid, steroid respectively (0.0004 g) was added and stirred for 5 minutes at RT. A second portion was added if after the indicated time all the amount of fatty acid or steroid was solubilized. The addition was repeated until the first symptom of precipitate appeared. The results were concluded by visual observation.

IV.8.4. General procedure for the dissolution of α - and γ -CD in ILs

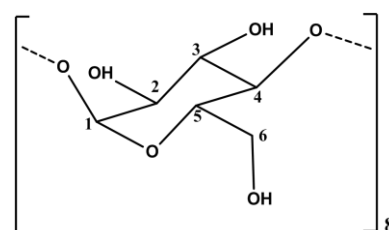
Following the general procedure for α - and γ -CD dissolution studies, RTILs were selected based on phosphonium, ammonium, methylimidazolium cations connected to chloride, dicyanamide and ethylsulfate anions. To a 1 ml vial, 0.2-0.3g of ILs were added and also 0.1-0.15g of α - and γ -CD until saturation was observed. The α - and γ -CDs solubility was determined visually. The

samples were stirred for 24 hours at room temperature and filtrated. The percentage of α - and γ -dissolved in ILs was confirmed using ^1H NMR spectra of the mixture after 24 hours by comparing the well known peaks of α - and γ -CD with the ILs peaks.

α -CD ^1H NMR (400.13 MHz, DMSO) δ 5.51 (m, 6H, H_1), 5.43 (s, 6H, 2-OH), 4.78 (s, 6H, 3-OH), 4.49 (t, $^3J_{\text{H}_5-\text{H}_6}=4$ Hz, $^3J_{\text{H}_5-\text{H}_6}=8$ Hz, 6H, H_5), 3.77 (m, 6H, H_2), 3.62-3.55 (m, 12H, 6-OH, H_6), 3.26 (m, 12H, H_3 , H_4). ^{13}C NMR (101 MHz, $(\text{CD}_3)_2\text{SO}$) δ 110.40 (C1), 83.51 (C4), 79.09 (C5), 74.30 (C2), 72.08 (C3), 60.97 (C6).



γ -CD ^1H NMR (400.13 MHz, DMSO) δ 5.73 (m, 8H, H_1), 5.67 (s, 8H, 2-OH), 4.81 (s, 8H, 3-OH), 4.46 (t, $^3J_{\text{H}_5-\text{H}_6}=4$ Hz, $^3J_{\text{H}_5-\text{H}_6}=8$ Hz, 8H, H_5), 3.61 (m, 8H, H_2), 3.60-3.53 (m, 16H, 6-OH, H_6), 3.31 (m, 16H, H_3 , H_4). ^{13}C NMR (100.61 MHz, DMSO) δ 101.99 (C1), 81.58 (C4), 73.09 (C5), 72.45 (C2), 72.08 (C3), 59.97 (C6).



IV.8.5. General procedure for the studies on improvement of water solubility of α - and γ -CDs

First, the solubilities of α - and γ -CDs in water without any additive were studied. In this context, to a flask with 0.5 ml of water, portions of α - or γ -CDs (0.005 g) were added. The addition was repeated until the first symptom of precipitate appeared. The results were concluded by visual observation. For the studies of solubility of α - and γ -CDs in water with additive, the α - or γ -CDs [Emim][EtSO₄] gels were prepared. α - or γ -CDs (0.05 g, 0.04 mmol) was mixed with [Emim][EtSO₄] (0.2 g, 0.85 mmol) and stirred for 24h at RT. To a flask with 0.5 ml of water, portions of α - or γ -CDs with [Emim][EtSO₄] (50 μl) additive were added and stirred to solubilize all the gel. The addition was repeated until the first symptom of precipitate appeared. The results were concluded by visual observation. Then, a solution of 0.9% sodium chloride in water (serum solution) was prepared (0.0045 g NaCl per 0.5 ml H₂O). The same procedures were repeated for α - and γ -CDs dissolution studies in water with sodium chloride buffer, pH=7.

CHAPTER V. Nucleobases

V. Ionic Liquids from nucleobases

Nucleotides are the building blocks of all nucleic acids and on the other hand, ILs have come under worldwide scrutiny mostly through their use as solvents. Mainly, the room temperature ionic liquids (RTILs), also known as “designer solvents” have been tested as greener replacement of common toxic organic solvents⁵. Their flexible nature in the solubility of various compounds, including pharmaceuticals and biological compounds, indicated us that ILs can be excellent for the dissolution of nucleobases. Nevertheless, the preparation of ILs derived from nucleotides has not been reported so far. Having this fact in mind, this chapter presents the development of novel CILs based on nucleosides such as adenosine, guanosine, thymidine and uridine as well as nucleotide based on adenosine monophosphoric acid (AMP).

V.1. *Synthesis of organic salts developed from nucleosides and AMP nucleotide*

It is interesting to note that the bases of nucleic acids are biological molecules constituted by heteroaromatic rings like imidazole from ionic liquid structures (Figure V.1). In this context, nucleosides can be manipulated in order to create novel nucleoside-based ILs according with combination with adequate counter-ions.

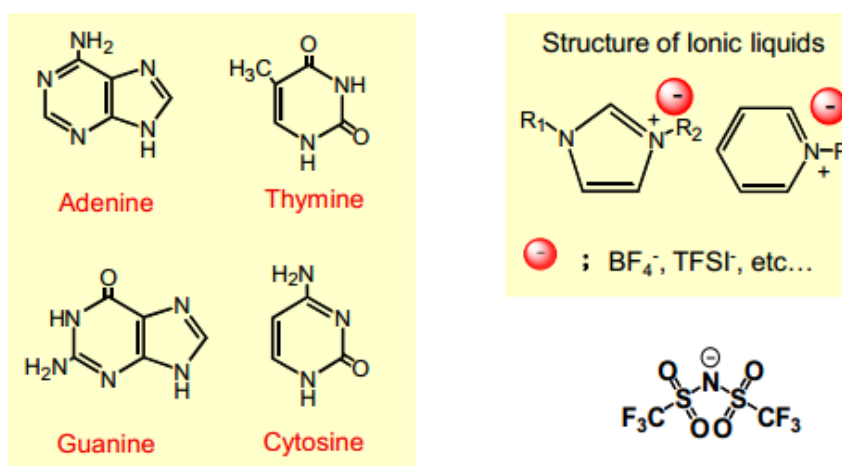
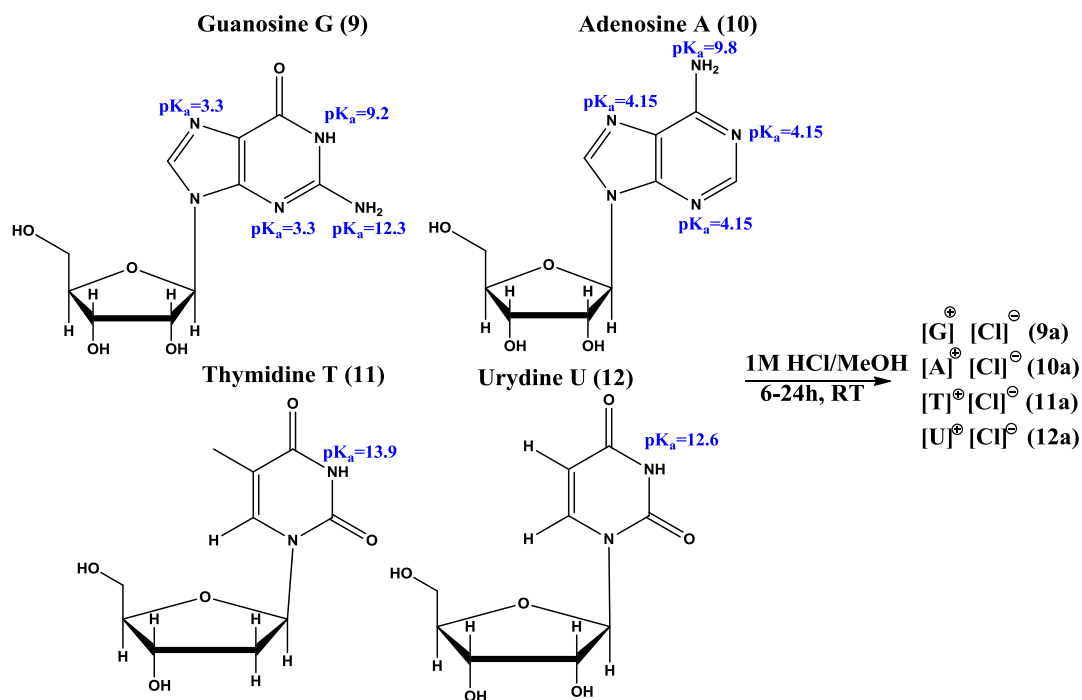


Figure V.1 - Comparison of nucleic acids cations with imidazolium cation.

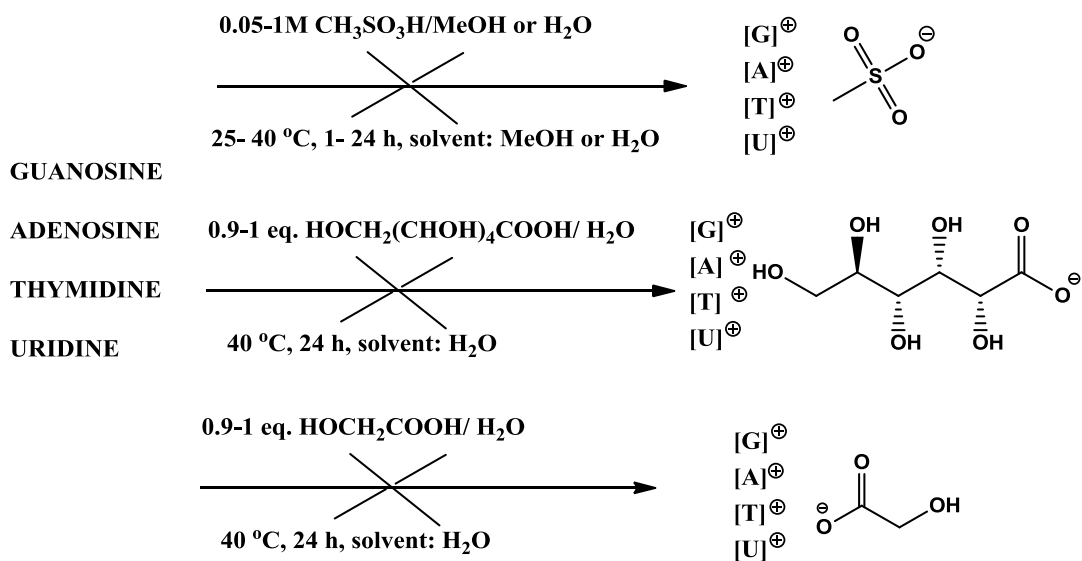
Initially, the protonation of four nucleosides, namely guanosine, adenosine, thymidine and uridine, using hydrochloric acid were performed as indicated in Scheme V.I. Then different organic acids were tested for the studies. Hydrochloric acid (1M) and mesylic acid (0.05 to 1M)

in methanol or water was firstly prepared for the adequate protonation of each nucleoside. ^1H NMR spectra showed that the protonation with hydrochloric acid is possible for all the cases. A characteristic chemical shift of all the protons was observed when compared to ^1H NMR spectra of the starting materials (all protons more deshielded). The protonation using mesylic acid was much more difficult to carry out. This procedure failed in all of the cases, probably due to solubility and stability problems of the nucleoside scaffolds (Scheme V.2). Different reaction conditions (acid concentration, type of solvents, temperature and reaction time, among others) were studied without positive results. It was concluded that solubility and chemical stability of nucleoside could be one of the limitations that made it difficult in order to obtain the correct proportion of nucleoside to mesylic acid. It is important to empathize that the degradation of the nucleoside sugar ring was observed when an excess of mesylic acid was added. Later experiments on the protonation of guanosine using solutions of gluconic (1: 0.9 eq) and glycolic (1: 1 eq.) acids in proportion to the adequate nucleoside were also performed. All this efforts failed as indicated in Scheme V.2. One of the reasons could be the fact that those acids are much weaker than mesylic and hydrochloric, thus aren't acidic enough to keep the positive charge on the nucleoside ($\text{pK}_a = 3.86$ for gluconic and $\text{pK}_a = 3.83$ for glycolic acids).

Similar to the procedure explained for the synthesis of CILs from amino acids (see chapter II and III), after the successful protonation with hydrochloric acid, the second step corresponded to anion exchange reaction using bis(trifluoromethanesulfonyl)imide ($[\text{NTf}_2]$), docusate ($[\text{AOT}]$) and p-toluenesulfonate ($[\text{TsO}]$) as selected anions. The studies showed the importance of the appropriate selection of counter-ions. $[\text{NTf}_2]$ anion wasn't acidic enough to keep the positive charge on the nucleoside, while $[\text{TsO}]$ anion created too acidic condition for the compound to be stable. After these reactions, it was possible to conclude the limited success related with the preparation of organic salts based on three nucleosides as cations when combined with docusate $[\text{AOT}]$ as biocompatible anion (Figure V.2). It seems that larger alkylsulfonate anions can be appropriate for these combinations. Only in the case of adenosine the degradation of the nucleoside was observed. Interestingly, both guanosine and adenosine contain a primary amine attached directly to the heterocyclic ring, nevertheless they showed different solubility behaviour and pK_a values as presented in Scheme V.1. Figures V.3 and V.4 present the ^1H NMR spectra of $[\text{T}][\text{AOT}]$, **11b**, and $[\text{U}][\text{AOT}]$, **12b**, respectively which elucidate about the expected cation/anion correlations by quantitative integration of their characteristic ^1H resonance peaks (1:1 for **11b** and 1.07:1 for **12b**). It is interesting to note that the ^1H NMR spectra of nucleoside ion combined with the large docusate anion comparing with the spectra of chloride as anion showed a significant chemical shift. Therefore it can be concluded that stronger interactions occur between the docusate anion (including sulfonate structure) and nucleoside cation as illustrated in additional NMR studies presented in subsection V.3.



Scheme V.1 - Protonation of nucleosides using hydrochloridic acid.



Scheme V.2 - Studies on the protonation of nucleosides using other organic acids.

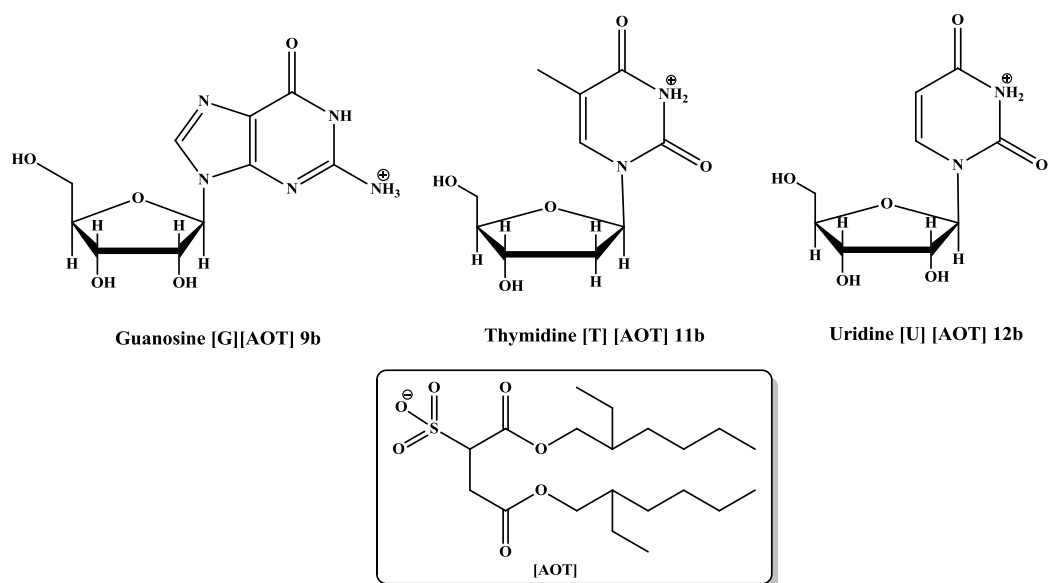


Figure V.2 - Structures of chiral salts synthesized from nucleosides as cations docusate [AOT] as anion.

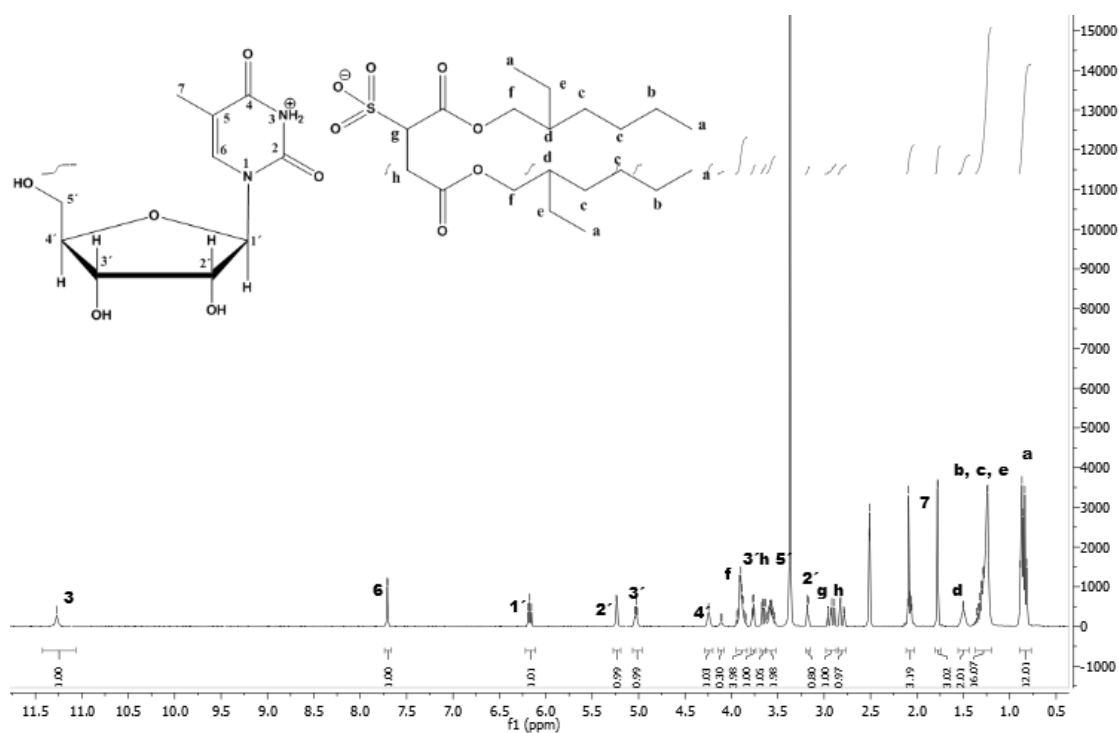


Figure V.3- ¹H NMR spectra of [T][AOT] 11b performed in dry DMSO.

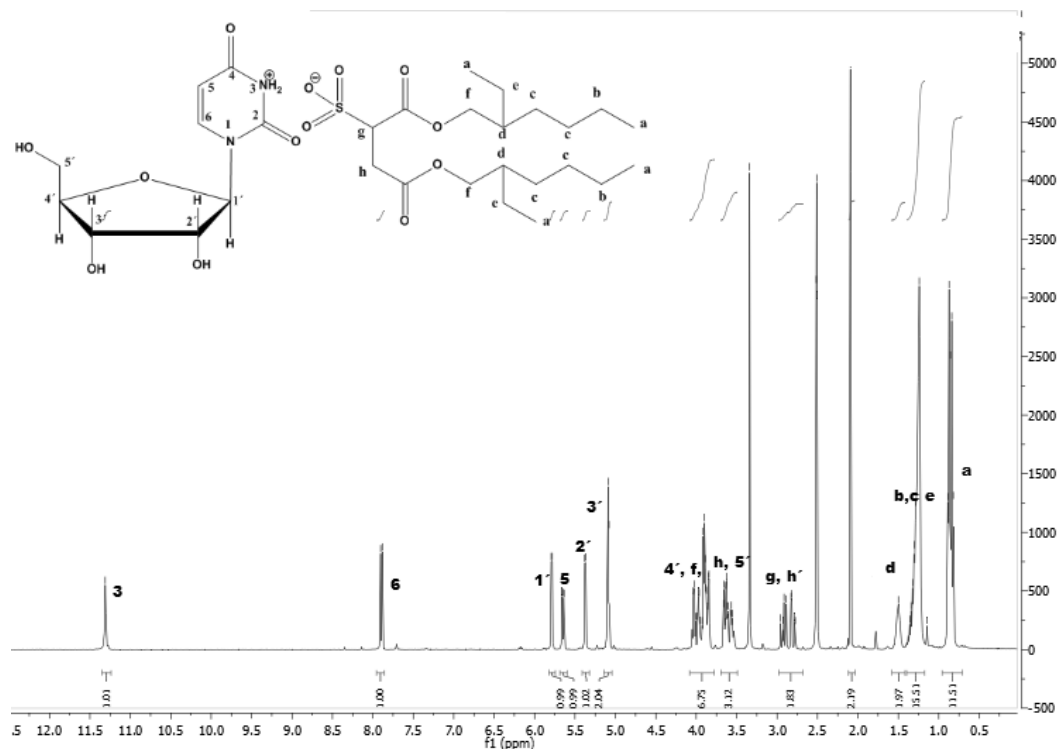


Figure V.4 - ^1H NMR spectra of [U][AOT] 12b performed in dry DMSO.

In addition, synthesis of chiral salts based on adenosine 5'-monophosphoric acid (AMP, Chapter I, Figure I.11) as nucleotide structure were also performed. According to this, Amberlyst A-26 resin (in the OH form) has been used to exchange halides (bromide or chloride) to hydroxide form and then this basic solution reacted with an adequate acid solution. The structures of the developed salts are presented in Figure V.5. The direct acid-base reaction yields the desired AMP salt combined with selected organic cations such as trihexyltetradecylphosphonium ([P_{6,6,6,14}]), **13a**, 1-ethyl-3-methylimidazolium ([Emim]), **13b**, and 1-(2-methoxyethyl)-3-methylimidazolium ([C₃Omim]), **13c**. In the case of choline ([Choline]) cation, a direct reaction (without resin column method) was performed from commercial available choline hydroxide, **13d**. ^1H NMR of an example of chiral salt based on AMP scaffold as the anionic unit is presented in Figure V.6.

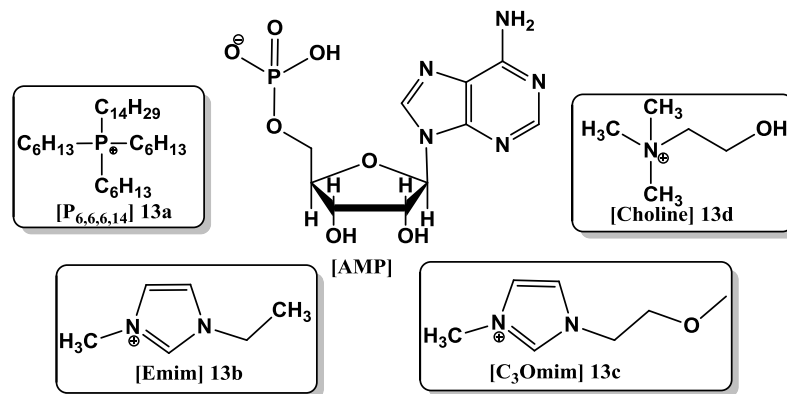


Figure V.5 - Structures of the salts developed from AMP nucleotide.

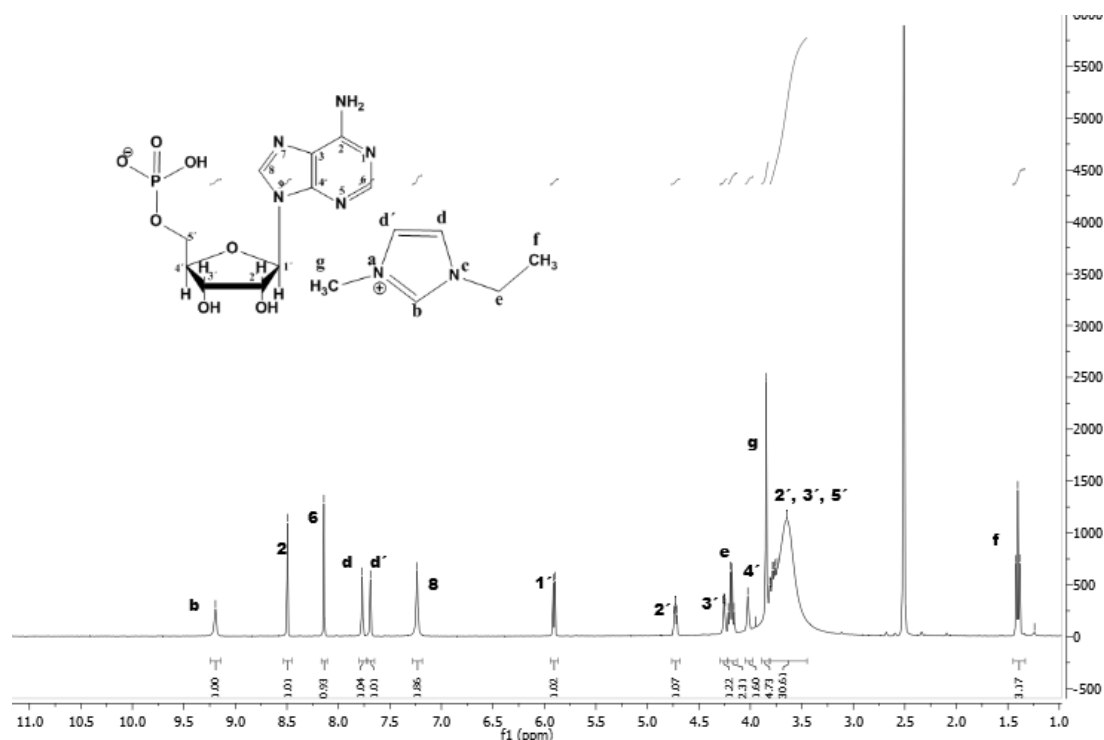


Figure V.6- ^1H NMR spectra of [Emim][AMP] **13b** performed in dry DMSO.

V.2. Characterization of salts developed from nucleosides and AMP

All isolated products were completely characterized by ^1H and ^{13}C NMR, FTIR spectra and elemental analysis in order to check their expected structures and final purities. The desired chiral nucleoside-based salts ([G][AOT], **9b**, [T][AOT], **11b**, and AMP-based salts ([P_{6,6,6,14}][AMP], **13a**, [Emim][AMP], **13b**, [C₃Omim][AMP], **13c**, and [Choline][AMP], **13d**, were obtained in high yields (76-99%) as well as high purities as indicated in Table V.I. Furthermore, the uridine based salt [U][AOT], **12b**, was obtained in lower yield (23% of yield) comparing with other cases. Table V.1 summarizes some physical and thermal characteristics of the synthesized salts from nucleosides and AMP-nucleotide. All protonated nucleosides with hydrochloric acid in methanol solution were obtained as white pastes and only characterized by ^1H and ^{13}C NMR spectroscopy. For cream-coloured pastes of chiral guanosine and thymidine-based salts [G][AOT], **9b**, and [T][AOT], **11b**, no T_g values were observed. Among all, the only solid synthesized was based on uridine [U][AOT], **12b**, with a melting point of 134 °C. Particularly relevant is the successful reduction of the initial melting point of commercial uridine (167.2 °C) by the appropriate selection of the organic anion. All the salts derived from AMP nucleotide were obtained as viscous yellow liquids. The T_g was determined at heating/cooling rate of 10 °C.min⁻¹ for all compounds and the values obtained were between -24.32 and -48.19 °C, except for [Emim][AMP], **13b**, in which the T_g was not detectable.

Decomposition studies were performed by TGA analysis for some of the synthesized compounds. In some cases it is possible to observe an improvement in the thermal stability of the original neutral nucleosides and AMP nucleotide compounds. This observation suggests that the stronger cation-anion interaction can stabilize better the final salt avoiding their thermal stability at lower temperatures.

According to the poor miscibility of AMP in most of organic solvents, the solubility behaviour of novel ILs derived from AMP was studied in order to show the possibility to enhance their miscibility.

Table V.1 - Characterization of new synthesized salts based on nucleosides and AMP scaffolds.

<i>Salt</i>	<i>Yield [%]</i>	<i>Purity [%]</i>	<i>Physical state</i>	<i>T_g [°C]^[a]</i>	<i>T_{dec} [°C]^[d]</i>
[G][Cl] 9a	>99	99	white paste	T _m < 250 (lit.)	^[e]
[A][Cl] 10a	99	99	white paste	T _m < 234 (lit.)	^[e]
[T][Cl] 11a	73	99	white paste	T _m < 186 (lit.)	^[e]
[U][Cl] 12a	76	99	white paste	T _m < 163 (lit.)	^[e]
[G][AOT] 9b	76	97	cream-coloured paste	-- ^[b]	^[e]
[T][AOT] 11b	≥99	99	cream-coloured paste	-- ^[b]	241.60
[U][AOT] 12b	23	97	cream-coloured solid	T _m =134 ^[c]	^[e]
[P _{6,6,6,14}][AMP] 13a	98	99	viscous yellow liquid	-48.19	269.20
[Emim][AMP] 13b	76	99	viscous yellow liquid	-- ^[b]	275.30
[C ₃ Oim][AMP] 13c	96	98	viscous yellow liquid	-24.32	260.10
[Choline][AMP] 13d	98	99	viscous yellow liquid	-30.51	270.50

^[a] Glass transition temperature (T_g) was determined by DSC measurements at a heating/cooling rate of 10 °C.min⁻¹ for all salts. ^[b] Not observed by DSC studies. ^[c] Melting temperature was determined on Electrothermal Melting Point Apparatus. ^[d] Decomposition temperature (T_{dec}) was determined by TGA studies. ^[e] Not determined.

V.3. NMR interaction cation-anion studies

Preliminary ¹H NMR studies were performed in the case of [T][AOT], **11b**, and [Emim][AMP], **13b**, at different temperatures to determine the degree of cation-anion interactions. Figure V.7 and Figure V.8 illustrate a comparative ¹H NMR measurements of both of the salts derived from nucleic acids bases either as cation (**11b**) or anion (**13b**) at five temperatures (25, 40, 55, 70 and 85 °C) in d-DMSO. In the case of **11b**, two different regions of the ¹H NMR spectra between 3.40 to 2.80 and around 2.10 ppm were particularly selected to check the heteroaromatic cationic part and the aliphatic signals close to the negative charge of docusate anion, respectively. In the case of CH₃ group attached to the pyrimidine ring of thymidine (singlet at 3.35 ppm), a chemical shift to right was observed between 25 °C and 85 °C. This variation of

the chemical shift (at least 0.37 ppm of difference between 25 °C to 85 °C) can be explained by the possible interaction of the protons close to the nucleoside positive charge with the aliphatic signals near to negative charge. The CH₂ peaks close to sulfonate anion (multiplet at 2.10 ppm) increase for higher temperature values (free rotation of the molecule). It is clear that increase of temperature from 25 °C up to 85 °C (hence decrease of viscosity), facilitates the cation-anion interaction close to ion charge.

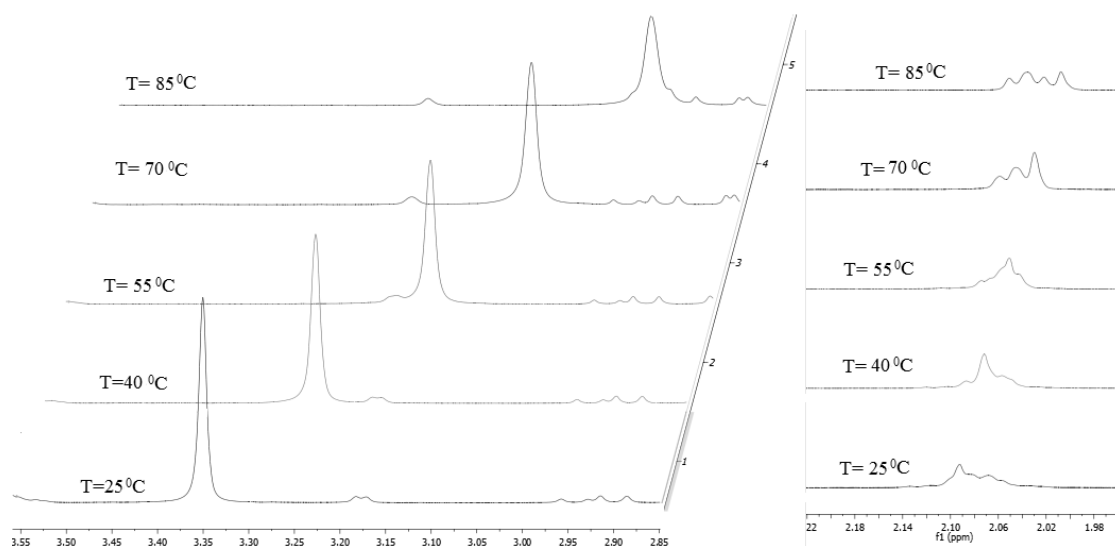


Figure V.7 - Comparative ¹H-NMR study of [T][AOT] for five temperatures (25, 40, 55, 70 and 85 °C) and two NMR regions (3.40 to 2.80 and at 2.10 ppm) in DMSO.

In the case of [Emim][AMP] **13b**, region between 4.00 to 3.00 ppm was chosen to see behaviour of imidazolium cation as presented in Figure V.6. Also for this sample the CH₃ peak close to the positive charge (singlet at 3.85 ppm), increase at higher temperature and a chemical shift to right was observed between 25 °C and 85 °C. This variation of the chemical shift (0.4 ppm of difference between 25 °C to 85 °C) can be explained by the possible interaction of the protons close to the nucleoside negative charge (monophosphate anion) with the protons near the positive charge of imidazolium cation.

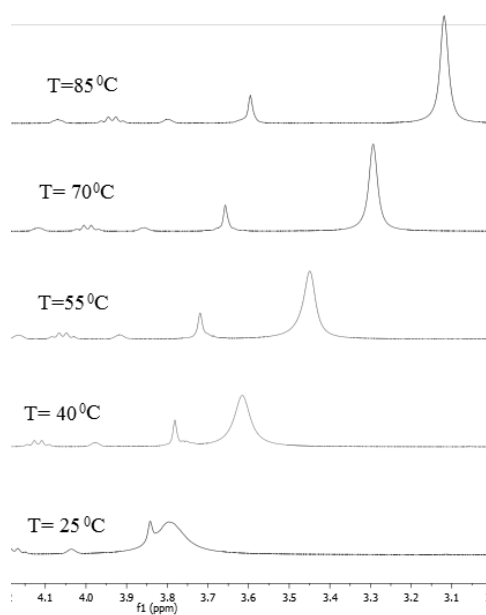


Figure V.8 - Comparative ^1H -NMR study of [Emim][AMP] for five temperatures (25, 40, 55, 70 and 85 °C) in DMSO.

V.4. *Critical micellar concentration studies*

In colloidal and surface chemistry, surfactants (also known as surface-active agents or detergents) are among the most adaptable chemicals available. Because of their unique functional properties, surfactants find a wide range of uses including chemistry (chemical kinetics or equilibria), biology (as membrane mimetics), and pharmacy¹⁴⁴. Depending on the type of product, these include improving the solubility (increase of bioavailability), stability of specific drugs in liquid preparation and extension of drug absorption. Surfactants can provoke direct effects on biological membranes thus altering drug transport across the membrane. Furthermore, they may reduce the effectiveness of antimicrobials or preservatives included in a specific biological formulation. Detergents are amphiphilic materials containing both apolar long-chain hydrocarbon ‘tail’ and polar, usually ionic, ‘head’ groups¹⁴⁵. In polar solvents, for example water, this property of the amphiphile leads to self-association: the surfactant molecules arrange themselves into organized molecular assemblies known as micelles or colloid-sized clusters as presented in Figure V.9. Amphiphilic molecules form micelles above a particular concentration which is called as critical micellar concentration (CMC)¹⁴⁵. The CMC is an important characteristic of a surfactant. Before reaching the CMC, the surface tension varies strongly with the concentration of the surfactant. After reaching the CMC, the surface tension stays relatively constant or changes with a lower slope. The value of the CMC for a specific dispersant in a given medium depends on temperature, pressure, and (sometimes strongly) on the presence and concentration of other surface active substances and electrolytes. CMC has been obtained by numerous researchers using different techniques such as surface

tension (tensiometer), conductivity (conductimeter) or absorption studies (UV/VIS spectrophotometer)¹⁴⁶. For example, the value of CMC for anionic surfactant [Na][AOT] at 20 °C, atmospheric pressure, measured by conductivity method is $2.40 \text{ (mol.dm}^{-3} \cdot 10^3)$.

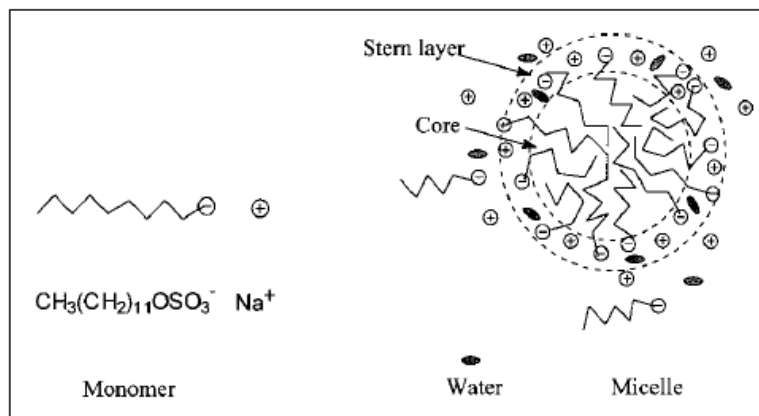


Figure V.9 - An idealized model for a spherical micelle of sodium dodecyl sulfate¹⁴⁴.

According to the surfactant nature of the biocompatible [AOT] used for the preparation of novel chiral salts based on nucleosides presented in this chapter, CMC measurements of **9b** and **11b** were performed firstly using Absorption Spectroscopy Method. Unfortunately, this method failed due to the strong interactions between the nucleosides derived salts and the chosen colored probe (acridine yellow G as well as normal acridine). In the second approach, electrical conductivity measurements were chosen in order to measure the type of micelles of the surfactants with two different nucleoside counterions (guanosine and thymidine). The possible CMC values were obtained by plotting conductance Λ against the concentration of the surfactant. There are some indications that chiral cations derived from nucleosides may lower CMC values comparing with common Na[AOT]. It seems that the size of counter-ion plays an important role: a bigger size of the counter-ion lowers its accessibility towards the head group and the chance for micellization at lower concentration is better. Nevertheless, in order to prove this hypothesis a large range of concentrations should be used for conductivity studies or other method such as surface tension should be examined. In order to measure the type of micelles, more detail studies should be performed using for instance Dynamic Light Scattering method (DLS).

V.5. Fluorescence studies

Nucleotides display environmentally sensitive fluorescence and therefore give strong signals upon a binding event which makes them a perfect probe for stopped- flow and equilibrium

analysis¹⁴⁷. It was observed that these new chiral salts derived from AMP nucleotide are fluorescent at ambient temperature as the neutral AMP nucleotide. Figure V.10 shows the comparative fluorescence between RTIL [Emim][AMP], **13b** (right) and original crystalline powder AMP (left) by UV light. In this context, novel RTILs [Emim][AMP], **13b** and [C₃Oimim][AMP] **13c** were chosen in order to evaluate their fluorescence. The studies were performed in aqueous solutions (10.⁻⁶ M), so for this reason water insoluble [P_{6,6,6,14}][AMP], **13a**, was not selected. The emission spectrum was monitored at wavelength $\lambda=521$ nm. The spectroscopic measurements showed that the starting material AMP is the least fluorescent material proving that the enhancement of the fluorescence of nucleotide in aqueous solution is possible when AMP was transformed to a chiral salt (Figure V.11). Specifically, [Emim][AMP] caused a 2-fold increase in the fluorescence intensity comparing with the initial nucleotide (increase from 1.13 to 2.23). In the case of [C₃Oimim][AMP] it was possible to obtain a 1.35-fold enhancement of fluorescence intensity. This fact could be explained by possible interactions between the acidic imidazolium proton (2-H) with the phosphate [AMP] anion.



Figure V.10 -An example of fluorescence material- photo of [Emim][AMP](right) and the solid AMP nucleotide (left) under UV lamp.

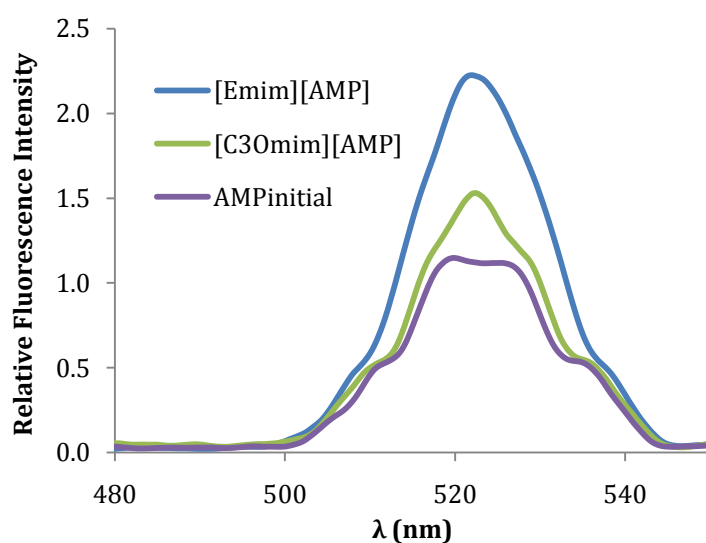


Figure V.11- Emission spectra of AMP nucleotide (violet) and new AMP-based chiral salts [Emim][AMP] in blue, and [C₃Oimim][AMP] in green at concentration 10.⁻⁶ M.

V.6. Conclusions

In the last chapter concerning the design of novel bio-derived ionic liquid, the attention is paid to bases of nucleic acids. These biological compounds that lead directly to the helical structure of DNA and RNA showed potential to be used as a source for design of novel pure chiral salts.

After optimizing the synthetic approaches, it was possible to protonate nucleosides and also to combine three of them (guanosine, thymidine and uridine) with biocompatible docusate anion. It was concluded that protonated nucleotides may form ILs. Nevertheless, aminoacids are easier to protonate when comparing with nucleosides. The surfactant docusate anion was crucial in order to reduce the melting temperature in the case of [U][AOT] **12b**, moreover because its large size facilitates stronger interactions with the cationic unit than chloride anion. Nevertheless, different organic anions such as mesylate ([CH₃SO₃]), gluconate ([HOCH₂(CHOH)₄CO₂]), glycolate ([HOCH₂CO₂]) and bis(trifluoromethanesulfonyl)imide ([NTf₂]) were not enough acidic to keep the positive charge on the nucleoside scaffold.

Chiral salts developed from AMP nucleotide by using ion exchange resin method [P_{6,6,6,14}][AMP] **13a**, [Emim][AMP] **13b**, [C₃Omim][AMP] **13c**, [Choline][AMP] **13d** are the most promising examples as they all were obtained as RTILs. It is important to note that this synthetic approach was easier to control and the sugar ring of the nucleotide was more stable in these basic conditions. Glass transition temperatures were detected for AMP-based CILs in contrast to the initial crystalline AMP nucleotide with the melting point of 178 to 185 °C. All of novel chiral salts derived from natural nucleosides and nucleotides were synthesized with moderate to high yields and purities, except in the case of [U][AOT].

The attempt was to apply these new chiral salts for fluorescence enhancement of the initial AMP nucleotide. On the other hand, the idea was to determine the CMC in order to study their possibility to act as surfactants forming micelles.

In our work, we illustrated the opportunity to perform chiral salts and at the same time, some RTILs from AMP nucleotide, thus further investigation on their preparation method, toxicology as well as better understanding of solubility mechanism should be attained. Different synthetic approaches should be examined in order to develop other salts based on nucleic acid bases, eg. mixing the nucleobase with a buffer and using the ion exchange resin method.

From the biological, medical and pharmaceutical point of view, the possibility to prepare novel modified nucleosides is extremely attractive as the interest on their solubility chemistry is growing as well as the knowledge of its biochemical importance and applications is becoming better known¹⁴⁸. Molecules that act like nucleosides in DNA synthesis known as nucleosides analogues include a range of antiviral products used to prevent viral replication in infected cells. These agents can be used against hepatitis B virus, hepatitis C virus, herpes simplex as well as cancer (chemotherapy agents). Knowledge of the often complex interactions amongst antiretroviral drugs and their clinical implications is important to maintain their antiretroviral efficiency and avoid toxicity. Some studies on the development of drugs in form of gels to improve their activity and solubility were performed¹⁴⁹. In our work no additional media was needed in order to determine salts of nucleobases with a possible future application as antiviral drugs. Transformation of a drug from a neutral into salt form could improve the solubility, therapeutic activity and avoid the polymorphism as long as the derived salts are amorphous. Nucleobases are involved in two qualitatively diverse mutual interactions: hydrogen bonding and aromatic base stacking. Therefore, the correct choice of counter-ion could protect the drug, ease the transport and work as the drug carrier.

V.7. *Experimental part*

General: Commercially available reagents (Guanosine, MW= 283.24 g.mol⁻¹, CAS No. 118-00-3, Adenosine, MW= 267.24 g.mol⁻¹, CAS No. 58-61-7, Thymidine, MW= 242.23 g.mol⁻¹, CAS No. 50-89-5, Uridine, MW= 244.20 g.mol⁻¹, CAS No. 58-96-8 and adenosine 5'-monophosphoric acid, MW= 346.21 g.mol⁻¹, CAS No. 61-19-8), ionic liquids, solvents were purchased from Alfa Aesar, Aldrich, Solchemar and were used without further purification. The basic anion-exchange resin Amberlyst A-26 (OH-form with ion-exchange capacity 0.8 eq.mL⁻¹) was purchased from Supelco. ¹H and ¹³C NMR spectra were recorded at room temperature on a Bruker AMX400 spectrometer with TMS as internal standard. Chemical shifts are reported downfield in ppm. Dried DMSO was used as deuterated solvent in order to avoid any water content in the spectra of all the synthesized compounds. IR spectra were performed by Perkin Elmer model Spectrum 1000 using NaCl plates for neat liquids. DSC analysis was carried out using a TA Instruments Q-series™ Q200 DSC with a refrigerated cooling system. The decomposition temperatures were measured with the Simultaneous Thermal Analyser STA 449 F3 Jupiter, using a nitrogen atmosphere (mass changed in % or mg). The samples for elemental analysis were performed by Laboratório de Análises at REQUIMTE, Departamento de Química Faculdade de Ciências e Tecnologia (Monte da Caparica) using Thermo Finnigan-

CE Instruments equipment, model Elemental Analyser 1112 series. The melting point (mp) was determined by Electrothermal Melting Point Apparatus.

Absorption measurments: UV/Vis absorption spectra were recorded with a Varian-Cary 100 Bio UV/Vis Spectrophotometer at 20 °C.

Emission measurments: Emission spectra were performed using Perkin Elmer LS 45 Luminescence Spectrometer at 20 °C.

Conductivity measurments: CMC was determined by using Crison Conductimeter Basic 30, conductivity cell + Pt 1000 at 20 °C.

V.7.1. General procedure for protonation of nucleosides (9a), (10a), (11a), (12a)

The general approach of the protonation was to dissolve the nucleoside (**9**, **10**, **11**, **12**) in 40 ml of methanol and add slowly 1M solution of HCl in MeOH (1:1 eq., 1.77 ml) in order to protonate the amine group. The reaction mixture was stirred at room temperature for 24h. The solution was evaporated and dried *in vacuo* for ~24h. The adequate nucleoside hydrochloride **9a**, **10a**, **11a**, **12a** was obtained as a white solid.

9-(2R,3R,4S,5R)-3,4-dihydroxy-5-(hydroxymethyl)tetrahydrofuran-2-yl)-6-oxo-6,9-dihydro-1H-purin-2-aminium chloride (9a): (0.56 g, >99 %). ¹H NMR (400.13 MHz, DMSO) δ 11.71 (s, 1H, H₁), 9.12 (s, 1H, H₈), 7.30 (s, 3H, H₂), 5.82 (d, ³J_{H1'-H2'} = 4 Hz, 1H, H_{1'}), 5.78 (t, ^{2,3}J_{H2'-H2', H1'} = 4 Hz, 1H, H_{2'}), 4.51 (s, 3H, H_{2'}, H_{3'}, H_{5'}), 4.39 (t, ^{2,3}J_{H3'-H3', H2'} = 4 Hz, 1H, H_{3'}), 4.16 (m, 1H, H_{4'}), 3.97 (t, ^{2,3}J_{H2'-H3', H2'} = 4 Hz, 1H, H_{2'}), 3.72 (dd, ²J_{H5'-H5'} = 4 Hz, ³J_{H5'-H4'} = 16 Hz, 1H, H_{5'}), 3.61 (dd, ²J_{H5'-H5'} = 4 Hz, ³J_{H5'-H4'} = 16 Hz, 1H, H_{5'}). ¹³C NMR (100.61 MHz, DMSO) 155.85 (C₆), 154.25 (C₂), 150.04 (C₄), 135.65 (C₈), 109.76 (C₅), 88.75 (C_{1'}), 85.74 (C_{4'}), 74.55 (C_{2'}), 69.63 (C_{3'}), 49.04 (C_{5'}).

(2R,3R,4S,5R)-2-(6-amino-9H-purin-9-yl)-5-(hydroxymethyl)tetrahydrofuran-3,4-diol, chloride (10a): (0.63 g, 99%). ¹H NMR (400.13 MHz, DMSO) δ 9.51 (s, 3H, H₆), 8.74 (s, 1H, H₂), 8.54 (s, 1H, H₈), 5.97 (d, ³J_{H1'-H2'} = 4 Hz, 1H, H_{1'}), 4.52 (t, ^{2,3}J_{H2'-H2', H1'} = 4 Hz, 1H, H_{2'}), 4.18 (t, ^{2,3}J_{H3'-H3', H2'} = 4 Hz, 1H, H_{3'}), 3.68 (d, ³J_{H4'-H3'} = 4 Hz, 1H, H_{4'}), 3.61 (dd, ²J_{H5'-H5'} = 4 Hz, ³J_{H5'-H4'} = 16 Hz, 1H, H_{5'}), 3.58 (dd, ²J_{H5'-H5'} = 4 Hz, ³J_{H5'-H4'} = 16 Hz, 1H, H_{5'}). ¹³C NMR (100.61 MHz, DMSO) 155.85 (C₆), 151.25 (C₄), 150.04 (C₂), 136.33 (C₈), 108.88 (C₅), 87.52 (C_{1'}), 85.64 (C_{4'}), 72.35 (C_{2'}), 67.63 (C_{3'}), 48.97 (C_{5'}).

3-((2R,3R,4S,5R)-3,4-dihydroxy-5-(hydroxymethyl)tetrahydrofuran-2-yl)-5-methyl-2,6-dioxo-1,2,3,6-tetrahydropyrimidin-1-ium chloride (11a): (0.21 g, 73%). ¹H NMR (400.13 MHz, DMSO) δ 11.25 (s, 2H, H₃), 7.68 (s, 1H, H₆), 6.15 (t, ^{2,3}J_{H1'-H2'} = 4 Hz, 1H, H_{1'}), 4.22 (q,

$^3J_{H4'-H3', H5'} = 4$ Hz, 1H, $H_{4'}$), 5.01(t, $^3J_{H5'-H5', H4'} = 4$ Hz, 1H, $H_{5'}$), 3.55 (m, 2H, $H_{5'}$, $H_{3'}$), 2.09 (m, 2H, $H_{2'}$), 2.05 (s, 3H, H_7). ^{13}C NMR (100.61 MHz, DMSO) δ 164.20 (C_4), 150.93 (C_2), 136.58 (C_6), 109.82 (C_5), 87.71 ($C_{1'}$), 84.19 ($C_{4'}$), 70.90 ($C_{3'}$), 61.80 ($C_{5'}$), 49.06 ($C_{2'}$), 12.72 (C_7).

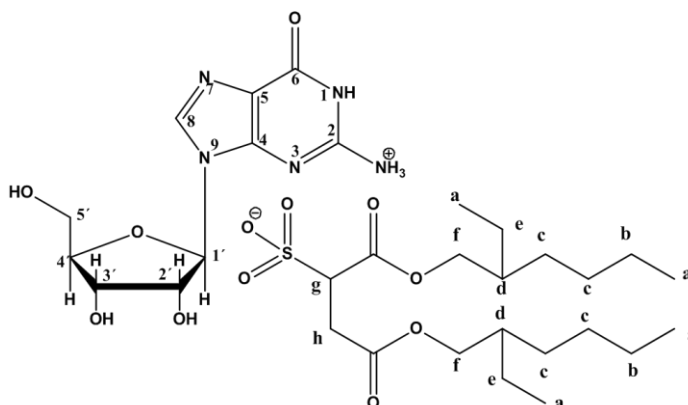
3-((2R,3R,4S,5R)-3,4-dihydroxy-5-(hydroxymethyl)tetrahydrofuran-2-yl)-2,6-dioxo-

1,2,3,6-tetrahydropyrimidin-1-ium chloride (12a): (0.21 g, 76%). ^1H NMR (400.13 MHz, DMSO) δ 11.329 (s, 2H, H_3), 7.88 (d, $^3J_{H6-H5} = 8$ Hz, 1H, H_6), 5.76 (d, $^3J_{H1'-H2'} = 4$ Hz, 1H, $H_{1'}$), 5.56 (d, $^3J_{H5-H6} = 8$ Hz, 1H, H_5), 4.01-3.83 (m, 3H, $H_{3'}$, $H_{4'}$, $H_{2'}$), 3.53 (m, 2H, $H_{5'}$). ^{13}C NMR (100.61 MHz, DMSO) δ 163.59 (C_4), 151.22 (C_2), 141.19 (C_6), 102.21 (C_5), 88.14 ($C_{1'}$), 85.30 ($C_{4'}$), 74.00 ($C_{2'}$), 70.35 ($C_{3'}$), 61.31 ($C_{5'}$).

V.7.2. Synthesis of 9-(2R,3R,4S,5R)-3,4-dihydroxy-5-(hydroxymethyl)tetrahydrofuran-2-yl)-6-oxo-6,9-dihydro-1H-purin-2-aminium 1,4-bis((2-ethylhexyl)oxy)-1,4-dioxobutane-2-sulfonate (9b)

After the protonation was finished, the isolated guanosine hydrochloride (0.2 g; 0.63 mmol) was dissolved in 10ml of methanol and Na[AOT] was added to perform the ion exchange (0.33 g; 0.75 mmol).

The reaction was stirred for 24 h

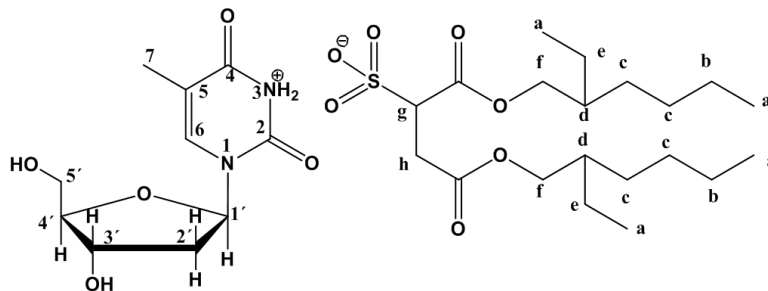


at room temperature. Then the solvent was evaporated and the crude was redissolved in acetone in order to remove the inorganic salts by precipitation. The solution was evaporated and dried *in vacuo* for 24 h. The desired product was obtained as a cream-coloured paste (0.33 g, 76%). ^1H NMR (400.13 MHz, DMSO) δ 11.72 (s, 1H, H_1), 9.00 (s, 1H, H_8), 7.26 (s, 3H, H_2), 6.17 (t, $^2J_{H2'-H2', H1'} = 4$ Hz, 1H, $H_{2'}$), 5.78 (d, $^3J_{H1'-H2'} = 4$ Hz, 1H, $H_{1'}$), 5.38 (d, $^3J_{H3'-H2'} = 4$ Hz, 1H, $H_{3'}$), 4.40 (m, 1H, $H_{4'}$), 3.90- 3.86 (m, 4H, H_f), 3.77 (m, 1H, $H_{3'}$), 3.62 (dd, $^2J_{Hh-Hh} = 4$ Hz, $^3J_{Hh'-Hg} = 8$ Hz, 1H, H_h), 3.58 (m, 2H, $H_{5'}$), 3.13 (d, $^3J_{H2'-H3'} = 1$ Hz, $H_{2'}$), 2.96 (m, 1H, H_g), 2.79 (dd, $^2J_{Hh'-Hh} = 4$ Hz, $^3J_{Hh'-Hg} = 8$ Hz, 1H, $H_{h'}$), 1.52 (m, 2H, H_d), 1.35 – 1.23 (m, 16H, H_b , H_c , H_e), 0.91-0.84 (m, 12H, H_a). ^{13}C NMR (100.61 MHz, DMSO) δ 171.51 ($-C=O$), 158.39 (C_6), 153.77 (C_2), 149.47 (C_4), 136.66 (C_8), 117.81 (C_5), 108.36 ($C_{1'}$), 89.11 ($C_{4'}$), 81.64 ($C_{2'}$), 71.33 ($C_{3'}$), 68.23 (C_f), 65.12 (C_g), 61.87 ($C_{5'}$), 38.59 (C_d), 30.20 (C_c), 30.02 (C_e), 28.80 (C_h), 23.65 (C_b), 22.86 (C_e), 11.28 (C_a), 11.25 (C_a). FTIR (NaCl) $\nu = 3424, 2960, 2930, 2868, 2588, 2364, 1716, 1642, 1613, 1526, 1463, 1371, 1219, 1169, 1092, 1045, 924, 818, 772, 733, 678, 573, 467, 450$ cm^{-1} .

Elemental analysis (%) calcd for $C_{30}H_{51}N_5O_{12}S$ (MW= 705.82 $g \cdot mol^{-1}$): C 51.05; H 7.28; N 9.92; S 4.54; found: C 50.79; H 7.32; N 9.88; S 4.51.

V.7.3. Synthesis of 3-(2*R*,3*R*,4*S*,5*R*)-3,4-dihydroxy-5-(hydroxymethyl)tetrahydrofuran-2-yl)-5-methyl-2,6-dioxo-1,2,3,6-tetrahydropyrimidin-1-ium 1,4-bis((2-ethylhexyl)oxy)-1,4-dioxobutane-2-sulfonate (11b)

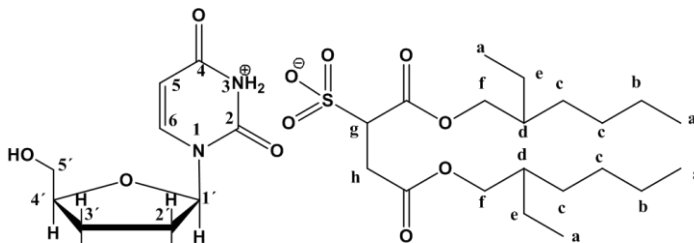
The isolated protonated thymidine hydrochloride (0.21 g; 0.74 mmol) was dissolved in 10ml of methanol and Na[AOT] was added to perform the ion



exchange (0.39 g; 0.89 mmol). The reaction was stirred for 24 h at room temperature. Then the solvent was evaporated and the crude was redissolved in acetone in order to remove the inorganic salts by precipitation. The solution was evaporated and dried *in vacuo* for 24 h. The desired product was obtained as a cream-coloured paste (0.49 g, $\geq 99\%$). 1H NMR (400.13 MHz, DMSO) δ 11.27 (s, 2H, H₃), 7.71 (s, 1H, H₆), 6.17 (t, $^2, ^3J_{H1'-H2}=4$ Hz, 1H, H_{1'}), 5.24 (q, $^3J_{H4'-H3'}, H5'=4$ Hz, 1H, H_{4'}), 5.01 (t, $^3J_{H3'-H2}=4$ Hz, 1H, H_{3'}), 4.25 (m, 1H, H_{5'}), 3.91- 3.87 (m, 4H, H_f), 3.77 (m, 1H, H_{3'}), 3.66 (dd, $^2J_{Hh-Hh}=4$ Hz, $^3J_{Hh'-Hg}=8$ Hz, 1H, H_h), 3.53 (m, 1H, H_{5'}), 2.96 (m, 1H, H_g), 2.82 (dd, $^2J_{Hh'-Hh}=4$ Hz, $^3J_{Hh'-Hg}=8$ Hz, 1H, H_{h'}), 2.06 (m, 1H, H_{2'}), 1.75 (s, 3H, H₇), 1.51 (m, 2H, H_d), 1.36 – 1.24 (m, 16H, H_b, H_c, H_e), 0.89-0.82 (m, 12H, H_a). ^{13}C NMR (100.61 MHz, DMSO) δ 171.06 (C₄, -C=O), 168.39 (-C=O), 163.75 (C₂), 150.47 (C₆), 136.13 (C₅), 109.36 (C_{1'}), 87.26 (C_{4'}), 83.74 (C_{2'}), 70.45 (C_{3'}), 66.23 (C_f), 66.16 (C_g), 61.42 (C_{5'}), 38.18 (C_d), 29.74 (C_c), 29.57 (C_c), 28.80 (C_c), 28.34 (C_h), 23.20 (C_b), 23.17 (C_e), 13.92 (C₇), 12.24 (C_a), 10.78 (C_a). FTIR (NaCl) ν = 3862, 3450, 2959, 2929, 2865, 2362, 1732, 1657, 1463, 1391, 1218, 1048, 853, 766, 734, 667, 585, 468 cm^{-1} . Elemental analysis (%) calcd for $C_{30}H_{52}N_2O_{13}S$ (MW= 680.80 $g \cdot mol^{-1}$): C 52.93; H 7.70; N 4.11; S 4.71; found: C 52.66; H 8.02; N 3.90; S 4.47.

V.7.4. Synthesis of 3-(2*R*,3*R*,4*S*,5*R*)-3,4-dihydroxy-5-(hydroxymethyl)tetrahydrofuran-2-yl)-2,6-dioxo-1,2,3,6-tetrahydropyrimidin-1-ium 1,4-bis((2-ethylhexyl)oxy)-1,4-dioxobutane-2-sulfonate (12b)

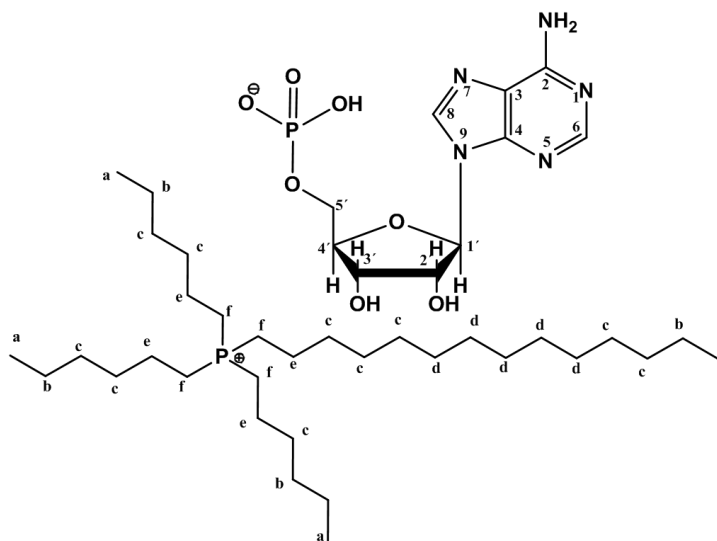
The isolated protonated uridine hydrochloride (0.21 g; 0.74 mmol) was dissolved in 10ml of methanol and Na[AOT] was added to perform the ion exchange (0.39 g; 0.89 mmol).



The reaction was stirred for 24 h at room temperature. Then the solvent was evaporated and the crude was redissolved in acetone in order to remove the inorganic salts by precipitation. The solution was evaporated and dried *in vacuo* for 24 h. The desired product was obtained as a cream-coloured solid (0.11 g, 23%). $T_m=134\text{ }^{\circ}\text{C}$. ^1H NMR (400.13 MHz, DMSO) δ 11.31 (s, 2H, H₃), 7.90 (d, $^3J_{\text{H}_6\text{-H}_5}=4\text{ Hz}$, 1H, H₆), 5.79 (d, $^3J_{\text{H}_1\text{'-H}_2\text{'}}=4\text{ Hz}$, 1H, H₁'), 5.66 (d, $^3J_{\text{H}_5\text{'-H}_6\text{'}}=4\text{ Hz}$, 1H, H₅), 5.38 (d, $^3J_{\text{H}_2\text{'-H}_1\text{'}}=4\text{ Hz}$, 1H, H₂'), 5.09 (t, $^3J_{\text{H}_3\text{'-H}_2\text{'}}=4\text{ Hz}$, 1H, H₃'), 4.02 (m, 1H, H₄'), 3.91-3.85 (m, 4H, H_f), 3.77 (m, 1H, H₃'), 3.62 (dd, $^2J_{\text{H}_h\text{'-H}_h\text{'}}=4\text{ Hz}$, $^3J_{\text{H}_h\text{'-H}_g\text{'}}=8\text{ Hz}$, 1H, H_h'), 3.34 (m, 2H, H₅'), 3.18 (d, $^3J_{\text{H}_2\text{'-H}_3\text{'}}=4\text{ Hz}$, 1H, H₂'), 2.91 (m, 1H, H_g'), 2.82 (dd, $^2J_{\text{H}_h\text{'-H}_h\text{'}}=4\text{ Hz}$, $^3J_{\text{H}_h\text{'-H}_g\text{'}}=8\text{ Hz}$, 1H, H_h'), 1.50 (m, 2H, H_d'), 1.34 – 1.24 (m, 16H, H_b, H_c, H_e), 0.89-0.82 (m, 12H, H_a). ^{13}C NMR (100.61 MHz, DMSO) δ 176.28 (C₄), 173.60 (-C=O), 168.33 (C₂), 155.97 (C₆), 145.99 (C₅), 109.96 (C₁'), 92.90 (C₄'), 90.06 (C₂'), 78.76 (C₃'), 75.10 (C_f), 71.40 (C_g), 66.64 (C₅'), 39.32 (C_d'), 35.90 (C_c'), 34.96 (C_c'), 33.56 (C_c'), 28.39 (C_c'), 28.34 (C_h'), 27.63 (C_b'), 23.20 (C_e'), 19.11 (C₇'), 16.00 (C_a'), 15.97 (C_a'). FTIR (KBr) ν = 3454, 3323, 3051, 2967, 2927, 2862, 2362, 1715, 1679, 1456, 1418, 1257, 1218, 1076, 1044, 910, 853, 767, 722, 658, 581, 447, 425 cm^{-1} . Elemental analysis (%) calcd for C₂₉H₅₀N₂O₁₃S (MW= 666.78 $\text{g}\cdot\text{mol}^{-1}$): C 52.24; H 7.56; N 4.20; O 31.19; S 4.81; found: C 52.03; H 7.54; N 4.17; S 4.

V.7.5. Synthesis of trihexyl(tetradecyl)phosphonium ((2*R*,3*S*,4*R*,5*R*)-5-(6-amino-9H-purin-9-yl)-3,4-dihydroxytetrahydrofuran-2-yl)methyl hydrogenphosphate (13a)

For the preparation of trihexyl(tetradecyl)phosphonium ((2*R*,3*S*,4*R*,5*R*)-5-(6-amino-9H-purin-9-yl)-3,4-dihydroxytetrahydrofuran-2-yl)methyl hydrogenphosphate, a column ion exchange method was used. The [P_{6,6,6,14}]Cl (0.74 g; 1.44 mmol) was first transformed into hydroxide by the use of an ionic exchange column (Amberlyst A-26 OH) in



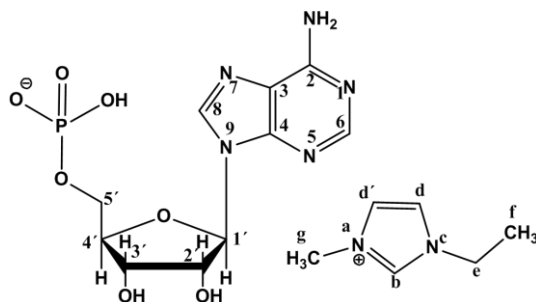
methanol and then this basic solution was neutralized by reacting with the AMP acid (0.5 g; 1.44 mmol) in methanol solution. The mixture was stirred at room temperature for 24 h. After the indicated time, the established water was evaporated and dried *in vacuo* for 24 h. The final product was obtained as a viscous yellow liquid (1.17 g, 98%). $T_g = -48.19^\circ\text{C}$. ^1H NMR (400.13 MHz, DMSO) δ 8.50 (s, 1H, H₆), 8.14 (s, 1H, H₈), 7.23 (s, 2H, H₂), 5.91 (d, $^3J_{\text{H}_1-\text{H}_2}=4$ Hz, 1H, H₁), 4.72 (t, $^3J_{\text{H}_2'-\text{H}_1}=8$ Hz, $^2J_{\text{H}_2'-\text{H}_2}=4$ Hz, 1H, H_{2'}), 4.27 (m, 2H, H_{3'}, H_{4'}), 3.81- 3.73 (m, 4H, H_{2'}, H_{3'}, H_{5'}), 2.17 (m, 8H, H_f), 1.38 (m, 16H, H_b, e), 1.29-1.25 (m, 32H, H_c), 0.86 (m, 12H, H_a). ^{13}C NMR (100.61 MHz, DMSO) δ 155.92 (C₂), 152.50 (C₆), 149.88 (C₄), 139.43 (C₈), 118.67 (C₃), 86.31 (C_{1'}), 84.69 (C_{4'}), 74.22 (C_{2'}), 71.51 (C_{3'}), 63.95 (C_{5'}), 31.28 (C_c), 30.39 (C_c), 29.85 (C_d), 29.79 (C_d), 29.64 (C_d), 28.99 (C_b), 28.94 (C_b), 28.69 (C_b), 22.08, 21.79, 20.54 (C_e), 20.50 (C_e), 13.93 (C_a), 13.84 (C_a). FTIR (NaCl) $\nu = 3334, 2927, 2857, 1674, 1609, 1465, 1420, 1337, 1302, 1213, 1107, 990, 925, 830, 720, 646, 584\text{ cm}^{-1}$. Elemental analysis (%) calcd for C₄₂H₈₁N₅O₇P₂ (MW= 830.07 g.mol⁻¹): C 60.77; H 9.84; N 8.44; found: C 60.46; H 9.88; N 8.40.

V.7.6. Synthesis of 1-ethyl-3-methyl-1H-imidazol-3-ium ((2*R*,3*S*,4*R*,5*R*)-5-(6-amino-9H-purin-9-yl)-3,4-dihydroxytetrahydrofuran-2-yl)methyl hydrogenphosphate (13b)

For the preparation of 1-ethyl-3-methyl-1H-imidazol-3-ium ((2*R*,3*S*,4*R*,5*R*)-5-(6-amino-9H-purin-9-yl)-3,4-dihydroxytetrahydrofuran-2-yl)methyl hydrogenphosphate, a column ion exchange method was used. The [Emim]Br (0.28 g; 1.44 mmol) was first transformed into hydroxide by the use of an ionic exchange column (Amberlyst A-26 OH) in methanol and then this basic solution was neutralized by reacting with the AMP acid (0.5 g; 1.44 mmol) in

methanol solution. The mixture was stirred at room temperature for 24 h. After the indicated time, the established water was evaporated and dried *in vacuo* for 24 h. The final product was obtained as a viscous yellow liquid (0.65 g, 99 %). ^1H NMR (400.13 MHz, DMSO) δ 9.19 (s,

1H, H_b), 8.50 (s, 2H, H_2), 8.14 (s, 1H, H_6), 7.77 (s, 1H, H_d), 7.69 (s, 1H, $\text{H}_{d'}$), 7.24 (s, 1H, H_8), 5.91 (d, $^3J_{\text{H}_1'-\text{H}_2}=4$ Hz, 1H, H_1'), 4.73 (t, $^3J_{\text{H}_2'-\text{H}_1}=8$ Hz, $^2J_{\text{H}_2'-\text{H}_2}=4$ Hz, 1H, H_2'), 4.26 (m, 2H, H_3', H_4'), 4.21-4.16 (q, $^3J_{\text{H}_e-\text{H}_f}=8$ Hz, 2H, H_e), 4.02 (s, 1H, H_4), 3.85 (s, 3H, H_g), 3.78-3.65 (m, 4H, H_2 , H_3 , H_5), 1.40 (t, $^3J_{\text{H}_e-\text{H}_f}=8$ Hz, 3H, H_f). ^{13}C NMR (100.61 MHz, DMSO) δ 156.38 (C_2), 153.05 (C_6), 150.32 (C_8), 139.90 (C_b), 124.00 (C_d), 122.38 ($\text{C}_{d'}$), 119.10 (C_3), 86.76 (C_1), 74.61 (C_4), 71.95 (C_2'), 64.45 (C_3'), 44.56 (C_5'), 39.14 (C_e), 36.13 (C_g), 15.56 (C_f). FTIR (KBr) $\nu = 3407, 2930, 2857, 1654, 1576, 1478, 1424, 1391, 1389, 1300, 1216, 1171, 1065, 989, 930, 871, 816, 765, 721, 644, 474$ cm^{-1} . Elemental analysis (%) calcd for $\text{C}_{16}\text{H}_{24}\text{N}_7\text{O}_7\text{P}$ (MW = 457.38 $\text{g}\cdot\text{mol}^{-1}$): C 42.02; H 5.29; N 21.44; found: C 41.82; H 5.32; N 21.33. FTIR (NaCl) $\nu = 3407, 2930, 2857, 1654, 1576, 1478, 1424, 1391, 1389, 1300, 1216, 1171, 1065, 989, 930, 871, 816, 765, 721, 644, 474$ cm^{-1} .

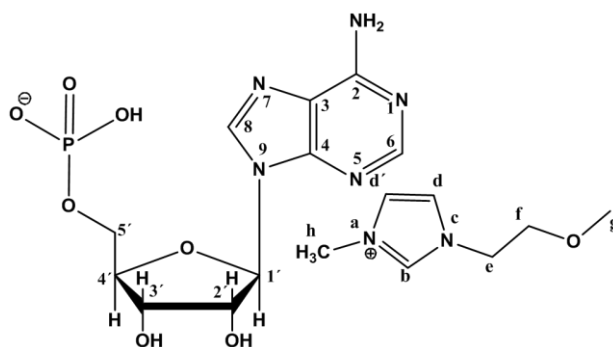


V.7.7. Synthesis of 1-(2-methoxyethyl)-3-methyl-1H-imidazol-3-ium ((2R,3S,4R,5R)-5-(6-amino-9H-purin-9-yl)-3,4-dihydroxytetrahydrofuran-2-yl)methyl hydrogenphosphate (13c)

For the preparation of 1-(2-methoxyethyl)-3-methyl-1H-imidazol-3-ium ((2R,3S,4R,5R)-5-(6-amino-9H-purin-9-yl)-3,4-

dihydroxytetrahydrofuran-2-yl)methyl hydrogenphosphate, a column ion exchange method was used. The

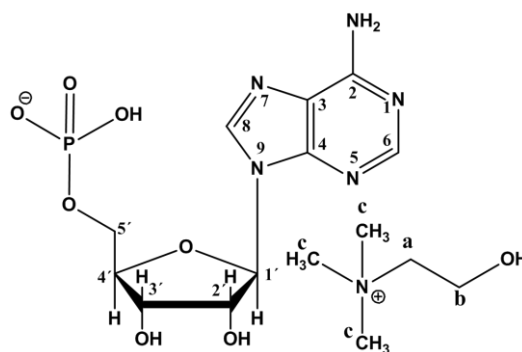
[C_3Oimim] Cl (0.26 g; 1.44 mmol) was first transformed into hydroxide by the use of an ionic exchange column (Amberlyst A-26 OH) in methanol and then this basic solution was neutralized by reacting with the AMP acid (0.5g; 1.44 mmol) in methanol solution. The mixture was stirred at room temperature for 24 h. After the indicated time, the established water was evaporated and dried *in vacuo* for 24 h. The final product was obtained as a viscous yellow liquid (0.50 g, 98 %). $T_g = -24.32$ $^{\circ}\text{C}$. ^1H NMR (400.13 MHz, DMSO) δ 9.15 (s, 1H, H_b), 8.46 (s, 1H, H_6), 8.15 (s, 1H, H_8), 7.68 (d, $^3J_{\text{H}_d-\text{H}_{d'}}=12$ Hz 2H, H_d , $\text{H}_{d'}$), 7.12 (s, 2H, H_2), 5.92 (d, $^3J_{\text{H}_1'-\text{H}_2}=4$ Hz, 1H, H_1'), 4.68 (t, $^3J_{\text{H}_2'-\text{H}_1}=8$ Hz, $^2J_{\text{H}_2'-\text{H}_2}=4$ Hz, 1H, H_2'), 4.35 (m, 2H, H_3', H_4'), 4.25 (t,



$^3J_{\text{He-Hf}} = 4\text{Hz}$, 2H, H_e), 4.15-4.06 (m, 4H, $H_{2'}$, $H_{3'}$, $H_{5'}$), 3.86 (s, 3H, H_h), 3.66 (t, $^3J_{\text{Hf-He}} = 4\text{Hz}$, 2H, H_f), 3.25 (s, 1H, H_g). ^{13}C NMR (100.61 MHz, DMSO) δ 155.95 (C_2), 152.64 (C_6), 149.81 (C_8), 139.34 (C_b), 123.45 (C_d), 122.61 ($C_{d'}$), 118.72 (C_3), 86.45 ($C_{1'}$), 84.23 ($C_{4'}$), 73.98 ($C_{2'}$), 71.18 ($C_{2''}$), 69.61 ($C_{3'}$), 64.34 ($C_{5'}$), 58.04 (C_g), 48.62 (C_e), 35.75 (C_h). FTIR (NaCl) $\nu = 3421$, 2932, 2363, 1650, 1576, 1479, 1423, 1336, 1302, 1174, 1084, 921, 821, 722, 645, 585, 481 cm^{-1} .
¹. Elemental analysis (%) calcd for $\text{C}_{17}\text{H}_{26}\text{N}_7\text{O}_8\text{P}$ (MW = 487.40 $\text{g}\cdot\text{mol}^{-1}$): C 41.89; H 5.38; N 20.12; found: C 41.71; H 5.41; N 20.05.

V.7.8. Synthesis of 2-hydroxy-N,N,N-trimethylethanaminium ((2R,3S,4R,5R)-5-(6-amino-9H-purin-9-yl)-3,4-dihydroxytetrahydrofuran-2-yl)methyl hydrogenphosphate (13d)

For the preparation of 2-hydroxy-N,N,N-trimethylethanaminium ((2R,3S,4R,5R)-5-(6-amino-9H-purin-9-yl)-3,4-dihydroxytetrahydrofuran-2-yl)methyl hydrogenphosphate, a direct acid base reaction was performed. Initially, the adenosine 5'-monophosphoric acid AMP (0.5 g; 1.44 mmol)



was dissolved in 25 ml H_2O and a solution of choline hydroxide in MeOH 45% (0.43 ml; 1.44 mmol) was added dropwise. The reaction mixture was stirred at room temperature overnight. After the indicated time, the pH was measured to confirm that the reaction was completed (pH = 8.0) and the water was evaporated and dried *in vacuo* for 8h. The final product was obtained as a viscous yellow liquid, (0.63 g, 98%). $T_g = -30.51$ $^{\circ}\text{C}$. ^1H NMR (400.13 MHz, DMSO) δ 8.46 (s, 1H, H_6), 8.14 (s, 1H, H_8), 7.25 (s, 2H, H_2), 5.91 (d, $J_{H1'-H2'} = 4$ Hz, 1H, $H_{1'}$), 5.75 (m, 1H, $H_{2'}$), 4.67 (m, 1H, $H_{3'}$), 4.19 (m, 2H, $H_{4'}$, $H_{3''}$), 4.04 (m, m, 1H, $H_{2''}$), 3.83 (m, 4H, H_b , $H_{5'}$), 3.40 (m, 2H, H_a), 3.11 (s, 9H, H_c). ^{13}C NMR (100.61 MHz, DMSO) δ 156.41 (C_2), 153.08 (C_6), 150.27 (C_4), 139.81 (C_8), 119.17 (C_3), 86.91 ($C_{1'}$), 74.48 ($C_{4'}$), 71.69 ($C_{2'}$), 67.47 ($C_{3'}$), 64.70 (C_a), 55.62 ($C_{5'}$), 53.63 (C_b), 49.05 (C_c). FTIR (NaCl) $\nu = 3387$, 2933, 2365, 1659, 1609, 1481, 1423, 1392, 1337, 1302, 1217, 1173, 1104, 1061, 991, 960, 872, 821, 767, 719, 641, 479 cm^{-1} . Elemental analysis (%) calcd for $\text{C}_{15}\text{H}_{27}\text{N}_6\text{O}_8\text{P}$ (MW = 450.16 $\text{g}\cdot\text{mol}^{-1}$): C 40.00; H 6.04; N 18.66; found: C 39.80; H 6.05; N 18.58.

V.7.9. General procedure for critical micelle concentration (CMC) of surfactant **9b** and **11b**

The CMC determination of synthesised compounds was performed using two methods, UV-VIS spectroscopy and conductivity.

Absorption measurments: In the first method it was necessary to resort to a molecular probe due to the lack of absorption by compounds. Therefore, two probes based on the same structure but with slight differences were used: Acridine Yellow G in the first place and Acridine as a second choice. Stock solutions (100mL) of probes were prepared in distilled water and stored. The same procedure was followed with chiral organic salts **9b** and **11b** combined with [AOT] anion. Then, absorption solutions (25mL) were prepared at different concentrations of product from compounds stock-solutions and with the same probe solution volume (5mL), in distilled water. The absorption spectra were measured but it wasn't possible determine any CMC with both probes.

Conductivity measurments: Conductivities were measured at 20°C by using a digital Conductimeter Basic 30. Compounds stock solutions (100 mL) were prepared and stored. A series of compounds solutions (10 mL) of different concentrations were prepared by dilutions from stock-solutions. The conductivities were measured in duplicate and CMC was determined.

V.7.10. General procedure for fluorencence studies

Solutions method: Emission spectra were performed using Perkin Elmer LS 45 Luminescence Spectrometer at 20 °C with a slit width of 2.0 nm, an excitation value of 255 nm and at room temperature. Emission solutions (10 mL) were prepared at the same concentration for each target compound in distilled water (10^{-6} M).

Film method: The apparatus used was the same as in the previous method. In this method, instead of preparing a solution with a specific concentration a compound film from a quartz cell emission was prepared. The spectrum was measured in the same conditions previously used.

CHAPTER VI. Ethyl Lactate

VI. Ethyl Lactate

The aim of this chapter was to highlight the relevant relations and interactions between CILs and biological molecules such as amino acids, cyclodextrins and nucleobases. The concept of this thesis is strongly correlated with sustainability and green chemistry. Therefore, as an additional final subject (in the closure) the idea of ethyl lactate will be demonstrated.

VI.1. *Ethyl Lactate - an alternative green solvent besides ILs*

Green chemistry consists in the use of chemicals and chemical processes designed to reduce or eliminate negative environmental impacts. Applying this concept can also lead to reducing waste products, substitution of toxic for non-toxic components and simultaneously improve the reactions efficiency. The world demand for solvents is predicted to grow in the next years and the industrial requirements will lead to an increased claim for new fluids and alternative solvents¹⁵⁰. Due to the very poor environmental and toxicological profiles and the volatile character of the most generally used solvents, there is a need for alternatives that may replace the current ones^{151, 152}. Within the idea of green chemistry, a number of approaches have been proposed in the last few years. According to the principles of green chemistry, supercritical fluids and ILs have been the most promising and extended ones amongst academia (Figure VI.1)¹⁵³.

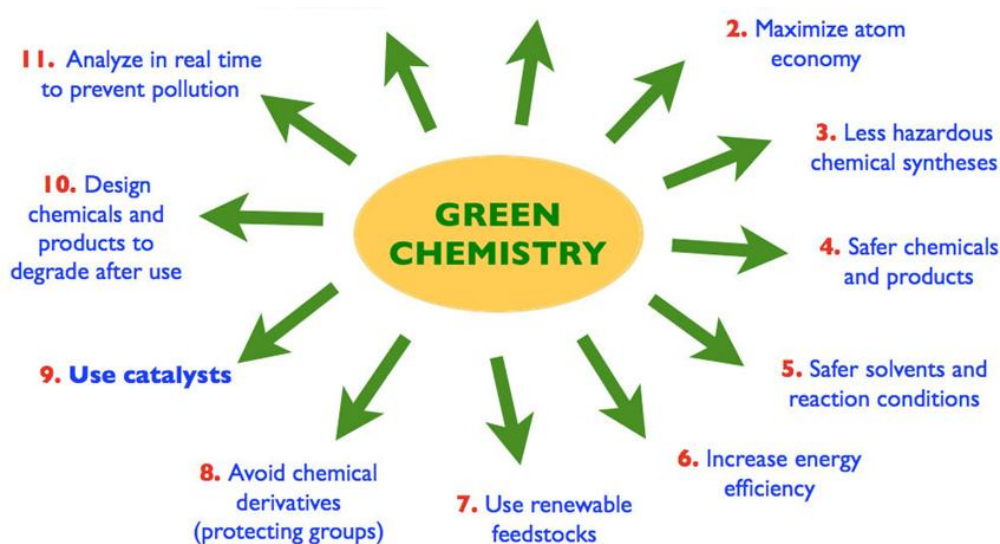


Figure VI.1 - Twelve principles of green chemistry.

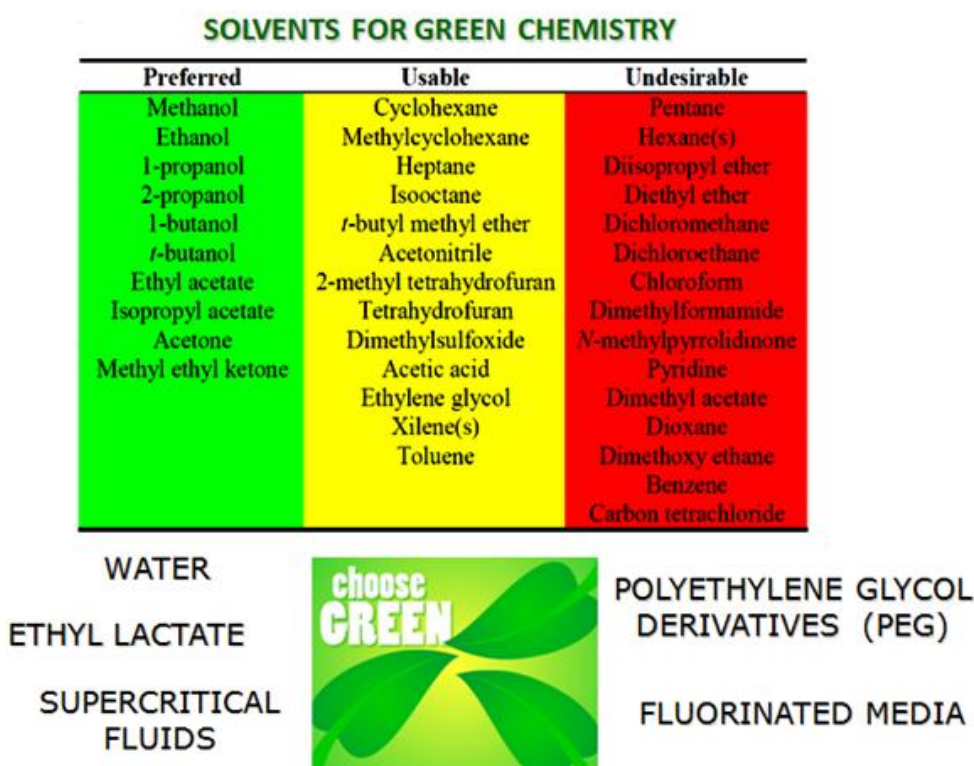


Figure VI.2 – Green technologies in industry- Pfizer solvent selection guide for medicinal chemistry.

In recent years, among these optional organic solvents, ethyl lactate (EL) has gathered much attention, a fact indicated by the growth of the number of articles published.

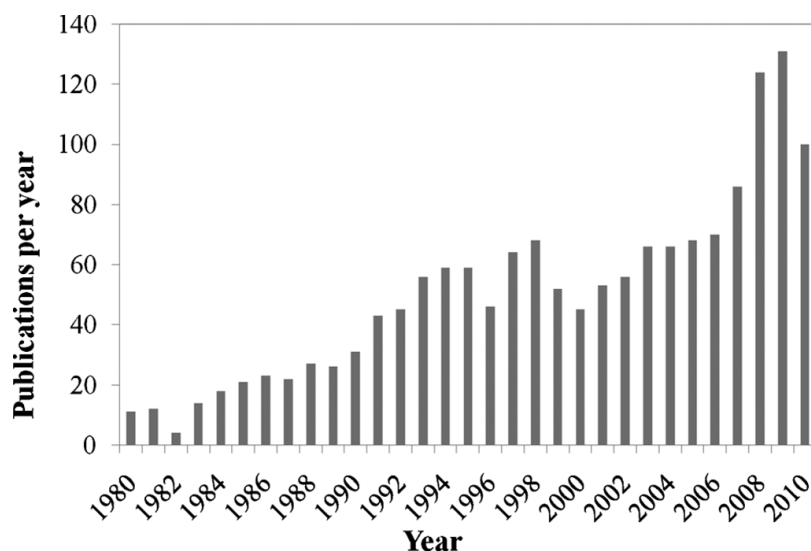


Figure VI.3 - Publications related to ethyl lactate since 1980 using all databases¹⁵⁴.

VI.2. Ethyl Lactate- properties and applications

Ethyl lactate is a green and economically viable monobasic unit of the lactate esters scaffold, also known as lactic acid ethyl ester (IUPAC name: Ethyl (*S*)- 2-hydroxypropanoate). It is formed by the reversible esterification reaction of ethanol and lactic acid, which can be generated from biomass raw materials through fermentation (Figure VI.4). EL can be either in the levo (*L*) or dextro (*D*) forms and it is industrially produced as a racemic mixture.

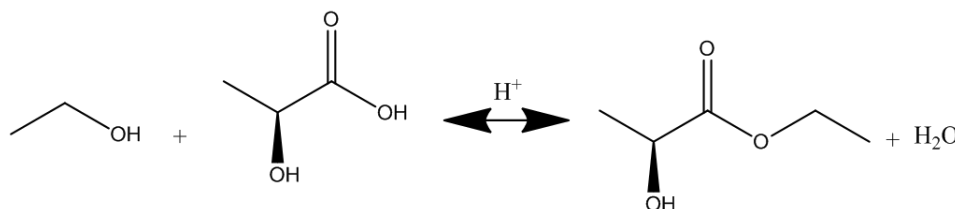


Figure VI.4 - Synthesis of ethyl lactate (EL) from lactic acid.

EL, similar to [choline], has very convenient toxicological properties¹⁵⁵, it does not demonstrate any potential health risks and it undergoes metabolic hydrolysis due to the esterase enzymatic activity to ethyl alcohol and lactic acid, with this last compound being a natural metabolite in humans. Its environmental profile is very adequate considering that it is completely biodegradable in a very short time¹⁵⁶. In case of vapors release, EL is a non-ozone depleting fluid. Considering its high solvency power, high boiling point, low vapour pressure and low surface tension, EL may be successfully applied in different areas such as a cleaning solvent¹⁵⁷, for the manufacturing of magnetic and electronic devices¹⁵⁸, as well as in the pharmaceutical¹⁰⁴ and paint industries¹⁵⁹. It can be also used in food industry (as food additive), in perfumery, (as

flavour chemicals and solvent, which can dissolve acetic acid cellulose and many resins)¹⁰⁴. Some of its peculiar properties are presented in Table VI.1.

Table VI.1 Major advantages of using Ethyl Lactate.

100% Biodegradable	Reusable- made from corn and other carbohydrates
Approved by the FDA as a food additive No carcinogenic	EPA approved SNAP solvent
Excellent penetration characteristics	Noncorrosive High dissolving power for resins, polymers and colors
Easily washable with water	Easy to recycle and cheap
High boiling point	It does not destroy the ozone layer
Low VOC	
Very low vapor pressure	
Does not pollute the air	

Some recent tests suggest that EL can replace conventional solvents in 80% of their applications. Nevertheless, there are some conflicting opinions because this is a high boiling solvent as well as a polar protic solvent. The price of EL has decreased significantly in recent years according to its greater use and application, being currently 50-74€ per kg for small suppliers (ex. Sigma-Aldrich or Alfa Aesar) or less than 15€ per kg in major suppliers for industrial production.

VI.3. Application of Ethyl Lactate in organic synthesis

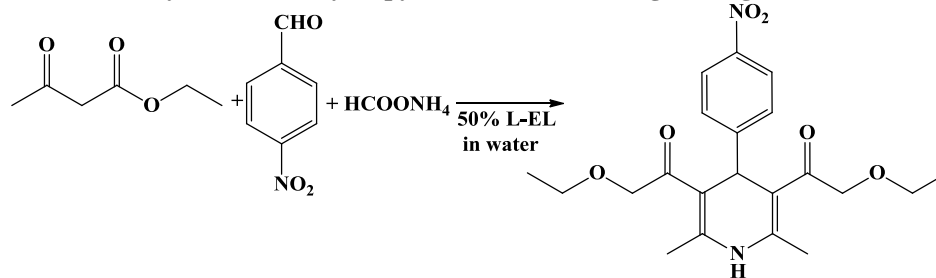
The use of EL as green solvent in organic synthesis is still little explored. Some recent examples reported in the literature demonstrated the potential use of EL in organic synthesis with synthetic advantages. Recently, the possibility of using a solvent system based on EL and H₂O as a co-solvent for Suzuki- Miyaura reaction has been reported by Wan et al¹⁶⁰. This reaction is classified as a coupling reaction where the coupling partners are boronic acids with a halide catalyzed by a palladium (0) complex. Through this reaction, it is possible to prepare organic compounds significant for pharmaceutical industry and fine chemistry. The use of EL for Suzuki- Miyaura reaction allowed reducing the reaction time and improved the final product yields. The desired product was obtained with 93% of yield in a solvent system H₂O/ EL (1:1) while in conventional organic solvent such as DMSO, the yield didn't exceed 70% (Table VI.2).

Table VI.2 – Use of EL in Suzuki-Miyaura reaction¹⁶⁰.

Entry	Catalyst (mol%)	Base	Solvent (ml)	Yield (%) ^b
1	Pd(OAc) ₂ (1)	K ₂ CO ₃	EL:H ₂ O (2:1)	26
2	Pd(OAc) ₂ (1)	K ₂ CO ₃	EL (3)	62
3	Pd(OAc) ₂ (1)	K ₂ CO ₃	H ₂ O (3)	60
4	Pd(OAc) ₂ (1)	K ₂ CO ₃	EL:H ₂ O (1.5:1.5)	56
5	Pd(OAc) ₂ (1)	K ₂ CO ₃	EL:H ₂ O (1:1)	93
6 ^c	Pd(OAc) ₂ (1)	K ₂ CO ₃	EL:H ₂ O (1:1)	47
7	Pd(OAc) ₂ (1)	Na ₂ CO ₃	EL:H ₂ O (1:1)	62
8	Pd (OAc) ₂ (1)	Et ₃ N	EL:H ₂ O (1:1)	53
9	Pd(OAc) ₂ (1)	NaHCO ₃	EL:H ₂ O (1:1)	44
10	Pd(OAc) ₂ (0.5)	K ₂ CO ₃	EL:H ₂ O (1:1)	52
11	Pd(OAc) ₂ (0.25)	K ₂ CO ₃	EL:H ₂ O (1:1)	44
12	PdCl ₂ (1)	K ₂ CO ₃	EL:H ₂ O (1:1)	23
13	Pd(OAc) ₂ (1)	K ₂ CO ₃	DMF:H ₂ O (1:1)	70
14	Pd(OAc) ₂ (1)	K ₂ CO ₃	DMSO:H ₂ O (1:1)	57
15	Pd(OAc) ₂ (1)	K ₂ CO ₃	Dioxane:H ₂ O (1:1)	58
16	Pd(OAc) ₂ (1)	K ₂ CO ₃	EA:H ₂ O (1:1)	15

^a Unless specified, the general conditions: 1a (0.5 mmol), 2a (0.75 mmol) and base (2 eq) at 60 °C for 2h. EA-ethyl acetate. ^b Isolated yield based on 1a. ^c This reaction was performed at 45 °C.

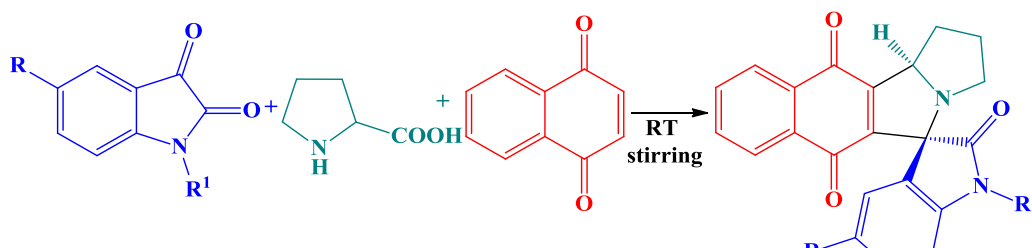
Additionally, the synthesis of dihydropyridines plays an important role due to the biological and pharmacological activity of these compounds. Nevertheless, the current research has been looking for more sustainable synthetic approaches. Last year, the synthesis of dihydropyridines and polytetrahydroquinolines in a solvent system of EL and water (1:1), by irradiation with visible light has been demonstrated¹⁶¹. This green solvent proved to be efficient, sustainable and no catalyst support or promotor was required. An addition of 50% of water to EL permits a significant improvement in reaction yield from 75% to 92%.

Table VI.3 - Synthesis of dihydropyridines with visible light using L-EL¹⁶¹.

Entry	Solvent	Yield (%) ^a
1	Toluene	49
2	Acetonitrile	52
3	DMSO	67
4	Ethanol	70
5	Water	60
6	L-EL	75
7	100% L-EL	75
8	85% L-EL in water	80
9	75% L-EL in water	86
10	50% L-EL in water	92
11	25% L-EL in water	82
12	10% L-EL in water	73
13	5% L-EL in water	66

^a Isolated yield of the pure compound.

The use of EL in water was first used for 1,3-dipolar cycloaddition reactions¹⁶². Again the mixture of EL with water led to a significant improvement in the reactivity of the reaction process. The effect of the solvent can be observed in detail by comparing the 30% of yield obtained after 18h in a conventional solvent DMF, with the 82% yield obtained after a 1h reaction using pure EL. The addition of water allowed to obtain yields even higher, up to 93%.

Table VI.4 - The use of EL in water used for 1, 3-dipolar cycloaddition reactions, optimization of solvent¹⁶².


Entry	Solvent	Time (h)	Yield (%) ^a
1	Toluene	24	22
2	Acetonitrile	20	16
3	THF	14	25
4	DMF	18	30
5	Methanol	24	^c
6	Ethanol	24	^c
7	EL	1	82

^a Isolated yield. ^b All reactions were carried out at RT. ^c No reaction.

VI.4. Application of Ethyl Lactate in asymmetric organocatalysis

Taking advantage of the chirality of EL (L- and D-isomers), it is possible to apply them for asymmetric organocatalysis in order to introduce chirality into the system. While Chapter II presented the application of new synthesized CILs based on L-cysteine derivatives as catalyst for asymmetric aldol reaction and Chapter III the L-proline based RTILs for Michael addition, this final Chapter includes both of the C-C bond forming reactions, this time using conventional catalyst L-proline, but testing the ability of EL as solvent.

The aldol condensation was first chosen as a model reaction to explore the possibility of using L-EL as an alternative green solvent to conventional organic solvents. The optimization of reaction conditions for the use of both the L-EL had been previously performed at the laboratory. Different reaction conditions have already been tested in particular in terms of temperature, amount of catalyst, reaction time, concentration and type of substrate used. As the model reaction acetone or cyclohexanone (ketone) and *ortho*- or *para*-nitrobenzaldehyde (aldehyde) were tested using L-proline as organocatalyst and DMSO or L-EL as solvent (Table VI.5). According to the literature, the use of water as a co-solvent in combination with organic solvents can increase its reactivity and the yield of the final product. In this context, additional studies were performed, in order to compare the EL: H₂O (1:1) solvent mixture with the optimal

conditions using pure DMSO or EL. As shown in Table VI.5, the presence of 50% of water had an adverse effect on this reaction.

Table VI.5 - Asymmetric aldol reaction using different solvents.

Entry	Ketone/Benzaldehyde ^[a]	Solvent	Conversion [%] ^[b]
1	Acetone/2-Nitro	DMSO	100
2	Acetone/2-Nitro	EL	100
3	Cyclohexanone/2-Nitro	DMSO	85
4	Cyclohexanone/2-Nitro	EL	84
5	Cyclohexanone/4-Nitro	EL: H ₂ O	20

^[a] Reaction conditions: acetone (1mmol) or cyclohexanone (2 mmol) and 2 or 4-nitrobenzaldehyde (0.5 or 1 mmol), loading of catalyst L-proline 10 mol% at room temperature, 24 h to 48 h. ^[b] The conversions were determined from 400Hz ¹H NMR spectroscopy.

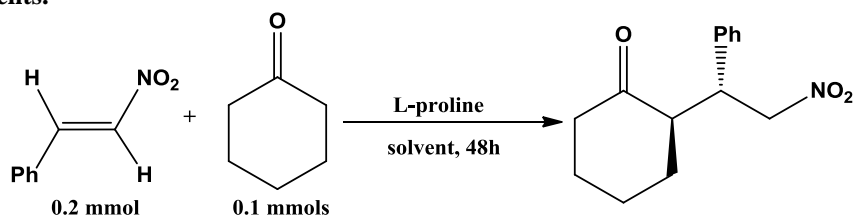
In order to evaluate in detail the potential use of L-EL as an alternative solvent for Michael reaction, the effect of different reaction conditions was tested in our laboratory, in particular the effect of temperature (0 °C, 24 °C and 50 °C); reaction time (24, 48, and 72h); amount of catalyst L-proline (30 to 50 mol%); concentration (0.2 and 0.4 mmol in relation to the *trans*-nitrostyrene) and the use of water (10% to 50%) or ethanol (20%, 80%) as co-solvents. The results are summarized in Table VI.6. All the products of the reactions were analyzed by ¹H NMR in comparison with the starting materials, thus allowing to evaluate the conversion of final product. It was found that different temperatures could promote the reaction process using L- EL. It was observed that with the increase of temperature the conversion of the product increased after the first 24h. While for the use of conventional solvents such as ethanol at 24 °C seems to be more favorable. The reaction time does not appear to be particularly relevant after 24h of reaction. Conversions of the products didn't vary significantly after 24h. The amount of L-proline as a common catalyst had an important effect on the values of final conversion product. The use of 50 mol % L-proline catalyst allowed conversions and *ee* values to be comparable with the conventional Michael reaction (81% conversion, 96% *ee*). The use of co-solvents based on alcohols (EtOH) 20% or 80% showed no significant difference in conversions of the product. With the use of water as co-solvent and the other conditions optimized, it was found that the reaction has not progressed and no product was detected after 24 hours. Water has clearly a negative effect on the Michael reaction.

Table VI.6 - The effect of changing different conditions of Michael additon of cyclohexanone to *trans*-nitrostyrene.

Entry	Tested conditions	Solvent	Conversion [%] ^[e]	
1	Temperature [°C]	24	EtOH	100
2		24	L-EL	44
3		4	L-EL	67
4		50	L-EL	81
5	Reaction time [h]	24 ^[a]	L-EL	81
6		24 ^[b]	L-EL	67
7		48 ^[a]	L-EL	84
8		48 ^[b]	L-EL	71
9	Co-solvent	20:80 ^[c]	L-EL: EtOH	65
10		80:20 ^[c]	L-EL: EtOH	61
11		1:1	L-EL: H ₂ O	0
12		8:2	L-EL: H ₂ O	0
13	Loading of catalyst	30 ^[d]	L-EL	44
14	(mol %)	50 ^[d]	L-EL	81

^[a] Loading of catalyst was increased from 30 to 50 mol%. ^[b] Reaction was performed at 4 °C. ^[c] The reaction time was 72 [h]. ^[d] Conversion after 24 [h]. ^[e] The conversions were determined from 400Hz ¹H NMR spectroscopy.

Having in hand the best reaction model, it was important to determine the enantiomeric excess values of the products obtained, in order to verify the effect of the chiral solvent in the reaction. The *ee* values of the final products were determined for four products. The results obtained are summarized in Table VI.7. The best conversions and *ee* values were achieved using the conventional system with EtOH. It seems clear that using the L-EL as an alternative solvent for Michael reaction is not much competitive when compared with the common solvent.

Table VI.7 Michael addition reaction of cyclohexanone to *trans*-nitrostyrene catalyzed by L-proline in different solvents.

Entry	Solvent	Temp. [°C]	Loading of catalyst [mol%]	Conversion [%] ^[b]	<i>ee</i> % ^[c]
1	EtOH	24	30	100	97
2	L-EL	24	30	44	53
3	EtOH	24	50	81	96
4	L-EL	50	30	81	62

^[a] Reagents concentrations: *trans*-nitrostyrene (0.4 mmol), cyclohexanone (0.2mmol). ^[b] The conversions were determined from 400Hz ¹H NMR spectroscopy. ^[c] Enantiomeric excesses determined by HPLC using Phenomenex Lux 5 μ m 250x10 cellulose column, flow 1ml/min., 25 °C column oven, hexane: i-PrOH 90:10, λ =230nm.

VI.5. Conclusions

This additional work presented in the closure chapter, suggests that in future, L- EL can be a possible alternative for common organic solvents used in aldol condensation and Michael reaction, but some optimization steps are still required. It seems that using L-EL as a chiral solvent doesn't contribute to improve the *ee* values. The presence of L-proline as a chiral catalyst is crucial. Nevertheless, to confirm this fact, studies using the racemic EL for organocatalysis should be made. Based on the preliminary results obtained, it would be appealing to develop a more complex system for organocatalysis, by combining the idea of CIL catalyst with chiral L-EL solvent.

VI.6. Experimental Part

General: Commercially available reagents L-proline (MW= 115.13 g.mol⁻¹, CAS No. 147-85-3), L-ethyl lactate (MW= 118.13 g.mol⁻¹, CAS No.687-47-8) and solvents were purchased from Alfa Aestar, Aldrich, Solchemar and were used without further purification. ¹H and ¹³C NMR spectra were recorded at 25 °C on a Bruker AMX400 spectrometer with TMS as internal standard. Chemical shifts are reported downfield in parts per million (ppm).

VI.6.1. General procedure for asymmetric aldol reaction

Asymmetric aldol reaction between aromatic *p*-nitroaldehyde and cyclohexanone was carried out in organic solvent (0.5 ml). As the organic solvent DMSO (conventional solvent), L-ethyl lactate or ethyl lactate and water mixture (1:1) were chosen. The suspension of L-proline as chiral catalyst (30 mol%) and ketone (100 µl, 2 mmol) was stirred for 30 minutes at RT. After that time aromatic aldehyde (0.0756 g, 1mmol) was added and the resulting mixture was allowed to stirr at RT for 24-48 hours as indicated in TablesVI.5. Relative and absolute configurations of the products were determined by comparison with the known ¹ H NMR as in chapter II. In some cases, the possibility of isolating the product by extracting the reaction mixture with diethyl ether or ethyl acetate was tested. In the case of the experiments with the addition of ethyl lactate, the addition of water allowed the product to precipitate and isolate.

VI.6.2. General procedure for the Michael reaction of cyclohexanone and β -nitrostyrene

To a suspension of L-proline as catalyst (30 or 50 mol%) and cyclohexanone (210 μ l, 2 mmol) in 1ml of solvent (EtOH, L-ethyl lactate and L-ethyl lactate systems with ethanol or water as co-solvent) *trans*- β -nitrostyrene (0.149 g, 1.0 mmol) was added. The resulting mixture was allowed to stir at 4, 25, 40 °C, for 24-72 hours, then evaporated in vacuo and the resulting residue was purified by extraction with Et₂O or ethyl acetate (in the case with L-ethyl lactate) or by adding water to allow precipitation of the final product. Relative and absolute configurations of the products were determined by comparison with the known ¹ H NMR and chiral HPLC analysis. The enantiomeric excess was determined by chiral HPLC analysis on a Phenomenex Lux 5 μ m 250x10 cellulose column, flow 1ml.min⁻¹, 25 °C column oven, hexane: i-PrOH 90:10, λ =230 nm. *t* major = 13.7 min and *t* minor = 15.0 min.

VII. Annex

VII.1. NMR data for NMR assignment

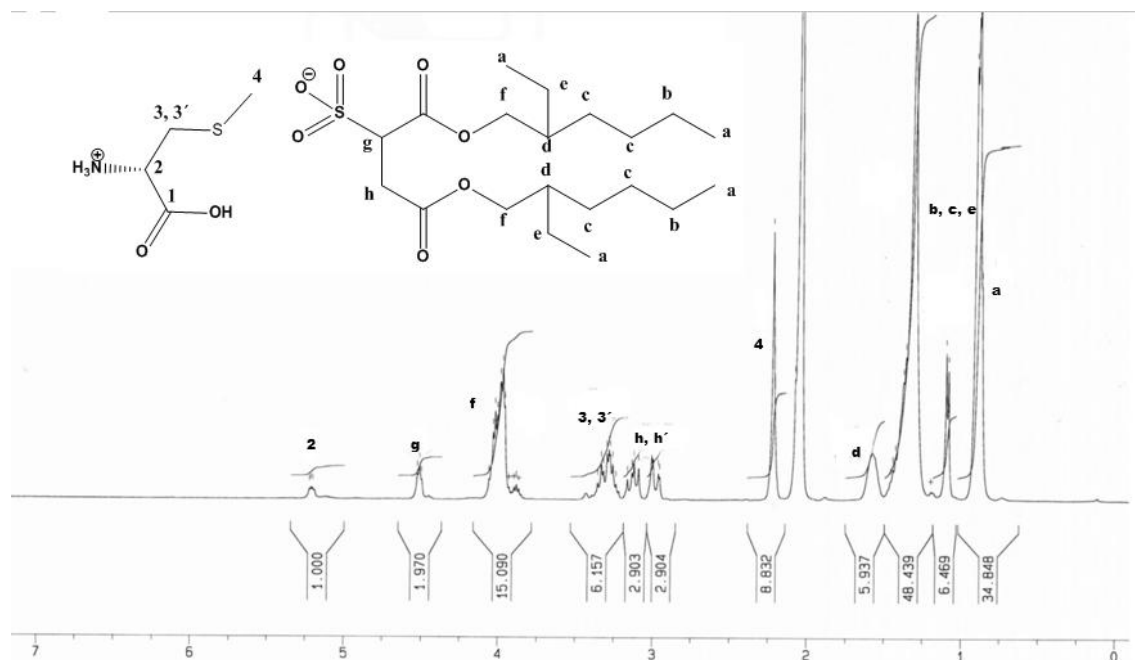


Figure VII.1 - ^1H NMR data for compound (S)-1-carboxy-2-(methylthio)ethanaminium 1,4-bis((2-ethylhexyl)oxy)-1,4-dioxobutane-2-sulfonate (2b).

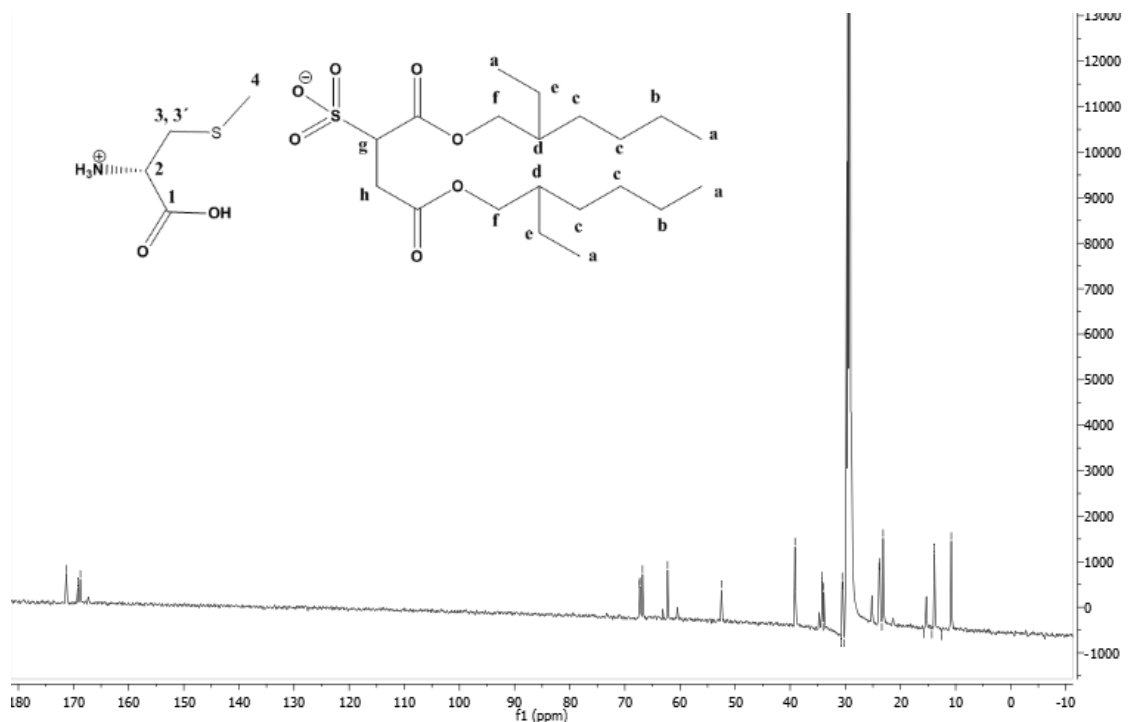


Figure VII.2 - ^{13}C NMR data for compound (S)-1-carboxy-2-(methylthio)ethanaminium 1,4-bis((2-ethylhexyl)oxy)-1,4-dioxobutane-2-sulfonate (2b).

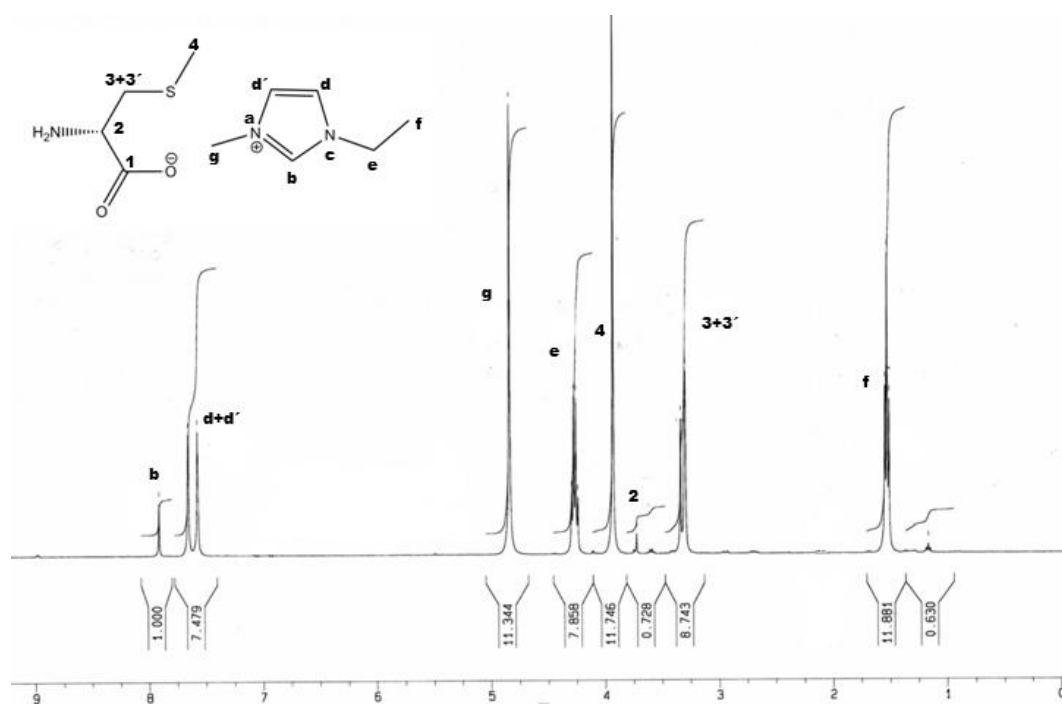


Figure VII.3 - ¹H NMR data of compound ethyl-3-methyl-1H-imidazol-3-ium (S)-2-amino-3-(methylthio)propanoate (3c).

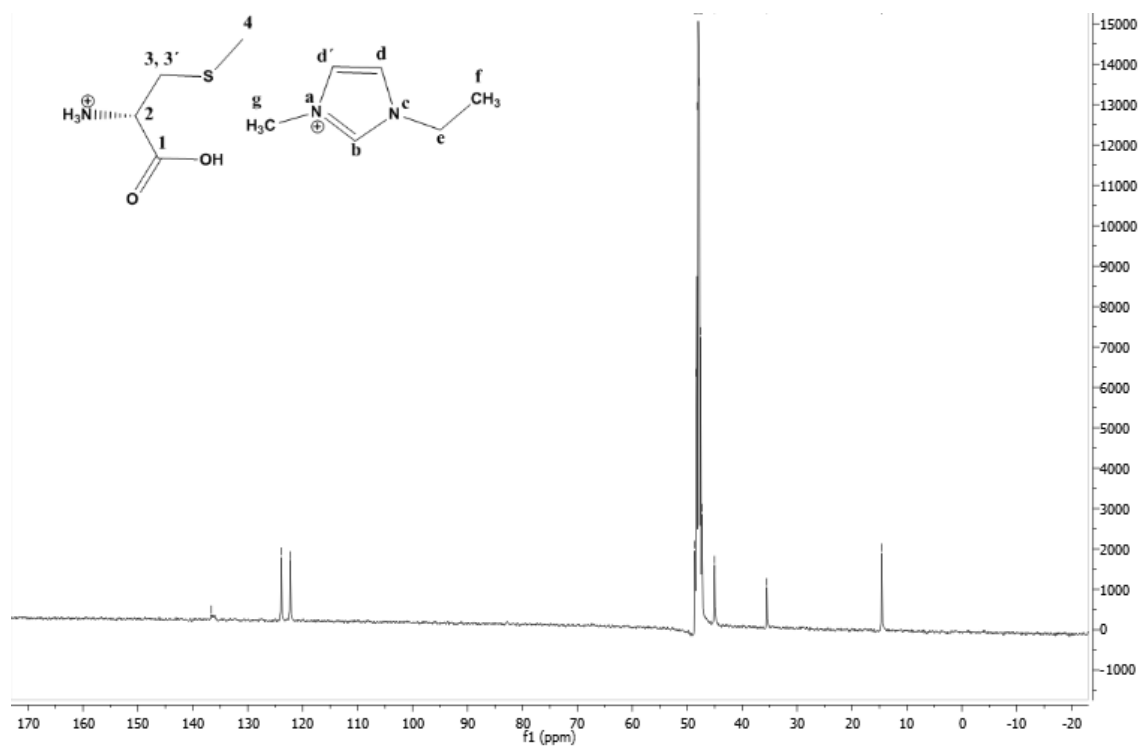


Figure VII.4 - ¹³C NMR data of compound ethyl-3-methyl-1H-imidazol-3-ium (S)-2-amino-3-(methylthio)propanoate (3c).

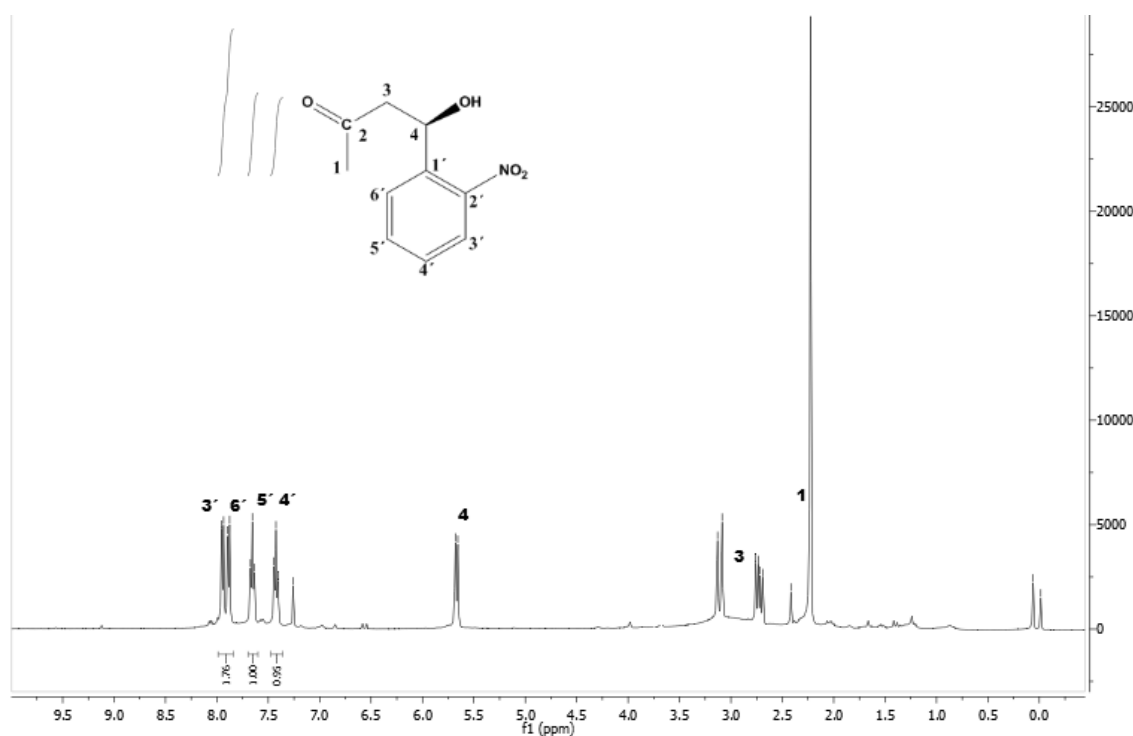


Figure VII.5 - ¹H NMR data of aldol product 4-hydroxy-4-(2-nitrophenyl)butan-2-one.

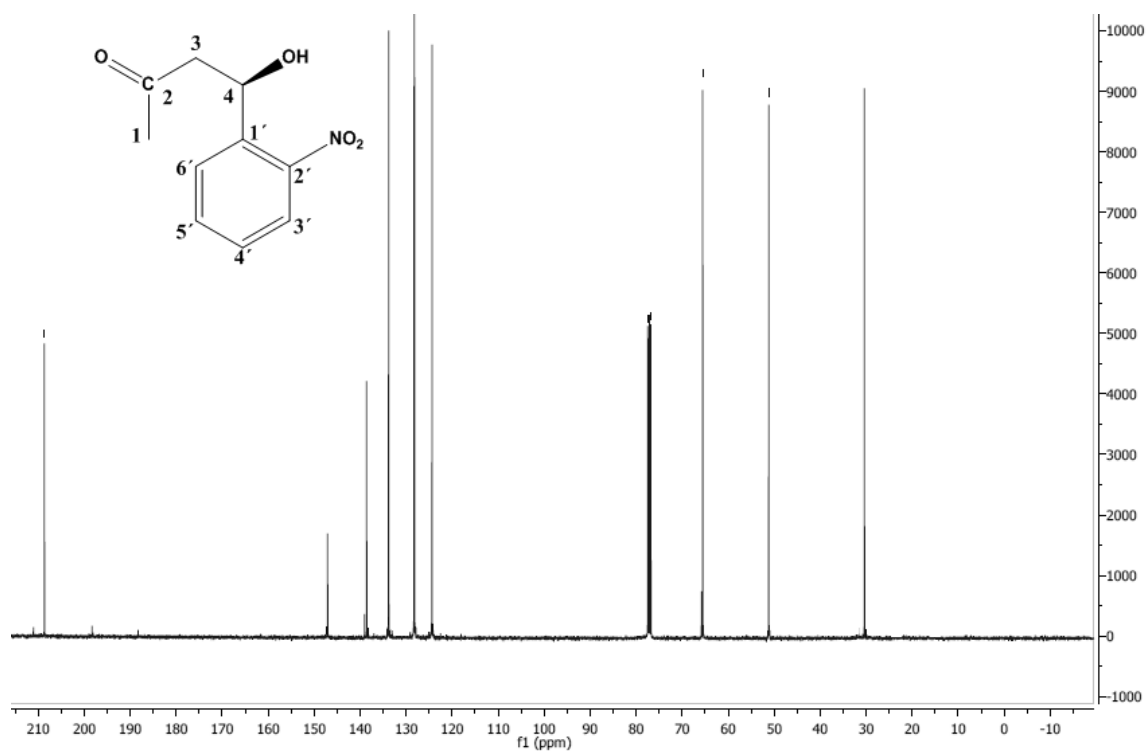


Figure VII.6 – ¹³C NMR data of aldol product 4-hydroxy-4-(2-nitrophenyl)butan-2-one.

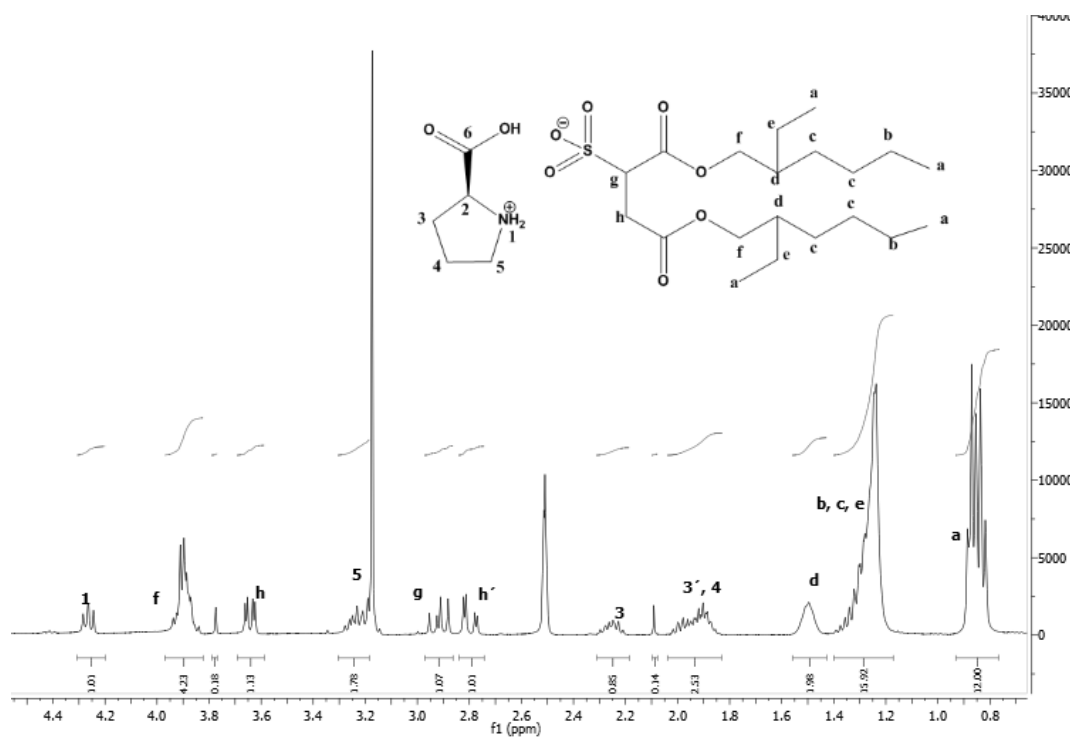


Figure VII.7 - ^1H NMR data of compound (S)-2-carboxypyrrolidin-1-ium 1,4-bis((2-ethylhexyl)oxy)-1,4-dioxobutane-2-sulfonate (7b).

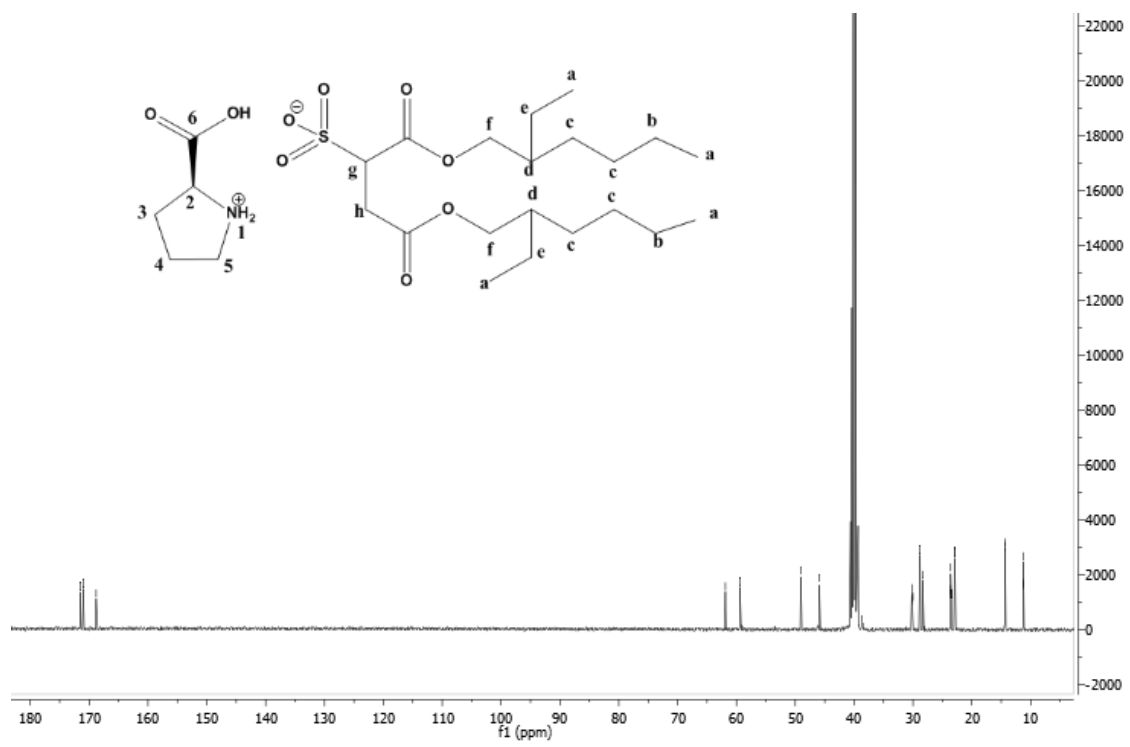


Figure VII.8 - ^{13}C NMR data of compound (S)-2-carboxypyrrolidin-1-ium 1,4-bis((2-ethylhexyl)oxy)-1,4-dioxobutane-2-sulfonate (7b).

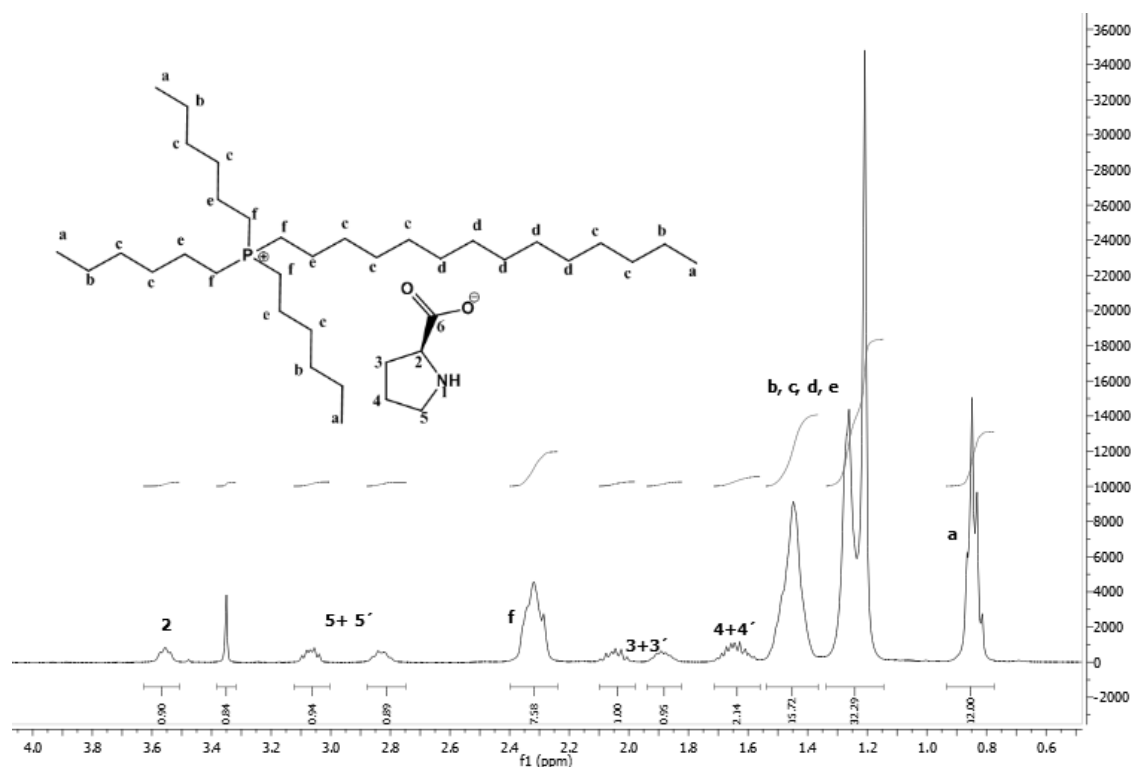


Figure VII.9 - ^1H NMR data of compound trihexyl(tetradecyl)phosphonium (S)-pyrrolidine-2-carboxylate (8a).

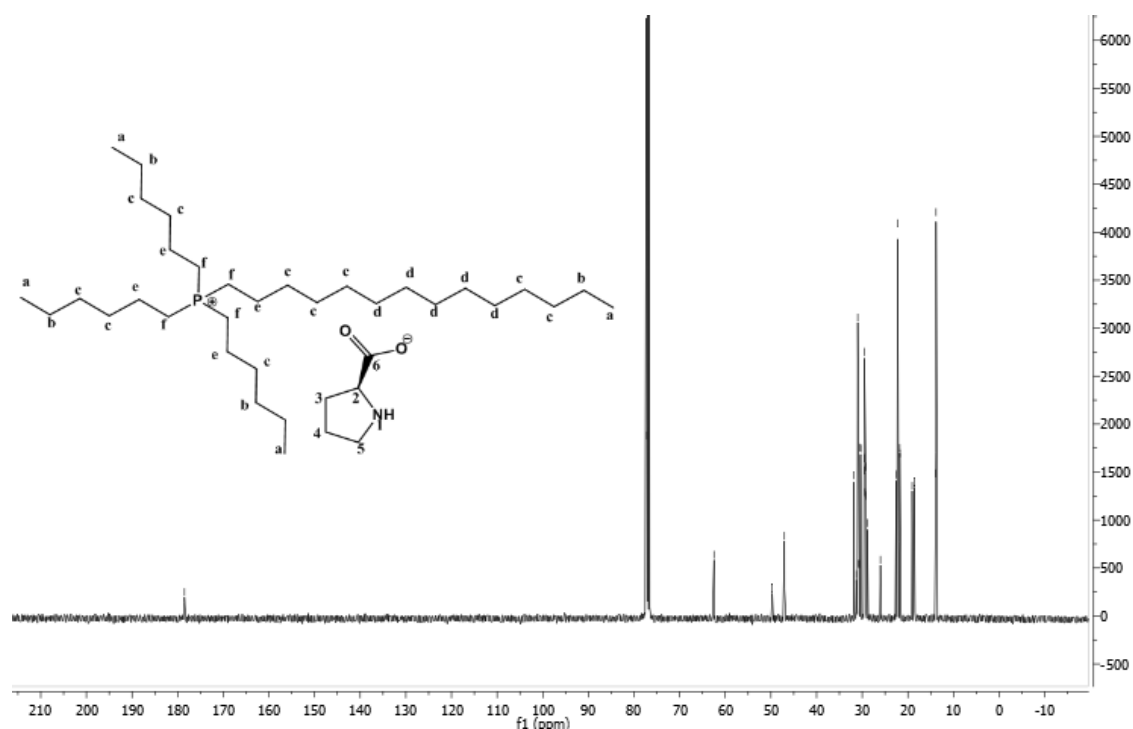


Figure VII.10 - ^{13}C NMR data of compound trihexyl(tetradecyl)phosphonium (S)-pyrrolidine-2-carboxylate (8a).

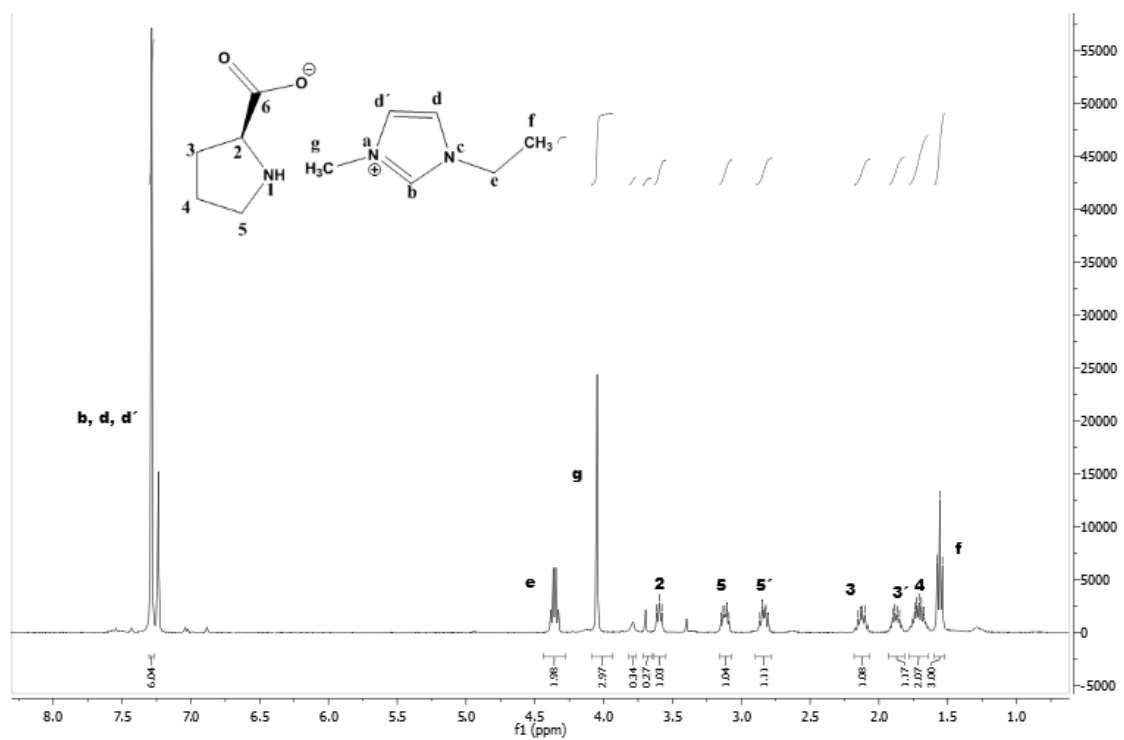


Figure VII.11 - ^1H NMR data of compound 1-ethyl-3-methyl-1H-imidazol-3-ium pyrrolidine-2-carboxylate (8b).

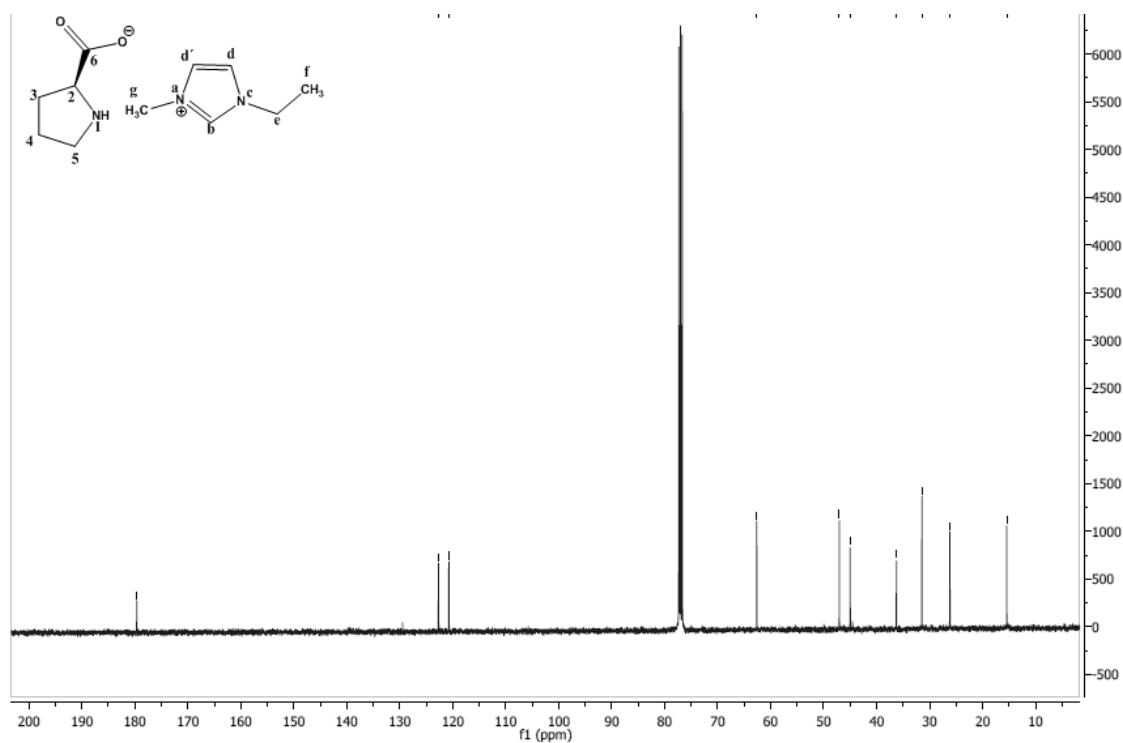


Figure VII.12 - ^{13}C NMR data of compound 1-ethyl-3-methyl-1H-imidazol-3-ium pyrrolidine-2-carboxylate (8b).

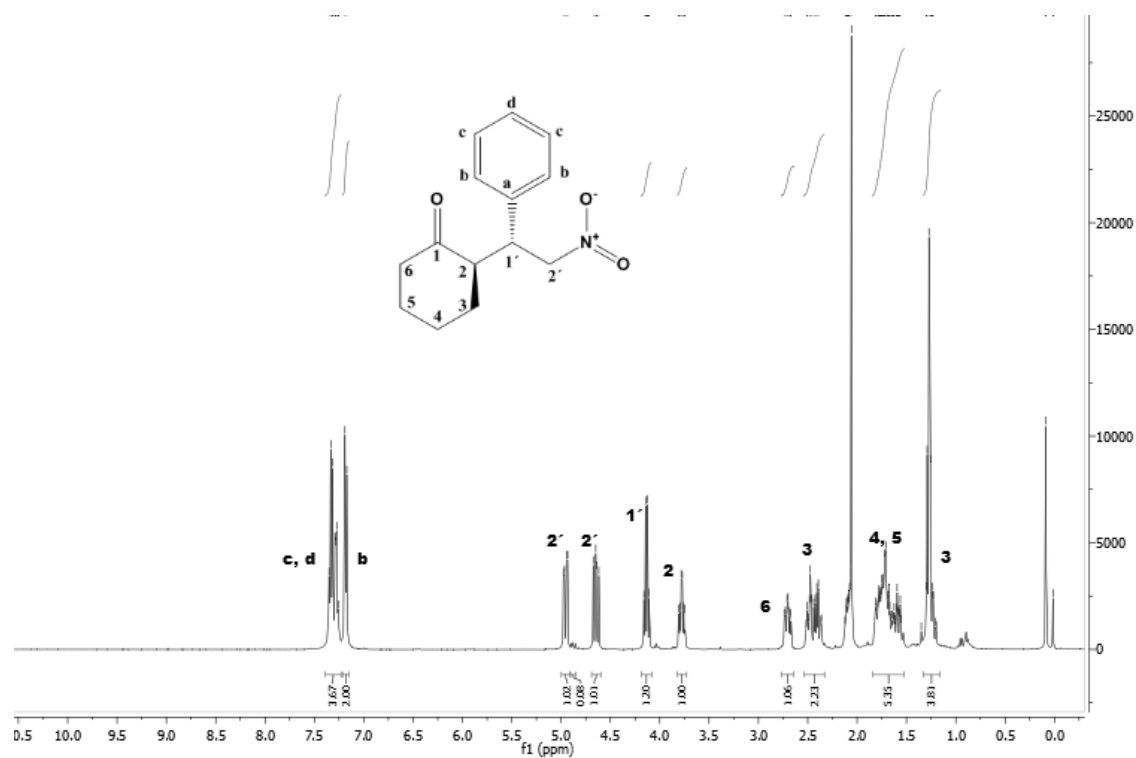


Figure VII.13- ^1H NMR data of compound (S)-2-[(R)-2-Nitro-1-phenylethyl]cyclohexanone (Michael product).

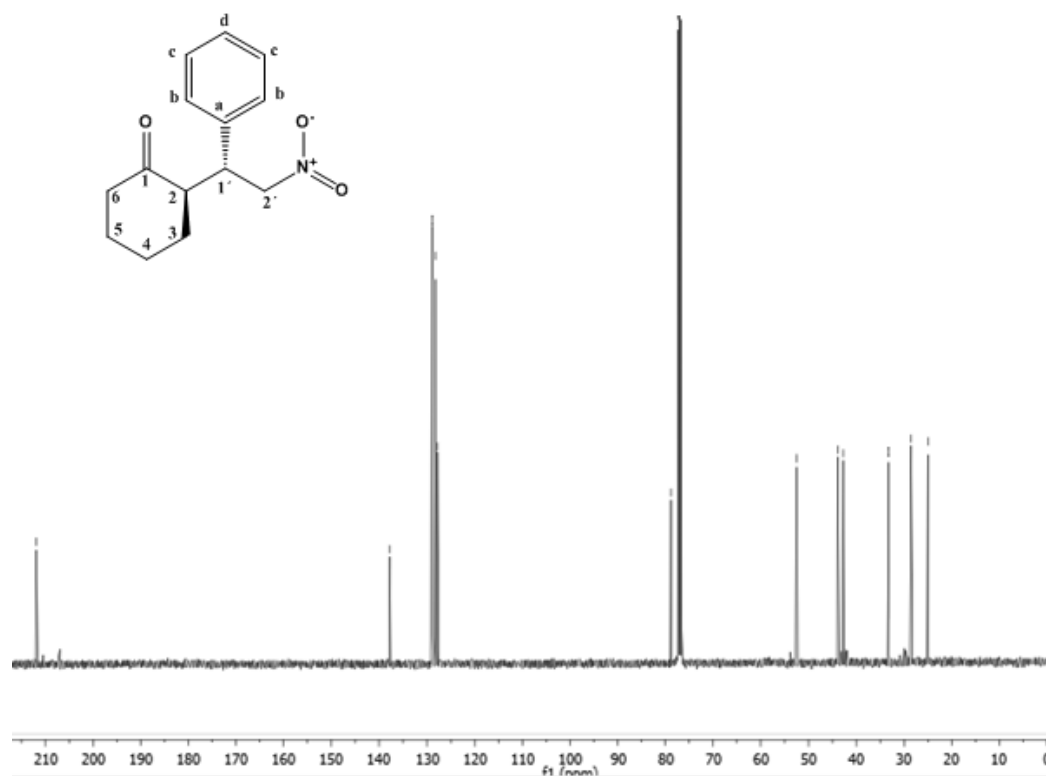


Figure VII.14 - ^{13}C NMR data of compound (S)-2-[(R)-2-Nitro-1-phenylethyl]cyclohexanone (Michael product).

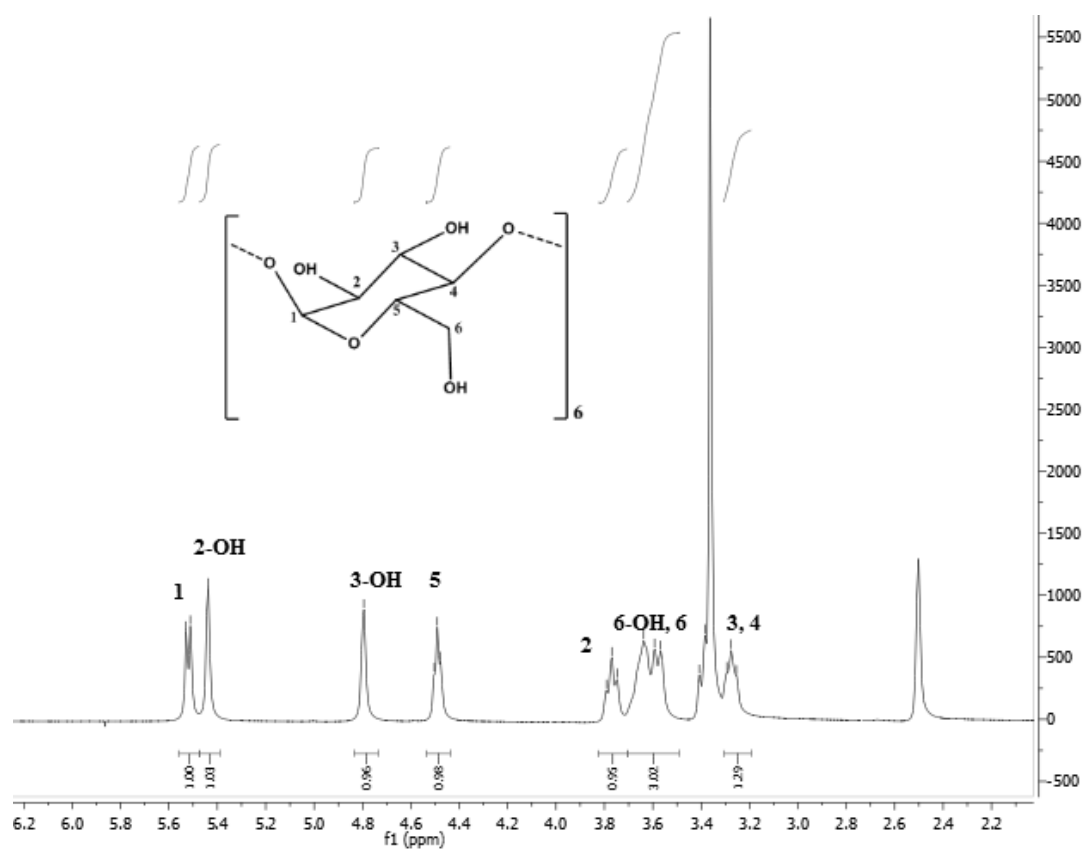


Figure VII.15 - ^1H NMR data of compound α - CD.

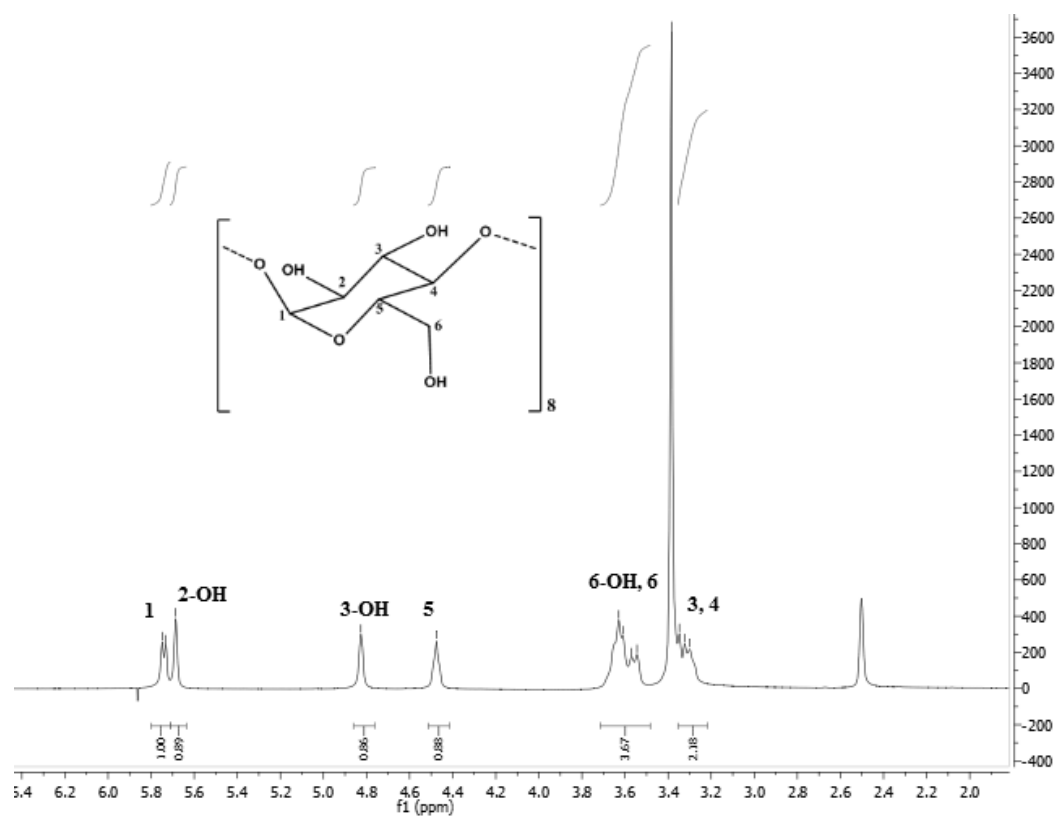


Figure VII.16 - ^1H NMR data of compound γ - CD.

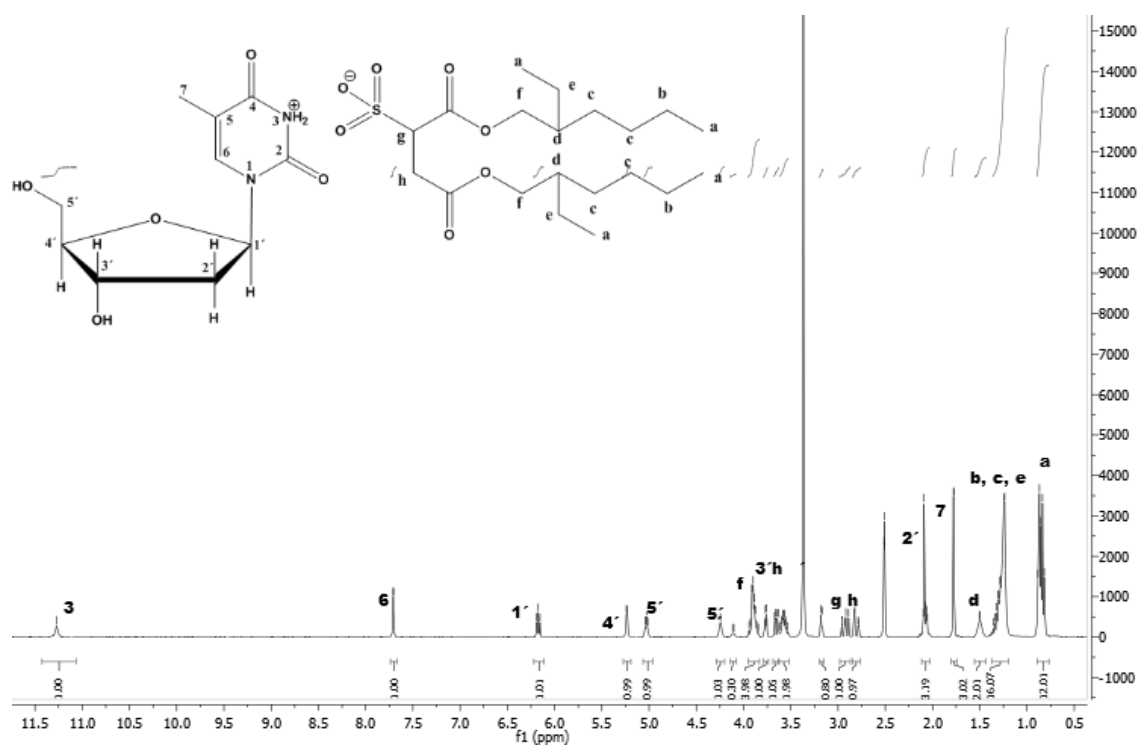


Figure VII.17 - ^1H NMR data of compound 3-((2R,3R,4S,5R)-3,4-dihydroxy-5-(hydroxymethyl)tetrahydrofuran-2-yl)-5-methyl-2,6-dioxo-1,2,3,6-tetrahydropyrimidin-1-ium 1,4-bis((2-ethylhexyl)oxy)-1,4-dioxobutane-2-sulfonate (11b).



Figure VII.18 - ^{13}C NMR data of compound 3-((2R,3R,4S,5R)-3,4-dihydroxy-5-(hydroxymethyl)tetrahydrofuran-2-yl)-5-methyl-2,6-dioxo-1,2,3,6-tetrahydropyrimidin-1-ium 1,4-bis((2-ethylhexyl)oxy)-1,4-dioxobutane-2-sulfonate (11b).

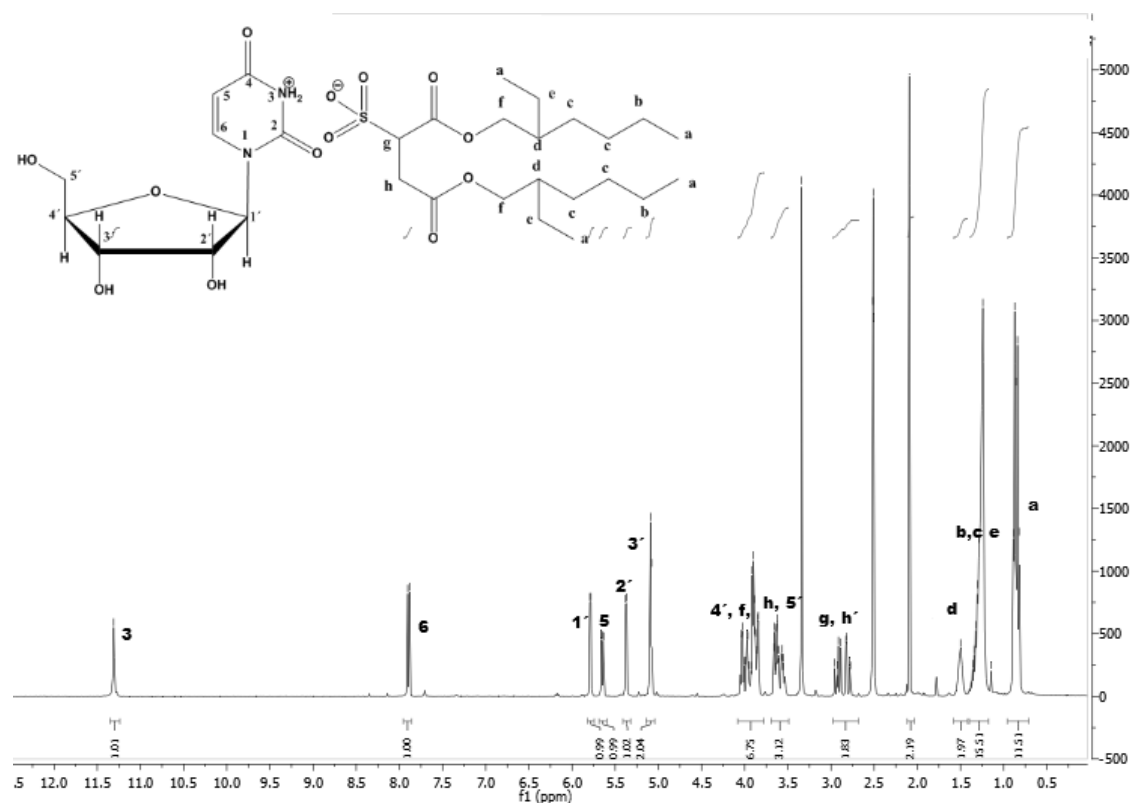


Figure VII.19 ^1H NMR data of compound 3-((2R,3R,4S,5R)-3,4-dihydroxy-5-(hydroxymethyl)tetrahydrofuran-2-yl)-2,6-dioxo-1,2,3,6-tetrahydropyrimidin-1-ium 1,4-bis((2-ethylhexyl)oxy)-1,4-dioxobutane-2-sulfonate (12b).

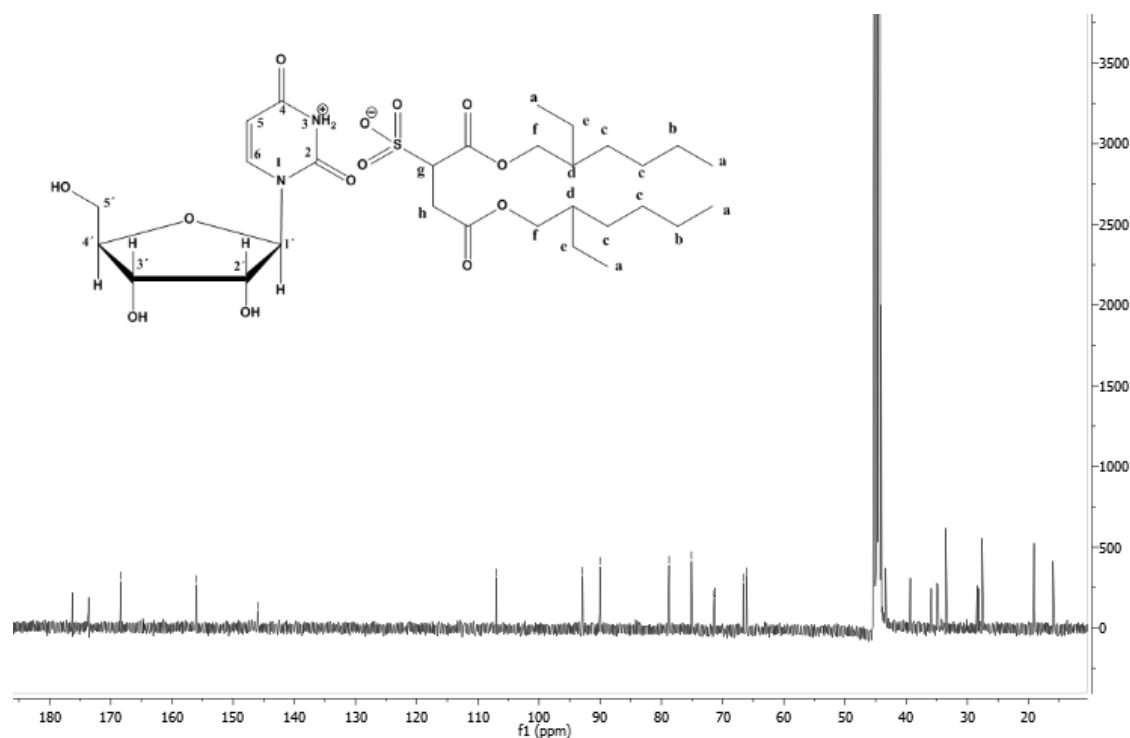


Figure VII.20 ^{13}C NMR data of compound 3-((2R,3R,4S,5R)-3,4-dihydroxy-5-(hydroxymethyl)tetrahydrofuran-2-yl)-2,6-dioxo-1,2,3,6-tetrahydropyrimidin-1-ium 1,4-bis((2-ethylhexyl)oxy)-1,4-dioxobutane-2-sulfonate (12b).

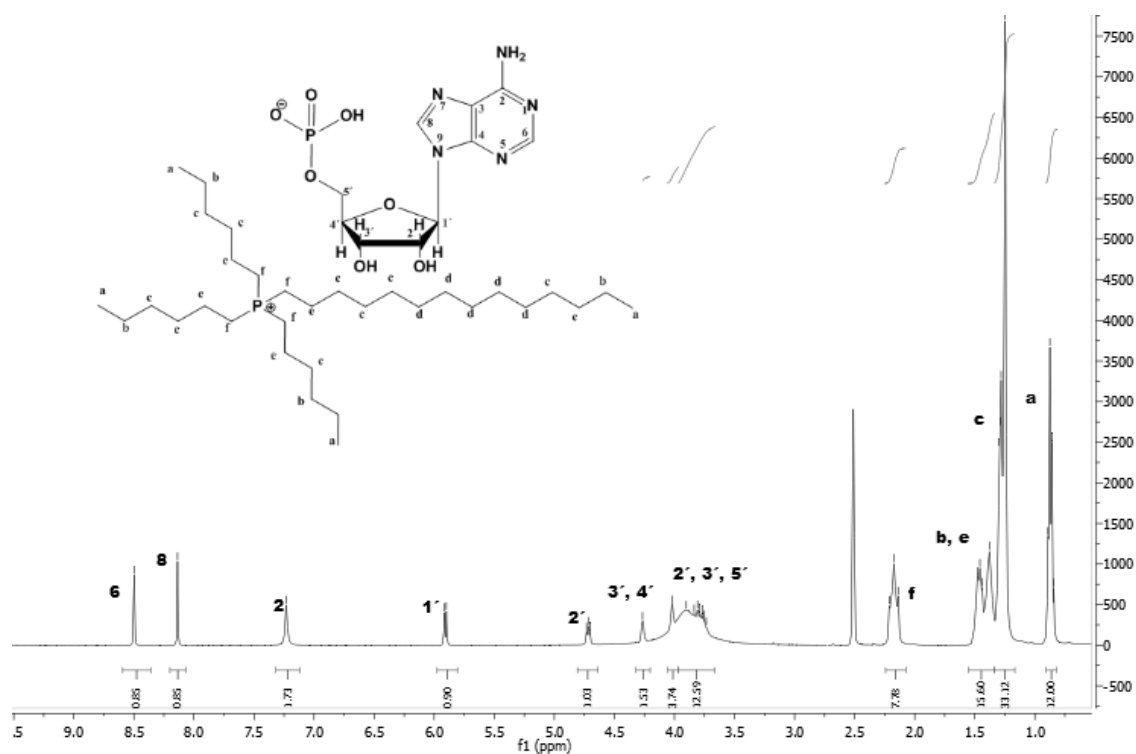


Figure VII.21 - ^1H NMR data of compound trihexyl(tetradecyl)phosphonium ((2R,3S,4R,5R)-5-(6-amino-9H-purin-9-yl)-3,4-dihydroxytetrahydrofuran-2-yl)methyl hydrogenphosphate (13a).

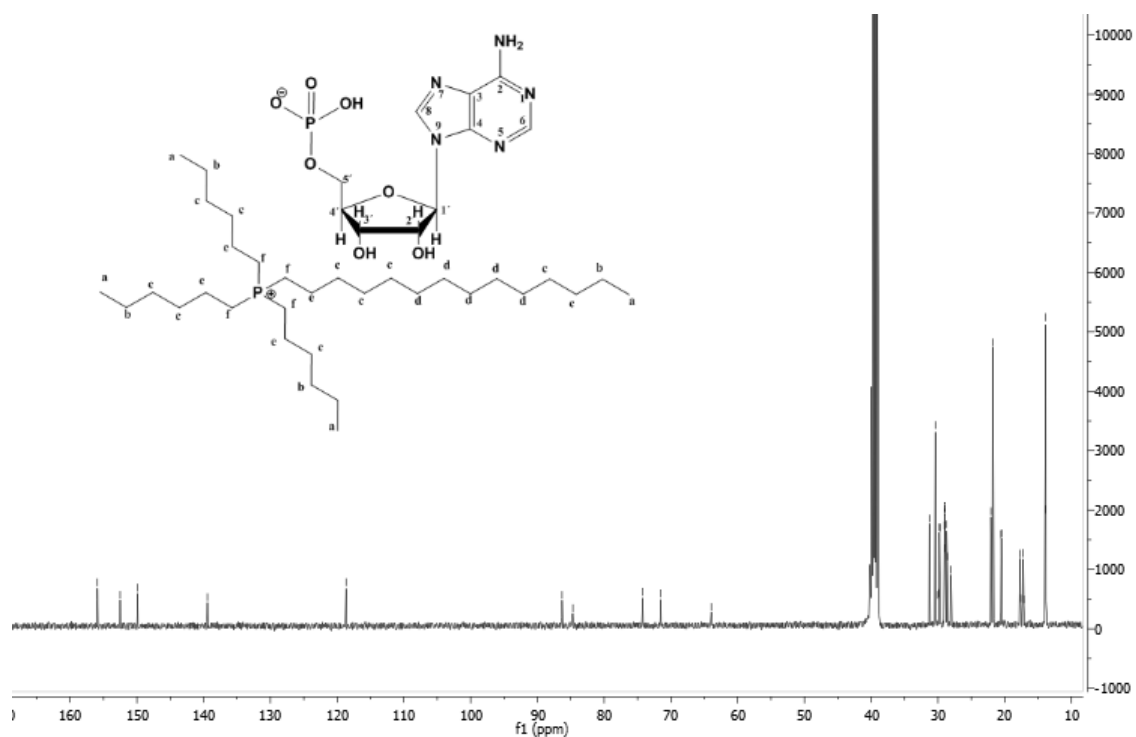


Figure VII.22 - ^{13}C NMR data of compound trihexyl(tetradecyl)phosphonium ((2R,3S,4R,5R)-5-(6-amino-9H-purin-9-yl)-3,4-dihydroxytetrahydrofuran-2-yl)methyl hydrogenphosphate (13a).

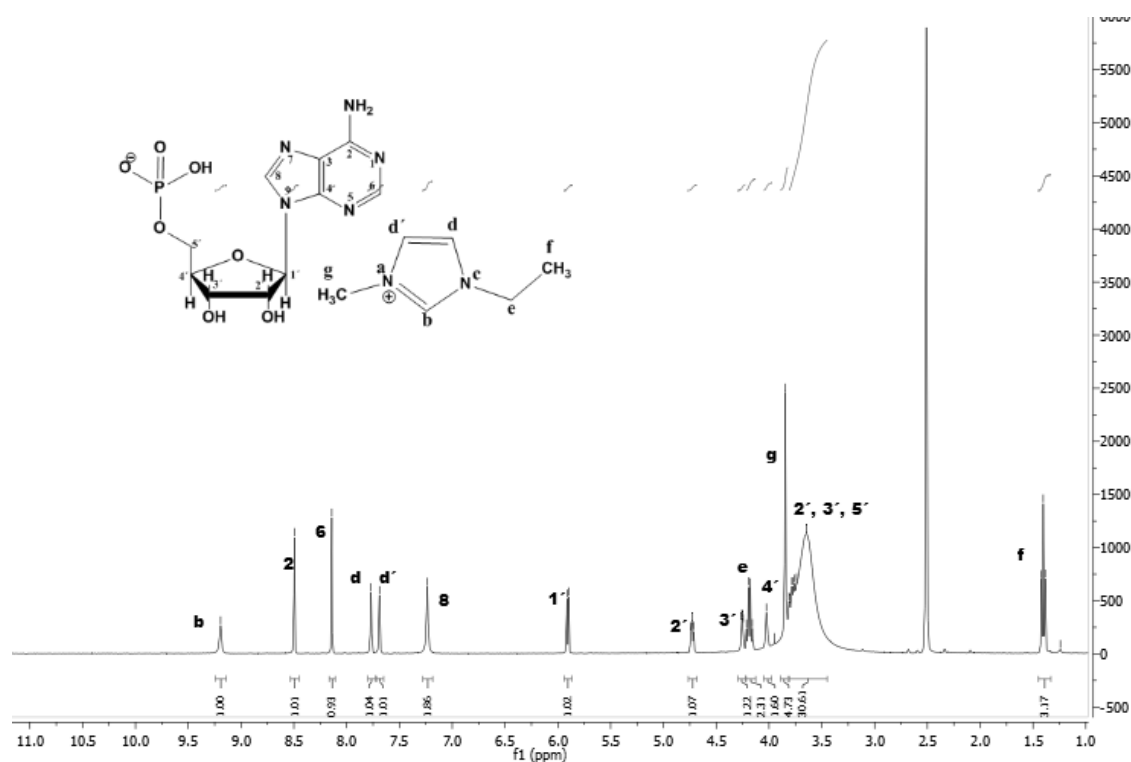


Figure VII.23 - ^1H NMR data of compound 1-ethyl-3-methyl-1H-imidazol-3-ium ((2R,3S,4R,5R)-5-(6-amino-9H-purin-9-yl)-3,4-dihydroxytetrahydrofuran-2-yl)methyl hydrogenphosphate (13b).

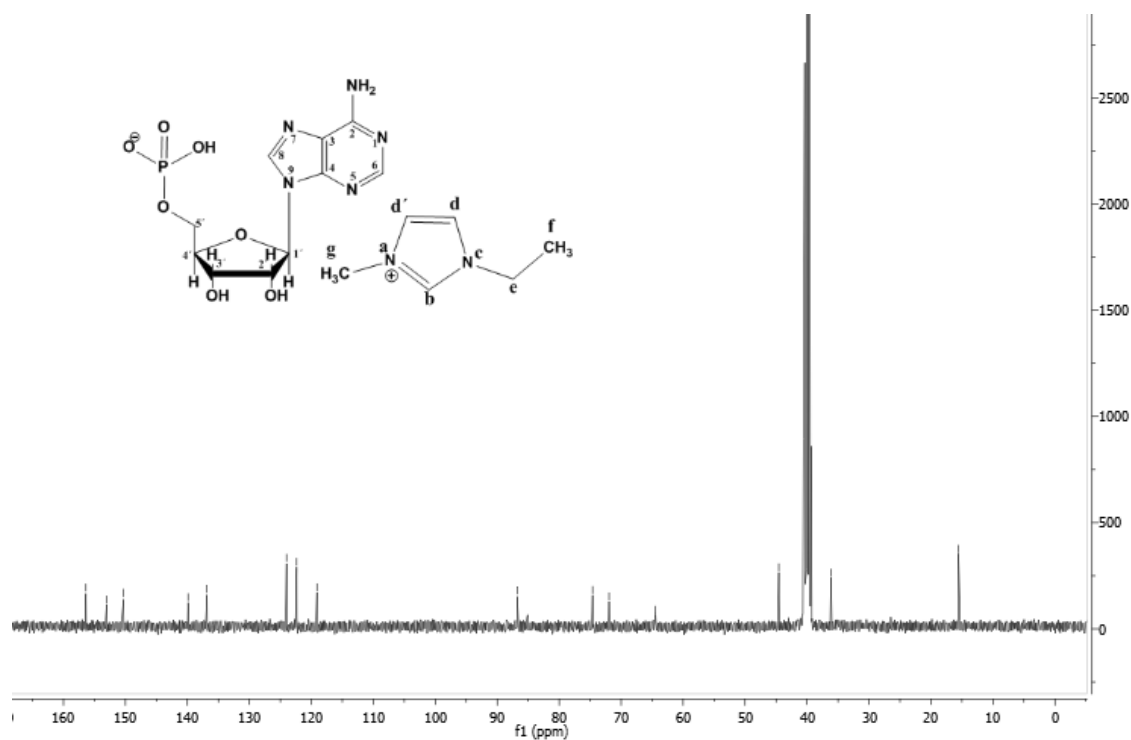


Figure VII.24 – ^{13}C NMR data of compound 1-ethyl-3-methyl-1H-imidazol-3-ium ((2R,3S,4R,5R)-5-(6-amino-9H-purin-9-yl)-3,4-dihydroxytetrahydrofuran-2-yl)methyl hydrogenphosphate (13b).

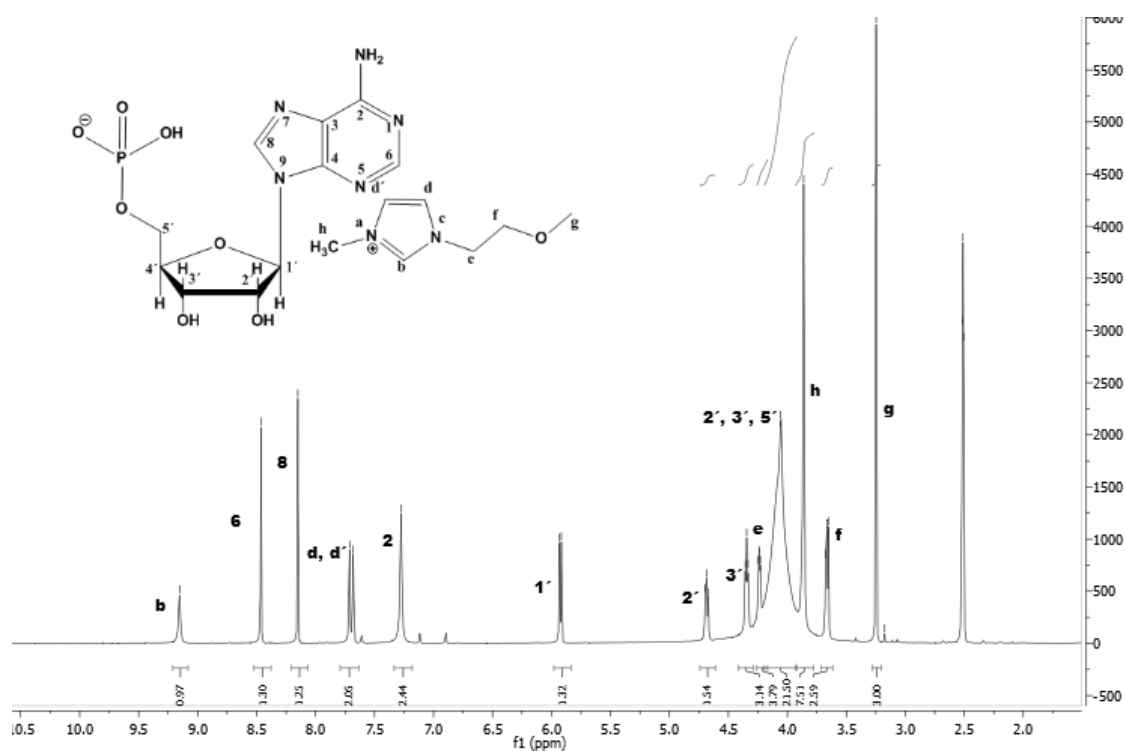


Figure VII.25 - ^1H NMR data of compound 1-(2-methoxyethyl)-3-methyl-1H-imidazol-3-ium ((2R,3S,4R,5R)-5-(6-amino-9H-purin-9-yl)-3,4-dihydroxytetrahydrofuran-2-yl)methyl hydrogenphosphate (13c).

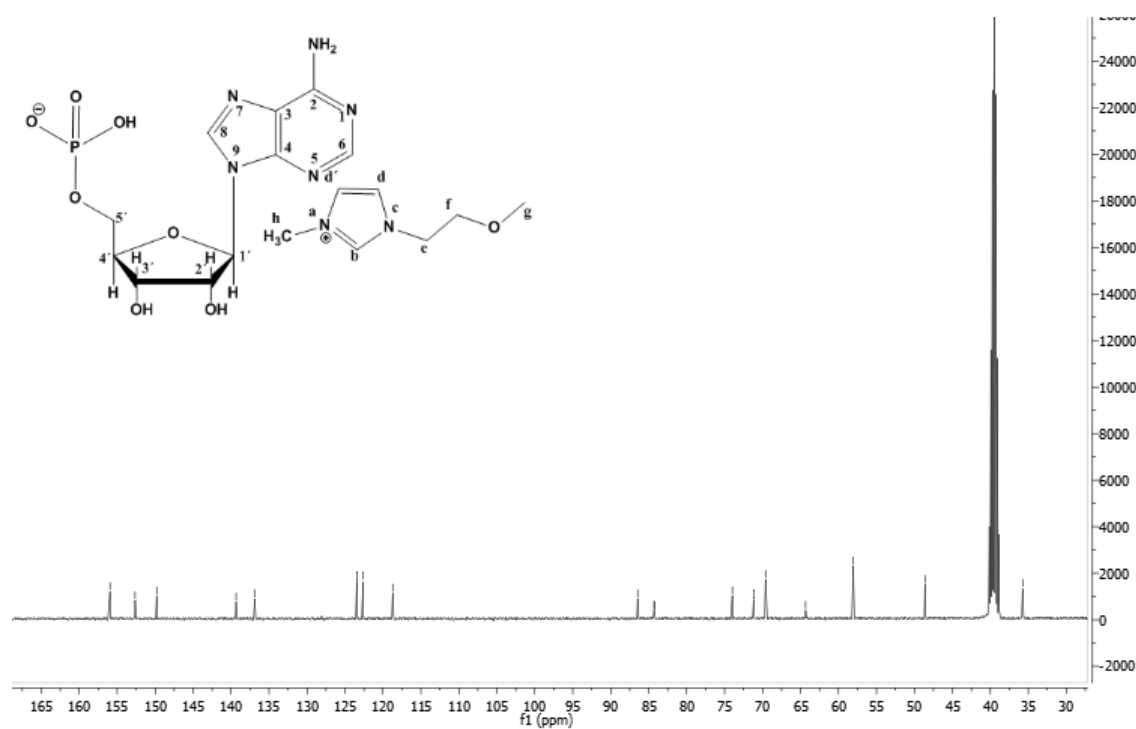


Figure VII.26 - ^{13}C NMR data of compound 1-(2-methoxyethyl)-3-methyl-1H-imidazol-3-ium ((2R,3S,4R,5R)-5-(6-amino-9H-purin-9-yl)-3,4-dihydroxytetrahydrofuran-2-yl)methyl hydrogenphosphate (13c).

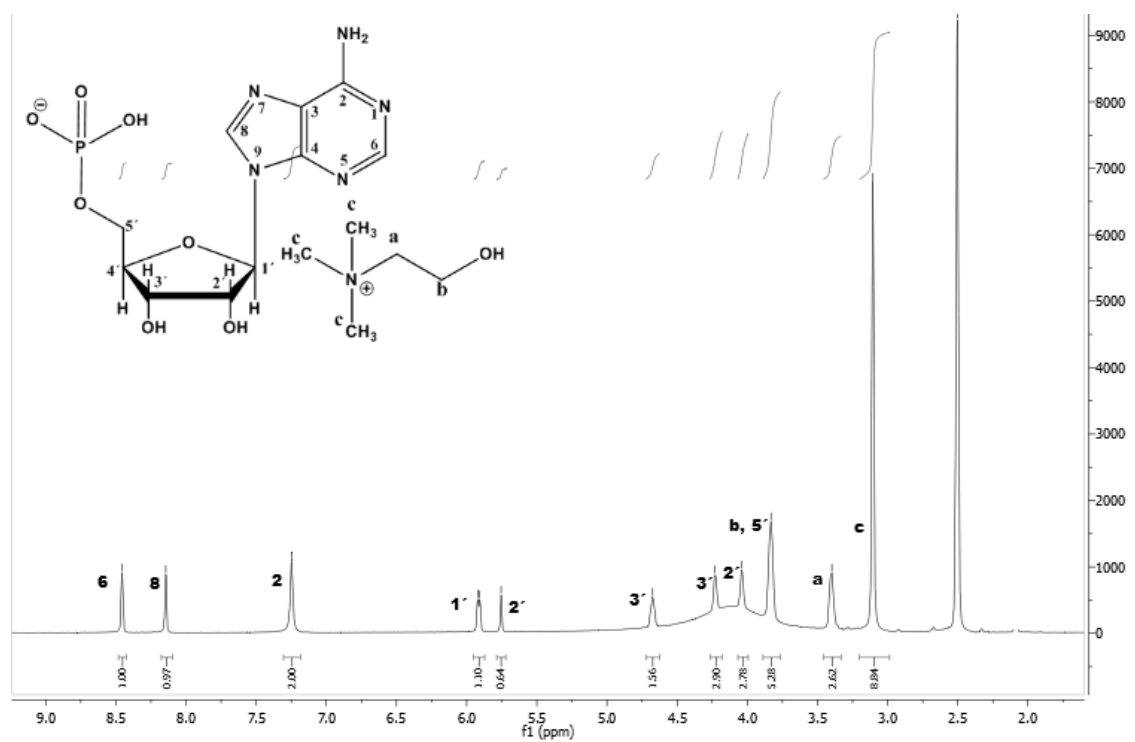


Figure VII.27 – ^1H NMR data of compound 2-hydroxy-N,N,N-trimethylethanaminium ((2R,3S,4R,5R)-5-(6-amino-9H-purin-9-yl)-3,4-dihydroxytetrahydrofuran-2-yl)methyl hydrogenphosphate (13d).

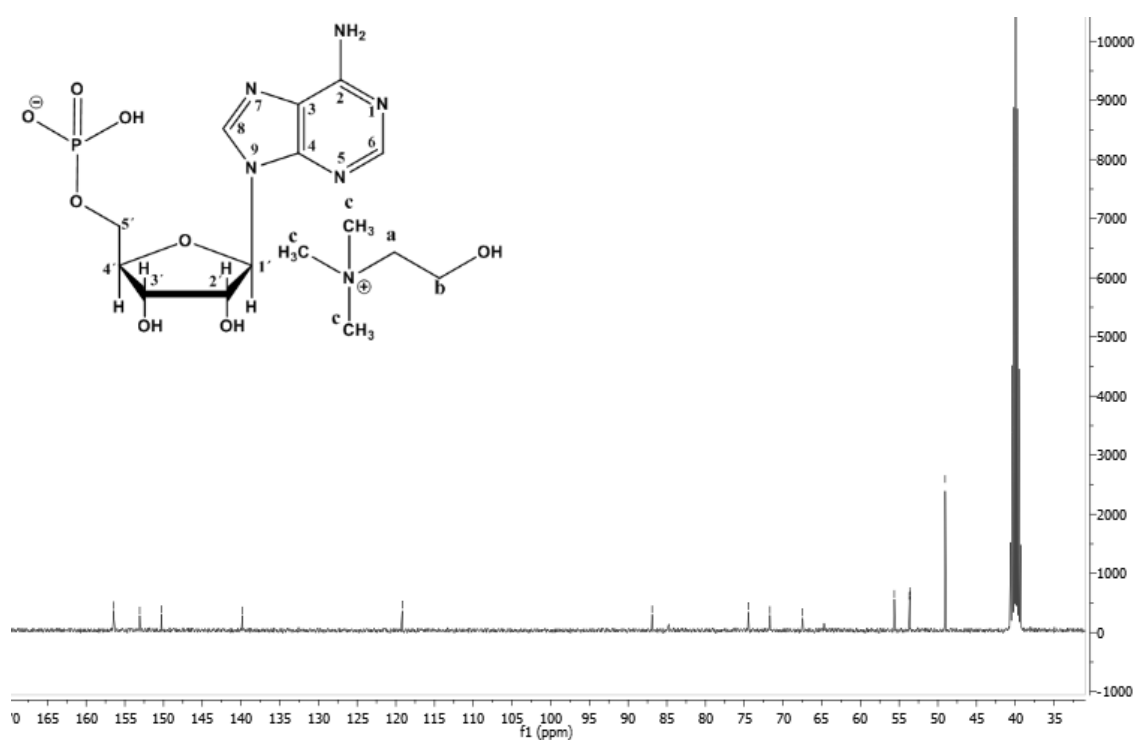


Figure VII.28 - ^{13}C NMR data of compound 2-hydroxy-N,N,N-trimethylethanaminium ((2R,3S,4R,5R)-5-(6-amino-9H-purin-9-yl)-3,4-dihydroxytetrahydrofuran-2-yl)methyl hydrogenphosphate (13d).

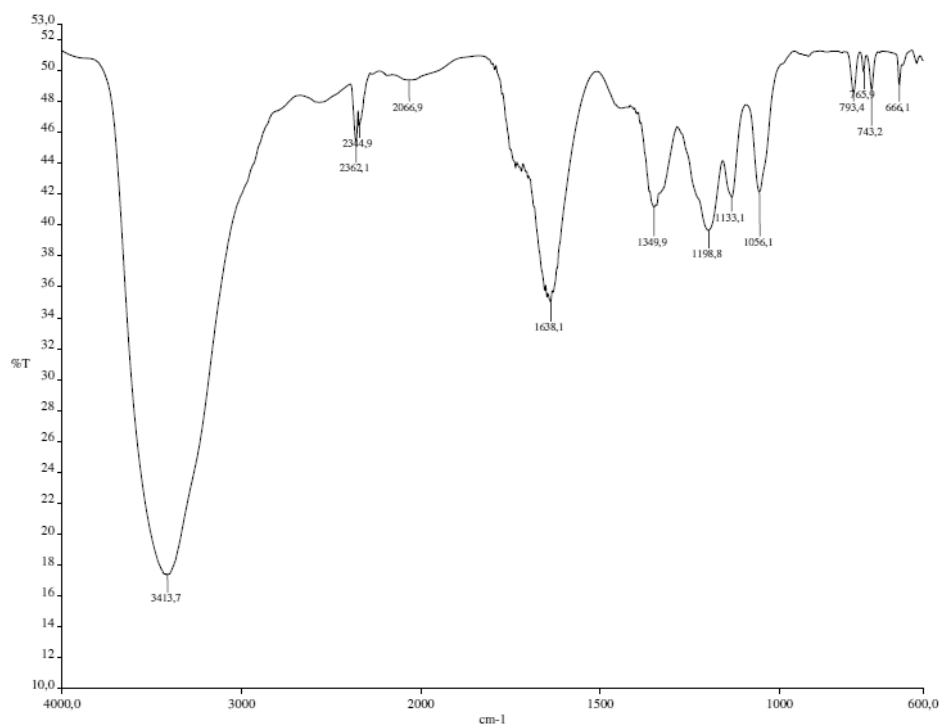
VII.2. FTIR data

Figure VII.29 - FTIR data for compound (L)-2-carboxypyrrolidin-1-ium bis((trifluoromethyl)sulfonyl)amide (7a).

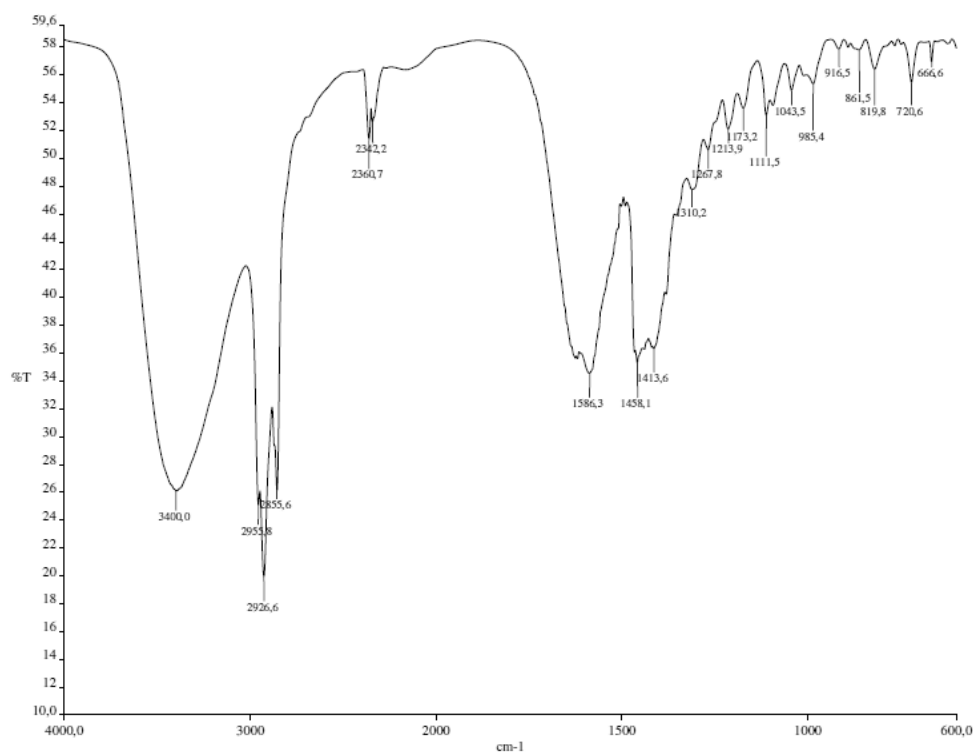


Figure VII.30 - FTIR data for compound trihexyl(tetradecyl)phosphonium (L)-pyrrolidine-2-carboxylate (8a).

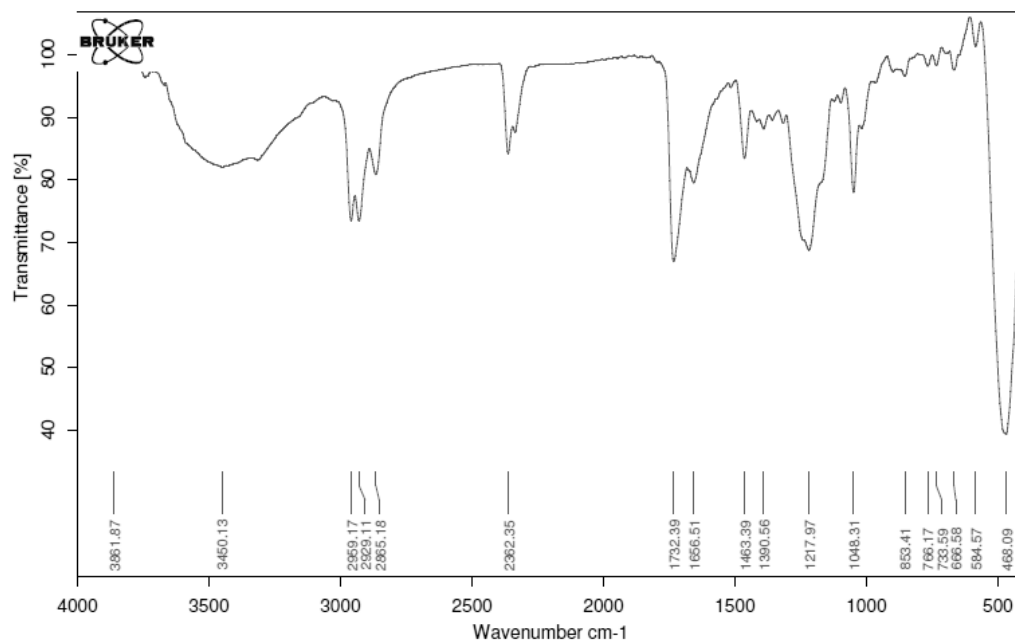


Figure VII.31 - FTIR data for compound 3-((2D,3D,4L,5D)-3,4-dihydroxy-5-(hydroxymethyl)tetrahydrofuran-2-yl)-5-methyl-2,6-dioxo-1,2,3,6-tetrahydropyrimidin-1-ium 1,4-bis((2-ethylhexyl)oxy)-1,4-dioxobutane-2-sulfonate (11b).

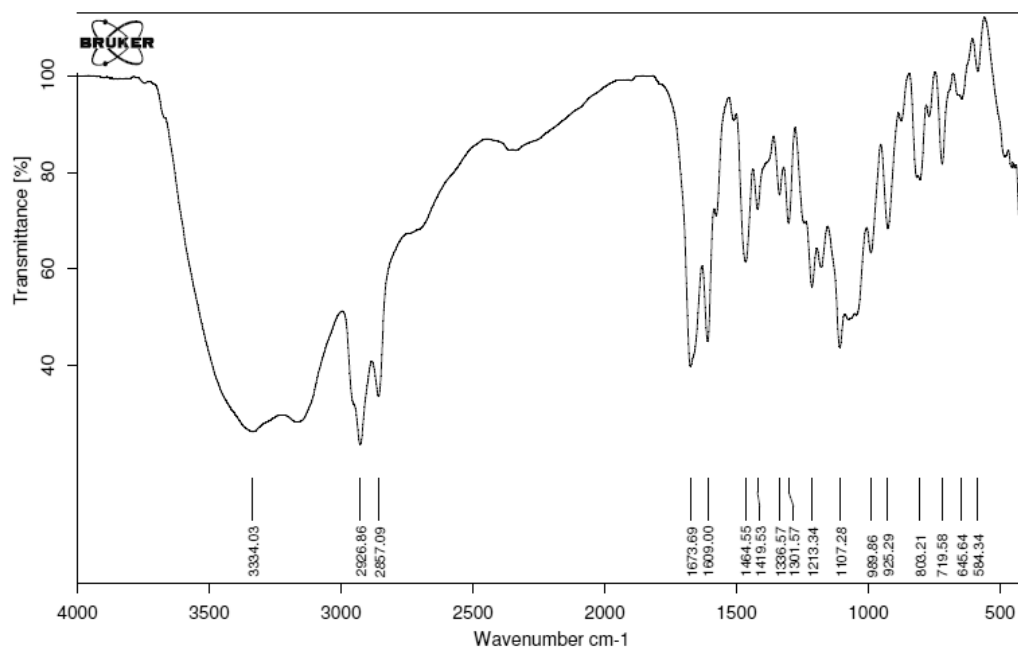


Figure VII.32 - FTIR data for compound trihexyl(tetradecyl)phosphonium ((2D,3L,4D,5D)-5-(6-amino-9H-purin-9-yl)-3,4-dihydroxytetrahydrofuran-2-yl)methyl hydrogenphosphate (13a).

VII.3. DSC curves data

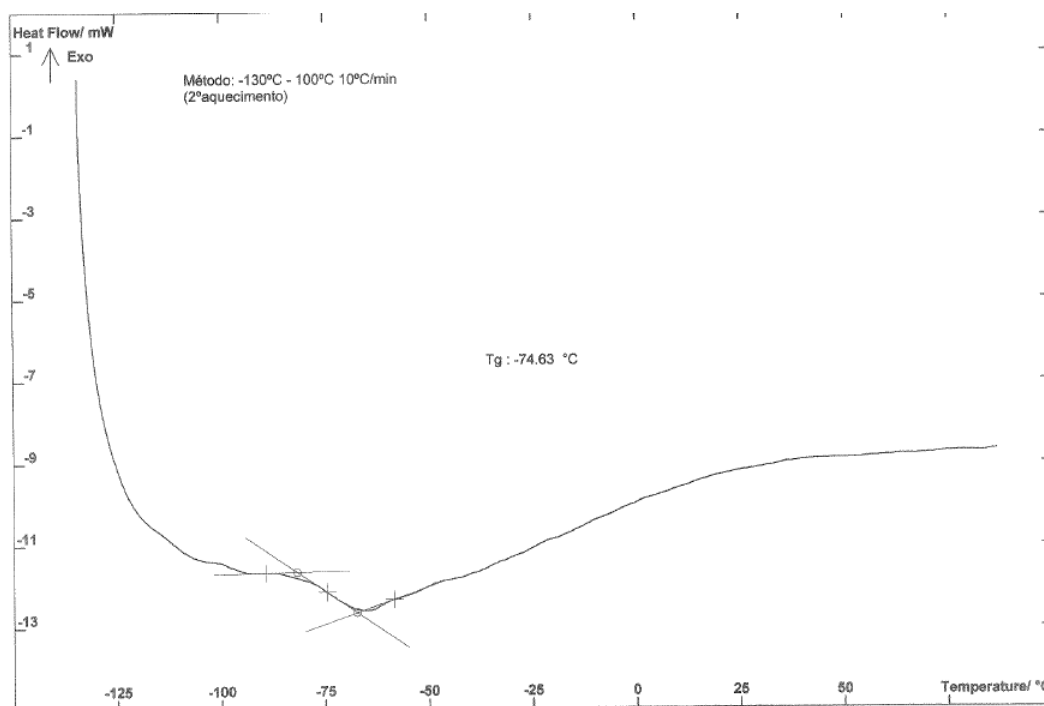


Figure VII.33 - DSC curve for compound (L)-1-carboxy-2-(methylthio)ethanaminium bis((trifluoromethyl)sulfonyl)amide (2a) in a heating cycle.

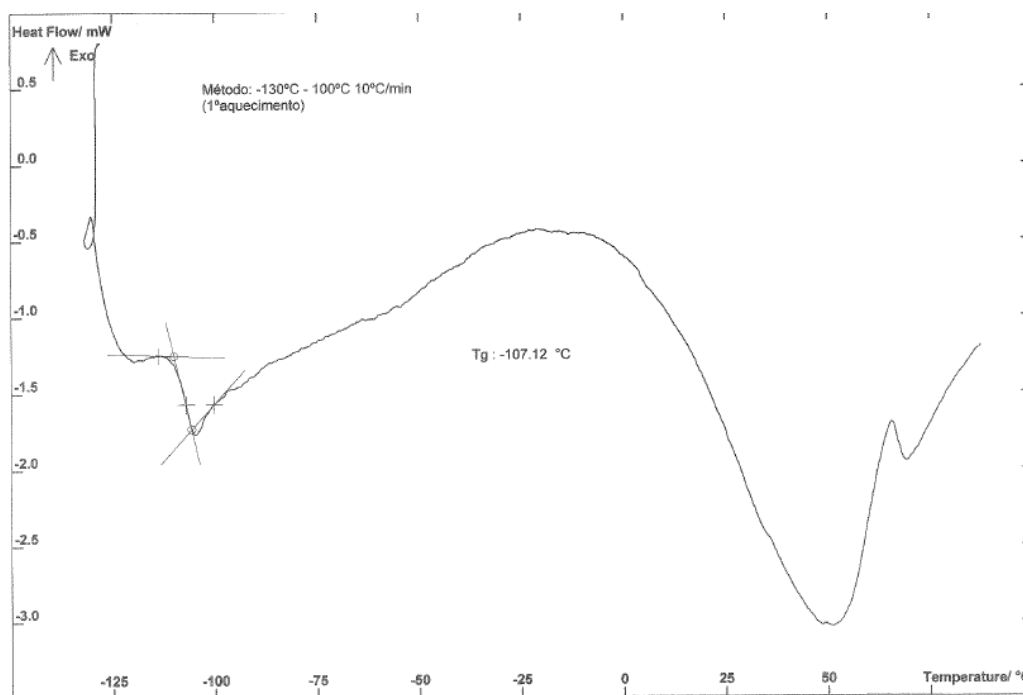


Figure VII.34 - DSC curve for compound trihexyl(tetradecyl)phosphonium (S)-2-amino-3-(methylthio)propanoate (3a) in a heating cycle.

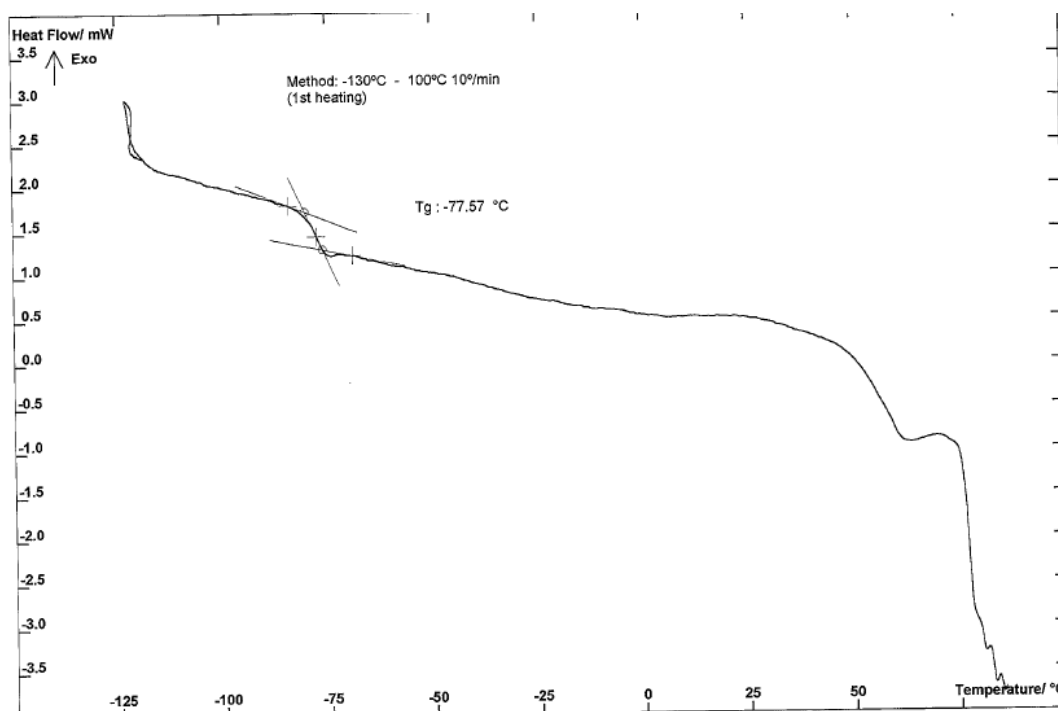


Figure VII.35 - DSC curve for compound 1-ethyl-3-methyl-1H-imidazol-3-ium pyrrolidine-2-carboxylate (8b) in a heating cycle.

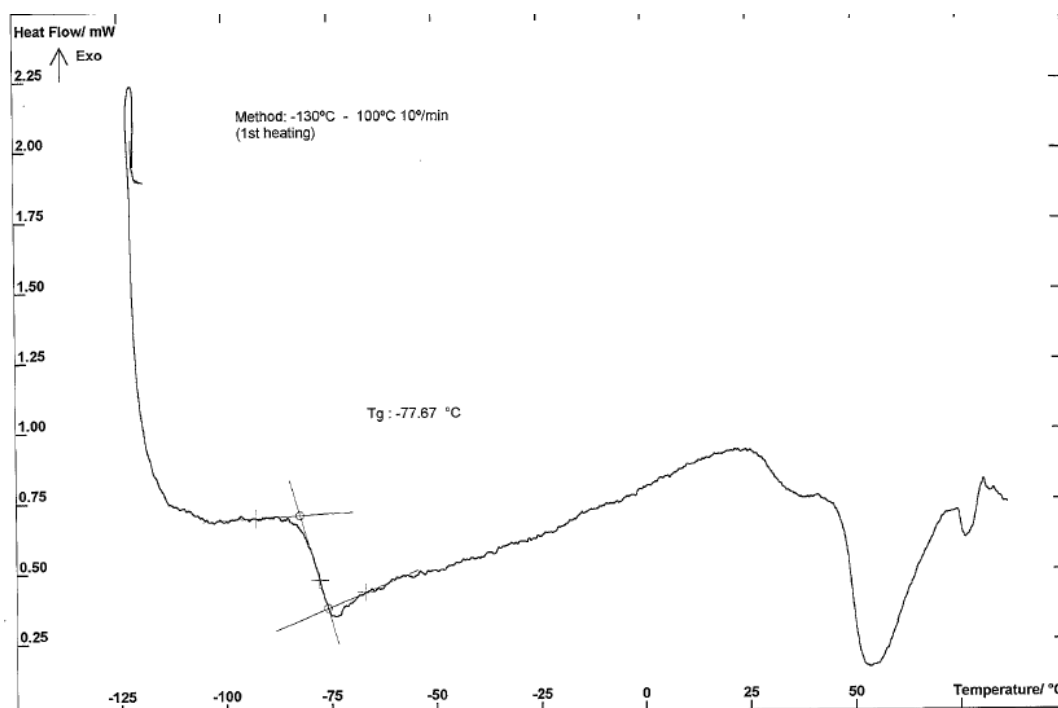


Figure VII.36 - DSC curve for compound (L)-2-carboxypyrrolidin-1-ium bis((trifluoromethyl)sulfonyl)amide (7a) in a heating cycle.

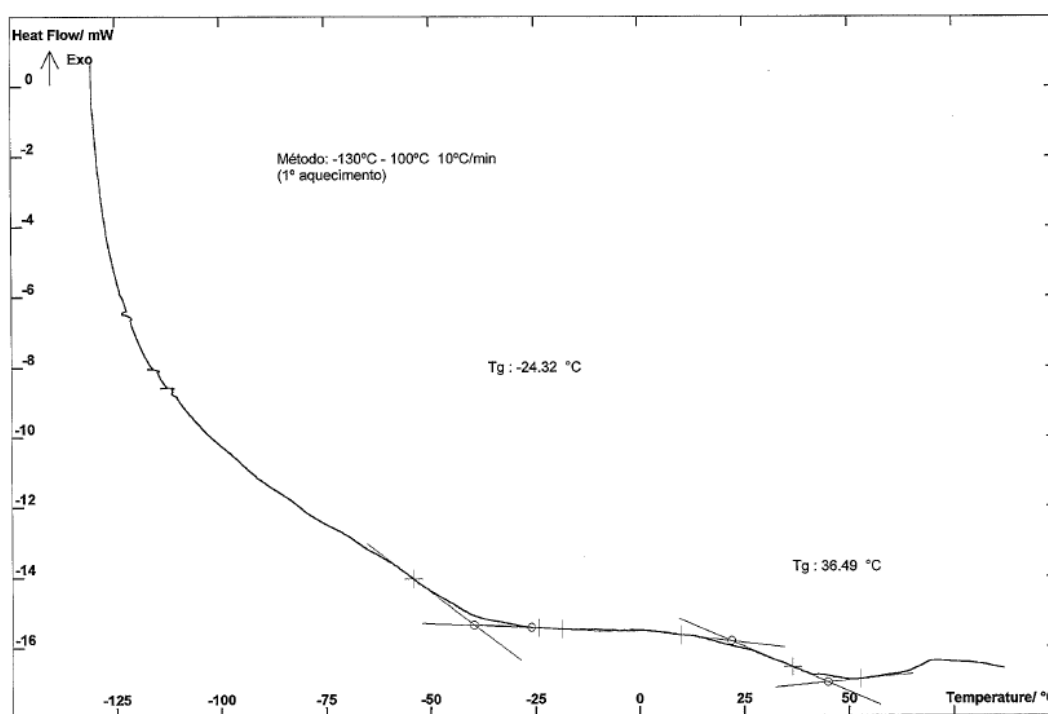


Figure VII.37 - DSC curve for compound 1-(2-methoxyethyl)-3-methyl-1H-imidazol-3-ium ((2D,3L,4D,5D)-5-(6-amino-9H-purin-9-yl)-3,4-dihydroxytetrahydrofuran-2-yl)methyl hydrogenphosphate (13c) in heating cycle.

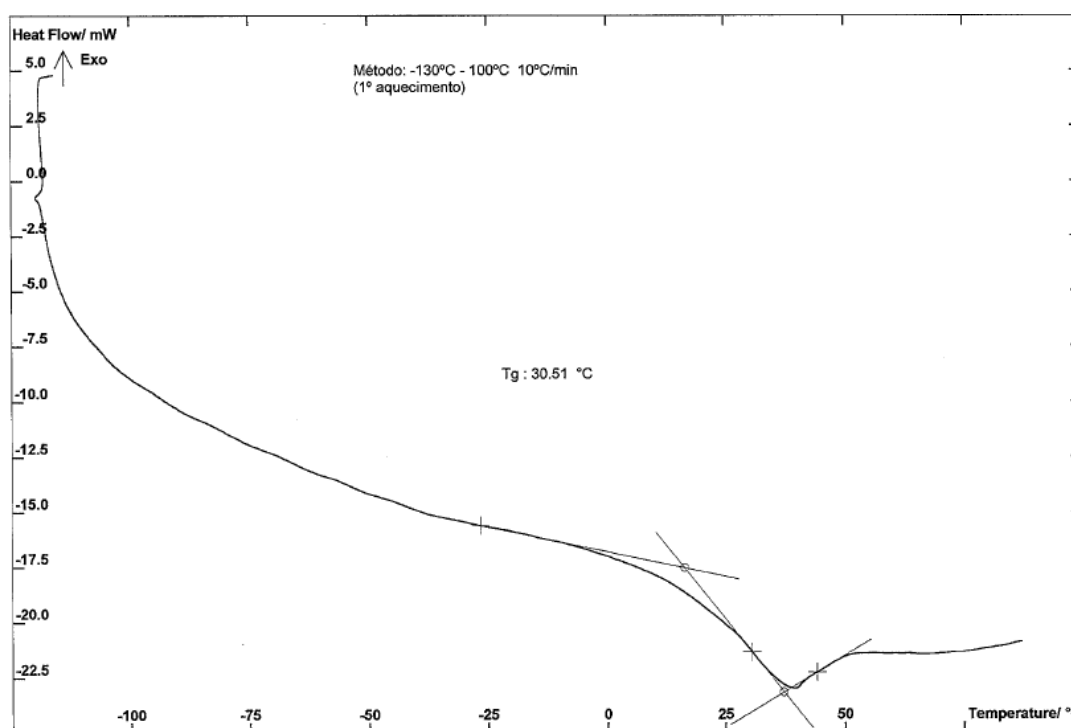


Figure VII.38 - DSC curve for compound 2-hydroxy-N,N,N-trimethylethanaminium ((2D,3L,4D,5D)-5-(6-amino-9H-purin-9-yl)-3,4-dihydroxytetrahydrofuran-2-yl)methyl hydrogenphosphate (13d) in heating cycle.

CHAPTER VIII. References

VIII. References

- ¹ A. D. Headley, B. Ni, *Aldrichimica Acta*, **2007**, 40, 107-117 and references therein.
- ² http://www.epa.gov/glo/SIPToolkit/ctg_act/197805_voc_epa450_2-78-022_stationary_sources.pdf
- ³ P. Walden, *Bull. Acad. Imper. Sci. Sant Petersburg*, **1914**, 1800.
- ⁴ J. Ding, D. W. Armstrong, *Chirality*, **2005**, 17, 281-292.
- ⁵ P. Wasserscheid, T. Welton, Eds. *Ionic Liquids in Synthesis*, Wiley-VCH, Weinheim, Germany, **2003** and references therein.
- ⁶ M. Freemantle, *An Introduction to ionic liquids* (Book), **2010**, RSC Publishing.
- ⁷ R. Rogers, K. R. Seddon, *Ionic Liquids: Industrial Applications for green chemistry* (Book), **2002**, ACS Series.
- ⁸ A. Kokorin, *Ionic Liquids: Applications and Perspectives* (Chapter 17), **2011**, Intech.
- ⁹ A. Kokorin, *Ionic Liquids: Theory, Properties, New Approaches* (Book), **2011**, Intech.
- ¹⁰ W. L. Hough, M. Smiglak, H. Rodriguez, R. P. Swatloski, S. K. Spear, D. T. Daly, J. Pernak, J. E. Grisel, R. D. Carliss, M. D. Soutullo, J. H. Davis, R. D. Rogers, *New J. Chem.* **2007**, 31, 1429-1436.
- ¹¹ C. Baudequin, *Tetrahedron Asymmetry*, **2003**, 14, 3081-3093.
- ¹² D. Seebach, A. H. Oei, *Angew. Chem. Int. Ed.* **1975**, 14, 634-636.
- ¹³ J. Dupont, P. A. Z. Suarez, R. F. de Souza, R. A. Burrow, J. P. Kintzinger, *Chem. Eur. J.* **2000**, 6, 2377-2381.
- ¹⁴ M. J., Earle, P. B., McCormac, K. R. Seddon, *Green Chem.* **1999**, 1, 23-25.
- ¹⁵ J. Kyoon Park, P. Sreekanth, B. Moon Kim, *Adv. Synth. Catal.* **2004**, 346, 49-52.
- ¹⁶ M. Lombardo, F. Pasi, S. Easwar, C. Trombini, *Adv. Synth. Catal.* **2007**, 349, 2061-2065.
- ¹⁷ S. Z. Luo, X. L. Mi, H. Xu, L. Zhang, S. Liu, J. P. Cheng, *Angew. Chem. Int. Ed.* **2006**, 118, 3165-3169.
- ¹⁸ L. C. Branco, A., Serbanovic, M. N. Ponte, C. A. M. Afonso, *ACS Catal.* **2011**, 1, 1408-1413.
- ¹⁹ C. Baudequin, D. Bregeon, J. Levillain, F. Guillen, J.-C. Plaquevent, A.-C. Gaumont, *Tetrahedron: Asymmetry*, **2005**, 16, 3921-3945.
- ²⁰ C. D. Tran, D. Oliveira, S. F. Yu, *Anal. Chem.* **2006**, 78, 1349-1356.
- ²¹ A. S. Shamsi, N. D. Danielson, *J. Sep. Sci.* **2007**, 30, 1729 - 1750.
- ²² W. A. Herrmann, L. J. Goossen, C. Köcher, G. R. Artus, *Angew. Chem. Int. Ed.* **1996**, 35, 2805 - 2807.
- ²³ B. Ni, A. D. Headley, G. Li, *J. Org. Chem.* **2005**, 70, 10600-10602.
- ²⁴ W. Bao, Z. Wang, Y. Li, *J. Org. Chem.* **2003**, 68, 591-593.

- ²⁵ Y. Génisson, N. Lauth-de Viguerie, C. André, M. Baltas, L. Gorrichon, *Tetrahedron: Asymmetry*, **2005**, 16, 1017-1023.
- ²⁶ E. J. Kim, S. Y. Ko, E. K. Dziadulewicz, *Tetrahedron Lett.* **2005**, 46, 631-633.
- ²⁷ M. Y. Machado, R. Dorta, *Synthesis*, **2005**, 15, 2473-2475.
- ²⁸ M. Tosoni, S. Laschat, A. Baro, *Helv. Chim. Acta.* **2004**, 87, 2742-2749.
- ²⁹ J. J. Jodry, K. Mikami, *Tetrahedron Lett.* **2004**, 45, 4429-4431.
- ³⁰ Z. Wang, Q. Wang, Y. Zhang, W. Bao, *Tetrahedron Lett.* **2005**, 46, 4657-4660.
- ³¹ T. Biedron, P. Kubisa, *J. Polym. Sci., Part A: Polym. Chem.* **2005**, 43, 3454-3459.
- ³² B. Ni, A. D. Headley, *Tetrahedron Lett.* **2006**, 47, 7331-7334.
- ³³ H. Ohno, K. Fukumoto, *Acc. Chem. Res.* **2007**, 40, 1122-1129.
- ³⁴ S.-P. Luo, D.-Q. Xu, H.-D. Yue, L.-P. Wang, W.-L. Yang, Z.-Y. Xu, *Tetrahedron: Asymmetry*, **2006**, 17, 2028-2033.
- ³⁵ A. D. Headley, S. R. S. Saibabu Kotti, B. Ni, *Heterocycles*, **2007**, 71, 589-596.
- ³⁶ A. D. Headley, S. R. S. Saibabu Kotti, J. Nam, K. Li, *J. Phys. Org. Chem.* **2005**, 18, 1018-1022.
- ³⁷ W.-H. Ou, Z.-Z. Huang, *Green Chem.* **2006**, 8, 731-734.
- ³⁸ S. Luo, X. Mi, L. Zhang, S. Liu, H. Xu, J.-P. Cheng, *Angew. Chem. Int. Ed.* **2006**, 45, 3093-3097.
- ³⁹ W. Miao, T. H. Chan, *Adv. Synth. Catal.* **2006**, 348, 1711-1718.
- ⁴⁰ F. Hannig, G. Kehr, R. Fröhlich, G. Erker, *J. Organomet. Chem.* **2005**, 690, 5959-5972.
- ⁴¹ F. Guillen, D. Brégeon, J.-C. Plaquevent, *Tetrahedron Lett.* **2006**, 47, 1245-1248.
- ⁴² Y. Ishida, H. Miyauchi, K. Saigo, *Chem. Commun.* **2002**, 2240-2241.
- ⁴³ B. Ni, S. Garre, A. D. Headley, *Tetrahedron Lett.* **2007**, 48, 1999-2002.
- ⁴⁴ M. L. Patil, C. V. L. Rao, K. Yonezawa, S. Takizawa, K. Onitsuka, H. Sasai, *Org. Lett.* **2006**, 8, 227-230.
- ⁴⁵ B. Ni, Q. Zhang, A. D. Headley, *J. Org. Chem.* **2006**, 71, 9857-9860.
- ⁴⁶ B. Ni, Q. Zhang, A. D. Headley, *Tetrahedron Lett.* **2008**, 49, 1249-1252.
- ⁴⁷ E. Tourneux, H. Gornitzka, J. Marty, N. Lauth-de Viguerie, *Molecules*, **2007**, 12, 1940-1949.
- ⁴⁸ J. Pernak, J. Feder-Kubis, *Tetrahedron: Asymmetry*, **2006**, 17, 1728-1737.
- ⁴⁹ T. Payagala, D. W. Armstrong, *Chirality*, **2012**, 24, 17-53.
- ⁵⁰ P. Wasserscheid, A. Bösmann, C. Bolm, *Chem. Commun.* **2002**, 200-201.
- ⁵¹ G. Vo-Thanh, B. Pegot, A. Loupy, *Eur. J. Org. Chem.* **2004**, 5, 1112-1116.
- ⁵² G.-H. Tao, L. He, N. Sun, Y. Kou, *Chem. Commun.* **2005**, 44, 3562-3564.
- ⁵³ J. Levillain, G. Dubant, I. Abrunhosa, M. Gulea, A.-C. Gaumont, *Chem. Commun.* **2003**, 2914-2915.
- ⁵⁴ S. T. Handy, M. Okello, *Tetrahedron Lett.* **2003**, 44, 8399-8402.

- ⁵⁵ S. T. Handy, M. Okello, G. Dickenson, *Org. Lett.* **2003**, 5, 2513–2515.
- ⁵⁶ L. Poletti, C. Chiappe, L. Lay, D. Pieraccini, L. Polito, G. Russo, *Green Chem.* **2007**, 9, 337–341.
- ⁵⁷ O. N. Van Buu, G. Vo-Thanh, *Lett. Org. Chem.* **2007**, 4, 158–167.
- ⁵⁸ V. Kumar, C. E. Olsen, S. J. C. Schaeffer, V. S. Parmar, S. V. Malhotra, *Org. Lett.* **2007**, 9, 3905–3908.
- ⁵⁹ P. G. J. Plaza, B. A. Bhongade, G. Singh, *Synlett*, **2008**, 2973–2976.
- ⁶⁰ K. Fukumoto, M. Yoshizawa, H. Ohno, *J. Am. Chem. Soc.* **2005**, 127, 2398–2399.
- ⁶¹ X. Chen, X. Li, A. Hu, F. Wang, *Tetrahedron: Asymmetry*, **2008**, 19, 1–14.
- ⁶² C. R. Allen, P. L. Richard, A. J. Ward, L. G. A. Van de Water, A. F. Masters, T. Maschmeyer, *Tetrahedron Lett.* **2006**, 47, 7367–7370.
- ⁶³ L. C. Branco, P. M. P. Gois, N. M. T. Lourenco, V. B. Kurteva, C. A. M. Afonso, *Chem. Commun.* **2006**, 2371–2372.
- ⁶⁴ M. Y. Machado, R. Dorta, *Synthesis*, **2005**, 2473–2475.
- ⁶⁵ T. Yamada, P. J. Lukac, T. Yu, R. G. Weiss, *Chem. Mater.* **2007**, 19, 4761–4768.
- ⁶⁶ T. Yu, T. Yamada, G. C. Gaviola, R. G. Weiss, *Chem. Mater.* **2008**, 20, 5337–5344.
- ⁶⁷ G. V. S. M. Carrera, A. Costa, M. N. Ponte, L. C. Branco, *Synlett*, **2013**, 24, 2525–2530.
- ⁶⁸ A. Villiers, *Compt. Rend. Acad. Sci.* **1891**, 112, 536–538.
- ⁶⁹ T. Loftsson, D. Duchêne, *Int. J. Pharm.* **2007**, 329, 1–11.
- ⁷⁰ F. Schardinger, *Z. Unters. Nahr.- Genussm.* **1903**, 6, 865–880.
- ⁷¹ F. Schardinger, *Zentralbl. Bakteriол. Parasitenkd. Abt. II*, **1911**, 29, 188–197.
- ⁷² H. Dodziuk (Ed.), *Cyclodextrins and their complexes*, **2006**, Wiley- VCH, Weinheim.
- ⁷³ J. Szejtli, T. Osa, (eds.) *Comprehensive Supramolecular Chemistry*, Vol. 3, *Cyclodextrins*, **1996**, Elsevier Science Ltd., Oxford, UK.
- ⁷⁴ M. Sardo, A. M. Amadob, P. J. A. Ribeiro-Claroa, *J. Raman Spectrosc.* **2009**, 40, 1624–1633.
- ⁷⁵ J. Szejtli, *Chem. Rev.* **1998**, 98, 1743–1754.
- ⁷⁶ A. R. Hedges, *Chem. Rev.* **1998**, 98, 2035–2044.
- ⁷⁷ T. Loftsson, M. E. Brewster, *J. Pharmaceutical Sciences*, **1996**, 85, 1017–1025.
- ⁷⁸ Y. Zheng, X. Xuan, J. Wang, M. Fan, *J. Phys. Chem. A* **2010**, 114, 3926–3931.
- ⁷⁹ Q. Liu, M. H. A. Janssen, F. van Rantwijk, R. A. Sheldon, *Green Chem.* **2005**, 7, 39–42.
- ⁸⁰ Y. Gao, X. Zhao, B. Dong, L. Zheng, N. Li, S. Zhang, *J. Phys. Chem. B* **2006**, 110, 8576–8581.
- ⁸¹ C. D. Tran, S. H. De Paoli Lacerda, *Anal. Chem.* **2002**, 74, 5337–5341.
- ⁸² S. Amajjahe, H. Ritter, *Macromolecules*, **2008**, 41, 3–12.
- ⁸³ E. Vranic, A. Uzunovic, *Bosnian J. of Basic Med. Sc.* **2010**, 10, 197–205.
- ⁸⁴ H.- G. Li, Q. Zhang, M. Liu, J. Liu, D.- Z. Sun, *Ind. J. Chem.* **2010**, 49A, 752–756.

- ⁸⁵ D.W. Armstrong, Y. Tang, J. Zukowski, *Anal. Chem.* **1991**, 63, 2858-2861.
- ⁸⁶ D.W. Armstrong, W. Li, J. Pitha, *Anal. Chem.* **1990**, 62, 214-217.
- ⁸⁷ Z.S. Breitbach, D.W. Armstrong, *Anal. Bioanal. Chem.* **2008**, 390, 1605-1617.
- ⁸⁸ C.F. Poole, *Adv. Chromatogr.* **2007**, 45, 89-124.
- ⁸⁹ A. Berthod, L. He, D.W. Armstrong, *Chromatographia*, **2001**, 53, 63-68.
- ⁹⁰ K. Huang, X. Zhang, D. W. Armstrong, *J. Chromatogr. A.* **2010**, 1217, 5261-5273.
- ⁹¹ J. L. Anderson, R. F. Ding, A. Ellern, D. W. Armstrong, *J. Am. Chem. Soc.* **2005**, 127, 593-604.
- ⁹² N. Costa, S. Matos, M. D. R. Gomes da Silva, M. M. A. Pereira, *ChemPlusChem.* **2013**, 78, 1466 – 1474.
- ⁹³ G. M. Blackburn, M. J. Gait, D. Loakes, D. M. Williams, *Nucleic Acids in Chemistry and Biology- 3rd ed.* **2006**, The Royal Society of Chemistry Publishing.
- ⁹⁴ G. Chen, X. Han, L. Zhang, J. Ye, *J Chromatogr. A.* **2002**, 954, 267–276.
- ⁹⁵ D. M. Huryn, M. Okabe, *Chem. Rev.* **1992**, 92, 1745-1768.
- ⁹⁶ J. N. C. Lopes, L. P. N. Rebelo, *Chimica Oggi/Chem. Today*, **2007**, 25, 37-39.
- ⁹⁷ Y. F. Zheng, H. W. Kong, J. H. Xiong, S. Lv, G. W. Xu, *Clin Biochem.* **2005**, 38, 24–30.
- ⁹⁸ J. D. Watson, F. H. C. Crick, *Nature*, **1953**, 171, 737-738.
- ⁹⁹ V. Kumar, V. S. Parmar, S. V. Malhotra, *Biochimie*, **2010**, 92, 1260-1265.
- ¹⁰⁰ J. M. M. Araújo, R. Ferreira, I. M. Marrucho, L. P. N. Rebelo, *J. Phys. Chem. B.* **2011**, 115, 10739–10749.
- ¹⁰¹ S. Ishiwata, K. Itoh, T. Yamaguchi, N. Ishida, M. Mizugaki, *J. Exp. Med.* **1995**, 176, 61–68.
- ¹⁰² N. Q. Tran, S. Tabor, C. J. Amarasiriwardena, A. W. Kulczyk, C. C. Richardson, *J. Biol. Chem.* **2012**, 287, 29468–29478.
- ¹⁰³ Z. M. Qian, J. B. Wan, Q. W. Zhang, S. P. Li, *J. Pharm. Biomed. Anal.* **2008**, 48, 1361–1367.
- ¹⁰⁴ W. Wang, L. Zhou, S. Wang, Z. Luo, Z. Hu, *Talanta*, **2008**, 74, 1050–1055.
- ¹⁰⁵ L. Yu, K. Chu, H. Ye, X. Liu, X. Xu, G. Chen, *Anal. Chem.* **2012**, 34, 140–151.
- ¹⁰⁶ F. Li, F.-Q. Yang, Z.-N. Xia, *Chromatographia*, **2013**, 76, 1003–1011.
- ¹⁰⁷ K. Bica, P. Gaertner, *Eur. J. Org. Chem.* **2008**, 19, 3235-3250.
- ¹⁰⁸ R. S. Schwab, F. Z. Galetto, J. B. Azeredo, A. L. Braga; *Tetrahedron Lett.* **2008**, 49, 5094–5097.
- ¹⁰⁹ A Vass, K. Bélafi-Bakó, N. Nemestóthy, P. Cserjési, Z. Csanádi, *Desanilation*, **2009**, 246, 370-374.
- ¹¹⁰ P. S. Kulkarni, L.C. Branco, J.G. Crespo, M.C. Nunes, A. Raymundo; C.A.M. Afonso, *Chem. Eur. J.* **2007**, 13, 8478-8488.
- ¹¹¹ D.H. Baker, G.L. Czarnecki-Maulden, *J. Nutr.* **1987**, 117, 1003–10.

- ¹¹² T.-C Huang, C.-T. Ho, Y. H. Hui, W.-K.Nip, R. Rogers, *Meat Science and Applications*. CRC. **2001**, 71–102.
- ¹¹³ <http://www.fda.gov/>, Food and Drug Administration, *Food Ingredients and Colors*, **2004**.
- ¹¹⁴ G. Gonfa, M.A. Bustam, Z. Man, M. I. Abdul Mutalib, *Asian Transactions on Engineering (ATE)*, **2011**, 1, 24-34.
- ¹¹⁵ W. Zhao, F. Leroy, B. Heggen, S. Zahn, B. Kirchner, S. Balasubramanian, F. M. Iler-Plathe, *J. Am. Chem. Soc.* **2009**, 31, 15825–15833.
- ¹¹⁶ D. K. Bwambok, S. Challa, M. Lowry, I. M. Warner, *Anal. Chem.* **2010**, 82, 5028–5037.
- ¹¹⁷ V. Kumar, C.E. Olsen, S.J.C. Schaeffer, V.S. Parmar, S.V. Malhotra, *Org. Lett.* **2007**, 9, 3905–3908.
- ¹¹⁸ S. Yu, S. Lindeman, C. D. Tran, *J. Org. Chem.* **2008**, 73, 2576-2591.
- ¹¹⁹ S. L. De Rooy, M.Li, D. K. Bwambok, B. El-Zahab, S. Challa, I.M. Warner, *Chirality*, **2011**, 23, 54-62.
- ¹²⁰ J. Ding, D. W. Armstrong, *Chirality*, **2005**, 17, 281–292.
- ¹²¹ A. G. Hajos, D. R.Parrish, *J. Org. Chem.* **1974**, 39, 1615-1621.
- ¹²² A. Heine, G. DeSantis, J. G. Luz, M. Mitchell, C.-H. Wong, I. A. Wilson, *Science*, **2001**, 294, 369-374.
- ¹²³ B. List, *Tetrahedron*, **2002**, 58, 5573-5590.
- ¹²⁴ H. E. Zimmermann, M. D. Traxler, *J. Am. Chem. Soc.* **1957**, 79, 1920-1923.
- ¹²⁵ D. E. Siyutkin, A. S. Kucherenko, M.I. Struchkova, S.G. Zlotin, *Tetrahedron*, **2009**, 65, 1366–1372.
- ¹²⁶ S. D. Yang, L. Y. Wu, Z. Y. Yan, Z. L. Pan, Y. M. Liang, *J. Mol. Catal. A.* **2007**, 268, 107–111.
- ¹²⁷ W. Chuanlong, F. Xiangkai, L. Shi, *Eur. J. Org. Chem.* **2011**, 7, 1291-1299.
- ¹²⁸ U. Eder, G. Sauer, R. Wiechert, *Angew. Chem. Int. Ed.* **1971**, 10, 496-497.
- ¹²⁹ Y. Fukaya, Y. Iizuka, K. Sekikawa, H. Ohno, *Green Chem.* **2007**, 9, 1155-1157.
- ¹³⁰ S. G. Giap, *J. Phys. Sc.* **2010**, 21, 29–39.
- ¹³¹ Y. Hayashi, H. Gotoh, T. Tamura, H. Yamaguchi, R. Masui, M. Shoji, *J. Am. Chem. Soc.* **2005**, 127, 16028-16029.
- ¹³² B. List, *Chem. Rev.* **2007**, 107, 5471-5569.
- ¹³³ S. Saito, H. Yamamoto, *Acc. Chem. Res.* **2004**, 37, 570–579.
- ¹³⁴ D. Seebach, J. Golinski, *Helv. Chim. Acta*, **1981**, 64, 1413–1423.
- ¹³⁵ Y. Qian, S. Xiao, L. Liu, Y. Wang, Wang, *Tetrahedron: Asymmetry*, **2008**, 19, 1515- 1518.
- ¹³⁶ a) http://en.wikipedia.org/wiki/Supercritical_carbon_dioxide#cite_note-1, b) J.A. Mendiola, M. Herrero, A. Cifuentes, E. Ibañez, *J. Chrom. A.* **2007**, 1152, 234–246.
- ¹³⁷ C. Wang, H. Luo, D-E. Jiang, H. Li, S. Dai, *Angew. Chem. Int. Ed.* **2010**, 49, 5978-5981.

- ¹³⁸ C. Wang, S. M. Mahurin, H. Luo, G. A. Baker, H. Li, S. Dai, *Green Chem.* **2010**, 12, 870-874.
- ¹³⁹ C. A. Angell, Y. Ansari, Z. Zhao, *Faraday Discuss.* **2012**, 154, 9–27.
- ¹⁴⁰ K. Dua, K. Pabreja, M. V. Ramana, V. Lather, *J. Pharm. Bioallied Sci.* **2011**, 3, 417–425.
- ¹⁴¹ <http://www.wisegeek.com/what-is-ergosterol.htm>.
- ¹⁴² P. Asa, R. Wilson, R. F. Garry, *Exp. Mol. Path.* **2002**, 73, 19–27.
- ¹⁴³ G. Zhang, S. Shuang, C. Dong, J. Pan, *Spectrochimica Acta Part A*, **2003**, 59, 2935-2941 and references therein.
- ¹⁴⁴ A. Domínguez, A. Fernández, N. González, E. Iglesias, L. Montenegro, *J. Chem. Ed.* **1997**, 74, 1227-1231.
- ¹⁴⁵ <http://pt.slideshare.net/tabirsir/polymeric-micelles-and-their-applications>.
- ¹⁴⁶ A. Chakraborty, S. Chakraborty, S. K. Saha, *J. Disper. Sci. Tech.* **2007**, 28, 984–989 and references therein.
- ¹⁴⁷ M. H. Chowdhury, K. Ray, M. L. Johnson, S.K. Gray, J. Pond, J. R. Lakowicz, *J. Phys. Chem. C. Nanomater Interfaces.* **2010**, 114, 7448-7461.
- ¹⁴⁸ J. F. Jr. Banks, C. M. Whitehouse, *Int. J. Mass Spectrom. Ion Proc.* **1997**, 162, 163-172.
- ¹⁴⁹ T. N. Kakuda, M. Schöller- Gyüre, R. M. W. Hoetelmans, *Antiviral Theraphy*, **2010**, 15, 817-829.
- ¹⁵⁰ S. Aparicio, R. Alcalde, *Green Chem.* **2009**, 11, 65–78.
- ¹⁵¹ J. M. DeSimone, *Science*, **2002**, 297, 799-803.
- ¹⁵² R. A. Sheldon, *Green Chem.* **2005**, 7, 267-278.
- ¹⁵³ N. V. Plechkova, K. R. Seddon, *Chem. Soc. Rev.* **2008**, 37, 123-150.
- ¹⁵⁴ C. S. M. Pereira, V. M. T. M. Silva, A. E. Rodrigues, *Green Chem.* **2011**, 13, 2658–2671.
- ¹⁵⁵ J. J. Clary, V. J. Feron, J. A. van Velthuijsen, *Regul Toxicol. Pharmacol.* **1998**, 27, 88-97.
- ¹⁵⁶ C. T. Bowner, R. Hooftman, A.O. Hanstveit, P.W.M. Venderbosch, N. van der Hoeven, *Chemosphere*, **1998**, 37, 1317-1333.
- ¹⁵⁷ K. Trychta, D. A. Sandberg, M. Henry, *Pollution Prevention Rev.* **2001**, 44, 33-34.
- ¹⁵⁸ W. Den, F. Ko, T. Huang, *IEEE T. Semicond. M.* **2002**, 15, 540-551.
- ¹⁵⁹ D. L. White, J. A. Bardole, *Paint and Finish Removers*, Kirk-Othmer encyclopedia of chemical technology, John Wiley and Sons, New York, **2000**.
- ¹⁶⁰ J.-P. Wan, C. Wang, R. Zhou, Y. Liu, *Tetrahedron Lett.* **2012**, 2, 8789–8792.
- ¹⁶¹ P. P. Ghosh, S. Paul, A.R. Das, *Tetrahedron Lett.* **2013**, 54, 138–142.
- ¹⁶² A. Dandia, A. K. Jain, A. K. Laxkar, *Tetrahedron Lett.* **2013**, 54, 3929–3932.